University of Cincinnati

Date: 6/10/2013

I, Xinjian He , hereby submit this original work as part of the requirements for the degree of Doctor of Philosophy in Industrial Hygiene (Environmental Health).

It is entitled:

Effects of Faceseal Leakage, Combustion Material, Particle Size, Breathing Frequency and Flow Rate on the Performance of Respiratory Protection Devices

Student's name: **Xinjian He**

This work and its defense approved by:

Committee chair: Sergey Grinshpun, Ph.D.

Committee member: Pramod Kulkarni, D.Sc.

Committee member: Roy Mckay, Ph.D.

Committee member: Marepalli Rao, Ph.D.

Committee member: Tiina Reponen, Ph.D.

3541

Effects of Faceseal Leakage, Combustion Material, Particle Size, Breathing Frequency and Flow Rate on the Performance of Respiratory Protection Devices

A dissertation submitted to the

Division of Research and Advanced Studies

of the University of Cincinnati

In partial fulfillment of the requirements for the degree of

DOCTOR OF PHILOSOPHY

In the Department of Environmental Health of the College of Medicine

June 2013

By

Xinjian (Kevin) He

M.S., West Virginia University, 2010

B.S., China University of Mining & Technology, 2004

Committee Chair: Sergey A. Grinshpun, Ph.D.

ProQuest LLC.
789 East Eisenhower Parkway
P.O. Box 1346
Ann Arbor, MI 48106 - 1346

ABSTRACT

The main goal of this study was to investigate multiple factors (faceseal leakage, combustion material, particle size, breathing flow rate, and breathing frequency) that affect the performance offered by negative pressure respiratory protection devices, including an elastomeric full facepiece, an elastomeric half-mask, an N95 filtering facepiece respirator (FFR), and a surgical mask. Challenge aerosols included NaCl particles and combustion particles generated by burning different materials. This research effort consists of five related studies.

In study one (Chapter 1), the effects of faceseal leakage and origin of challenge aerosol (combustion of wood, paper and plastic) on the performance of a full facepiece and a half-mask elastomeric respirator were tested. The study revealed that the origin of challenge aerosol significantly affects the particle penetration through unsealed and partially sealed half-mask. Increasing leak size increased the total particle penetration.

In study two (Chapter 2), the effect of particle size on the performance of an elastomeric half-mask respirator against combustion aerosols was examined. For the partially sealed and unsealed respirators, the penetration through the faceseal leakage reached maximum at particle sizes > 100 nm when challenged with plastic aerosol, whereas no clear peaks were observed for wood and paper aerosols. The particles aerosolized by burning plastic penetrated more readily than wood and paper.

Study three (Chapter 3) was focused on the effect of breathing frequency on the total inward leakage (TIL) of an elastomeric half-mask respirator donned on an advanced manikin headform challenged with combustion aerosols. The frequency effect was less significant than

flow rate. The greatest penetration occurred when respirators were challenged with plastic aerosol at 30 L/min and 30 breaths/min.

Study four (Chapter 4) was conducted to investigate the effect of breathing frequency on the filter penetration (P_{filter}) and the TIL for a N95 facepiece filtering respirators (FFR) and a surgical mask. For the tested FFR and SM, results show that P_{filter} was significantly affected by particle size and breathing flow rate; surprisingly P_{filter} as a function of particle size exhibited more than one peak under all tested breathing conditions. The breathing frequency effect on P_{filter} was generally less pronounced, especially for lower MIFs. TIL was not significantly affected by particle size and breathing frequency for particles > 50 nm; however, the effect of MIF remained significant.

In study five (Chapter 5), a conventional and a modified elastomeric half-mask respirators were fit tested using 25 human subjects. The modified half-mask (with polymeric micro-patterned adhesives tapes applied on the sealing surface to minimize the faceseal leakage) exhibited higher overall fit factors (geometric mean, GM = 7,907) than the non-modified half-mask (GM = 4,779) under the normal test condition (dry and shaved face). For all challenge facial conditions, including wet and/or unshaved face, the modified half-mask showed significantly higher fit factors than the conventional one, suggesting a special advantage offered by the former respirator.

Overall, the results presented in this dissertation provide an extensive database, which is useful for respirator manufacturers, regulatory agencies, respiratory protection researchers, and end-users operating in various occupational environments.

Table of Contents

Acknowledgements

I would like to express my deepest gratitude to my advisor, Dr. Sergey Grinshpun, whose expertise, encouragement, patience, generous guidance and support made it possible for me to work on a topic that was of great interest to me. He was a constant source of motivation and the driving force behind my achievements for which I will always treasure. Without his help and instruction, my completion of PhD dissertation would not have been possible. It was an honor and great pleasure working with him.

I am hugely indebted to Dr. Tiina Reponen for being ever so kind to provide constant help, and for giving her precious advice regarding the topic of my research. Her friendship and support will always be remembered.

I am very greatly thankful to Dr. Roy McKay for his valuable suggestions, endless help and great interest in my research work. His expertise in respiratory protection research was always beneficial to me.

Special thanks go to my committee members: Dr. Marepalli Rao for his statistical insight, and Dr. Pramod Kulkarni for his background in aerosol science.

I also would like to acknowledge that this research was supported by the NIOSH Targeted Research Training Program and Pilot Research Project Training Program (University of Cincinnati, Education and Research Center, Grant T42/OH008432-07) as well as by the Chemical and Biological Defense (CBD) SBIR program (Contract No. W911NF-10-C-0060). The BRSS was made available thanks to courtesy of Koken Ltd. (Tokyo, Japan); the advanced manikin headform was provided by Mr. Michael S. Bergman, and Dr. Ziqing Zhuang of NIOSH.

I am offering my special appreciation to all the team members in our lab, especially Dr. Mike Yermakov for his constant support and technical assistance.

Finally, I would like to express my great gratitude to my wife, my parents and my younger sister for their love and support throughout these years. My wife Lina and I feel blessed to have our newborn baby – Ben.

List of Peer-reviewed Publications

This dissertation includes the results presented in the following seven peer-reviewed journal articles:

1. **He X,** Yermakov M, Reponen T, McKay RT, James K, and Grinshpun SA: Manikin-based performance evaluation of elastomeric respirators against combustion particles. *Journal of Occupational and Environmental Hygiene*; 10(4): 203-212 (2013) (See Chapter 1)
2. **He X,** Son SY, James K, Yermakov M, Reponen T, McKay RT, and Grinshpun SA: Exploring a Novel Ultrafine Particle Counter for Utilization in Respiratory Protection Studies. *Journal of Occupational and Environmental Hygiene*; 10(4): D52-D54 (2013) (See Chapter 1)
3. **He X,** Grinshpun SA, Reponen T, Yermakov M, McKay RT, Haruta H, and Kimura K: Laboratory Evaluation of the Particle Size Effect on the Performance of an Elastomeric Half-mask Respirator against Ultrafine Combustion Particles. (Published online). *Annals of Occupational Hygiene*. *doi:10.1093/annhyg/met014* (2013) (See Chapter 2)
4. **He X,** Grinshpun SA, Reponen T, McKay RT, Bergman MS, and Zhuang Z: Effect of Breathing Frequency and Flow Rate on the Total Inward Leakage of an Elastomeric Half-Mask Donned on an Advanced Manikin Headform. *Annals of Occupational Hygiene*. (Submitted in March 2013) (See Chapter 3)
5. **He X,** Reponen T, McKay RT, and Grinshpun SA: How does breathing frequency affect the performance offered by an N95 filtering facepiece respirator and a surgical mask against surrogates of viral particles? *Journal of Occupational and Environmental Hygiene.* (Submitted in May 2013) (See Chapter 4)
6. **He X,** Reponen T, McKay RT, and Grinshpun SA: Effect of Particle Size on the Performance of an N95 Filtering Facepiece Respirator and a Surgical Mask at Various Breathing Conditions. *Aerosol Science & Technology.* (Submitted in May 2013) (See Chapter 4)
7. **He X,** Grinshpun SA, Reponen T, McKay RT, Lu J, and Soroushian P: Performance Characteristics of an Elastomeric Half-mask Respirator Modified with a Polymer Micro-Patterned Adhesive. *Journal of the International Society for Respiratory Protection*. (In preparation) (See Chapter 5)

The full manuscripts are presented in Appendices A1 through A7. These seven papers comprise the main body of this dissertation.

The findings described in this dissertation were also presented in four conference presentations/posters listed below.

1. **X.He,** S.A. Grinshpun, T. Reponen, "*Effects of Breathing Frequency on the Performance of an Elastomeric Half-mask Against Combustion Aerosols Using an Advanced Manikin Headform*", Student Poster #35. American Industrial Hygiene Conference & Exposition (AIHce) 2013, Montréal, Canada, 18-23 May. (awarded "Best Student Poster")
2. **X.He,** S.A. Grinshpun, T. Reponen, "*How Does Breathing Frequency Affect the Filter Efficiency of an N95 Filtering Facepiece Respirator?*", Podium 111. American Industrial Hygiene Conference & Exposition (AIHce) 2013, Montréal, Canada, 18-23 May.
3. **X. He,** M. Yermakov, T. Reponen, S.A. Grinshpun, "*Performance Evaluation of an Elastomeric Half-mask Respirator on a Manikin with Combustion Aerosol*", International Society for Respiratory Protection 16th International Conference 2012, Boston, USA, 23-27 September.
4. **X. He,** S.A. Grinshpun, M. Yermakov, T. Reponen, "*Effects of Faceseal Leakage, Flow Rate and Combustion Material on the Performance of Elastomeric Respirators with P-100 Filters*", Student Poster #30, American Industrial Hygiene Conference & Exposition (AIHce) 2012, Indianapolis, 17-22 June. (awarded "Best of Session").

List of Figures

List of Tables

INTRODUCTION

Objective

This study was conducted to evaluate how faceseal leakage, combustion material, particle size, breathing frequency and flow rate affect the performance of an elastomeric full facepiece, an elastomeric half-mask, an N95 filtering facepiece respirator (FFR), and a surgical mask.

Hypothesis

The performance offered by negative pressure respiratory protection devices (including elastomeric full facepiece, elastomeric half-mask, N95 FFR, and surgical mask) depends on, the faceseal leakage, combustion material, particle size, breathing frequency and flow rate.

Specific Aims

Aim 1. Evaluate the performance of an elastomeric full facepiece and half-mask respirators against combustion aerosols using size-independent measurement.

Aim 2. Quantify particle size effect on the performance of an elastomeric half-mask respirator challenged with combustion aerosols.

Aim 3. Investigate the effect of breathing frequency on the TIL of an elastomeric half-mask donned on an advanced manikin headform and challenged with combustion aerosols.

Aim 4. Evaluate the effects of breathing frequency and particle size on the filter penetration and TIL of an N95 FFR and a surgical mask challenged with NaCl particles representing the viral particles, as well as other health-relevant sub-micrometer particles.

Aim 5. Study the performance of a modified elastomeric half-mask integrated with polymer micro-patterned adhesive tapes, and compare it to the performance of a conventional (non-modified) half-mask respirator.

Executive Summary

A respirator is a protective device that covers the nose and mouth or the entire face or head to guard the wearer against hazardous air environments. The U.S. Occupational Safety and Health Administration (OSHA) requires respirators be provided to employees whenever engineering and work practice control measures are not adequate to reduce the employees' exposure to acceptable levels. Among the non-powered air purifying respirators, filtering facepiece respirators (FFRs) are the most commonly used respiratory protection devices (share = 49%) followed by elastomeric half-masks (34%), and full facepiece (15%) according to the survey conducted in private industry by the U.S. Bureau of Labor Statistics (BLS) and the National Institute for Occupational Safety and Health (NIOSH).

Research presented in this thesis was carried out to investigate multiple factors that affect the performance offered by negative pressure respirators, including an elastomeric full facepiece, an elastomeric half-mask, an N95 filtering facepiece respirator (FFR), and a surgical mask. These primarily included particle size, breathing flow rate, and breathing frequency. Two particle penetration pathways –filter media and faceseal leakage – were investigated. Challenge aerosols included NaCl particles and combustion particles generated by burning of different materials. This research effort consists of five related studies respectively responding to the five above-listed specific aims.

In the first study (**Chapter 1, Specific Aim 1**), one elastomeric half-mask and one full facepiece respirators were examined. Each respirator was equipped with two P100 filters. These types of respirators are commonly used by firefighters and first responders during fire overhaul (after the fire has been extinguished). Respirators were tested on a breathing manikin exposed to aerosols produced by combustion of three materials (wood, paper, and plastic) in a room-size

(24.3 m^3) exposure chamber. Testing was performed using a single constant flow (30 L/min) and three cyclic flows (mean inspiratory flow rates, MIFs = 30, 85, and 135 L/min). Four sealing conditions ("unsealed", "nose-only sealed", "nose & chin sealed", and "fully sealed") were examined to evaluate the respirator faceseal leakage. The total (size-independent) aerosol concentration was measured inside (C_{in}) and outside (C_{out}) of the respirator using a condensation particle counter (CPC) and an ultrafine particle counter (prototype) developed at the University of Cincinnati (UC UPF counter). The total penetration through the respirator was determined as a ratio of the two (C_{in}/C_{out}). The experimental results suggested that the faceseal leakage, breathing flow rate and type, and combustion material were all significant factors affecting the performance of the half-mask and full facepiece respirators. The efficiency of P100 respirator filters met the NIOSH certification criteria (penetration $\leq 0.03\%$); it was not significantly influenced by the challenge aerosol and flow type, which supports the current NIOSH testing procedure utilizing a single challenge aerosol and a constant air flow. However, contrary to the NIOSH total inward leakage (TIL) test protocol assuming that the result is independent on the type of the test aerosol, this study revealed that the challenge aerosol significantly affects the particle penetration through unsealed and partially sealed half-mask respirators. Increasing leak size increased the total particle penetration. The findings of this study point to some limitations of the existing TIL test in predicting protection levels offered by half-mask elastomeric respirators.

In the second study (**Chapter 2, Specific Aim 2**), the particle size effect on the performance of an elastomeric half-mask respirator challenged with three (wood, paper, and plastic) combustion aerosols was quantified. The half-mask respirator equipped with two P100 filters was donned on a breathing manikin connected to a breathing simulator. Testing was

conducted with respirators that were fully sealed, partially sealed (nose area only), or unsealed to the face of a breathing manikin to simulate different faceseal leakages. Three cyclic flows with MIFs of 30, 85, and 135 L/min were tested for each combination of sealing condition and combustion material. Additional testing was performed with plastic combustion particles at other cyclic and constant flows. Particle penetration was determined by measuring particle number concentrations inside and outside the respirator with size ranges from 20 to 200 nm. Study results showed that the breathing flow rate, particle size, and combustion material all had significant effects on the performance of the respirator. For the partially sealed and unsealed respirators, the penetration through the faceseal leakage reached maximum at particle sizes above 100 nm when challenged with plastic aerosol, whereas no clear peaks were observed for wood and paper aerosols. The particles aerosolized by burning plastic penetrated more readily into the unsealed half-mask than those aerosolized by the combustion of wood and paper. The difference may be attributed to the fact that plastic combustion particles differ from wood and paper particles by physical characteristics such as a charge, shape and density. For the partially sealed respirator, the highest penetration values were obtained at MIF = 85 L/min. The unsealed respirator had approximately 10-fold greater penetration than the one partially sealed around the bridge of the nose, which indicates that the nose area was the primary leak site.

In the third study (**Chapter 3, Specific Aim 3**), we investigated the effect of breathing frequency on the TIL of an elastomeric half-mask donned on an advanced manikin headform and challenged with combustion aerosols. The half-mask respirator equipped with P100 filters was donned on an advanced manikin headform covered with life-like soft skin and challenged with aerosols originated by burning three materials: wood, paper and plastic. TIL was determined as the ratio of aerosol concentrations inside and outside of the respirator (C_{in}/C_{out}) measured with a

nanoparticle spectrometer operating in the particle size range of 20 to 200 nm. The testing was performed under three cyclic breathing flows (MIFs = 30, 55, and 85 L/min) and five breathing frequencies (10, 15, 20, 25, and 30 breaths/min). A completely randomized factorial study design was chosen with four replicates for each combination of breathing flow rate and frequency. The results demonstrated that the particle size, MIF and combustion material had effects on TIL regardless of breathing frequency. Increasing breathing flow decreased TIL. Testing with plastic combustion aerosol produced higher mean TIL values than wood and paper aerosols. The effect of the breathing frequency was found to be rather complex. When analyzed using all combustion aerosols and MIFs (pooled data), breathing frequency did not significantly affect TIL. However, once the data were stratified according to combustion aerosol and MIF, the effect of breathing frequency became significant for all MIFs challenged with wood and paper combustion aerosols, and for MIF = 30 L/min only when challenged with plastic combustion aerosol. It is concluded that the effect of breathing frequency on TIL was less significant than the effects of combustion aerosol and breathing flow rate for the tested elastomeric half-mask respirator. The greatest penetration occurred when challenged with plastic aerosol at 30 L/min and at a breathing frequency of 30 breaths/min.

The fourth study (**Chapter 4, Specific Aim 4**) was to evaluate the effects of particle size and breathing frequency on the filter penetration and TIL of an N95 filtering facepiece respirator (FFR) and a surgical mask (SM) challenged with NaCl particles representing the viral particles, as well as other health-relevant sub-micrometer particles (20 to 500 nm). First, the tested FFR/SM fully sealed on a hard plastic manikin headform connected to a breathing simulator was exposed to the challenge aerosol (charge equilibrated NaCl particles). Four MIF rates (15, 30, 55 and 85 L/min) combined with five breathing frequencies (10, 15, 20, 25 and 30 breaths/min)

were tested. With the sealed FFR/SM, filter penetration (P_{filter}) was determined as the ratio of aerosol concentration inside/outside the FFR/SM (C_{in}/C_{out}) using a CPC (size-independent measurements) and a nanoparticle spectrometer (size-selective measurements). Second, the same model of the FFR/SM was donned on an advanced manikin headform covered with skin-like material. Total inward leakage (TIL) was measured under the conditions identical to the filter experiment. The "faceseal leakage-to-filter" (*FLTF*) ratios were calculated as $P_{leakage}/P_{filter}$ (P_{leakge}= TIL – P_{filter}). The results suggested that showed significant effects on P_{filter} and TIL. Increasing MIF increased P_{filter} and decreased TIL resulting in decreasing *FLTF* ratio. Most of *FLTF* ratios were >1, suggesting that the faceseal leakage was the primary particle penetration pathway at various breathing frequencies. P_{filter} was significantly affected by particle size and breathing flow rate ($p < 0.05$) for the tested FFR and SM. Surprisingly, for both respiratory protection devices, P_{filter} as a function of the particle size exhibited more than one peak under all tested breathing conditions. The effect of breathing frequency on P_{filter} was generally less pronounced, especially for lower MIFs. For the FFR and SM, TIL increased with increasing particle size up to about 50 nm; for particles above 50 nm, the total penetration was not significantly affected by particle size and breathing frequency; however, the effect of MIF remained significant.

The aim of the fifth study (**Chapter 5, Specific Aim 5**) was to evaluate the fitting characteristics of an elastomeric half-mask respirator modified with a polymeric micro-patterned adhesive (PMA) applied to the sealing surface; to compare the performance of the modified respirator to that of a conventional (non-modified) one. Twenty-five adult subjects representing a NIOSH bivariate panel were tested with a modified and non-modified elastomeric half-mask respirators while participating in a standard OSHA fit testing protocol. NaCl particles were

generated as the challenge aerosol and the concentrations inside and outside of the respirator were measured to determine the fit factor (FF) for each subject. Additional tests were performed with one subject under challenge facial conditions, including wet and/or unshaved face. Results: The modified half-mask exhibited higher fit factors (geometric mean, GM = 7,907) than the non-modified half-mask (GM = 4,779). For all challenge facial conditions, the modified half-mask prototype was consistently achieving significantly ($p < 0.05$) higher fit factors than the conventional half-mask. Overall, applying a polymeric micro-patterned adhesive to the sealing surface of an elastomeric half-mask respirator was found to improve respirator fit and showed promise towards improving performance with various facial conditions..

CHAPTER 1

Manikin-Based Performance Evaluation of Elastomeric Respirators against Combustion Particles (Specific Aim 1)

Introduction

While on duty, firefighters are exposed to a wide range of chemicals and particulate matter (NIOSH, 2007). Smoke from a fire contains fine (≤ 1 μm) and ultrafine (≤ 0.1 μm) particle size fractions. In a large-scale fire test laboratory study, ultrafine particles were found to account for more than 70% of the total number concentration of particles during fire knockdown and overhaul (Baxter *et al.*, 2010). Fine particle exposures at various workplace environments have been associated with impairment of cardiovascular function and other adverse health outcomes (Schwartz *et al.*, 1996; Peters *et al.*, 1997; Timonen *et al.*, 2005).

There are approximately 1.1 million firefighters in the United States (including 300,000 career firefighters). Their leading cause of death is heart disease (Fahy *et al.*, 2009). Sudden cardiac death is responsible for 50% and 39% of the on-duty deaths for volunteers and professional firefighters, respectively (CDC, 2006). Firefighters have greater mortality rates associated with cardiovascular disease and elevated cancer rates than the general population (LeMasters *et al.*, 2006; Yoo *et al.*, 2009).

Respirators used for structural firefighting should meet the certification requirements of the National Institute for Occupational Safety and Health (NIOSH) and the National Fire Protection Association (NFPA, 1981; NIOSH, 1995). Ironically, there is very limited information on the efficiency of the full facepiece used by firefighters during actual firefighting.

Furthermore, during fire overhaul (entering the structure after the fire has been extinguished), firefighters commonly use negative pressure elastomeric half-mask or Filtering Facepiece Respirators (FFR) or no respirators at all (Bolstad-Johnson *et al.*, 2000; Burgess *et al.*, 2001). According to the Occupational Safety and Health Administration (OSHA), the assigned protection factors (APF) given for negative pressure air-purifying full and half-mask respirators are 50 and 10 (OSHA, 2006) which corresponds the equivalent penetration values of 2% and 10%, respectively (P = 100/APF, %).

Respiratory protection offered by negative pressure respirators significantly (and often primarily) depends on the faceseal fit (Grinshpun *et al.*, 2009; Cho *et al.*, 2010b). Very little data are available on faceseal aerosol penetration under the cyclic flow regime and even less is known about the filter versus faceseal penetration under actual breathing conditions. The early investigation carried out by Hinds and Kraske (Hinds and Kraske, 1987) addressed the performance of half-mask and single-use respirators by measuring particle penetration through the filter and the artificially induced cylindrical leaks; the tests were conducted under a constant flow regime at rates between 2 to 150 L/min. Chen and Willeke (Chen *et al.*, 1992), who deployed a breathing manikin with artificially created slit-like or circular leaks to assess the faceseal versus filter penetration for 0.5 – 5 μm particles, also tested under the constant flow regime. However, artificial fixed leaks and constant flows are not representative of real world conditions. Workplace protection factor (WPF) studies are representative of real world conditions with human subjects wearing respirators (Myers *et al.*, 1996; Myers *et al.*, 1998; Lee *et al.*, 2005a; Lee *et al.*, 2005b; Cho *et al.*, 2010a) and thus, the WPF results include both filter and faceseal penetration. However, the contribution of faceseal leakage to total penetration cannot be calculated from WPF.

The above limitations were overcome in recent studies (Lee, Grinshpun, *et al.*, 2008a; Grinshpun *et al.*, 2009; Cho *et al.*, 2010a; Cho *et al.*, 2010b; Reponen *et al.*, 2011) either by inclusion of human subjects without induced fixed leaks or through partial sealing of respirators on a manikin tested under cyclic flow. Grinshpun *et al.* (2009) found that the primary particle penetration pathway was faceseal leakage for both a N95 FFR and a surgical mask. Cho *et al.* (2010b) reported that despite having a well-fitted N95 FFR, the majority of particles penetrated through the faceseal leaks and the penetration decreased with an increase in respiration flow and in particle size.

Finally, most of the published data on the performance of respirators were collected using an ambient aerosol or nebulizer-generated NaCl particles. Some investigators utilized polystyrene latex (PSL) spheres as challenge aerosol in their tests (Myers *et al.*, 1991; Qian *et al.*, 1998). Others used fungal spores, bacteria or viruses (Qian *et al.*, 1998; Lee *et al.*, 2005a; Bałazy, Toivola, Adhikari, *et al.*, 2006; Eninger *et al.*, 2008). Eninger *et al.* (2008) compared the effects of NaCl and three virus aerosols (all having significant ultrafine components) on the performance of fully sealed N99 and N95 FFRs. The authors concluded that filter penetration of the tested biological aerosols did not exceed that of NaCl aerosol, which suggests that NaCl may generally be appropriate for modeling filter penetration of similarly sized virions. However, particles used in the above-quoted studies are not representative of the exposures experienced by firefighters. The differences are concerned with the particle shape, density, electric charge, and possibly other properties. To our knowledge, the effects of combustion material on respirator performance have not been previously studied.

The present investigation was designed to examine the effects of faceseal leakage, breathing flow type and rate, and combustion material on the overall (non-size selective) aerosol

particle penetration through elastomeric half and full facepiece respirators equipped with P-100 filters.

Materials and Methods

Experimental Design

Two elastomeric respirators (one half-mask and the other a full facepiece) were tested on a breathing manikin exposed to aerosols produced by combustion of three different materials. Testing was performed using two different flow patterns (constant and cyclic breathing regimes). Cyclic flow testing was conducted at three flows selected to represent breathing at different workload levels. Four facepiece sealing conditions were established to evaluate faceseal leakage. Total aerosol concentration was measured inside (C_{in}) and outside (C_{out}) of the respirator. Particle penetration (P) through the respirator was determined as C_{in} / C_{out}.

The experimental set-up for investigating particle penetration through the respirator is schematically shown in Figure 1-1. Inside the exposure chamber (142×95×102 inches, L×W×H), the tested respirator was donned on a manikin headform made of hard plastic (Allen Display^{SM}, Model: Full round molded male manikin display head). A copper pipe (1 inch diameter) was installed into the headform to simulate airflow through the upper respiratory tract. One end of the pipe was sealed between the upper and lower lips of the manikin. For cyclic flows, the other end was connected to an electromechanical Breathing Recording and Simulation System (BRSS) (Koken Ltd., Tokyo, Japan) with a HEPA filter placed in between to keep particles from re-entering into the respirator cavity with the exhalation air flow. The constant flow was created by a vacuum pump (Model: G272X, Doerr Electric Corp., Cedarburg, WI). The aerosol concentrations inside and outside of the respirator were measured with a condensation particle

counter (TSI CPC, Model: 3007, TSI Inc., Minneapolis, MN) which detects particles in a size range from 0.01 to >1.0 μm.

In addition, a novel ultrafine particle counter recently developed at the University of Cincinnati (UC UFP counter) (S. Y. Son *et al.*, 2011), was operated in selected experiments side-by-side with the TSI CPC. The operation principle of this device, like any CPC, involves condensation on nuclei; however, the novelty of this instrument is that the condensation takes place on nano-materials entering through the input channel. After passing a PM filter (cyclone), the particles enter a non-wetting, porous, evaporation-condensation tube. Enlarged due to condensation growth, they are detected with an optical laser counter. Capillary force spontaneously generated on the surface of the non-wetting tube, prevents flooding regardless of orientation and movement. This makes the instrument particularly advantageous for field applications. Additionally, its time of response to a change in aerosol concentration is as low as approximately 0.3 seconds. The detection particle size range is 4.5 nm to >1.0 μm, which, in contrast to conventional CPCs, includes a low nano-scale. The present prototype of the UC UFP counter is portable; however, it is undergoing additional miniaturization to make the device wearable. This device is being developed for a future field study aimed at evaluating workplace protection factors for elastomeric respirators worn by firefighters and first responders during fire activities. The comparison of the new UC UFP counter with the conventionally used TSI CPC is an important step in the development of the personal sampler for field studies.

Data collected with the UC UFP counter were only used for direct comparison to the values obtained with the TSI CPC. All the conclusions listed in this paper regarding the factors affecting the aerosol penetration were drawn solely from data generated with the TSI CPC.

Respirators and Test Conditions

Two types of respirators were tested in this study: (1) Half-mask elastomeric respirator (size: medium) equipped with two P-100 filters and (2) Full facepiece elastomeric respirator (size: medium) equipped with the same type of P-100 filters.

Several studies have reported common facepiece leak locations as the nose, chin and cheek (Oestenstad *et al.*, 1992; Crutchfield *et al.*, 1997; Oestenstad *et al.*, 2010). In the present study, four sealing conditions ("unsealed", "nose-only sealed", "nose & chin sealed" and "fully sealed") were utilized when testing the half-mask respirator. For the full facepiece respirator, only two sealing conditions ("unsealed" and "fully sealed") were used because our pilot study revealed that these two conditions produced similar penetration levels, which made unnecessary to evaluate partially sealed conditions. Silicone sealant was applied in between the manikin's face and the edge of the respirator to form seals. Sealing configurations for the half-mask with "nose-only" and "nose & chin" sealing conditions are shown in Figure 1-2. Respirator straps were tightened and placed around the manikin's head and neck as conventionally used. For each sealing condition, once the respirator was positioned, it was not removed until another sealing condition was evaluated.

Wood (BBQ long match, 0.23 ± 0.03 g), paper (Multifold brown paper towel, 0.25 ± 0.04 g) and plastic (Ziploc^{TM} plastic bag, 0.24 ± 0.04 g) were selected for this study. Wood, paper and plastic are the most common materials encountered by firefighters during fire activities. All three materials were ignited by a long reach lighter and burnt separately inside the testing chamber. The aerosol measurements were initated15 minutes after burning to allow the combustion aerosol to reach a homogenous concentration. To assess the effect of breathing flow on the particle penetration through respirators, we selected three mean inspiratory flows (MIF) of 30, 85, and

135 L/min, with breathing rates of 15, 25, and 25 breaths/min (achieved by adjusting the tidal volume) , respectively. These were established to simulate breathing at moderate, high, and strenuous workloads, respectively. The selection of the breathing rates was based on average respiratory rates reported in a healthy adult (Tortora *et al.*, 1990; Sherwood, 2006). In addition, one constant flow (30 L/min) was selected to investigate the effects of the flow type (constant vs. cyclic).

Three replicates were conducted for each condition, resulting in 144 and 72 measurements for the half and full facepiece respirators, respectively. The manikin breathing flow with three replicates was completely randomized throughout the entire study. A summary of experimental conditions is listed in Table 1-1.

Data Analysis

Collected data from the TSI CPC were entered into a spreadsheet, and descriptive and inferential statistical analyses were performed using SAS version 9.2 (SAS Institute Inc., Cary, NC). The total aerosol penetration was the sum of filter and faceseal penetration ($P = P_F + P_L$), where P_F is the penetration solely through the filter and P_L represents faceseal penetration. For each combination of experimental conditions, the average value of the overall penetration and the standard deviation were calculated from the three replicates. Analysis of Variance (ANOVA) with Tukey's range test and paired *t*-test were performed to study effects of sealing condition, burning material, manikin breathing rate and respirator type on aerosol penetration value. *P*-values of < 0.05 were considered significant.

Results and Discussion

Particle Size Distribution of Combustion Aerosols

Prior to the experiments involving respirators, challenge aerosols – produced by combustion of wood, paper and plastic, respectively – were characterized with respect to their particle size distributions determined with a Nanoparticle Spectrometer (Model: Nano-ID NPS500, Particle Measuring System, Inc., Boulder, CO). This instrument is capable of measuring particle diameter in a range of 5 to 500 nm. Particle size distribution curves obtained 30 minutes after burning are presented in Figure 1-3. The peak particle size for wood combustion aerosol was around 45 nm, and 95% of the particles fell within the size range of 20–200 nm. The peak size for paper and plastic combustion aerosols were 56 nm and 89 nm, respectively, with 95% of the particles falling in size ranges of 20–200 nm and 20–300 nm, respectively. In general, wood combustion produced smaller particles; all three peak concentrations were observed at particle sizes below 100 nm. More than 70% of particles generated by combustion of wood and paper and slightly more than 50% of particles generated by plastic combustion were ultrafine, which is consistent with the earlier findings (Baxter *et al.*, 2010).

Half-mask Elastomeric Respirator with P-100 Filters

1. Respirator Donned on the Manikin (Unsealed)

a. Constant flow. As shown in Table 1-2, for the constant flow 30 L/min, the overall particle penetration was very high: average values were 43.97 ± 2.44 % (wood aerosol), 48.37 ± 0.15 % (paper aerosol), and 50.67 ± 0.61 % (plastic aerosol). ANOVA revealed a statistically significant (p-value < 0.05) effect of combustion material, but from the practical standpoint it does not play an important role since all measured penetration values fell between 40% and 52%. The important finding is that the obtained penetration level is over three orders of magnitude higher than the one expected based solely on the

filter efficiency. Indeed, the respirator was equipped with a P100 filter that has a collection efficiency 99.97% for the most penetrating particle size at a constant flow of 85 L/min, which corresponds to an overall penetration of $\leq 0.03\%$ at 85 L/min and even lower at 30 L/min (no data are available for 135 L/min). This means that most of the penetrated particles entered through the faceseal leakage; only one out of thousands of the penetrated particles entered through the filter media. When testing with an unsealed respirator, a sizeable gap (~ 1 mm) located around the nose of the manikin was observed, indicating a poor fit for the tested respirator donned on the manikin, which could result in unexpectedly high penetration values. This was likely caused by the fact that the manikin was made of hard plastic. Softer human skin would likely form a better seal, resulting in lower penetration values for the elastomeric half-mask respirator.

The total particle penetration results from two components: the filter penetration (P_F) at the corresponding flow through the filter (Q_F) and the leakage penetration (P_L) at the corresponding air flow (Q_L). It can be expressed as:

$$P = \frac{C_{in}}{C_{out}} = \frac{N_{in}}{N_{out}} = \frac{N_F + N_L}{N_{out}} = \frac{N_F}{N_{out}} + \frac{N_L}{N_{out}} = \frac{P_F N_{out} \frac{Q_F}{Q}}{N_{out}} + \frac{P_L N_{out} \frac{Q_L}{Q}}{N_{out}}$$

$$= P_F \frac{Q_F}{Q} + P_L \frac{Q_L}{Q} = P_F \frac{Q_F}{Q} + P_L (1 - \frac{Q_F}{Q}) \qquad \textbf{(1-1)}$$

where: N_{in} – Particle numbers inside the respirator,

N_{out} – Particle number outside the respirator,

N_F – Number of particle penetrating through the filters,

N_L – Number of particles penetrating through the leakage,

Q – Breathing flow = $Q_F + Q_L$.

We concluded from Eq.(1-1) that it is crucial to determine the relative contribution of the air flow through the filter to the total air flow. Therefore, a separate experiment was conducted to measure Q_F when the half-mask was donned on the manikin. A flow meter (Model: 4043, TSI Inc.) was placed between the filter and the respirator. Three breathing (constant) flows (30, 85, and 135 L/min) were selected. For each flow, the respirator was taken off from the manikin, and put back on. Then the filter flow was recorded after each re-donning the respirator. Seven replicates were performed for each flow (which makes the total number of runs equal to 21). It was determined that the fraction of the breathing flow entering through the filter (Q_F/Q) was 56.0 ± 7.2 % at 30 L/min, 61.7 ± 4.4 % at 85 L/min, and 61.0 ± 4.0 % at 135 L/min. Given that P_F of a P100 filter is negligibly low (<0.03%) compared to P_L, and Q_F and Q_L are comparable (according to the above experimental data), Eq. (1-2) can be simplified as:

$$P \approx P_L\left(1-\frac{Q_F}{Q}\right) \quad \textbf{(1-2)}$$

The particle loss inside the gap (~ 1 mm) was estimated to be negligibly low according to a classic particle diffusion theory (Kulkarni *et al.*, 2011). For these conditions, P_L is close to 100%, which allows further simplifying the equation for the overall particle penetration:

$$P \approx 1-\frac{Q_F}{Q} \quad \textbf{(1-3)}$$

According to this assessment, the overall penetration values are expected to be slightly below 50% at 30 L/min and about 40% at 85 and 135 L/min, which is in a reasonable agreement with the penetration values experimentally obtained for an unsealed half-mask tested against three combustion aerosols under constant flow of 30

L/min (listed in Table 1-2). However, Eq. (1-3) is limited to constant flow only, and cannot be applied to cyclic flow conditions representing a much more complex two-direction flow regime.

b. Cyclic flow. The data on the overall aerosol penetration through the *unsealed* half-mask respirator obtained for different MIFs and different combustion materials are presented in Table 1-2.

b.1. *Cyclic versus constant flow.* For wood combustion aerosol with a cyclic MIF of 30 L/min, the penetration was 8.27 ± 0.25 %, which is approximately 5-fold lower than the one obtained in the same experiment with constant flow (43.97 ± 2.44 %). Similar results were observed for paper and plastic combustion aerosols. Overall, P_{cyclic}-values were approximately 4 – 8 times lower than the corresponding $P_{constant}$-values. One reason for this difference is that with constant flow, aerosol particles continuously penetrate into the respirator (mostly through the leakage). However, under the cyclic flow regime, no particles enter during exhalation (half of the period). The return flow is particle-free since it is supplied back into the respirator through a HEPA filter installed between the manikin and the breathing simulator. This time factor causes a two-fold decrease in aerosol concentration inside the respirator with cyclic breathing compared to constant flow, which explains a 50% drop in the measured penetration. In addition, the returning clean air flow dilutes the particle-contaminated air inside the respirator by a volumetric factor of two, thus further decreasing the aerosol concentration C_{in}. Consequently, it should be anticipated that P_{cyclic} is at least 4 times below the corresponding $P_{constant}$. This explanation is valid when the majority of particles detected inside the respirator penetrate directly through facepiece leaks (not the filter). The situation is different when the

aerosol enters solely through the filter (see Table 1-2 – fully sealed respirator). Additionally, with cyclic flow, the relative contribution of air flow through the faceseal leak and filter changes with time, which affects the difference between the penetration levels obtained in the two protocols (constant vs. cyclic flow). The large and consistent difference between $P_{constant}$ and P_{cyclic} found in this study points to a significant limitation of the existing respirator evaluation protocols that are based on the constant flow design.

b.2. *MIF effect on P_{cyclic}.* As MIF of the cyclic flow increased, the particle penetration decreased. This was observed for all three combustion materials and was statistically significant (see Table 1-3). One possible explanation is changing leak size with increasing cyclic flows. Higher flows can generate higher negative pressures inside the respirator during breathing, which improves the sealing performance of the respirator. It should be stressed that P_{cyclic} values that ranged from a low of 5.37 ± 0.29 % (wood, 135 L/min) to a high of 11.4 ± 0.10 % (plastic, 30 L/min) are still well above the expected penetration level of P100 filters (< 0.03%). This suggests faceseal leakage was the primary penetration pathway for the unsealed half-mask respirator.

b.3. *Effect of combustion material on the particle penetration.* The data obtained with the three tested combustion materials revealed similar trends, with paper and plastic producing slightly higher penetrations than wood (see Table 1-4). There was no statistically significant difference in penetration between paper and plastic combustion aerosols. As this study is the first one of a kind dealing with combustion aerosols, no direct comparisons can be made with previous studies.

2. Respirator Partially Sealed on the Manikin (Nose-only Sealed and Nose & Chin Sealed)

a. Effect of partial sealing on penetration. As seen from Table 1-2, penetration values obtained under these two conditions were significantly lower than those determined for the unsealed respirator (see Table 1-5). In most cases the decrease was almost two orders of magnitude. The data indicate that most of the leakage occurred around the manikin's nose.

b. Difference between two types of partial sealing. There were no significant differences in penetration between the two partial sealing conditions labeled as "nose-only" and "nose & chin" regardless on the combustion material and the breathing air flow (see Table 1-5). This further suggests that sealing the nose area (rather than the chin area) reduced penetration on average from approximately 5 – 11% (unsealed) to 0.11 – 0.48% (nose-only sealed) for the cyclic flow regime, and from approximately 44 – 51% (unsealed) to 0.66 – 1.19% (nose-only sealed) for the constant flow regime. This finding is consistent with other studies (Oestenstad *et al.*, 1992; Crutchfield *et al.*, 1997; Oestenstad *et al.*, 2010) that suggest the nose is frequently the primary leak location.

c. Penetration pathway. Although partial sealing reduced the total particle penetration to the levels below 1%, these levels are still much higher than that for a P100 filter alone (<0.03% or <<0.3%). Thus, although offering much greater protection against combustion particles, partial sealing still left a considerable opportunity for penetration through faceseal leakages so that full advantage could not be taken of the efficient P100 filter deployed in a half-mask elastomeric respirator.

d. MIF effect on P_{cyclic}. For nose-only sealed condition, we found that penetration remained at the same level at 30 and 85 L/min but was significant higher at 135 L/min (see Table

1-3). For nose-chin sealed condition, there were significant differences between the outcome observed at three MIFs (30, 85, and 135 L/min). Compared to the unsealed condition, the P_{cyclic} values obtained for the two partial sealing conditions were 10 to 100 times lower as determined at the same MIF. The results also show that increasing the flow does not always reduce the faceseal penetration. In another study, Cho *et al.* (2010b) reported that faceseal penetration was reduced significantly (p-value < 0.001) with increasing breathing flow. A different type of respirator (N95 FFR partially sealed on a manikin) tested in the quoted study may exhibit faceseal leaks of different sizes, which could cause the disagreement between the two studies.

e. Effect of combustion material on penetration. Penetration values were higher for wood combustion aerosol as compared to paper and plastic combustion aerosols in both "nose-only" and "nose & chin" sealed conditions (see Table 1-4). In contrast, for an unsealed respirator, plastic combustion aerosol exhibited the highest penetration. It is not exactly clear why the particles generated by combustion of the three tested materials featured different penetration ability. The differences may be attributed to the physical properties of these aerosols. Ziploc™ plastic bags burned in our experiments are made of polyethylene (PE). This material burns much differently from wood and plastic, and forms more toxic products than the other two. Paper is cellulose (plus various additives and coatings), which burns faster than PE because more than half of its molecular weight is oxygen. Wood is half cellulose and half lignin, which is a complex mixture including some aromatic structures; it has lower amount of hydrogen and oxygen than paper. All three materials (wood, paper and plastic) are expected to generate particles that differ in shape, density, electric charge, and possibly other properties. The capture of sub-

micrometer particles is driven primarily by the mechanisms such as impaction, interception, diffusion and electrostatic attraction. The first two are quantitatively characterized by the particle aerodynamic diameter – a diameter determined by particle density and shape. The third (diffusion) has a great influence for small particles (<300 nm). Conversely, the electrostatic attraction mechanism relies on the charges acquired by the particles. Provided that particles aerosolized due to combustion of wood, paper and plastic feature different density, shape and electric charge, the penetration of those particles may not be exactly the same.

The finding suggests that a better sealing may produce different effect on the respiratory protection level for different aerosols, e.g., be more beneficial for protecting against plastic combustion particles than against other materials. This seems to have a significant practical relevance, especially given that burning plastic generates more toxic combustion particles making their elimination by a respirator particularly important.

3. Respirator Fully Sealed on the Manikin

For a fully sealed half-mask respirator, the total penetration should be equal to the filter penetration, which is supposed to be below 0.03% at 85 L/min for a NIOSH-certified P100 filter. In our experiments, no particle penetration was detected at constant flow rate of 30 L/min. For low to moderate cyclic flows, filter penetration was 0.002% or below. At the highest flow (MIF = 135 L/min), the average penetration was around 0.011%.

It is noted that the P-100 filter penetration values obtained in this study reflect the total particle count regardless of the particle size. The filter penetration generally depends on the particle size reaching the highest value for the most penetrating particle size (MPPS). One size-

selective investigation revealed – for a specific P-100 FFR filter – that the penetration could be as high as 0.048% at the MMPS of 50-200 nm (Eshbaugh *et al.*, 2008).

Full Facepiece Elastomeric Respirator with P-100 Filters

1. Respirator Donned on the Manikin (Unsealed)

a. Penetration values. As seen from Table 1-6, penetration values for unsealed condition were extremely low for all flows and materials. At 30 L/min, $P_{constant}$ ranged from 0.017% (wood) to 0.035% (plastic). The values of P_{cyclic} were even lower: from 0.003% for MIF = 30 L/min (all three combustion materials) to 0.025% (135 L/min, plastic). These levels were approximately three orders of magnitude lower than the penetrations obtained for the half-mask elastomeric respirator. This difference is likely associated with the leak size. The nose has been identified as the primary leak location for half-mask respirators (see the half-mask section above), whereas full facepiece does not have a nose leak (thus penetration dramatically reduced). The difference between the cyclic and constant flow regimes for the full facepiece was not as big as we observed with the half-mask. Again, this also can be explained by the leak size. As the full facepiece does not have nose leak, it is more comparable to a partially sealed half-mask rather than a fully sealed half-mask.

b. MIF effect on P_{cyclic}. The lowest MIF (30 L/min) produced the lowest penetration; as the flow increased, the penetration increased (p-value < 0.05). Since the penetration values were so low and closer to those expected from the filter material, one would suggest that the role of faceseal leakage pathway is not as great for the full facepiece elastomeric respirator if compared to the half-mask, and the particle deposition on the *filter* governs the process, at least to a significant extent. For ultrafine particles used in this study, the

primary filtration mechanism is diffusion. As the flow increases, the residence time decreases, and the diffusion becomes less effective. This explains the experimentally observed effect of MIF on the particle penetration.

2. Respirator Fully Sealed on the Manikin

The data obtained with the fully sealed full facepiece were similar to those obtained with the fully sealed half-mask. This is understandable because testing of a fully sealed respirator (both half and full facepiece) is essentially equivalent to examining the performance of the respirator filter (with an exhalation valve attached). As the same type of filter was used for the half and full facepiece respirators, there was no significant difference in the filter efficiency. The results are consistent with the fact that the efficiency of a P100 filter is 0.03% or below at 85 L/min.

Data obtained with the UC UFP counter versus the TSI CPC 3007

The penetration values obtained from the measurement of aerosol concentrations inside and outside of the two respirators (half and full) by UC UFP counter and TSI CPC operating in parallel are plotted in Figure 1-4. The figure contains all data collected for all tested conditions. A favorable agreement is seen (slope ≈ 1.16, $R^2 \approx 0.99$; paired *t*-test, *p*-value = 0.91), suggesting that the new counter, once miniaturized to serve as a field compatible personal sampling device, can produce meaningful data comparable to a conventional TSI CPC instrument. Given the data variability (specifically two clusters at penetration around 0.1% and 1% as measured by the TSI CPC), a follow-up study is warranted to improve the sensitivity and stability of the UC UFP.

Limitations

The HEPA filter (supposed to mimic the respiratory tract) placed between the headform and the breathing simulator removed all particles, which passed through the manikin's mouth during the inhalation and exhalation cycles, whereas in real life situation only a fraction of particles is captured inside the respiratory tract (determined by the respiratory deposition curve). The above represents a difference between the manikin-based and human subject-based measurement protocols, although the former seems to better represent the actual penetration of particles from the breathing zone into the respirator. Additionally, there is a dead space between the respirator and the HEPA filter. Given that the tubing volume between the respirator and the HEPA filter is 0.038 L [length ~30 cm; diameter = 1.27 cm (0.5″)] and the respirator dead space is ~0.2 L, the total dead space volume is ~0.238 L. As the tidal volume of the breathing machine ranges from 1 to 2.7 L, some particles may be trapped inside the dead space especially at the lowest breathing rate (1 L/min), suggesting that the tubing/respirator volume may have an effect on the particle concentration inside the respirator. However, this effect is likely insignificant considering the difference between the total dead space and the tidal volume. The above limitations also apply to studies II, III and IV.

Conclusions

Two elastomeric respirators (half-mask and full facepiece) were evaluated as to the overall particle penetration with respect to faceseal leakage, breathing flow type and rate, and combustion material. All these factors were found to have significant impact on the performance of the respirators. The total penetration through the fully sealed half and full facepiece respirators did not exceed the NIOSH certification level established for P-100 respirator filters (<0.03%).

Increasing leak size increased total penetration. Effects of combustion material and breathing flow were significant and heavily dependent on sealing condition. The results suggest that eliminating or minimizing the faceseal leakage is the key aspect for improving the efficiency of elastomeric respirators used by firefighters against combustion particles regardless of particle composition and size distribution.

Significant difference in penetration was found between cyclic and constant flow; however, this difference was mainly observed for the unsealed half-mask. For the half-mask (fully sealed) and full facepiece (unsealed or fully sealed), the penetration remained the same when challenged with three different combustion aerosols (wood, paper and plastic). While under sealing conditions such as “nose-only”, “nose & chin”, and “unsealed”, the combustion material did show a significant effect on the total penetration for the half-mask. This effect was not consistent – plastic aerosol produced the highest penetration under the unsealed condition, whereas for the two partial sealing conditions wood aerosol was associated with the highest penetrations.

This study provides meaningful information related to the NIOSH respirator testing program in accordance with Title 42 of the Code of Federal Regulations, Part 84. The results indicate that the efficiency of a P-100 respirator filter is not significantly influenced by the challenge aerosol and the flow type (constant versus cyclic). This supports the approach implemented in the current NIOSH respirator testing of P-100 filters that utilizes a non-combustion challenge aerosol and constant air flow. However, the NIOSH total inward leakage (TIL) test assumes that the result is independent on the type of the tested aerosol, while this study revealed that the challenge aerosol significantly affects the particle penetration through unsealed and partially sealed half-mask elastomeric respirators. The differences between the currently

utilized challenge(s) and actual combustion aerosols are concerned with the particle shape, density, electric charge, and possibly other properties. The findings generated by the presently adopted TIL test protocol (utilizing ambient or NaCl model aerosols) may have limitations in predicting protection levels offered by half-mask elastomeric respirators.

One limitation of this study is that a stationary (non-moving) manikin headform was used. It is acknowledged that this type of headform is not capable of mimicking human speaking, head movements, or facial expressions, which could affect the leak size. We believe that the next step in testing the elastomeric half-mask and full facepiece respirators could involve robotically articulating headforms.

CHAPTER 2

Laboratory Evaluation of the Particle Size Effect on the Performance of an Elastomeric Half-mask Respirator against Ultrafine Combustion Particles (Specific Aim 2)

Introduction

The US Bureau of Labor Statistics has reported that firefighting ranks among the most dangerous occupations in the United States (BLS, 2003). Firefighters are known to have respiratory problems due to smoke inhalation resulting from combustion (Musk *et al.*, 1982; Materna *et al.*, 1992; CDC, 2006). First responders as well as other workers exposed to combustion aerosols are at a similar health risks as firefighters although their associated health effects are not as well documented. Smoke generated from a fire consists primarily of fine ($\leq$ 1μm) and ultrafine ($\leq$ 0.1 μm) particles. These smoke particles contain a variety of reactive free radicals and other chemical compounds, which pose a potential health risk (Leonard *et al.*, 2007). Baxter *et al.* (2010) reported more than 70% (by number) of smoke particles present during fire knockdown and overhaul are ultrafine. With an increase in surface area, ultrafine particles can be toxicologically more reactive than those of larger sizes (Lam *et al.*, 2004; Shvedova *et al.*, 2005).

During fire overhaul (after the fire has been extinguished), firefighters enter the structure to examine areas for possible re-ignition. At that stage, it has been reported that firefighters may use elastomeric half-mask respirators equipped with a highly efficient P-100 filters (Bolstad-Johnson *et al.*, 2000; Burgess *et al.*, 2001). When subjected to the National Institute for Occupational Safety and Health (NIOSH) respirator certification test, a P-100 filter must provide at least a 99.97% efficiency when challenged to polydisperse dioctyl phthalate (DOP) particles

having a count median diameter (CMD) of 185±20 nm and a geometric standard deviation (GSD) of <1.60 (Shaffer *et al.*, 2009).

Numerous studies have been conducted to determine the filter efficiency of commercially available respirators (Martin *et al.*, 2000; Eninger *et al.*, 2008; Eshbaugh *et al.*, 2008; Rengasamy *et al.*, 2008; Rengasamy *et al.*, 2009). However, the respirator performance is affected not only by the filter efficiency but also by the faceseal leakage. Furthermore, several studies have shown that particle penetration through the faceseal leakage may be much higher than through the filter media (Coffey *et al.*, 1998; Zhuang *et al.*, 1998; Grinshpun *et al.*, 2009; Cho *et al.*, 2010b). To account for these two penetration pathways, NIOSH has proposed the total inward leakage (TIL) method for testing respirators (NIOSH, 2009). However, the NIOSH TIL test does not consider particle size, as it is based on non-size-selective measurement. TIL was investigated as a function of particle size (aerodynamic size: 0.04–1.3 μm) in our previous research performed with N95 respirators and surgical masks (Lee, Grinshpun, *et al.*, 2008a). The lowest protection factors (PFs) were observed in the size range of 0.04–0.2 μm (which includes the ultrafine fraction). Faceseal leaks on one brand of half-mask respirator (US Safety Series 200 Half-mask) worn by 73 subjects were studied by Oestenstad and Perkins (1992). They found respirator leakage was strongly affected by leaks at the nose and chin, and consideration should be given to including nasal dimensions when selecting a respirator for an individual wearer. Our recent study with a half-mask respirator tested on a breathing manikin revealed that the nose was the primary leak site (He *et al.*, 2013).

There are no data available about the ultrafine particle penetration through faceseal leaks of elastomeric respirators even for a relatively simple case when the breathing flow rate is assumed to be constant. It is much more complex to quantify the particle penetration under

actual breathing conditions (when the air flow through a respirator is not constant but has a cyclic nature). Early researchers addressed the effects of faceseal leakage on the particle penetration (Hinds and Kraske, 1987; Chen *et al.*, 1990; Chen *et al.*, 1992). A recent study conducted by Rengasamy and Eimer (2011) investigated the TIL of nanoparticles through Filtering Facepiece Respirators (FFRs), and reported that penetration increased with increasing leak size. With smaller size leaks (< 1.65 mm), the penetration values measured for 50 nm size particles were ~2-fold higher than the values determined for 8 and 400 nm size particles. However, the quoted studies were conducted using either constant flow or artificially induced leaks. Cho *et al.* (2010b) investigated a more realistic faceseal leakage by partially sealing a N95 respirator on a manikin face with breathing patterns simulated (as a sinusoidal function) by a breathing simulator. That paper showed that most of particles penetrated into the respirator through the faceseal leakage, rather than through the filter. A similar conclusion was drawn by Grinshpun *et al.* (2009) for a N95 FFR and a surgical mask.

Different challenge aerosols (non-biological and biological) have been utilized for various respiratory protection research including NaCl, Ag, DOP and viruses (enterobacteriophages MS2, T4 and Bacillus subtilis phage) (Bałazy, Toivola, Adhikari, *et al.*, 2006; Huang *et al.*, 2007; Eninger *et al.*, 2008; Shaffer *et al.*, 2009; Cho *et al.*, 2010a; Rengasamy *et al.*, 2011). In most of the previous respirator evaluation studies the challenge aerosol was charge neutralized/equilibrated. To our knowledge, besides our latest investigation (He *et al.*, 2013), no peer-reviewed published study has yet reported respirator performance using combustion aerosols which likely have different charge, shape, and density.

The present investigation is a follow-up to the study of He *et al.*, (2013) performed with challenge aerosols originating from the combustion of wood, paper, and plastic. Similar to our

earlier study, the present investigation aims at testing the performance of an elastomeric half-mask respirator; however, a distinct difference is that the current experimental design includes particle size as an independent variable. Accordingly, a particle size selective measurement technique was deployed in this effort to characterize the effect of particle size along with other factors such as inhalation flow, combustion material, and faceseal leakage on the efficiency of a half-mask respirator.

Materials and Methods

Respirator and challenge aerosols

In this study an elastomeric half-mask respirator was tested, which is widely used by firefighters during fire overhaul. This type of respirator is also commonly used by first responders and other workers exposed to combustion aerosols. The model selection was also influenced by feedback from the Cincinnati Fire Department, which indicated that their firefighters frequently wear elastomeric 3M 6000 series half-mask respirators with P-100 filters for medical responses and fire overhaul. Based on this rationale, a medium size 3M 6000 series half-mask respirator equipped with two 3M 2091 P-100 filters was chosen for this study. This same make and model was tested in our latest study on the overall (non-particle-size-selective) particle penetration (He *et al.*, 2013).

Three combustion aerosols were generated by burning the following materials inside a test chamber: wood (24 cm BBQ long matches, 1.9±0.5 g), paper (23 cm ×24 cm brown multifold paper towel, 2.1±0.2 g), and plastic (23 cm ×20 cm Ziploc^{TM} sandwich bags, single layer, 1.7±0.3 g). Wood, paper and plastic were selected to represent common sources of combustion particles in the environments encountered by firefighters and first responders. It is

noted that aerosol particles originated by combustion are usually highly charged; unlike many earlier investigations, no charge neutralization or equilibration was conducted in this study in order to preserve the original properties of combustion particles.

Study design and experimental set-up

The experiments were carried out in the University of Cincinnati indoor testing chamber (volume = 24.3 m^3). The experimental set-up is presented in Figure 2-1.

In each experiment, the elastomeric half-mask respirator was donned on a breathing manikin and challenged with one of the three test combustion aerosols. Tests were conducted at three cyclic flows, with mean inspiratory flows (MIFs) of 30, 85, and 135 L/min. These flows represent breathing at medium, high and strenuous workloads (Lafortuna *et al.*, 1984; Anderson *et al.*, 2006). The cyclic breathing was simulated by a Breathing Recording and Simulation System (BRSS, Koken Ltd., Tokyo, Japan). The BRSS consists of an electromechanical drive-cylinder and two air cylinders connected to each other. A sinusoidal air flow is generated as the electromechanical cylinder moves back (inspiratory duration, half a period) and forth (expiratory duration, half a period) (Haruta *et al.*, 2008). The cylinder moving distance simulates the human tidal volume. By adjusting the speed and distance of the cylinder, the breathing frequency was set at 25 breaths/min for all three cyclic flows. Choosing the same breathing frequency for all cyclic flows eliminated frequency as an additional variable from the study design.

To examine the effect of the faceseal leakage on the performance of the respirator, three sealing conditions, namely “fully sealed”, “partially (nose area) sealed”, and “unsealed”, were established. A silicone sealant was applied to the respirator when it was necessary to seal the facepiece to the manikin. The fully sealed condition essentially targeted the efficiency of the P-100 filters installed on the half-mask respirator assuming no penetration through the exhalation

valve. The unsealed and partially sealed conditions permitted evaluation for both penetration pathways: filter penetration and faceseal leakage. Several studies have reported that faceseal leakage occurs mostly in the nose and chin area (Holton *et al.*, 1987; Crutchfield *et al.*, 1997; Oestenstad *et al.*, 2007; Oestenstad *et al.*, 2010). Our previous study (He *et al.*, 2013) showed that there was no significant difference between two conditions "nose-only sealed" and "nose & chin sealed" in terms of the penetration level for the same half-mask respirator. Based on this rationale, only one partially sealed condition – a nose area seal – was chosen for this study (the length of the seal was 12.7 cm, which is approximately 30% of the 40.6 cm total respirator sealing length).

For each combination of the test conditions, the experiment was repeated four times. The particle concentrations outside and inside of the respirator were measured size-selectively using a recently developed Nanoparticle Spectrometer (Model: Nano-ID NPS500, Naneum Ltd., Kent, UK). To sample from inside the respirator, the half-mask was probed between the nose and upper lip of the manikin using the TSI Model 8025-N95 Fit Test Probe Kit. The Nano-ID is capable of measuring an aerosol particle size distribution over a range of mobility diameters (an equivalent diameter of a spherical particle of the same mobility, Kulkarni *et al.*, 2011) from 5 to 500 nm (referred to as a scan range). The particle counts are recorded in up to 128 user-selectable channels at a sampling flow rate 0.2 L/min, which is sufficiently low (compared to the breathing flow 30 – 135 L/min) and, therefore, is unlikely to cause significant influence in the measured particle concentration inside the respirator. Myers *et al.* (1988) stated that biased sampling often occurs because aerosol does not mix well within the respirator cavity during the inhalation phase of the respiratory cycle. To minimize the effect of non-homogeneity of the concentration inside the respirator resulting from poor mixing, a 3-minute scan time was chosen

for each measurement; this time allows integrating many cycles in one measurement, e.g., as many as 75 cycles in 3 minutes at 25 breaths/min.

The particle penetration (through both pathways) was determined for each particle size (d_p) as the ratio of inside and outside concentrations:

$$P(d_p) = \frac{C_{in}}{C_{out}} \times 100\% \quad \textbf{(2-1)}$$

Data analysis

For each combination of experimental conditions, the mean value of the total penetration and the standard deviation were calculated from the four replicates. One-way analyses of Variance (ANOVA) was performed to quantify the effect of sealing condition on the particle penetration, and three-way ANOVA was used to study the significance of combustion material, breathing flow and particle size using SAS version 9.2 (SAS Institute Inc., Cary, NC). *P*-values of < 0.05 were considered to represent significant differences in the outcomes.

Results and Discussion

Particle size distribution of challenge combustion aerosols

Figure 2-2 shows the particle size distributions of the three combustion aerosols measured at 10, 30, 50, 70, and 90 minutes after the burning stopped. Each aerosol produced a single-mode distribution. The peak concentrations occurred in the mobility diameter range of 40 to 80 nm for wood and paper combustion aerosols, whereas the peaks shifted slightly toward a larger size range (50 to 100 nm) for plastic combustion aerosols.

The majority of particles detected by the Nanoparticle Spectrometer fell between 20 and 200 nm. This is in a good agreement with the above quoted findings of Baxter *et al.* (2010), who

suggested that the scan range could be narrowed down. In addition to a better representation of the challenge aerosol, a narrower scan range improves the instrument performance in a specific time interval (by providing a more accurate particle count per channel). Accordingly, the size range of 20–200 nm discriminated through 30 scan channels (representing 30 particle size fractions) was selected. The above choice was consistent with an important aim of the particle size selective sampling – to identify the most penetrating particle size (MPPS).

The natural decay of airborne particle concentration was found to be dependent on particle size. It is seen in Figure 2-2 that the natural decay was very slow for wood and paper combustion particles above 80 nm, and plastic combustion particles above 100 nm. The slower decay for larger particles can be explained by weakening diffusion as well as continuous coagulation (Kulkarni *et al.*, 2011). The curves demonstrate a pronounced concentration decrease during approximately the first 50 min, which slowed down afterwards. On average, approximately 40% of particles remained airborne after 90-minutes. This assured a sufficient number of particles available for counting in each Nano-ID channel.

Fully sealed half-mask respirator with P-100 filters

The fully sealed respirator prevented particles from penetrating through the faceseal leakage. Therefore, total particle penetration equals filter penetration ($P = P_{filter}$) assuming no penetration through the exhalation valve. A separate experiment was conducted to test the assumption that exhalation valve operated properly, thus introducing no additional pathway for particles to penetrate inside the respirator. In this experiment, the same respirator with a functional exhalation valve was compared to a sealed valve. The penetration was determined at a constant flow of 135 L/min as well as at a cyclic flow of MIF=135 L/min. For either flow conditions, no significant difference in the penetration values was found. The results confirmed

that the exhalation valve had no influence on particle penetration, which supports the fundamental postulate of our study design of only two particle penetration pathways (filter and faceseal).

Figure 2-3 presents the particle penetration values for the fully sealed half-mask respirator equipped with two P-100 filters challenged with particles aerosolized by wood combustion. Our previous study (He *et al.*, 2013) conducted with an identical fully sealed half-mask indicated that the effect of combustion material on the particle penetration was not significant (*p*-value > 0.05); therefore, only one combustion material (wood) was tested here. Except for a few points obtained at 135 L/min, all the other values were below 0.005% regardless of the particle size and flow rate. The two peak points that occurred at the lower (~30 nm) and higher (~180 nm) sizes could be outliers as there were not sufficient number of particles (C_{out} <10,000 particles/channel, C_{in} <1 particle/channel) generated at those two sizes especially after 90 minutes measurement (see Fig. 2, Wood Aerosol). However, even if these two peaks were considered as valid data points, the maximum filter penetration would still fall below 0.025% (Fig. 3). Overall, the results demonstrate that the tested P-100 filters exhibited the efficiency levels exceeding the NIOSH certification requirement (P ≤0.03%). This finding is in agreement with our earlier results obtained using a non-particle-size-selective aerosol measurement technique (He *et al.*, 2013). Several other studies also reported similarly low particle penetration for P-100 filters (Eshbaugh *et al.*, 2008; Rengasamy *et al.*, 2011).

Partially (nose area) sealed half-mask respirator with P-100 filters

Figure 2-4 presents the particle penetration data for partially sealed half-mask with two P-100 filters, which was tested at three MIFs (30, 85, and 135 L/min) while exposed to three combustion aerosols (wood, paper and plastic). Data analysis revealed that combustion material

and particle size had a significant effect on penetration values (p<0.001). For all three materials, the highest particle penetration values occurred at 85 L/min throughout the entire tested particle size range (20 to 200 nm) except for the first channel; the 135 L/min flow generated the second highest penetration levels followed by 30 L/min. All penetration values obtained with the three combustion aerosols were approximately between 0.05% and 0.7% except a few points obtained for smaller particles at 30 L/min. Insufficient number of particles detected by the Nanoparticle Spectrometer (C_{out} <1,000 particles/channel, C_{in} <1 particle/channel) prevented us from reporting penetration values for plastic particles between 20 and approximately 30 nm (see Fig. 2, Plastic Aerosol).

Compared to the fully sealed test condition, even the lowest penetration values obtained for the partially sealed half-mask at 30 L/min were at least 10-fold greater, regardless of flow rates (30, 85, and 135 L/min). This shows that any additional faceseal leakage can substantially compromise the protection offered by a half-mask respirator.

The penetration curves obtained for wood and paper combustion aerosols were of similar shapes. While not perfectly monotonic, the curves showed an overall increase of penetration with increasing particle size. For plastic combustion particles, the curves are slightly different from those found for wood and paper aerosols with the penetration reaching the maximum approximately at 120–160 nm at 85 and 135 L/min. One possible reason is that the particles generated by burning plastic, a synthetic material, may differ in composition and physical characteristics such as a charge, shape and density (see full explanations in Chapter 1 on page 21). It is also to be noted that the measurement of particles in this study was based on their electrical mobility (not an aerodynamic diameters), and there are no data, to our knowledge, that would allow establishing a relationship between the two, at least, for the challenge aerosol.

The order of curves in Figure 2-4 was somewhat unexpected: at the same particle size the penetration increased as the MIF increased from 30 to 85 L/min but then decreased as the flow continued rising from 85 to 135 L/min at MIF. In order to identify the flow rate(s) associated with the maximum particle penetration, four more cyclic flows (50, 70, 100 and 120 L/min) were added to the testing program for the partially sealed half-mask. This additional experiment was conducted using plastic combustion aerosol only. It is believed that the finding would have higher practical significance because plastic aerosol is comparatively more toxic and more health-relevant than the ones produced by burning wood or paper (UL, 2010). Thus, seven flows (30, 50, 70, 85, 100, 120, and 135 L/min) were tested at the same manikin breathing frequency (25 breaths/min) with four replicates for each flow. The experimental results are presented in Figure 2-5. The penetration values are shown for particle sizes of and above of 30 nm (as mentioned earlier, the count of plastic combustion particles below 30 nm was insufficient).

Firstly, the curves (upper section of Figure 2-5) corresponding to seven different MIFs are similarly non-monotonic. Although the trend is not completely clear for particle diameters up to 40–50 nm, all the curves indicated that penetration increased with increasing particle size up to approximately 100–140 nm (depending on the flow rate) and then decreased for larger particles. The flow rate of 85 L/min indeed appeared to be the one producing the highest penetration values when particle size was > 40 nm. The flow rate of 100 L/min produced the second highest penetration (the values are approximately the same compared to 85 L/min in the particle size range of 80 to 100 nm). Further increase in flow rate resulted in decrease in penetration. Results also showed the lowest penetration values at the lowest tested MIF (30 L/min). The following explanations are offered to address the flow effect: as the breathing flow increased from 30 to 85 L/min, more combustion particles were brought into the respirator cavity

(greater penetration) while the outside concentration remained unchanged. However, it is anticipated that at higher flows (>85 L/min) the negative pressure inside the respirator during inhalation became sufficiently high to suck the respirator toward the face of the manikin and consequently reduce faceseal leak size. In turn, a smaller leak could correspond to a lower relative contribution of the total air flow entering the facepiece, resulting in penetration of fewer particles. During exhalation, exhaled air is released primarily through the exhalation valve (rather than the faceseal leakage or filters) of the half-mask respirator so that a higher flow should not substantially increase the leak size during exhalation.

Secondly, the lower section of Figure 2-5 shows the particle penetration as a function of MIF at four particle sizes (52, 83, 104 and 153 nm) that were selected to fairly represent the entire scan range. This figure conveys that the particle penetration was largely dependent on the cyclic breathing flow, with the highest penetration values occurred at the MIF = 85 L/min. As particle size increased from 52 nm to 104 nm, the penetration values showed a clear increasing trend regardless of the flow rate. However, penetration values obtained at the larger particle size (153 nm) were close to or higher than those acquired at 104 nm (depending on the flow rate). This indicates that the MPPS for this partially sealed half-mask (nose area only) was within a size range of approximately 100 to 160 nm when challenged to plastic combustion aerosols.

Unsealed half-mask respirator with P-100 filters

The findings for the unsealed half-mask are presented in Figure 2-6. The ANOVA results showed that both particle size and material type had strong significant effects ($p<0.001$) on the particle penetration. The penetration values ranged from 4% to 8% for wood aerosol, from 3% to 10% for paper aerosol, and from 3% to 16% for plastic aerosol. Plastic aerosol produced higher penetration values for particles between 100 and 200 nm as compared to wood and paper

combustion aerosols. This finding is important in light of previously published evidence that combustion of plastic generates toxic particles that may be associated with human health effects (Linak *et al.*, 1989; Wong *et al.*, 2007).

The average penetration of the unsealed half-mask respirator exceeded that of fully sealed respirator by a factor of more than 100, given that most of penetration values obtained for the fully sealed half-mask were below 0.05% (see Figure 2-3). Therefore, more than 99% of particles entering the unsealed half-mask respirator cavity penetrated through faceseal leakage (not through the P-100 filter media). This finding is consistent with the conclusions presented in He *et al.* (2013) for the same type of respirator based on total particle concentration measurement (not size-selective).

For plastic aerosol, the size of particles most readily penetrating through faceseal leakage fell in a range of 120–140 nm for all three MIFs, whereas it is difficult to determine the MPPS for wood and paper aerosols as the penetration curves do not show clear peaks in the particle size range of 20 to 200 nm. Many previous studies on respirator filter efficiency have reported the MPPS for tested filters (Brown, 1993; Martin *et al.*, 2000; Grafe *et al.*, 2001; Bałazy, Toivola, Adhikari, *et al.*, 2006; 2006; Eninger *et al.*, 2008). However, there are very limited data available on the MPPS for respirator faceseal leakage. Rengasamy and Eimer (2011) reported that the MPPS for a cylindered leak (<1.65 mm diameter) was ~50 nm. It is commonly assumed that size and location of faceseal leakage are constantly changing during breathing, talking, and head/body movement (Myers *et al.*, 1996), which contributes to additional variability when trying to determine the MPPS. Additional challenge is that the MPPS can be affected by aerosol type as shown in this study.

Unlike the fully sealed condition, an unsealed respirator involves two primary particle penetration pathways (filter media and faceseal leakage). While numerous studies have addressed the effect of breathing flow on the filter efficiency (e.g., increasing flow rate was shown to promote higher penetration of ultrafine particles due to diffusion) (Bałazy, Toivola, Adhikari, *et al.*, 2006; 2006; Eninger *et al.*, 2008; Rengasamy *et al.*, 2011), it is less certain how the breathing flow affects the faceseal penetration. Interestingly, several published FFR studies have documented that faceseal penetration decreased with increase in breathing flow when challenged with particles above 500 nm (Chen *et al.*, 1990; Huang *et al.*, 2007; Cho *et al.*, 2010b). On the other hand, another FFR evaluation effort failed to observe significant increase or decrease in faceseal penetration when increasing the breathing flow (Rengasamy and Eimer, 2011) for particles ranging from 8 to 400 nm. In our study, increasing flow seemed to decrease particle penetration through the faceseal leakage, and such effect was most dominant for plastic aerosol and particle size of >100 nm (see Fig. 6). It is acknowledged that our study tested a different respirator (elastomeric half-mask) with different challenge aerosols compared to the three studies referenced above.

To interpret the above finding (faceseal penetration decreases with increasing flow rate), an experiment with breathing flow held constant was conducted. The same unsealed half-mask was tested using three constant flow rates (30, 85, and 135 L/min) while challenged with plastic aerosol. The results are shown in Figure 2-7. First, constant inhalation flow produced much higher penetration values than cyclic flow. Peak penetration was close to 50% for a constant flow rate of 30 L/min (Figure 2-7) as compared to 16% for cyclic flow of the same MIF (Figure 2-6); similar trends were observed for 85 and 135 L/min. These differences were explained in our previous study (He *et al.*, 2013). The important finding is that increasing constant flow was

generally associated with a decrease in particle penetration (with the exception of data obtained at 85 versus 135 L/min for larger particles). Due to the high efficiency of the P-100 filter, the total particle penetration through the half-mask elastomeric respirator is almost fully determined by the number of particles penetrating through faceseal leakage. Most of tested particles are small enough to have their motion governed primarily by diffusion and electrostatics. Assuming that (a) the exhalation valve provides a perfect seal, (b) the particle loss inside the faceseal leakage is negligibly small, and (c) the capture efficiency of the P-100 filter is close to 100%, the total particle penetration (P_{Total}) into a respirator is determined by the relative contributions of the air flows through the filter and the leakage (He *et al.*, 2013):

$$P_{Total} \approx 1 - \frac{Q_F}{Q} = \frac{Q_L}{Q} \times 100\% \qquad \textbf{(2-2)}$$

Where Q_F is the constant air flow through filter media, Q_L is the constant air flow through faceseal leakage, and $Q = Q_F + Q_L$ is the constant total flow. If the respirator is equipped with an absolute filter, the penetration value calculated by Eq. (2-2) can be considered as maximum possible particle penetration.

Depending on the position of the respirator and the tightness of the straps, the gap between the respirator and the face of the manikin is likely variable. In our experiment, the most sizeable leakage (~1 mm) was observed around the nose area. However, in areas around the chin and cheeks the faceseal leakage could be 0.1 mm or lower. According to the classic particle diffusion theory (Kulkarni *et al.*, 2011), the particle losses inside a 1-mm gap are estimated to be negligibly low (with the Brownian displacement of ~0.01 mm). At the same time, the diffusional deposition inside a 0.1 mm gap is not negligible, especially for particles below ~50 nm. Larger particles (well above 50 nm) are not subjected to appreciable diffusional deposition, but some of

them may carry substantial electrical charges, which could cause losses inside the faceseal leakage and consequently decrease the particle penetration. This effect is expected to be more pronounced as the particle size increases (further increase of the particle size adds interception and impaction losses). The above explains the non-monotonic curves shown in Fig. 7. The MPPSs ranging approximately from 70 to 90 nm (depending on the flow rate) represent the condition when the particles are too large for substantial diffusional losses inside the leakage but at the same time too small to expect notable deposition due to electrostatic mechanism, interception, and impaction. In these cases, the penetration is close to the theoretically maximum level, Q_L/Q [Eq. (2-2)]. These thresholds are shown in Fig. 7 for each of the three flow rates as straight lines.

The proportion of total flow through the faceseal leakage was experimentally determined for an unsealed half-mask donned on the manikin under the constant flow condition. This was done as follows. First, the respirator was fully sealed on the manikin, and the air flow was established (entirely through the filter in absence of the faceseal leakage). By adjusting the speed of a vacuum pump, seven constant flow rates (Q_F) ranging from 10 to 100 L/min were achieved and the seven corresponding static pressures (pressure drop) were recorded. Second, an unsealed respirator was donned on the manikin with both P-100 filters removed and all inhalation openings fully covered to allow the air pass solely through the leakage. Using the same pre-recorded static pressures, seven flow rates (Q_L) were established by adjusting the vacuum pump. Subsequently, the seven total flow rates were calculated ($Q = Q_F + Q_L$, see Fig. 8 for the seven tested Q-values marked as black dots).

The relationship between Q_L/Q and total flow Q is plotted in Figure 2-8. The graph reveals that Q_L/Q values decreased along with increasing total flow rate. As indicated above, this

likely occurred due to high negative pressure inside of the respirator that sucks it towards the manikin surface, thus reducing the faceseal leakage and producing higher flow resistance, which, in turn, reduced the proportion of total flow (Q_L/Q) passing through the leakage. Increase in total flow decreased the slope of the curve shown in Figure 2-8. At a total flow of 30 L/min, the ratio of Q_L/Q was as high as 53%, which, based on our theoretical considerations presented above, was supposed to produce $P_{Total} \approx Q_L/Q = 53\%$ (see Figure 2-7, the 53% straight line). Similarly, when the total flow was 85 and 135 L/min, the Q_L/Q was 38% and 33%, respectively.

The above explanations can be applied to a more complex case of the cyclic flow regime, which – in contrast to the constant flow – exhibits both inhalation and exhalation. During exhalation, particle concentration inside the respirator is diluted by the purified exhalation air (in our experimental set-up, a HEPA filter installed between the manikin and the breathing simulator). At the same time, the particles cannot be entirely removed from the respirator cavity as there are always particles trapped inside the respirator after exhalation. Thus, the particle penetration obtained under the cyclic flow regime is expected to be lower than those obtained under the constant flow regime (see a more detailed explanation in He *et al.*, 2013). However, the effects of the flow rate on the faceseal penetration remained the same for both constant flow and cyclic flow regimes – higher flow associated with lower penetration, which was proven by the theoretical calculation (Eq. 2-2) combined with the flow measurements (Fig. 8). No previously published studies were found to address the flow type (cyclic vs. constant) effect on the total inward leakage for the elastomeric half-masks.

Conclusions

Performance of the elastomeric half-mask respirator was significantly affected by the particle size ($p < 0.001$). When testing the partially sealed half-mask, the highest penetration was detected at 180 nm for wood and paper combustion aerosols, and at around 120 to 160 nm for plastic aerosol. Under the unsealed conditions, the peak penetration occurred at 120 nm for plastic combustion aerosol while no clear peaks were identified for wood and paper. Results suggest that the MPPS for the faceseal leakage was >100 nm for the partially sealed and unsealed conditions when challenged with plastic aerosol. The partially sealed (nose area only) half-mask respirator resulted in 10-fold lower penetration levels when compared to the unsealed condition. This suggests that the nose area was a primary leak site.

Material type was another significant factor ($p<0.001$). For the unsealed half-mask challenged with plastic combustion aerosol, higher penetration values were observed as compared to wood and paper aerosols for particles >100 nm.

The effect of cyclic flow rate was found to be significant as well ($p<0.001$). For the partially sealed respirator, increasing flow rate was associated with an increase in penetration up to MIF = 85 L/min. For higher flow rates, the trend changed to a decrease in penetration as the flow increased. For unsealed conditions, increasing flow rate resulted in consistent decrease of penetration and this trend was most apparent for the plastic aerosol with size >100 nm.

One major limitation of this study is that a hard plastic manikin headform was used, which was not capable of mimicking the texture and softness of human skin. This may potentially create larger leaks for equivalent strap tension. An advanced headform covered with soft skin-like material may be considered as an appropriate alternative in future studies. Only one

model of the elastomeric half-mask was tested, which also represents a study limitation. Additionally, it is acknowledged that all the cyclic flows tested in this study used the same breathing frequency (25 breaths/min), which may not fully represent the real world situation. Future studies are needed to investigate the effects of the breathing frequency on the performance of respiratory protection devices.

CHAPTER 3

Effect of Breathing Frequency on the Total Inward Leakage of an Elastomeric Half-Mask Donned on an Advanced Manikin Headform (Specific Aim 3)

Introduction

The U.S. Occupational Safety and Health Administration (OSHA) requires respirators be provided to employees whenever engineering and work practice control measures are not adequate to reduce the employees' exposure to acceptable levels (OSHA, 2006). Among the non-powered air purifying respirators, filtering facepiece respirators (FFRs) are the most commonly used respiratory protection devices (share = 49%) followed by elastomeric half-masks (34%), according to the survey conducted in private industry by the U.S. Bureau of Labor Statistics (BLS) and the National Institute for Occupational Safety and Health (NIOSH) (BLS/NIOSH, 2003).

Smoke from a fire contains primarily ultrafine particles (< 0.1 μm). The latter were found to account for more than 70% of airborne particles (by number) measured in a large-scale fire test laboratory study (Baxter *et al.*, 2010). Exposure to ultrafine particles has been associated with impairment of cardiovascular function and other adverse health outcomes (Schwartz *et al.*, 1996; Peters *et al.*, 1997; Timonen *et al.*, 2005; Schulte *et al.*, 2008).

Many studies have evaluated the most penetrating particle size (MPPS) (Martin *et al.*, 2000; Grafe *et al.*, 2001; Bałazy, Toivola, Adhikari, *et al.*, 2006; 2006; Eninger *et al.*, 2008; Rengasamy *et al.*, 2008; Cho *et al.*, 2010a) of NIOSH-certified N95 FFRs. These studies consistently report a MPPS in a range of 30 to 100 nm. Elastomeric half-masks, which offer the

benefits of reusability, improved face seal, and enhanced user seal check capability – and can be decontaminated multiple times – (Roberge *et al.*, 2010), have not been studied as extensively as N95 FFRs. One study involving three half-masks and 10 FFRs tested on a panel of 10 human subjects concluded that the performance of elastomeric half-masks was better than that of FFRs (Han *et al.*, 2005). Another study (Lawrence *et al.*, 2006) involving a panel of 25 subjects with varying face sizes reported superior performance of elastomeric N95 half-masks (15 models tested) over N95 FFRs (15 models tested) and surgical masks (6 models tested). However, these investigations used non-size-selective aerosol measurement devices that did not allow exploring potential differences in penetration by different particle sizes, and none of these studies studied the effect of breathing frequency.

Respirator filter efficiency is significantly affected by breathing flow rate. This has been demonstrated for mechanical and "electret" filters tested under constant and cyclic flow conditions (Chen *et al.*, 1990; Brown, 1993; Qian *et al.*, 1998; Martin *et al.*, 2000; Bałazy, Toivola, Reponen, *et al.*, 2006; Huang *et al.*, 2007; Eninger *et al.*, 2008; Rengasamy *et al.*, 2008; Rengasamy *et al.*, 2009; Cho *et al.*, 2010b). A constant inhalation flow rate of 85 L/min is currently used in the NIOSH respirator certification program (NIOSH, 1995); however, constant flow does not accurately represent human breathing patterns. Stafford *et al* (1973) reported that human breathing is more reasonably approximated by a sinusoidal waveform, which can be better approximated with different flow rates and breathing frequencies (breaths/min) (Haruta *et al.*, 2008). Breathing frequency differs between population groups (e.g., healthy vs. sick, young vs. old) and is significantly affected by the level of physical activity (e.g., rest vs. active) (Tortora *et al.*, 1990; Sherwood, 2006). Several studies using cyclic flow, have reported an effect of flow rate on filter efficiency and faceseal leakage (Myers *et al.*, 1991; Eshbaugh *et al.*,

2008; Haruta *et al.*, 2008; Cho *et al.*, 2010b). However, with the exception of Wang et al. (2012) no published study has yet fully addressed the effect of the breathing frequency. Wang *et al.* (2012) did investigate two breathing frequencies (32 and 50 breaths/min) with a single MIF (100 L/min), but the data generated in their study were too limited to draw conclusions about breathing frequency. Furthermore, they selected a breathing frequency (50 breaths/min) that is excessive for most workplace populations.

Respiratory protection offered by negative pressure respirators is dependent not only on the filter efficiency but also on faceseal leakage (Zhuang *et al.*, 1998; Grinshpun *et al.*, 2009; Cho *et al.*, 2010b). To account for these two penetration pathways (filter and faceseal leakage), NIOSH has proposed the total inward leakage (TIL) method for testing respirators (NIOSH/CDC, 2009). Several studies addressed this issue by creating artificial slit-like or circular leaks to assess the faceseal leakage (Hinds and Bellin, 1987; Myers *et al.*, 1991; Chen *et al.*, 1992; Rengasamy *et al.*, 2011). However, artificial fixed leaks are not representative of actual conditions when a respirator is worn by humans. It is commonly assumed that size and location of faceseal leaks are constantly changing during breathing, talking, and head/body movement (Myers *et al.*, 1996). Some studies tested respirators worn by human subjects (Zhuang *et al.*, 1998; Grinshpun *et al.*, 2009) but these were, obviously, limited to a non-toxic challenge aerosol (NaCl). Comprehensive testing of respirator performance in a toxic aerosol environment and at higher challenge concentrations requires use of a manikin headform. Conventional static manikin headforms (either made of a rigid material or coated with a thin layer of rubber, plastic, or other compressible materials) have been shown in the literature to have high TIL levels for half-mask elastomeric respirators and filtering facepiece respirators (Cooper *et al.*, 1983; Tuomi, 1985; Golshahi *et al.*, 2012). These older type headforms do not simulate the properties of human facial

tissue (e.g., skin softness and local depth) which deforms under stress in ways that solid elastomers cannot simulate (Hanson *et al.*, 2007). To address this gap, an advanced manikin headform was developed that is capable of mimicking the softness and thicknesses of the human skin (Hanson *et al.*, 2006; Bergman *et al.*, 2013).

Aiming at testing the performance of elastomeric half-mask respirators challenged with combustion aerosols, this study is a follow-up to recent studies (He *et al.*, 2013a; 2013b) conducted in the same laboratory. The present study specifically addresses breathing frequency and flow rate as factors affecting TIL of an elastomeric half-mask respirator. The testing was conducted with respirators donned on an advanced headform that enables an adequate simulation of the human facial characteristics, which is crucial for measuring the TIL of a respirator. The advance manikin was challenged with three combustion aerosols: wood, paper and plastic.

Materials and Methods

Respirator

An elastomeric 3M 6000 series half-mask respirator equipped with two 3M 2091 P100 filters (3M Corp., St. Paul, MN, USA) was chosen for the testing to assure the continuity of our previous research (He *et al.*, 2013a; 2013b). The rationale for selecting the above respirator was described in detail in He *et al.* (2013a). An 11 mm long flush probe with a 14 mm diameter flange and a 4 mm diameter inlet was mounted on the surface of the respirator centerline between the manikin's nose and upper lip. The end of the probe (14 mm flange) was flush with the interior surface of the half-mask. The probe was located approximately 25 mm from the manikin's nose/mouth.

Challenge Aerosols

The challenge aerosols were separately generated by burning the following three materials inside a test chamber: wood (24 cm long and 0.4 cm diameter pellets, 1.9 ± 0.5 g), paper (23 cm × 24 cm brown multifold paper towel, 2.1 ± 0.2 g), and polyethylene (23 cm × 20 cm, 1.7 ± 0.3 g – further referred to as plastic) (He *et al.*, 2013a). Each material held by a caliper was ignited by a long reach lighter and completely burnt inside the chamber. All burnt materials were captured in a water-filled basin placed on the floor. The measurements were initiated 15 minutes after burning to allow the combustion aerosol to reach a spatial uniformity. As our previous measurements revealed that 90% of particles so generated were within the range 20 to 200 nm (He *et al.*, 2013a), we focused on this size range.

Advanced Manikin Headform

The specifications of the advanced manikin headform chosen for this study were reported in detail by Bergman *et al.* (2013). Briefly, the headform is of the medium size defined by the NIOSH Principal Component Analysis panel created using data from a large-scale anthropometric survey of U.S. workers conducted in 2003 (Zhuang *et al.*, 2007). A human-like skin with locally correct thicknesses was mounted on the headform skull. The material used to generate the skin is called Frubber™ (Hanson *et al.*, 2004), a fluid-filled cellular matrix composed of an elastomer that compresses, elongates and otherwise deforms in ways that simulates human skin (Hanson *et al.*, 2004).

Experimental Design and Test Conditions

The experimental set-up is shown in Figure 3-1. The respirator was donned on the advanced manikin headform, which was then challenged with one of three combustion aerosols (wood, paper and plastic). The donning was performed according to the manufacturer's user

instructions. After donning, the respirator was not re-donned or repositioned until the completion of the study, which allowed maintaining the size and shape of the faceseal leaks. Obviously, the static headform design did not allow fit testing of the respirator prior to the study. The P100 filters were changed after every 15 runs to minimize the effect of loading of combustion products on the filter media. The filters were changed carefully to minimize the effect of this procedure on the respirator faceseal leakage. After each filter change, the particle penetration was measured to assure that the size of the leak was consistent with the one existing before the change under the same experimental conditions. Temperature and relative humidity were kept at 17-22 ℃ and 30-50 %, respectively.

The headform was connected to a Breathing Recording and Simulation System (BRSS, Koken Ltd., Tokyo, Japan) with a HEPA filter placed in between to keep particles from re-entering the respirator cavity in exhaled air. The BRSS consists of an electro-mechanical drive-cylinder coupled with two air cylinders. As the electromechanical cylinder stroke moves back (inspiratory duration, half a period) and forth (expiratory duration, half a period), a sinusoidal air flow is generated (Haruta *et al.*, 2008). The stroke moving distance and frequency can be adjusted with a resolution of 0.1 mm and 0.01 Hz, respectively, thus allowing for precise changes to breathing flow rate and frequency when human breathing is simulated (Haruta *et al.*, 2008).

The test were conducted under three cyclic breathing flows (mean inspiratory flow – time weighted average flow rate over the width of an inspiration, MIF = 30, 55 and 85 L/min) and five breathing frequencies (10, 15, 20, 25 and 30 breaths/min). A completely randomized factorial study design was chosen with four replicates for each combination of the tested breathing flow rate and frequency. A summary of the experimental conditions is presented in Table 3-1.

Aerosol concentrations inside (C_{in}) and outside (C_{out}) the respirator were measured using a nanoparticle spectrometer (Nano-ID NPS500, Naneum Ltd., Kent, UK) size-selectively in 10 channels between 20 and 200 nm at a sampling flow rate of 0.2 L/min. Each concentration measurement took 3 minutes. The corresponding mean sizes for the 10 chosen channels were 22.4, 28.2, 35.5, 44.7, 56.2, 70.8, 89.1, 112.2, 141.3 and 177.8 nm. TIL was determined for each particle size (d_p) as the ratio of inside to outside concentration:

$$\mathrm{TIL}_{d_p} = \frac{C_{\mathrm{in},d_p}}{C_{\mathrm{out},d_p}} \times 100\% \quad \textbf{(3-1)}$$

In addition, by combining the 10 channels, size-independent (overall) TIL was calculated for all combustion particles ranging from 20 to 200:

$$\mathrm{TIL} = \frac{\sum_{i=1}^{10} N_{\mathrm{in},i}}{\sum_{i=1}^{10} N_{\mathrm{out},i}} \times 100\% \quad \textbf{(3-2)}$$

where N_{in} is the number of particles measured in a specific channel inside the respirator, N_{out} is the number of particles measured in a specific channel outside the respirator, and i is the i^{th} particle size channel.

Data analysis

Data analysis was performed using SAS version 9.3 (SAS Institute Inc., Cary, NC, USA). For the size-selective TIL, the effect of particle size was analyzed using the one-way analysis of variance (ANOVA) on the pooled data. Three-way ANOVA was used to study the significance of combustion material, breathing flow and breathing frequency for the size-independent TIL. One-way ANOVA was performed to quantify the effect of breathing frequency on the size-independent TIL after stratifying the data by the combustion material and breathing flow. All

pairwise comparisons were performed using Tukey's range test. *P*-values < 0.05 were considered significant.

Results and Discussion

Size-selective Total Inward Leakage (TIL_{d_p})

The size-selective TIL values determined within the chosen ten-channel size range are shown in Figure 3-2. The graphs represent three MIFs, five breathing frequencies, and three combustion aerosols (error bars are not shown as they make it difficult to see the data lines for each breathing frequency).

The reported TIL data were compared to the filter penetration data. The latter were obtained in our earlier study, which examined the performance of a fully sealed half-mask equipped with two P100 filters while challenged with wood, paper and plastic combustion particles of 20 to 200 nm (He *et al.*, 2013a). For most of the particle sizes, TIL was much greater than the filter penetration (< 0.03%) suggesting that the faceseal leakage was the primary particle penetration pathway for the tested elastomeric half-mask (an additional experiment was conducted to confirm that exhalation value did not leak).

The average size-selective TIL values obtained from this study were comparable to those reported in our previous study with a partially sealed (nose or nose-chin area) half-mask donned on a hard plastic manikin headform (He *et al.*, 2013a, 2013b), and 5~10-fold lower than those obtained with the unsealed half-mask donned on the plastic headform. This improvement can be attributed to the softness of the manikin skin, which deforms under stress, thus increasing the contact surface area and consequently forming a better seal.

Figure 3-2 demonstrates that particle size affected TIL_{d_p} ($p < 0.0001$) only for particles < 40 nm. For all three aerosols, the TIL_{d_p} values obtained at the lowest tested sizes, 20–40 nm, fell below those obtained at > 40 nm regardless of the breathing flow and frequency. This can be explained by the diffusional deposition which is more pronounced for smaller particles (consequently, a smaller fraction could penetrate inside the respirator more readily). For particles 40~50 nm and larger, the TIL_{d_p} curves showed no consistent increasing or decreasing trend. Furthermore, ANOVA results showed no significant differences in TIL_{d_p} ($p = 0.36$) among the six channels between 45 to 200 nm. The relatively flat curves obtained for the half-mask indicate a wide range for the MPPS. No TIL MPPS data were available in the literature for elastomeric respirators until our recent study (He *et al.*, 2013a), which measured an MPPS of 120–140 nm for the same half-mask donned on a plastic manikin headform and challenged with plastic combustion aerosol. The cited study did not detect an MPPS for wood and paper aerosols due to multiple peaks in the TIL_{d_p} curves. Previous TIL studies have focused on N95 FFRs or surgical masks, for which the particle size effect was found significant and the TIL values were close to the penetration levels observed for the filters only (Myers *et al.*, 1991; Cho *et al.*, 2010a; Rengasamy *et al.*, 2011). At the same time, little information has been generated with respect to the MPPS for faceseal leakage. When testing N95 FFRs with artificially created cylindered leaks, Rengasamy and Eimer (2011) found that for leak diameters ≤ 1.65 mm the MPPS was ~50 nm; we believe that this value likely represents the N95 filter penetration, whereas the TIL of the respirator used in this study (equipped with P100 filters) is primarily governed by the faceseal leakage penetration. This likely explains the suppressed peaks or the plateaus seen in the curves presented in Figure 3-2.

The effect of breathing frequency on TIL_{d_p} was complex. When challenged with wood combustion aerosol, frequencies of 30, 20 and 15 breaths/min produced the highest TIL_{d_p} values at MIF = 30, 55 and 85 L/min, for most size channels between 20 to 200 nm. MIF = 30 L/min produced the most notable effect of the breathing frequency on the TIL_{d_p}. The TIL_{d_p} curves obtained from testing with paper combustion aerosol showed some peaks at 30 and 10 breaths/min at MIF = 30 and 85 L/min, but no clear peak was identified for MIF = 55 L/min. The graphs representing TILs for plastic aerosol revealed separations between the TIL_{d_p} curves at MIF = 30 L/min, which essentially diminished at higher flow rates.

Increasing the MIF resulted in a decrease in the average TIL values for all challenge aerosols (wood, paper and plastic). For example, for the wood combustion aerosol, the average TIL values were 0.6~1.0 % at MIF = 30 L/min, 0.5~0.8 % at 55 L/min, and 0.3~0.6 % at 85 L/min. Several published FFR studies also reported that faceseal penetration decreased with increase in breathing flow when challenged with particles larger than 500 nm (Chen *et al.*, 1990; Cho *et al.*, 2010b). On the other hand, another FFR study observed no significant increase or decrease in faceseal penetration by 8–400 nm particles associated with increasing breathing flow (Rengasamy *et al.*, 2011).

Size-independent (overall) Total Inward Leakage (TIL)

The size-independent (overall) TIL values for the half-mask respirator challenged with the three tested combustion aerosols are presented in Figure 3-3. The highest TIL values were determined at MIF = 30 L/min and 30 breaths/min for all three challenge aerosols (peak TIL = 1.08%, 1.33% and 1.87% for wood, paper and plastic, respectively). The lowest TIL values (0.35%, 0.60% and 0.75% for wood, paper and plastic, respectively) were obtained at MIF = 85 L/min combined with 25 breaths/min. ANOVA with Tukey's range test was performed to study

the effects of combustion material, breathing flow and breathing frequency on the TIL, and the data analysis results are presented in Tables 3-2 through 3-5.

Effect of the combustion aerosol. A three-way ANOVA (see Table 3-2) shows that the non-size selective combustion aerosol significantly affected TIL ($p < 0.0001$). Pair wise multiple comparison analysis revealed the mean overall TIL values for wood, paper and plastic combustion aerosol were significantly ($p < 0.05$) different from each other (see Table 3-3). The plastic aerosol produced the highest mean TIL (1.14%) followed by wood (0.85%) and paper (0.70%). This finding is in agreement with our recent study (He *et al*., 2010b) conducted with the same type of half-mask donned on a hard plastic manikin headform. The difference in TIL can be attributed to differences in particle shape, density, electric charge, and possibly other properties. Plastic (polyethylene) is pure hydrocarbon, paper is cellulose (plus various additives and coatings), and wood is half cellulose and half lignin, which includes aromatics and relatively little hydrogen.

Effect of the breathing flow (MIF). Breathing flow had a significant effect on TIL ($p <0.0001$) as shown in Table 3-2. The interaction between the challenge aerosol and breathing flow (Aerosol*MIF) was significant ($p = 0.0096$). The pairwise comparison results for three MIF groups (30, 55 and 85 L/min) are presented in Table 3-4. The mean TIL obtained at MIF = 30 L/min was significantly ($p < 0.05$) higher than those determined for MIF = 55 and 85 L/min. The differences between the data series obtained at 55 and 85 L/min were not significant ($p > 0.05$). One possible explanation is that a higher breathing flow can create a higher negative pressure inside the half-mask respirator, which sucks the respirator toward the manikin's face, thus creating tighter contact with the manikin headform (i.e., reducing faceseal leakage).

Increasing the flow rate from 30 to 55 L/min significantly reduced TIL; however, TIL was not significantly reduced from 55 to 85 L/min.

Effect of the breathing frequency. Breathing frequency did not show a significant effect on the TIL($p > 0.05$, see Table 3-2) regardless of combustion aerosol, MIF and breathing frequency (pooled data). When the data was stratified by combustion aerosol and MIF (see Table 3-5), the effect of the breathing frequency became significant ($p < 0.05$) for all conditions challenged with wood and paper combustion aerosols, and for MIF = 30 L/min only if challenged with plastic aerosol. However, no significant breathing frequency effect was found at MIF = 55 L/min ($p = 0.99$) and MIF = 85 L/min ($p = 0.97$) for plastic aerosol. The pairwise multiple comparisons confirmed that the frequency of 30 breath/min produced the highest mean TIL value when MIF = 30 L/min, which was true for all three combustion aerosols (see Table 3-5). The findings were consistent with the results of size-selective TIL measurements (see Figure 3-2). At MIF = 55 L/min, the highest mean TIL values were recorded at 20 breaths/min for wood combustion aerosol (TIL = 0.89%) and at 30 breaths/min for paper aerosol (TIL = 0.88%); no peak TIL value was observed for plastic aerosol. For the MIF = 85 L/min, the highest mean TIL values were recorded at 15 breaths/min for wood combustion aerosol (TIL = 0.67%), at 10 breaths/min for paper aerosol (TIL = 0.90%); again, no peak TIL value was found for plastic aerosol.

In summary, the data suggest that the breathing frequency effect is rather complex and dependent on the combustion aerosol and MIF. It is concluded that the breathing frequency affects the TIL less than factors such as combustion aerosol and breathing flow rate. This finding points to the importance of a proper selection of challenge aerosol and MIF when testing the performance of the elastomeric half-mask respirators. Nevertheless, for a certain chosen

aerosol and MIF, different breathing frequencies can produce significant differences among the TIL values. For example, for wood aerosol and MIF = 30 L/min, the highest TIL (1.08%) obtained at 30 breaths/min was almost 1.5-fold higher than the one (0.74%) obtained at 15 breaths/min. At MIF = 85 L/min, the highest TIL found for the wood aerosol (0.67% at 15 breaths/min) was almost twice greater than the lowest TIL (0.35% at 25 breaths/min). In addition to characterizing the role of breathing frequency in the performance evaluation of an elastomeric respirator, the findings of this study support testing with cyclic flow (the present NIOSH certification protocol utilizes the constant flow condition). A similar conclusion was made for other types of respirators (Eshbaugh *et al.*, 2008; Haruta *et al.*, 2008; Grinshpun *et al.*, 2009).

A limitation of the study is that only one model of elastomeric half-mask respirators was tested. Generally, the results may differ from one model to another. In addition, only a single donning was conducted so that a contaminated respirator would not be subjected to a replicate testing. It remains unknown how the results would differ given that the respirator model characteristics and between-donning variability may cause leaks of different sizes and shapes. While we believe that the major trends would remain the same, it seems meaningful to expand the present study in the future involving alternative experimental designs and other half-mask models as well as, possibly, other classes of respirators (i.e., full facepiece and filtering facepiece respirators).

It was also noticed that the combustion aerosol in the breathing zone outside the respirator was diluted during exhalation phases by extraction through the HEPA filter and replacement with the particle-free air. This leaves fewer particles (by an absolute number) that

are capable of penetrating through the respirator. Consequently, the above affects the TIL results. The real TIL would have been higher if such dilution effect did not exist.

Conclusions

Breathing flow and combustion material had significant ($p < 0.001$) effects on the TIL regardless of the level of the breathing frequency. The particle size effect on the TIL was not significant ($p = 0.36$) for particles > 40 nm. The relatively flat curves generated in the size-selective experiments between approximately 40 to 200 nm serve as an evidence of a wide size range of particles, which most readily penetrate through faceseal leaks of half-mask respirators.

The effect of the breathing frequency was complex and differed for different combinations of the combustion aerosol and the MIF. For pooled data, the breathing frequency had no significant ($p = 0.08$) effect on the non-size selective TIL. However, after stratifying the data according to combustion aerosol and MIF, the breathing frequency effect became significant ($p < 0.05$) for all MIFs when challenged with wood and paper combustion aerosols, and specifically for MIF = 30 L/min when challenged with plastic aerosol. More studies are needed to fully understand the effect of breathing frequency.

Plastic aerosols produced higher overall mean TIL values ($p < 0.05$) as compared to wood and paper aerosols, suggesting potentially higher exposure to a wearer. The highest penetration occurred when challenged plastic aerosol, at 30 L/min, and at a breathing frequency of 30 breaths/min. The results also showed that an increase in the MIF leads to a decrease in TIL — a trend which lost its significance as the flow rate exceeded 55 L/min. In summary, the results suggest that when testing respirators on breathing manikins, a flow rate (not a breathing frequency) should be considered as a primary breathing characteristic to be addressed. The TIL results also indicate that for particles larger than 40 nm the particle size effect was not significant,

and particles < 40 nm produced lower penetration than those > 40 nm. This finding suggests that size-selective measurement may not be necessary when performing the TIL test.

CHAPTER 4

How Does Breathing Frequency Affect the Performance of an N95 Filtering Facepiece Respirator and a Surgical Mask Against Surrogates of Viral Particles? (Specific Aim 4)

Introduction

The National Institute for Occupational Safety and Health (NIOSH) certified N95 filtering facepiece respirators (FFRs) are widely used in various occupational environments to reduce the workers' exposure to hazardous aerosols. In healthcare environments, N95 FFRs and surgical masks (SMs) are the most commonly used devices to prevent transmission of infectious diseases (OSHA, 2007). N95 FFRs are certified by the National Institute for Occupational Safety and Health (NIOSH) in accordance with Title 42 of the Code of Federal Regulations (CFR, 1995. pp.30382-30383). The letter 'N' stands for non-oil-resistance, and the number '95' denotes the filter efficiency of at least 95% when the filter is challenged with NaCl aerosols having a mass median aerodynamic particle diameter of 300 nm (the most penetrating particle size, MPPS, for mechanical filters) at a constant flow of 85 L/min (NIOSH, 1995). Presently, the vast majority of FFRs are manufactured utilizing electrostatic fibers, which feature much smaller MPPS: 30 to 100 nm (Martin *et al.*, 2000; Grafe *et al.*, 2001; Bałazy, Toivola, Adhikari, *et al.*, 2006; 2006; Eninger *et al.*, 2008; Rengasamy *et al.*, 2008; Cho *et al.*, 2010a; Zuo *et al.*, 2013). The latter range includes many viral species. SMs are not subject to NIOSH filter certification approval; instead they are regulated by the US Food and Drug Administration (FDA). Previous studies have shown that the filter efficiency for SMs is much lower than that

for N95 FFRs (Willeke *et al.*, 1996; Bałazy, Toivola, Adhikari, *et al.*, 2006; Lee *et al.*, 2008b; Grinshpun *et al.*, 2009).

Besides filter penetration, faceseal leakage can have a significant impact on the performance of N95 FFRs and SMs. One study showed that the efficiency of N95 FFRs was high when sealed to a manikin headform but decreased significantly due to faceseal leakage when the same respirators were tested on human subjects (Qian *et al.*, 1998). NIOSH has proposed total inward leakage (TIL) testing to assess respirator performance since it takes into account both penetration pathways (NIOSH/CDC, 2009). Grinshpun and colleagues quantified the relative contributions of the two pathways for an N95 FFR and a SM by determining the filter penetration (P_{filter}) and faceseal leakage penetration ($P_{leakage}$) using manikin-based and human subject-based experimental protocols (Grinshpun *et al.*, 2009). The "faceseal leakage-to-filter" ratio ($FLTF = P_{leakage}/P_{filter}$) was > 1, indicating a greater number of particles penetrated through faceseal leaks than the filter media (Grinshpun *et al.*, 2009). While the quoted study addressed a wide range of particle sizes (30 – 1000 nm), it did not examine breathing frequency.

Viral airborne particles (known as virions) are generally much smaller than airborne bacteria. Most viruses referenced in the literature are between 20 and 300 nm in diameter (Collier *et al.*, 1998). For instance, coronavirus, the causative agent of severe acute respiratory syndrome (SARS), has a primary physical size ranging from 80 to 140 nm; the avian influenza virus (H5N1 and H1N1) is between 80 to 120 nm (Mandell *et al.*, 1995; Ksiazek *et al.*, 2003). Exposure to viral particles is best characterized by the number of inhaled particles rather than mass concentration (Kulkarni *et al.*, 2011). The size range of aerosols (often referred to as "carriers") containing viruses found in occupational setting is substantially larger than 500 nm because the actual aerosols contain not only the virus but also respiratory secretions, dead cells,

mucous, etc. However, particles < 500 nm are a worst-case situation (involving deeply inhaled particles and MPPS for N95 FFRs and SMs), and thus are more scientifically interesting than studying particles > 500 nm. In addition, the differences in filtration performance between surgical masks and FFRs are likely less noticeable for > 1 um aerosols. Therefore, this study focused on particles < 500 nm.

The Institute of Medicine estimates that during an influenza pandemic, more than 13 million health care workers, patients, family members and friends may need respiratory protection devices to protect them from receiving or spreading infectious illness (IOM, 2008). Between population groups (e.g., young vs. old, small vs. large, healthy vs. sick), breathing frequency (breaths/min) differs and will differ significantly with level of physical activity (e.g., at rest vs. active) (Tortora *et al.*, 1990; Sherwood, 2006). In addition, studies examined the physiologic impact of respirators on healthcare workers, reported that wearing a FFR did not impose any important physiological burden during 1 hour of use, at realistic clinical work rates, and using surgical mask use for 1 h at a low-moderate work rate was not associated with clinically significant physiological impact or significant subjective perceptions of exertion or heat (Roberge *et al.*, 2010). Human berating has a cyclic flow pattern, which is primarily determined by mean inspiratory flow (MIF, L/min) and breathing frequency (breaths/min). Unlike the constant flow with a fixed flow rate, the cyclic flow features a constantly changing flow that depends on the level of the breathing frequency. Various studies have addressed the effect of flow rate on filter efficiency and faceseal leakage (Myers *et al.*, 1991; Eshbaugh *et al.*, 2008; Haruta *et al.*, 2008; Cho *et al.*, 2010b). However, with exception to our recent study in which an elastomeric half-mask respirator was tested (He *et al.*, 2013c), no published study has

evaluated the effect of breathing frequency on the performance of N95 FFRs and SMs when both filter and faceseal leakage penetration pathways are present.

Although the nature of an inert aerosol (e.g., NaCl) differs from that of bioaerosols, several studies have confirmed that filter performance against biological particles is consistent with that determined using non-biological particles of the same size (Qian *et al.*, 1998; Bałazy, Toivola, Adhikari, *et al.*, 2006; Eninger *et al.*, 2008). This suggests that inert aerosol surrogates such as NaCl particles may generally be appropriate for predicting penetration of similarly sized virions. The present manikin-based study addresses the effects of breathing frequency and flow rate on the filter efficiency and faceseal leakage of an N95 FFR and a SM challenged with NaCl particles representative of viral size ranges, as well as other health-relavent particles (e.g., combustion generated or engineered nanoparticles). The tested N95 FFR/SM was sealed to plastic manikin headform to investigate filter performance. It was also donned without sealing to a different advanced manikin headform to quantify TIL. The advanced manikin utilized in this study was recently developed to mimic the properties of the human face (Hanson *et al.*, 2006; Bergman *et al.*, 2013). Faceseal leakage represents the difference between TIL and filter penetration.

This research was conducted to evaluate the effects of breathing frequency and particle size on the filter penetration and TIL of an N95 FFR and a surgical mask challenged with NaCl particles representing the viral particles, as well as other health-relevant submicrometer particles.

Materials and Methods

Tested N95 FFR and Surgical Mask

One N95 FFR and one SM were chosen for the study. Both models are commercially available and widely used in health-care environments. The model of the N95 FFR was identical to the one tested in our previous studies (Bałazy, Toivola, Adhikari, *et al.*, 2006; Bałazy, Toivola, Reponen, *et al.*, 2006). It has three principle layers with the middle layer composed of electrically charged polypropylene fibers to enhance filter capture efficiency (Bałazy, Toivola, Adhikari, *et al.*, 2006). The selected SM, according to the manufacturer, is fluid resistant and capable of providing at least 95% filter efficiency for 100 nm particles.

For filter efficiency testing, the FFR/SM was sealed to the face of a hard plastic manikin headform. For the TIL tests, it was donned on an advanced manikin headform according to the FFR/SM manufacturer's user instruction. After 20 tests, the tested FFR/SM was removed from the manikin and replaced with a new one to minimize the effect of NaCl loading on the filter media.

Challenge Aerosol

To produce the challenge agent (NaCl), a liquid salt solution was aerosolized using a particle generator (Model: 8026, TSI Inc., Shoreview, MN) and charge-equilibrated by passing through a ^{85}Kr electrical charge equilibrator (Model: 3054, TSI Inc., Shoreview, MN) prior to being released inside the test chamber. Before each experiment, the particle generator operated for at least one hour to achieve a uniform NaCl concentration in the chamber; it continued operating during the testing to maintain a stable particle concentration level. The challenge aerosol was log normally distributed with a size range of 20 – 500 nm, a count geometric mean of 125.4 nm, and a geometric standard deviation of 1.68 as measured with a Nanoparticle Spectrometer (Nano-ID NPS500, Naneum Ltd., Kent, UK). This size range covers the size of individual and aggregate virus particles.

Experimental Design and Test Conditions

Experiments were carried out in a room-size (24.3 m^3) test chamber described in recent studies.(He *et al.*, 2013a; He *et al.*, 2013c) Temperature and relative humidity inside the chamber were kept at 17–22 ℃ and 30–60 %, respectively. The headform was connected to a Breathing Recording and Simulation System (BRSS, Koken Ltd., Tokyo, Japan) with a HEPA filter placed in-between to keep particles from re-entering the respirator cavity during exhalation cycles. Details regarding the BRSS are described in our previous studies (Haruta *et al.*, 2008; He *et al.*, 2013a; He *et al.*, 2013b; He *et al.*, 2013c).

The experiments were conducted at four cyclic breathing flows (mean inspiratory flow, MIF =15, 30, 55 and 85 L/min) and five breathing frequencies (10, 15, 20, 25 and 30 breaths/min). Completely randomized factorial design was implemented for the breathing frequency and flow rate with three replicates. Particle size-independent (overall) concentrations inside and outside the FFR/SM were obtained using a condensation particle counter (Model: 3007, TSI Inc., Shoreview, MN) having a total sampling time of 3 min with a time resolution of 1 sec. Particle size-specific concentrations inside ($C_{in\_d_p}$) and outside ($C_{out\_d_p}$) of the FFR/SM were measured using a nanoparticle spectrometer (Nano-ID NPS500, Naneum Ltd., Kent, UK) operating in 28 channels within a range of d_p = 20 – 500 nm at a sampling flow rate of 0.2 L/min. Each particle size-specific concentration ($C_{in\_d_p}$ or $C_{out\_d_p}$) was sampled for 6 min.

Filter Penetration Test

The filter penetration (P_{filter}) was determined as the ratio of concentrations inside [$C_{in\_(Sealed)}$] and outside [$C_{out\_(Sealed)}$] of the FFR/SM sealed to the plastic headform; for each particle size, the filter penetration ($P_{filter\_d_p}$) was determined as the ratio of the corresponding

size-specific concentrations inside ($C_{in\_d_p\,(Sealed)}$) and outside ($C_{out\_d_p\,(Sealed)}$) of the FFR/SM sealed to the plastic headform:

$$P_{filter} = \frac{C_{in\_(Sealed)}}{C_{out\_(Sealed)}} \times 100\% \quad \textbf{(4-1)}$$

$$P_{filter\_d_p} = \frac{C_{in\_d_p(Sealed)}}{C_{out\_d_p(Sealed)}} \times 100\% \quad \textbf{(4-2)}$$

Total Inward Leakage Test

For TIL, the same experimental protocol and test conditions were used except the FFR/SM was not sealed onto the advanced manikin headform. TIL values were determined as the ratio of concentrations inside [$C_{in\_(Donned)}$] and outside [$C_{out\_(Donned)}$] of the FFR/SM; accordingly, the size-specific TIL values were determined as follows (Eq.4-4):

$$TIL = \frac{C_{in\_(Donned)}}{C_{out\_(Donned)}} \times 100\% \quad \textbf{(4-3)}$$

$$TIL_{d_p} = \frac{C_{in\_d_p(Donned)}}{C_{out\_d_p(Donned)}} \times 100\% \quad \textbf{(4-4)}$$

Faceseal Leakage to Filter (FLTF) Ratio

The TIL test measures total penetration through the filter and faceseal leakage (TIL = $P_{filter} + P_{leakage}$). The *FLTF* ratio represents the relative contribution for each and was calculated as:

$$FLTF = \frac{P_{leakage}}{P_{filter}} = \frac{TIL - P_{filter}}{P_{filter}} \quad \textbf{(4-5)}$$

In this study, the *FLTF* ratio was calculated using the average TIL and P_{filter} values over three replicates in order to identify the primary penetration pathway (leakage or filter penetration) for the entire particle size range of interest.

Data analysis

SAS version 9.3 (SAS Institute Inc., Cary, NC, USA) was used for data analysis. Two-way Analysis of Variance (ANOVA) was performed to analyze the effect of breathing frequency and flow rate on the filter penetration and TIL. All pairwise comparisons were conducted using Tukey's range test. A t-test was used to examine the differences in P_{filter} and TIL between the N95 FFR and the SM. *P*-values < 0.05 were considered significant.

Results and Discussion

1. N95 Filtering Facepiece Respirator

N95 Filter Penetration (P_{filter})

Filter penetration results for the N95 FFR are presented in Figure 4-1A. Filter penetration (P_{filter}) consistently increased with increasing MIF. This result can be explained by the differences in linear air velocities. Penetration of very small particles, which deposit on filter fibers primarily due to diffusion, increases with a decreasing residence time (also known as removal time). Thus, small particles are more likely to penetrate the filter at higher breathing flows. At the higher flows (MIF = 55 and 85 L/min), the P_{filter} curves are not flat, in contrast to those at the 15 and 30 L/min, suggesting that the effect of lower breathing frequencies are more pronounced at higher MIFs.

Two-way ANOVA performed on the P_{filter} data revealed that both the MIF and breathing frequency had a significant effect on filter penetration (p <0.0001, see Table 4-1). Pairwise multiple comparison results (see Table 4-1) show that the four MIFs produced four different P_{filter} groups with the highest mean P_{filter} (0.72%, Tukey grouping "A") occurring at the highest MIF of 85 L/min, and the lowest mean P_{filter} (0.05%, Tukey grouping "D") occurring at the lowest MIF of 15 L/min. The breathing frequency comparisons show that 10 and 15 breaths/min produced higher values of P_{filter} (0.39% and 0.38%, Tukey grouping "I") than those observed at 20, 25 and 30 breaths/min (0.25%, 0.23% and 0.26%, respectively, Tukey grouping "II").

N95 FFR Filter Penetration ($P_{filter\_d_p}$)

Figure 4-2 presents the size-specific $P_{filter\_d_p}$ values for the tested N95 FFR. It is seen that filter penetration increased with increasing MIF (p <0.05), which is consistent with the results of many previous N95 FFR studies (Bałazy, Toivola, Reponen, *et al.*, 2006; Eninger *et al.*, 2008; Rengasamy *et al.*, 2008; Cho *et al.*, 2010a; He *et al.*, 2013c).

Particle size had a significant effect on the $P_{filter\_d_p}$ (p <0.05). Interestingly, all the filter penetration curves show two peaks for all MIFs and breathing frequencies, indicating two possible MPPS for the tested N95 FFR. The first MPPS occurred at 30–40 nm, which was expected for conventional N95 FFRs composed of electrically charged fibers. Several studies have reported that the MPPS for a N95 FFR "electret" filter is < 100 nm while a "mechanical" filter has a MPPS of approximately 300 nm (Bałazy et al. 2006a; Bałazy et al. 2006b; Eninger et al. 2008; Martin and Moyer 2000; Huang et al. 2007; Rengasamy et al. 2009). The second MPPS identified at ~300 nm (Figure 4-2) was not reported in any of the above quoted studies. One reason is that the quoted investigations utilized a constant flow design, whereas the present

effort represents a cyclic flow condition. It is possible that under the cyclic flow some particles are trapped inside the respirator cavity. This phenomenon "artificially" increases the particle count inside the FFR, thus affecting the filter penetration calculated by Eq. (4-2). The effect is expected to be particularly pronounced at low $C_{out\_d_p}$. It is noted that the tested aerosol is characterized by a rapidly decreasing concentration in the particle size range of 200 to 400 nm – the area where the second peak was identified (Figure 4-2). The other reason of the observed departure of $P_{filter} = f(d_p)$ from the conventional single-mode function could be associated with a three-layer filter structure of the tested N95 FFR of which only the middle layer was electrostatically charged. The combination of electrostatic (the middle layer) and mechanical (the two outer layers) characteristics may produce a complex penetration function involving the particle diffusion, polarization force, interception and impaction, which is capable of generating two peaks. Alternatively, the second peak may be attributed to limitations associated with the mobility-based particle measurement in the 100 – 500 nm size range, specifically with biases in corona charging and uncertainties in defining charge as a function of the particle size for particles that differ by morphology and other characteristics (Dhaniyala et al., 2011). The above could affect the particle concentration values in this size range and consequently lead to an aberration of the penetration curve at $d_p > 100$ nm, especially for lower concentrations measured inside the respirator. Future studies are needed to determine if the observed second peak can, at least partially, be linked to the instrumental error. We envision that such a study would utilize mobility classified challenge aerosol particles (as an alternative to the polydisperse NaCl aerosol used in the present study).

The effect of breathing frequency on filter penetration is complex and heavily dependent on the particle size and the MIF. The effect was most clearly seen for particles around the MPPS

(see Figure 4-2). For example, at the first MPPS (30-40 nm) the lower breathing frequencies (10, 15 and 20 breaths/min) produced higher penetration values for MIF = 15, 55 and 85, but not for 30 L/min. It is hard to differentiate the breathing frequency effect on the penetration at the second MPPS at 200 – 300 nm for all four MIFs. Such complexity of breathing frequency effect was also reported in our other study using an elastomeric half-mask respirator equipped with P100 filters (He *et al.*, 2013c). As expected, the N95 FFR had P_{filter} below 5% for any particle size, breathing frequency, and MIF used in this study.

N95 Total Inward Leakage (TIL)

Figure 4-1B presents the results obtained from the TIL measurements for the tested N95 FFR. It is seen that the MIF of 15 L/min produced the highest TILs. Interestingly, the TIL increased with increasing the breathing frequency, especially at MIF = 15 L/min. The exhaled particle-free air dilutes the aerosol in the respirator cavity. At a higher breathing frequency, the dilution air volume per breathing cycle is lower, which results in a less efficient dilution and consequently increases the aerosol concentration inside the respirator. This explains why a higher breathing frequency produced a higher TIL. This finding suggests that fast-breathing people (e.g., children and adults with various health impairments) may benefit less from wearing N95 FFRs. It is acknowledged though that the latter statement is acceptable only as the first approximation. The aerosol particle transport into a FFR/SM worn by a human is more complex than the one when it is donned on a manikin (e.g., the exhalation air generally carries particles to the cavity).

Statistical analysis revealed significant effects of MIF (p =0.0019) and breathing frequency (p =0.0025) on TIL (see Table 4-2). The pairwise multiple comparison results presented in Table 4-2 show that the lowest MIF (15 L/min) was associated with the highest

mean TIL (1.93%, Tukey grouping “A”). The mean TIL values among the three higher MIFs (30, 55 and 85 L/min) were not significantly different from each other (1.37%, 1.31% and 1.29%, Tukey grouping “B”). The highest breathing frequency (30 breaths/min) produced the highest mean TIL (1.73%, Tukey grouping “I”) compared to the lowest mean TIL (1.22%, Tukey grouping “II”) with the lowest breathing frequency (10 breaths/min). The highest and lowest breathing frequencies were significantly different (Tukey groups I & II). As was pointed out in our previous study on elastomeric respirators, (He *et al.*, 2013c) higher MIF may create a higher sucking force that made a tighter contact between the respirator and the soft skin of the headform, possibly reducing the leak size. We anticipate that the quoted effect showed up when MIF increased to 30 L/min. The finding is consistent with previous FFR performance studies conducted using hard manikins and challenge aerosol particles above 500 nm (Chen *et al.*, 1990; Huang *et al.*, 2007; Cho *et al.*, 2010b).

N95 FFR Total Inward Leakage (TIL_{d_p})

The size-specific TIL results for the tested N95 FFR donned on an advanced manikin headform are presented in Figure 4-3. The TIL_{d_p} increased as the particle size increased from 20 to ~50 nm regardless of the MIF and the breathing frequency, which is consistent with the fact that the diffusional deposition effect is stronger for smaller particles. However, at the particle size of ~50 nm, the TIL_{d_p} curves reached a plateau. The effect of particle size on the TIL_{d_p} was not significant (p >0.05) for particles larger than 50 nm for any MIF and breathing frequency used in this study. One possible reason is that the penetration through the faceseal leakage (unlike the filter media) is not very sensitive to the particle size. Once the particles are large enough (for a typical leakage dimension, the estimated size must be above 40 – 70 nm) to have a low diffusional deposition efficiency (Kulkarni et al. 2011), their penetration through the

faceseal leak is essential particle size independent in a wide size range (it is in contrast to P_{filter} , which is influenced by other particle deposition mechanisms). As seen from the data presented in Figures 4-2 and 4-3, the leakage represents the major penetration pathway and thus has the major effect on the TIL, which explains the lack of its particle size dependence at > 50 nm. This finding is consistent with the conclusion of our recent study in which the performance of an elastomeric respirator was examined while it was donned on the same advanced manikin headform (He et al. 2013c). Little information is available about the MPPS for faceseal leakage of N95 FFRs. One investigation that measured TIL and filter penetration for N95 FFRs with artificially created leaks, reported MPPS ~50 nm for leak diameters as small as < 1.65 mm(Rengasamy and Eimer 2011). Experimental protocols with artificial faceseal leaks have a number of limitations because (i) the outcome may be dependent not only on the leak size but factors such as the leak shape, location and others unaccounted for and (ii) in reality, the leak is continuously changing as a wearer is breathing, talking and moving.

Statistical analysis showed that increasing MIF was associated with a decrease in TIL_{d_p} (p <0.05). Other FFR performance studies have shown decreased inward leakage with increasing the breathing flow (Cho *et al.*, 2010b; Rengasamy *et al.*, 2011; He *et al.*, 2013d). One explanation, as explained previously, is that higher MIF with cyclic flows create a greater negative pressure during the inspiratory cycle that pulls the facepiece towards the manikin surface with a reduction in leak size (Richardson *et al.*, 2007). This may be an advantage of the advanced manikin headform used in this study with simulated soft skin.

N95 Faceseal Leakage-to-Filter (FLTF) Ratio

The size-independent (overall) *FLTF* ratios calculated by Eq. (4-5) are presented in Figure 4-1C as a function of the breathing frequency and MIF. Except for MIF = 85 L/min, all

the *FLTF* ratios were > 1, which suggests that overall particle penetration through faceseal leaks exceeded N95 filter penetration at lower breathing rates. Remarkably, at the lowest MIF (15 L/min) the *FLTF* ratios ranged from 25 to 47, suggesting that the absolute majority of the measured virus-size aerosol particles penetrated through faceseal leaks. At MIF = 15 L/min, increase in breathing frequency was generally associated with increase in *FLTF* ratio. However, the breathing frequency effect was not clearly seen for the three higher MIFs (30, 55 and 85 L/min).

It is seen that increasing MIF resulted in decreasing *FLTF* ratio. This finding agrees with two other N95 FFR studies.(Grinshpun *et al.*, 2009; Rengasamy *et al.*, 2011) Grinshpun *et al* tested an N95 FFR using 25 human subjects, and reported that "deep breathing" produced higher *FLTF* ratios compared to "normal breathing".(Grinshpun *et al.*, 2009) Rengasamy and Eimer also reported higher *FLTF* ratios occurred at higher flow rates when testing the N95 FFRs with artificially created leaks.(Rengasamy *et al.*, 2011) In both quoted studies, all the *FLTF* ratios exceeded the unity, indicating that the faceseal leakage was the primary penetration pathway for N95 FFRs.

2. Surgical Mask

SM Filter Penetration (P_{filter})

The data on filter penetrations (P_{filter}) for the tested SM are shown in Figure 4-4A. Compared to the N95 FFR, the SM had a much higher filter penetration. This is not surprising given the less stringent filter penetration test requirements for SMs. In fact, previous studies have reported SMs providing much lower levels of respiratory protection than N95 FFRs when challenged with biological or non-biological particles.(Willeke *et al.*, 1996; Bałazy, Toivola, Adhikari, *et al.*, 2006; Lee *et al.*, 2008b; Grinshpun *et al.*, 2009) Increasing MIF frequently

resulted in an increase in filter penetration, especially at the lowest breathing frequency. Statistical analysis suggests that the effects of MIF and breathing frequency on the P_{filter} were both significant (p <0.05; see Table 4-3). The pairwise multiple comparisons (see Table 4-3) show the highest MIF (85 L/min) produced the highest mean P_{filter} (9.65%, Tukey grouping "A"), whereas the lowest P_{filter} (5.41%, Tukey grouping "C") occurred at the lowest MIF (15 L/min). Table 4-3 also shows that the mean P_{filter} = 7.81% (Tukey grouping "I") obtained at 30 breaths/min was significantly higher (p <0.05) than P_{filter} = 6.67% (Tukey grouping "II") obtained at 20 breaths/min. However, no consistent trend was identified throughout the frequency scale.

SM Filter Penetration ($P_{filter\_d_p}$)

The filter penetration ($P_{filter\_d_p}$) results for the tested SM are presented in Figure 4-5. Compared to the N95 FFR, the SM had a much higher filter penetration (p <0.05), which is expected given its primary function is to protect others from the aerosol exhaled by the wearer. Previous studies have reported that a typical SM provided much lower protection than a N95 FFR when challenged with biological or non-biological particles (Bałazy et al. 2006a; Grinshpun et al. 2009a; Lee et al. 2008b; Willeke et al. 1996; He et al. 2013d). It is also evident from Figure 4-5 that the filter penetration curve deviates from a single-peak function expected from a conventional mechanical filter. Similar to the interpretation offered above for the N95 FFR, we can attribute this difference to cyclic flow tested in this study compared to constant flow utilized by other researchers. As pointed out above, alternatively, the observed phenomenon may derive from an instrumental biases of Nano-ID associated with corona charging and certain challenges in defining the particle charge as a function of size for particles featuring different characteristics (Dhaniyala et al., 2011). No previous study has reported a multiple P_{filter} peaks for SMs. Three

peaks have been observed for P_{filter}: at ~30, ~100 and ~300 nm. The most prominent MPPS was ~300 nm for all MIFs and breathing frequencies. This is much higher than the MPPS obtained for the N95 FFR (30 – 40 nm). The latter is consistent with the fact that the tested SM had a mechanical filter with no electrically charged fibers (or the charges were negligible). These filters are known for their relatively low-efficiency and MPPS of ~300 nm.

As evident from Figure 4-5, the curves corresponding to different breathing frequencies are not distinct for MIF = 15 and 30 L/min and largely also for 55 L/min; the curve separation suggests that a more prominent effect of breathing frequency was observed at 85 L/min with the 10 and 15 breaths/min producing higher $P_{filter\_d_p}$ values and 20 breaths/min generating the lowest $P_{filter\_d_p}$ curve. This suggests that the MPPS was not directly affected by the MIF and the breathing frequency.

While, the model chosen for this study provides at least 95% filter efficiency for particles of 100 nm (according to its manufacturer, no flow rate is specified), Figure 4-5 shows that the filter penetration of 100 nm particles was > 5% for various breathing frequencies, especially when MIFs ≥ 55 L/min. This finding suggests that the tested SM may not provide the expected filter efficiency at higher breathing flows. Particles larger than 100 nm penetrated through the SM filter more readily. From this perspective, the 100 nm size used by the manufacturer as a reference point does not seem appropriate unless the SM is used specifically against 100-nm particles.

SM Total Inward Leakage (TIL)

TIL results for the SM are presented in Figure 4-4B. The average TIL values ranged from 17% to 35% compared to filter penetrations of 3 – 12%, suggesting that faceseal leakage had a

greater effect on the mask performance. Increasing MIF caused the mean TIL to decrease FFR (see Table 4-4), which is in agreement with the finding reported for the N95.

While ANOVA revealed that both MIF and breathing frequency had a significant effect on the TIL (p <0.05; see Table 4-4), no consistent trend of increase or decrease of TIL with breathing frequency was observed. For instance, increasing the breathing frequency from 10 to 15 breaths/min was associated with a decrease in TIL, whereas changing the frequency from 10 to 30 breaths/min at MIF = 55 or 85 L/min resulted in essentially no change in TIL. When comparing the mean TIL values among the five breathing frequencies, the highest mean TIL 5.7%, Tukey grouping "I") occurred at 30 breaths/min, and the lowest mean TIL (22.2%, Tukey grouping "II") at 15 breaths/min.

At the same time, the data produced by a pairwise comparison presented in Table 4-4 demonstrate that increasing MIF indeed decreased the TIL with MIF = 15 L/min generating the highest mean TIL (30%, Tukey grouping "A") and 85 L/min producing the lowest mean TIL (19.9%, Tukey grouping "C").

SM Total Inward Leakage (TIL_{d_p})

Figure 4-6 presents the TIL_{d_p} results for the SM. Similar to N95 FFR, the TIL_{d_p} of the SM increased rapidly with the particle diameter increasing up to 30 – 50 nm, but then its dependence on d_p became less pronounced (p >0.05). TIL_{d_p} was not significantly affected by breathing frequency (p >0.05) but had slightly different patterns at different MIFs. For particles >30 nm, a slow increase was observed at the lowest MIF (15 L/min), but this gradually leveled off as MIF increased to 85 L/min. This suggests a wide range of sizes producing essentially the same TIL (approximately 20% at MIF=85 L/min). It is also noticed that the variability in the

total penetration obtained for the SM is lower than that for the N95 FFR. The total particle penetration into the SM is about 10-fold greater than the penetration into the FFR, which means that the particle count inside the respirator is an order of magnitude lower than that inside the mask (given that C_{out} is the same). Lower count is usually associated with higher variability, which explains our finding. To our knowledge, no published study has reported the TIL's MPPS for surgical masks. Even though SMs are not considered personal respiratory protective devices, there are many circumstances where SMs are used to reduce human exposure to hazardous aerosols. In fact, the use of SMs as personal protective devices world-wide, likely exceeds the use of N95 FFRs. Given that the size of most of "naked" infectious airborne virions (Collier et al. 1998), diesel particles (Castranova et al. 2001), combustion particles generated from fire smoke (He et al. 2013a), and other hazardous aerosols falls into the above-indicated range, the data suggest that the tested SM may not be able to provide substantial protection against these particles at any relevant combination of the breathing frequency and flow rate.

SM Faceseal Leakage-To-Filter (FLTF) Ratio

The *FLTF* ratios calculated from the overall P_{filter} and the TIL data are presented in Figure 4-4C. It is seen that increasing MIF from 15 to 55 L/min resulted in a decrease in *FLTF*, with most of the *FLTF* ratios were > 1 (which means $P_{leakage} > P_{filter}$). Increasing MIF from 55 to 85 L/min had less effect, with FLTF ratios < 2 and even < 1 at the highest MIF (85 L/min) for the two lowest frequencies of 10 and 15 breaths/min. The results had a similar pattern to those presented for the N95 FFR. However, the *FLTF* ratios for the SM were lower. For example, at MIF = 15 L/min, the *FLTF* ratios for the SM were between 4 and 7 while those found for the N95 FFR ranged from 24 to 50. This difference is attributed to much higher filter penetration of the SM as compared to the N95 FFR.(Grinshpun *et al.*, 2009)

No clear trend was identified between the breathing frequency and the *FLTF* ratio for the three highest flows (MIF = 30, 55 and 85 L/min), where the curves are relatively flat (Figure 4-2C). For the lowest flow rate (15 L/min), increasing breathing frequency initially decreased *FLTF*, but this too leveled off.

Conclusions

Breathing frequency was found to be another factor (in addition to MIF) that can significantly affect the performance of N95 FFRs and SMs. For the tested N95 FFR, the increase of breathing frequency caused an increase in TIL, thus allowing more particles to penetrate inside the respirator. No consistent trend of increase or decrease of TIL with either MIF or breathing frequency was observed for the tested SM.

For the tested N95 FFR and SM, the filter penetration was significantly affected by the particle size and breathing flow rate ($p < 0.05$), whereas the breathing frequency effect on P_{filter} was generally less pronounced and less important from the practical viewpoint, especially for lower MIFs. Surprisingly, the P_{filter} curves show two peaks for the tested N95 FFR and three peaks for the SM, which was not reported in previous respiratory filter. Consequently, using data from a single MPPS may not always be representative of the filter performance, especially if the tested respirator is intended to be used against particles of a wide size range.

The *FLTF* ratios obtained for the N95 FFR were generally higher than those for the SM for all tested breathing frequencies and MIFs. It is primarily because of the higher efficiency of the N95 filter. Increasing MIF was also generally associated with decreasing *FLTF* ratio for the tested FFR/SM. Except for MIF = 85 L/min, all the calculated *FLTF* ratios were > 1, suggesting

that the faceseal leakage was the primary particle penetration pathway for the tested FFR/SM at various breathing frequencies.

For the FFR and SM, the total particle penetration increased with increasing particle size up to ~50 nm; when challenged with particles greater than 50 nm, only the breathing flow rate remained a significant (p <0.05) factor affecting the TIL, whereas the influence of particle size and breathing frequency was not significant (p >0.05). Increasing the MIF increased the filter penetration, but decreased the total penetration for both the FFR and SM. The SM produced much higher P_{filter} and TIL values than the N95 FFR, and the most predominate MPPS was also higher for the SM (~300 nm) than for the N95 FFR (30 – 40 nm). The results suggest that the tested SM may not be able to provide substantial protection against aerosol particles at least up to ~500 nm at any relevant combination of the breathing frequency and flow rate.

CHAPTER 5

Performance Characteristics of a Polymeric Micro-Patterned Adhesive on the Fit of an Elastomeric Half-mask Respirator Using a 25-subject Test Panel (Specific Aim 5)

Introduction

Elastomeric respirators are commonly used to protect workers from various hazardous airborne particulates, e.g., firefighters are reported to use elastomeric half-masks equipped with a highly efficient P-100 filters during fire overhaul (after the fire has been extinguished) (Bolstad-Johnson *et al.*, 2000; Burgess *et al.*, 2001). Unlike filtering facepiece respirators (FFRs), elastomeric half-masks offer the benefits of reusability, enhanced user seal check capability, improved face seal, and can be decontaminated multiple times (Roberge *et al.*, 2010).

According to the U.S. Occupational Safety and Health Administration (OSHA), every worker required to wear a tight fitting respirator such as the elastomeric half-mask shall be fit tested prior to initial use of the respirator (OSHA, 2006). There are two categories of fit testing: 1) qualitative fit test (QLFT), which relies on the wearer's ability to sense a test agent by taste, smell, or irritation, and 2) quantitative fit test (QNFT), which assesses the adequacy of respirator fit by numerically measuring the amount of leakage into the respirator, such as measuring the concentration of a test agent outside (C_{out}) and inside (C_{in}) the respirator. The ratio of the two (C_{out}/C_{in}) is called the fit factor (FF) (OSHA, 2006). A fit factor of 100 is the OSHA pass criterion for negative pressure elastomeric half-mask respirators.

One study involving three half-masks and ten FFRs tested on a panel of ten human subjects concluded that the FFs of elastomeric half-masks are higher than those of FFRs (Han *et*

al., 2005). Considering that elastomeric respirators are equipped with P-100 filters that offer a collection efficiency at least as high as 99.97%, the overall performance of these respirators is largely dependent on their fit (Eshbaugh *et al.*, 2008; Rengasamy *et al.*, 2008; He *et al.*, 2013a). Thus, efforts should be directed towards improving the fit of elastomeric respirators by reducing faceseal leakage. Many factors can interfere with a good face-to-respirator seal, e.g., positioning, strap adjustment, facial hair, facial scars, high cheekbones, excessive makeup, etc. Prior to the fit testing, a subject shall be free of stubble beard growth, beard, mustache or sideburns which cross the respirator sealing surface; no wetness on the subject's face is allowed. Accordingly, respirator fit-testing studies have usually been conducted under normal skin conditions (dry and clean-shaved). Thus, there are less data on respirator performance using other challenge conditions such as wet and/or unshaved skin.

Conventional elastomeric respirators have a flexible smooth sealing surface extending around the periphery and exhibit a uniform seal surface contour, which aims at creating a good faceseal (Beard, 1994; Starr *et al.*, 1996; Barnett *et al.*, 1999; Belfer *et al.*, 1999). One component of obtaining an effective seal is to be clean shaven prior to respirator donning. However, this requirement, cannot be met consistently in certain situations, e.g., in the battlefield or when respirators are needed during unforeseen emergency situations. The presence of sweat, facial hair, oil, dirt, or acne on facial skin could compromise the effectiveness of peripheral seals and thus negatively affect the performance of a conventional elastomeric respirator. To address the faceseal leakage issues, a conventional elastomeric half-mask was modified to reduce the faceseal leakage. A polymer micro-patterned adhesive (PMA) inspired by gecko-foot was applied to the peripheral area of the half-mask to improve its fit performance. Development of PMA has been actively pursued in recent years; arrays of relatively soft elastomeric fibrils such

as polydimethylsiloxane (PDMS) and polyurethane (PU) have been fabricated to mimic gecko's adhesion mechanism (Kim *et al.*, 2006; Del Campo and Arzt, 2007). The adhesion capacity of these synthetic adhesives can reach or even surpass that of gecko-foot (Qu *et al.*, 2008).

For this study, a conventional elastomeric respirator was modified with the addition of a PMA applied to the sealing surface. The modified respirator was then fit tested on a NIOSH bivariate (face length and width) 25-subject panel using the standard OSHA fit testing protocol (OSHA, 2006; Zhuang *et al.*, 2007). One of these 25 subjects then participated in a pilot study designed to investigate the fitting characteristics of the modified respirator with less than ideal facial conditions.

Materials and Methods

Fabrication of Polymer Micro-patterned Adhesives (PMA)

PMA was produced by soft-molding of elastomeric precursors on a photolithographically formed master template. The template was fabricated following a procedure described elsewhere (del Campo, Greiner, *et al.*, 2007). Fibrillar arrays were made with PU (ST-3040, BJB Enterprises, Inc). The templates were silanized with heptadecafluoro-1,1,2,2-tetrahydrooctyltrichlorosilane (hepta-fluorosilane). Gas-phase silanization was performed in an evacuated desiccator for one hour, followed by baking at 95°C for one hour. The PU ST-3040 A and B (20:17 by weight) mixture was degassed and poured on the silanized template. After curing at room temperature in light vacuum over 24 hours, the PU was demolded to avoid rupture of the polymer micro-fibrillar array. The micro-patterned structure had micro-fibrils 20 μm a diameter and 20 μm long with a center-to-center distance of 30 μm; in addition, every 60 rows of micro-fibrils were incorporated with one continuous micro-ribbon 20 μm wide, as shown

in Figure 5-1. The total thickness of the elastomer sheet (with fibrillar surface) was approximately 1 mm.

Respirators

This study was performed using a conventional elastomeric half-mask respirator equipped with two P100 pancake-shaped filters (Model: 2091, 3M, Minneapolis, MN, USA). The chosen respirator model (Model: 6000 series, 3M) is widely used in a variety of occupational environments; it was examined in our recent studies (He *et al.*, 2013a; 2013b) and available in three sizes (small, medium and large). The respirator was modified by manually attaching PMA strips with 2 cm width onto the presumed sealing surface of the half-mask respirator. A non-modified version of the same respirator model and size was used for comparison. The two half-masks (conventional and modified) are shown in Figure 2. An 11 mm long flush probe with a 14 mm diameter flange and a 4 mm diameter inlet was mounted on the surface of the respirator centerline approximately 25 mm from the manikin's nose/mouth. The end of the probe (14 mm flange) was flush with the interior surface of the half-mask.

The modified and non-modified respirators were tested on a given subject in random order. After each fit test the straps and yoke were removed from the respirator body and attached to the alternative respirator; this was accomplished without any adjustment to the straps themselves. We expected that the above procedure would eliminate and/or reduce variability due to strap adjustment.

Human Subjects and Test Conditions

Initially, 120 subjects were identified as available for screening. Twenty-five of these adult subjects were selected for fit testing. The selected subjects included all ten cells of the NIOSH bivariate 25-subject panel (see Figure 3). Of the selected subjects, six had relatively

small faces (cells # 1, 2, and 3), six had large faces (cells # 8, 9, and 10), and thirteen had medium faces (cells # 4, 5, 6, and 7). The tested cohort included 17 male and 8 female subjects; among them 13 were Caucasians, 8 Asians, and 4 African Americans/African origins. All subjects were medically cleared by completing an OSHA respirator medical clearance questionnaire. The study received an approval from the University of Cincinnati Institutional Review Board.

The subjects were asked not to eat or drink for at least one hour prior to the fit test. The main phase of this study was performed according to the standard OSHA fit testing protocol; accordingly, the 25 subjects involved in this phase were clean-shaved with dry faces and were fit-tested once with each respirator. For the pilot study, one male subject was fit tested with both respirators under the following facial conditions: dry-shaved (non-challenge condition), wet-shaved, dry-unshaved, and wet-unshaved. The "unshaved" facial condition was created after not shaving for ~40 hours. This condition is believed to reflect many real-life respirator usage situations in the military, the general population, and during certain unforeseen emergency situations. The "wet" face condition was created by applying a handful of water to the face using two hands, patting lightly with a napkin to remove large water droplets, and then waited for 30 seconds before donning the respirator. This condition was intended to simulate a wet sealing when a respirator is worn for some time. In this phase of the study, three replicates were conducted for each of the four above-listed combinations.

Measurements

The study was conducted in a room-size respirator test chamber (24.3 m^3). The challenge aerosol, NaCl, was generated using a particle generator (Model: 8026, TSI Inc., St. Paul, MN, USA). The concentration inside the chamber was maintained at 30,000 to 60,000 particles/cm^3

(such high ambient concentrations were chosen as to assure enough particles to be detected inside the respirator). For each subject, two fit tests were performed: one with the non-modified half-mask respirator and the other modified with the adhesives. A PortaCount Plus (Model: 8020, TSI Inc.) was used to measure the aerosol concentrations outside and inside the respirator.

Prior to the fit testing, all respirators were visually examined to eliminate any obvious defects or damages. The test subject was asked to select the respirator that provided the most comfortable fit; he/she was also shown how to don a respirator and how to adjust strap tension. After the tested respirator was donned on the subject and the straps were properly adjusted, a user seal check (positive pressure seal check) was performed.. Subsequently, the subject was fit-tested while performing the standard set of OSHA respiratory fit testing exercises: 1) normal breathing, 2) deep breathing, 3) turning head side to side, 4) moving head up and down, 5) talking, 6) grimace, 7) bending over and 8) returning to normal breathing. The individual and overall FFs were recorded for each subject. Based on the PortaCount-measured concentrations, each exercise-specific FF value was calculated as below:

$$FF_i = \frac{(C_{out})_i}{(C_{in})_i} \quad \textbf{(5-1)}$$

where FF_i is the fit factor for the i^{th} exercise, $(C_{out})_i$ and $(C_{in})_i$ are the aerosol concentrations measured outside and inside the respirator, respectively, for this exercise.

Data analysis

Data analysis was performed using SAS version 9.3 (SAS Institute Inc., Cary, NC, USA). The FF data were log-transformed. For comparison of respirator type (non-modified versus modified), paired *t*-test was performed using all 25 subjects' $FF_{overall}$ data. One-way analysis of

variance (ANOVA) was performed to study the differences among exercise-specific FFs. For $FF_{overall}$ results obtained under various facial challenge conditions, paired *t*-test was performed to compare the difference in $FF_{overall}$ between the non-modified and the modified respirator.

Results and Discussion

Tests under Normal Facial Condition (Dry and shaved Face, 25 Subjects)

The overall fit factor data for the control and modified half-masks are presented in Figure 5-3. FF values for the modified half-mask ranged from 159 (subject #T06) to 57,700 (subject #T11); geometric mean (GM) = 7,907 and geometric standard deviation (GSD) = 4.9. Since each respirator was equipped with P100 filters that are known to be at least 99.97% efficient when used against NaCl particles (results presented in He *et al*., 2013a). Therefore, a FF < 3,333 indicates face seal leakage, and 28% of subjects wearing the modified half-mask had FF < 3,333. Consequently, 72% of the tested modified respirators exhibited the particle penetration solely within the filter efficiency limit (allowing no measurable penetration through the face seal leakage. Furthermore, the majority of fit tests on the modified respirators had FF greater than 10,000. Only two subjects (#T06 and #T09) had overall FF's between 100 and 1,000.

The non-modified respirator had overall FF's ranging from 37 (subject #T10) to 92,800 (subject #12), with a GM = 4,779 and GSD = 9.1. The range and variability of the non-modified respirator were considerably greater than those for the modified one. Ten subjects (40%) had FF < 3,333 suggesting faceseal leakage was present in the non-modified respirator compared to 28% tested with the modified respirator.

Based on the comparison of the data presented in Figure 4, the performance of the modified half-mask appeared to be better than that of the non-modified. When tested with the

modified respirators, FF values exceeded 100 (the OSHA fit test passing criterion) for all 25 subjects, whereas 24 of 25 subjects wearing the non-modified respirators had FF > 100. However, paired *t*-test showed that this difference was not significant ($p = 0.07$, considered to be a boarder-line significance). Very high fit factors and between-subject variability were identified in this study, especially for the non-modified respirator, which presents a challenge in identifying statistical significance.

Comparison of Four Facial Conditions (dry/wet, shaved/unshaved, one subject)

Four facial conditions were compared: dry-shaved face, wet-shaved face, dry-unshaved face, and wet-unshaved face. One subject (#T01) participated in this evaluation with the non-modified and modified masks with three repeats for each condition. The results are presented in Figure 5-4. The PMA modified respirator produced higher mean FFs under all tested conditions compared to the non-modified respirator. For example, for the wet-shaved facial condition, the modified half-mask achieved a mean FF of 23,241 compared with 267 for the non-modified half-mask. Even the least remarkable difference identified for the dry-unshaved face was an order of magnitude higher for the modified respirator (mean FF = 974 versus 95). Paired *t*-test results showed that the modified respirator had significantly ($p < 0.05$) higher mean FFs for all facial conditions (dry-shaved, wet-shaved, dry-unshaved, and wet-unshaved). These test results indicate that the surface of the PMA material improved contact against a facial skin under various challenge conditions (shaved, unshaved, dry, and wet).

When the non-modified respirator was tested with the dry skin condition, the fit was higher for the unshaved face than for the shaved face condition (mean FF = 95 vs.74). This observation was made from a single subject and contradicts the conventional wisdom and our own experience that an unshaved facial condition will compromise respirator fit. However, the

difference was not statistically significant ($p > 0.05$). In the clean-shaved condition, the non-modified respirator fit this subject poorly with a mean FF below 100. The effect of facial hair may be less significant when respirators fit poorly. When the same subject participated in the 25-subject panel with a clean shaven face, his fit factor was higher (FF = 197 from Figure 4). This demonstrates the potentially high variability between donnings and the limitation of single-subject generated data. With respect to facial hair, it was an important observation that the PMA modified respirator initially fit very well, but FF dropped significantly ($p < 0.05$) after 40 hours of stubble. Although this finding is once again from a single subject, it demonstrates the potentially adverse effect of facial hair when respirators initially fit well in a clean shaven condition.

Limitations

The non-modified respirator selected for this study had very good fitting characteristics prior to adding the adhesive surface. It is challenging to demonstrate statistically significant improvement in fit when the "referenced" respirator already fitted well in most of the tests. Additionally, improvement in fit created a situation whereby the number of in-facepiece particles detected by the instrument was very small, which increased the margin of error and decreased the confidence in the measured FFs. However, this concern should have affected both the modified and non-modified respirators similarly since the donning order was randomized. Another limitation was the lack of a "control" respirator consisting of a material with similar thickness and width applied to the sealing surfaces but without the surface characteristics of the PMA. Lastly, conclusions regarding improved performance of the modified respirator using different facial (un-shave and/or wet) are preliminary as they derived from only a single subject with three

replicate measurements. A follow-up study seems to be warranted to address the above limitations.

It would be interesting to see how a control respirator would perform when using a material of similar thickness and width applied to the sealing surfaces but without the surface characteristics of the PMA.

Conclusions

An elastomeric half-mask respirator was modified by applying a polymer micro-patterned adhesive (PMA) material to the sealing surface. Twenty-five subjects with dry and clean-shaven faces and facial dimensions representing the NIOHS bivariate panel were fit tested using the modified respirator and its non-modified version. The modified respirator produced a geometric mean fit factor of 7,907 with a GSD of 4.9 compared to 4,779 (GSD = 9.1) for the non-modified respirator (p =0.07, paired t-test). In addition, pilot data were generated by testing a single subject under various facial conditions (shaved, unshaved, dry, and wet). The modified half-mask prototype was consistently achieving significantly (p <0.05) higher fit factors than the conventional half-mask. Future studies are needed to include more subjects with various face dimensions along with different shaving and wetting/sweating conditions.

Overall, the addition of a polymer micro-patterned adhesive to the sealing surface of an elastomeric half-mask respirator showed potential for improving the fitting characteristics and possibly respirator performance with less than ideal facial conditions.

OVERALL CONCLUSIONS AND FUTURE DIRECTIONS

Overall Conclusions

In summary, the faceseal leakage, combustion material, particle size, breathing frequency and flow rate were all found to be significant factors affecting the performance of the tested respiratory protection devices including an elastomeric full facepiece, an elastomeric half-mask, an N95 FFR, and a surgical mask. The significant effect of the faceseal leakage was dominant for these respirators under all tested conditions (except the fully sealed condition), which means that in most cases the particles penetrated inside the respirator/mask primarily through the faceseal leak rather than the filter media. Combustion aerosol effect was significant when tested for the unsealed and partially sealed half-mask; the plastic aerosol produced the highest penetration values compare to the paper and wood combustion aerosols. Effect of particle size on the filter penetration was significant for all tested respirators, whereas its effect on the TIL was significant only for the unsealed and partially sealed half-mask but not for the FFR and SM at particle size > 50 nm. The breathing flow was another significant factor in affecting the P_{filter} and TIL for all tested respirators. Compared to breathing flow rate, breathing frequency effect was complex and less pronounced especially from the practical stand point, suggesting that breathing flow rate should be given the primary consideration when choosing a breathing condition during a respirator testing.

Considering the predominant role of faceseal leakage in the TIL, minimizing the leakage is seen as the most meaningful direction in an effort to design and develop respirators with improved performance. A novel elastomeric respirator, which is currently being developed by

industry, addresses the faceseal leakage issue by introducing a polymeric micro-patterned adhesive (PMA) tape applied along its peripheral area. Our evaluation of this respirator showed the new concept that involves utilizing PMA on the sealing surface was found promising for improving the fit performance of an elastomeric half-mask respirator.

A great amount of data were reported in this dissertation providing an extensive data base, which is useful for respirator manufacturers, regulatory agencies, respiratory protection researchers, and end-users operating in various occupational environments.

Research to Practice

This dissertation research suggests the following three practical applications:

1. An unsealed half-mask respirator may not provide high level of protection, especially when challenged with plastic combustion aerosol, primarily because of considerable particle penetration through faceseal leakage. Therefore, a better fit respirator (e.g., full facepiece) should be provided. This is particularly relevant to firefighters (during fire overhaul) and first responders. Exposure to aerosols originated by burning plastic may be of particular concern given higher penetration of plastic particles through elastomeric respirators compared to other materials.
2. When testing respirators on breathing manikins, a breathing flow rate (not a breathing frequency) should be considered as a primary factor when choosing a specific breathing condition.
3. The TIL results (obtained using the advanced manikin headform) indicate that for particles larger than 50 nm the particle size effect was not significant, and particles <

50 nm produced lower penetration than those > 50 nm. This finding suggests that size-selective measurement may not be necessary when performing the TIL test.

Future Directions

The following two main directions are being considered for the future research efforts:

1. The workplace protection factor (WPF) set-up will be developed and used for testing the conventional and newly-developed elastomeric respirators during field studies when firefighters perform training activities as well as the actual firefighting (the fire overhaul phase).
2. For the filtering facepiece respirators, a novel approach is being currently developed by industry that also aims at minimizing the faceseal leak by modifying the peripheral area, but in this case a different material (with thermo-reconfigurational properties) is being considered. The future studies (already initiated) will include the fit testing of the new respirators as well as the measurement of their WPF in different occupational environments.

REFERENCES

Anderson NJ, Cassidy PE, Janssen LL, Dengel DR. (2006) Peak Inspiratory Flows of Adults Exercising at Light, Moderate and Heavy Work Loads. J Int Soc Resp Prot; 23 53-63.

Bałazy A, Toivola M, Adhikari A, Sivasubramani SK, Reponen T, Grinshpun SA. (2006) Do N95 respirators provide 95% protection level against airborne viruses, and how adequate are surgical masks? Am J Infect Control; 34 51-57.

Bałazy A, Toivola M, Reponen T, Podgorski A, Zimmer A, Grinshpun SA. (2006) Manikin-Based Performance Evaluation of N95 Filtering-Facepiece Respirators Challenged with Nanoparticles. Ann Occup Hyg; 50 259-69.

Barnett SS, M. HP, Sabo KK, Scarberry EN. (1999) Respiratory Mask Facial Seal.

Baxter CS, Ross CS, Fabian T, Borgerson JL, Shawon J, Gandhi PD, Dalton JM, Lockey JE. (2010) Ultrafine Particle Exposure During Fire Suppression-Is It an Important Contributory Factor for Coronary Heart Disease in Firefighters? J Occup Environ Med; 52 791-96.

Beard M. (1994) Seal for Respiratory Mask.

Belfer WA, Petillo P. (1999) Strapless Respiratory Facial Mask for Customerizing to the Wearer's Face.

Bergman MS, Viscusi DJ, Zhuang Z, Newcomb WE. (2012) Evaluation of Sampling Probes for Fit Testing N95 Filtering Facepiece Respirators. Ann Occup Hyg.

Bergman MS, Zhuang Z, Wander J, Hanson D, Heimbuch BK, McDonald M, Palmiero A, Shaffer RE, Husband M. (2013) Development of an Advanced Respirator Fit Test Headform. (To be submitted).

BLS. (2003) US Bureau of Labor Statistics, Occupational Injuries and Illnesses in the US by Industry International Association of Firefighters. Washington, DC. 1995-1996.

BLS/NIOSH. (2003) “Respirator Usage in Private Sector Firms, 2001”U.S. Department of Labor, Bureau of Labor Statistics/U.S. Department of Health and Human Services, Public Health Service, Centers for Disease Control and Prevention, National Institute for Occupational Safety and Health

Bolstad-Johnson DM, Burgess JL, Crutchfield CD, Storment S, Gerkin R, Wilson JR. (2000) Characterization of Firefighter Exposures During Fire Overhaul. AIHAJ - American Industrial Hygiene Association; 61 636-41.

Brosseau LM. (2010) Fit testing respirators for public health medical emergencies. J Occup Environ Hyg; 7 628-32.

Brown RC. (1993) Air filtration: An integrated approach to the theory and applications of fibrous filters. Oxford: Pergamon Press; p.109, Book (ISBN 0080412742).

Burgess JL, Nanson CJ, Bolstad-Johnson DM, Gerkin R, Hysong TA, Lantz RC, Sherrill DL, Crutchfield CD, Quan SF, Bernard AM, et al. (2001) Adverse Respiratory Effects Following Overhaul in Firefighters. J Occup Environ Med; 43 467-73.

Castranova V, Ma J, Yang H-M, Antonini JM, Butterworth L, Barger MW, Roberts J, Ma J. (2001) Effect of exposure to diesel exhaust particles on the susceptibility of the lung to infection. Environ Health Perspect; 109 609.

CDC. (2006) Fatalities among volunteer and career firefighters—United States, 1994-2004. The Journal of the American Medical Association; 295 2594-96.

CFR. (1995. pp.30382-30383) Code of Federal Regulations Title 42, Part 84. "Respirator Protection".

Chen CC, Ruuskanen J, Pilacinski W, Willeke K. (1990) Filter and leak penetration characteristics of a dust and mist filtering facepiece. Am Ind Hyg Assoc J; 51 632-39.

Chen CC, Willeke K. (1992) Characteristics of face seal leakage in filtering facepieces. Am Ind Hyg Assoc J; 53 533-39.

Cho KJ, Jones S, Jones G, McKay R, Grinshpun SA, Dwivedi A, Shukla R, Singh U, Reponen T. (2010a) Effect of Particle Size on Respiratory Protection Provided by Two Types of N95 Respirators Used in Agricultural Settings. J Occup Environ Hyg; 7 622-27.

Cho KJ, Reponen T, McKay R, Shukla R, Haruta H, Sekar P, Grinshpun SA. (2010b) Large Particle Penetration through N95 Respirator Filters and Facepiece Leaks with Cyclic Flow. Ann Occup Hyg; 54 68-77.

Coffey CC, Lawrence RB, Zhuang Z, Campbell DL, Jensen PA, Myers WR. (2002) Comparison of five methods for fit-testing N95 filtering-facepiece respirators. Applied occupational and environmental hygiene; 17 723-30.

Coffey CC, Zhuang Z, Campbell, D.L. M, W.R. . (1998) Quantitative fit testing of N95 respirators: part II - results, effect of filter penetration, fit test, and pass/fail criteria. J Int Soc Resp Prot; 16(1-4) 25-36.

Collier L, Balows A, Sussman M. (1998) Topley and Wilson's Microbiology and Microbial Infections, Volume 1, Virology: Hodder Arnold Publishers.

Cooper DW, Hinds WC, Price JM, Weker R, Yee HS. (1983) Common materials for emergency respiratory protection: leakage tests with a manikin. Am Ind Hyg Assoc J; 44 720-26.

Crutchfield CD, Park DL. (1997) Effect of Leak Location on Measured Respirator Fit. Am Ind Hyg Assoc J; 58 413-18.

Del Campo A, Arzt E. (2007) Design parameters and current fabrication approaches for developing bioinspired dry adhesives. Macromol Biosci; 7 118-27.

del Campo A, Greiner C, Arzt E. (2007) Contact shape controls adhesion of bioinspired fibrillar surfaces. Langmuir; 23 10235-43.

Eninger RM, Honda T, Adhikari A, Heinonen-Tanski H, Reponen T, Grinshpun SA. (2008) Filter Performance of N99 and N95 Facepiece Respirators Against Viruses and Ultrafine Particles. Ann Occup Hyg; 52 385-96.

Eshbaugh JP, Gardner PD, Richardson AW, Hofacre KC. (2008) N95 and P100 Respirator Filter Efficiency Under High Constant and Cyclic Flow. J Occup Environ Hyg; 6 52-61.

Fahy R, LeBlanc P, Molis J. (2009) Firefighter fatalities in the United States - 2008. National Fire Protection Association, Quincy, MA.

Golshahi L, Telidetzki K, King B, Shaw D, Finlay WH. (2012) A pilot study on the use of geometrically accurate face models to replicate ex vivo N95 mask fit. Am J Infect Control.

Grafe T, Gogins M, Barris M, Schaefer J, Canepa R. (2001) "Nanofibers in Filtration Applications in Transportation". Filtration 2001 Conference Proceedings, Chicago, IL; 1-15.

Grinshpun SA, Haruta H, Eninger RM, Reponen T, McKay RT, Lee SA. (2009) Performance of an N95 filtering facepiece particulate respirator and a surgical mask during human breathing: two pathways for particle penetration. J Occup Environ Hyg; 6 593-603.

Han D-H, Lee J. (2005) Evaluation of Particulate Filtering Respirators Using Inward Leakage (IL) or Total Inward Leakage (TIL) Testing—Korean Experience. Ann Occup Hyg; 49 569-74.

Hanson D, Bergs R, Tadesse Y, White V, Priya S. (2006) Enhancement of EAP Actuated Facial Expressions by Designed Chamber Geometry in Elastomers. Proc. SPIE's Electroactive Polymer Actuators and Devices Conf., 10th Smart Structures and Materials Symposium, San Diego.

Hanson D, Priya S. (2007) An Actuated Skin for Robotic Facial Expressions, NSF Phase 1 Final Report. National Science Foundation STTR award, NSF 05-557.

Hanson D, White V. (2004) Converging the Capabilities of ElectroActive Polymer Artificial Muscles and the Requirements of Bio-inspired Robotics. Proc. SPIE's Electroactive Polymer Actuators and Devices Conf., 10th Smart Structures and Materials Symposium, San Diego.

Haruta H, Honda T, Eninger RM, Reponen T, McKay R, Grinshpun SA. (2008) Experimental and theoretical investigation of the performance of N95 respirator filters against ultrafine aerosol particles tested at constant and cyclic flows. J Int Soc Resp Prot; 25 75-88.

He X, Grinshpun SA, Reponen T, McKay R, Bergman SM, Zhuang Z. (2013c) Effect of Breathing Frequency on the Total Inward Leakage of an Elastomeric Half-Mask Donned on an Advanced Manikin Headform. Submitted to the Annals of Occupational Hygiene.

He X, Grinshpun SA, Reponen T, Yermakov M, McKay R, Haruta H, Kimura K. (2013a) Laboratory Evaluation of the Particle Size Effect on the Performance of an Elastomeric Half-mask Respirator against Ultrafine Combustion Particles. (Accepted). Annals of Occupational Hygiene.

He X, Reponen T, McKay R, Grinshpun SA. (2013d) How does breathing frequency affect the performance of an N95 filtering facepiece respirator and a surgical mask against surrogates of viral particles? (Submitted). Am J Infect Control.

He X, Yermakov M, Reponen T, McKay RT, James K, Grinshpun SA. (2013b) Manikin-based performance evaluation of elastomeric respirators against combustion particles. J Occup Environ Hyg; 10 203-12.

Hinds WC, Bellin P. (1987) Performance of Dust Respirators with Facial Seal Leaks: II. Predictive Model. Am Ind Hyg Assoc J; 48 842-47.

Hinds WC, Kraske G. (1987) Performance of Dust Respirators with Facial Seal Leaks: I. Experimental. Am Ind Hyg Assoc J; 48 836-41.

Holton PM, Tackett DL, Willeke K. (1987) Particle Size-Dependent Leakage and Losses of Aerosols in Respirators. Am Ind Hyg Assoc J; 48 848-54.

Huang S-H, Chen C-W, Chang C-P, Lai C-Y, Chen C-C. (2007) Penetration of 4.5 nm to aerosol particles through fibrous filters. J Aerosol Sci; 38 719-27.

IOM. (2008) Institute of Medicine. Preparing for an Influenza Pandemic: Personal Protective Equipment for Healthcare Workers.

Kim S, Sitti M. (2006) Biologically inspired polymer microfibers with spatulate tips as repeatable fibrillar adhesives. Applied Physics Letters; 89.

Ksiazek TG, Erdman D, Goldsmith CS, Zaki SR, Peret T, Emery S, Tong S, Urbani C, Comer JA, Lim W, et al. (2003) A Novel Coronavirus Associated with Severe Acute Respiratory Syndrome. N Engl J Med; 348 1953-66.

Kulkarni P, Baron PA, Willeke K. (2011) Aerosol Measurement - Principles, Techniques, and Applications, 3rd Edition. John Wiley & Sons, New Jersey.

Lafortuna CL, Minetti AE, Mognoni P. (1984) Inspiratory flow pattern in humans. J Appl Physiol; 57 1111-19.

Lam C-W, James JT, McCluskey R, Hunter RL. (2004) Pulmonary Toxicity of Single-Wall Carbon Nanotubes in Mice 7 and 90 Days After Intratracheal Instillation. Toxicol Sci; 77 126-34.

Lawrence RB, Duling MG, Calvert CA, Coffey CC. (2006) Comparison of Performance of Three Different Types of Respiratory Protection Devices. J Occup Environ Hyg; 3 465-74.

Lee MC, Takaya S, Long R, Joffe AM. (2008a) Respirator Fit Testing: Does It Ensure the Protection of Healthcare Workers Against Respirable Particles Carrying Pathogens? Infect Control Hosp Epidemiol; 29 1149-56.

Lee S-A, Adhikari A, Grinshpun SA, McKay R, Shukla R, Zeigler HL, Reponen T. (2005a) Respiratory Protection Provided by N95 Filtering Facepiece Respirators Against Airborne Dust and Microorganisms in Agricultural Farms. J Occup Environ Hyg; 2 577-85.

Lee S-A, Grinshpun SA, Adhikari A, Li W, McKay ROY, Maynard A, Reponen T. (2005b) Laboratory and Field Evaluation of a New Personal Sampling System for Assessing the Protection Provided by the N95 Filtering Facepiece Respirators against Particles. Ann Occup Hyg; 49 245-57.

Lee SA, Grinshpun SA, Reponen T. (2008b) Respiratory performance offered by N95 respirators and surgical masks: human subject evaluation with NaCl aerosol representing bacterial and viral particle size range. Ann Occup Hyg; 52 177-85.

LeMasters GK, Genaidy AM, Succop P, Deddens J, Sobeih T, Barriera-Viruet H, Dunning K, Lockey J. (2006) Cancer Risk Among Firefighters: A Review and Meta-analysis of 32 Studies. J Occup Environ Med; 48 1189-202.

Leonard SS, Castranova V, Chen BT, Schwegler-Berry D, Hoover M, Piacitelli C, Gaughan DM. (2007) Particle size-dependent radical generation from wildland fire smoke. Toxicology; 236 103-13.

Linak WP, Ryan JV, Perry E, Williams RW, DeMarini DM. (1989) Chemical and biological characterization of products of incomplete combustion from the simulated field burning of agricultural plastic. International Journal of Air Pollution Control and Waste Management; 39 836-46.

Lu J, Soroushian P. (2012) Micropatterned Structures for Forming a Seal with the Face Skin and other Surfaces and Method of Make, US Patent Application. US Patent Application.

Mandell GL, Bennett JE, Dolin RD. (1995) Principles and practice of infectious diseases. New York: Churchill Livingstone.

Martin SB, Moyer ES. (2000) Electrostatic Respirator Filter Media: Filter Efficiency and Most Penetrating Particle Size Effects. Appl Occup Environ Hyg; 15 609-17.

Materna BL, Jones JR, Sutton PM, Rothman N, Harrison RJ. (1992) OCCUPATIONAL EXPOSURES IN CALIFORNIA WILDLAND FIRE FIGHTING. Am Ind Hyg Assoc J; 53 69-76.

Musk AW, Peters JM, Bernstein L, Rubin C, Monroe CB. (1982) Pulmonary function in firefighters: A six-year follow-up in the boston fire department. Am J Ind Med; 3 3-9.

Myers WR, Allender JR, Iskander W, Stanley C. (1988) Causes of In-Facepiece Sampling Bias - I. Half-Facepiece Respirators. Ann Occup Hyg; 32 345-59.

Myers WR, Kim H, Kadrichu N. (1991) Effect of particle size on assessment of faceseal leakage. J Int Soc Resp Prot; 6-21.

Myers WR, Zhuang Z. (1998) Field Performance Measurements of Half-Facepiece Respirators: Developing Probability Estimates to Evaluate the Adequacy of an APF of 10. Am Ind Hyg Assoc J; 59 796-801.

Myers WR, Zhuang Z, Nelson T. (1996) Field Performance Measurements of Half-Facepiece Respirators - Foundry Operations. Am Ind Hyg Assoc J; 57 166-74.

NFPA. (1981) National Fire Protection Association. Standard on Open-Circuit Self-Contained Breathing Apparatus (SCBA) for Emergency Services, 2007 Edition.

NIOSH. (1995) National Institute for Occupational Safety and Health. US DHHS, Public Health Service. "Respiratory Protective Devices; Final Rules and Notices" Federal Register 60:110, pp 30335-30393.

NIOSH. (2007) National Institute for Occupational Safety and Health. NIOSH document: Preventing fire fighter fatalities due to heart attacks and other sudden cardiovascular events 2007-133

NIOSH. (2009) National Institute for Occupational Safety and Health. "Total Inward Leakage for Half-mask Air-purifying Respirators,"

NIOSH/CDC. (2009) National Institute for Occupational Safety and Health. US DHHS, Public Health Service. "Total Inward Leakage for Half-mask Air-purifying Respirators".

Oestenstad RK, Bartolucci AA. (2010) Factors Affecting the Location and Shape of Face Seal Leak Sites on Half-Mask Respirators. J Occup Environ Hyg; 7 332-41.

Oestenstad RK, Elliott LJ, Beasley TM. (2007) The Effect of Gender and Respirator Brand on the Association of Respirator Fit with Facial Dimensions. J Occup Environ Hyg; 4 923-30.

Oestenstad RK, Perkins LL. (1992) An assessment of critical anthropometric dimensions for predicting the fit of a half-mask respirator. Am Ind Hyg Assoc J; 53 639-44.

OSHA. (2006) Occupational Safety & Health Administration. "Respirator Protection", 29 CFR 1910.134.

OSHA. (2007) Occupational Safety & Health Administration. Pandemic influenza preparedness and response guidance for healthcare workers and healthcare employers.

Parker F. (2011) Respirator fit testing for H1N1 Flu protection. Journal of Chemical Health and Safety; 18 2.

Peters A, Wichmann HE, Tuch T, Heinrich J, Heyder J. (1997) Respiratory effects are associated with the number of ultrafine particles. Am J Respir Crit Care Med; 155 1376-83.

Qian Y, Willeke K, Grinshpun SA, Donnelly J, Coffey CC. (1998) Performance of N95 Respirators: Filtration Efficiency for Airborne Microbial and Inert Particles. Am Ind Hyg Assoc J; 59 128-32.

Qu LT, Dai LM, Stone M, Xia ZH, Wang ZL. (2008) Carbon nanotube arrays with strong shear binding-on and easy normal lifting-off. Science; 322 238-42.

Rengasamy S, Eimer BC. (2011) Total Inward Leakage of Nanoparticles Through Filtering Facepiece Respirators. Ann Occup Hyg; 55 253-63.

Rengasamy S, Eimer BC, Shaffer RE. (2009) Comparison of Nanoparticle Filtration Performance of NIOSH-approved and CE-Marked Particulate Filtering Facepiece Respirators. Ann Occup Hyg; 53 117-28.

Rengasamy S, King WP, Eimer BC, Shaffer RE. (2008) Filtration Performance of NIOSH-Approved N95 and P100 Filtering Facepiece Respirators Against 4 to 30 Nanometer-Size Nanoparticles. J Occup Environ Hyg; 5 556-64.

Reponen T, Lee S-A, Grinshpun SA, Johnson E, McKay R. (2011) Effect of Fit Testing on the Protection Offered by N95 Filtering Facepiece Respirators Against Fine Particles in a Laboratory Setting. Ann Occup Hyg; 55 264-71.

Richardson A, Wang A, Hofacre K. (2007) Development of Skin-Like Material to Accommodate Respirator Sealing with Manikin Head Forms.

Roberge RJ, Coca A, Williams WJ, Powell JB, Palmiero AJ. (2010) Reusable elastomeric air-purifying respirators: Physiologic impact on health care workers. Am J Infect Control; 38 381-86.

S. Y. Son, J. Y. Lee, H. Fu, S. Anand, F. Romay, Collins A. (2011) "Personal and Wearable Ultrafine Particle Counter". Proceedings of the AAAR 30th Annual Conference, American Association for Aerosol Research, October 03-07, 2011, Orlando, Florida, USA.

Schulte P, Geraci C, Zumwalde R, Hoover M, Kuempel E. (2008) Occupational Risk Management of Engineered Nanoparticles. J Occup Environ Hyg; 5 239-49.

Schwartz J, Dockery DW, Neas LM. (1996) Is Daily Mortality Associated Specifically with Fine Particles? Journal of the Air & Waste Management Association; 46 927-39.

Shaffer R, Rengasamy S. (2009) Respiratory protection against airborne nanoparticles: a review. Journal of Nanoparticle Research; 11 1661-72.

Sherwood L. (2006) Fundamentals of Physiology: A Human Perspective. Thomson Brooks/Cole, p380.

Shvedova AA, Kisin ER, Mercer R, Murray AR, Johnson VJ, Potapovich AI, Tyurina YY, Gorelik O, Arepalli S, Schwegler-Berry D, et al. (2005) Unusual inflammatory and fibrogenic pulmonary

responses to single-walled carbon nanotubes in mice. Am J Physiol Lung Cell Mol Physiol; 289 L698-L708.

Stafford RG, Ettinger HJ, Rowland TJ. (1973) Respirator Cartridge Filter Efficiency under Cyclic- and Steady-Flow Conditions. Am Ind Hyg Assoc J; 34 182-92.

Starr EW, Starr JR, Walthour MT. (1996) Respiratory Mask Facial Seal.

Timonen KL, Vanninen E, de Hartog J, Ibald-Mulli A, Brunekreef B, Gold DR, Heinrich J, Hoek G, Lanki T, Peters A, et al. (2005) Effects of ultrafine and fine particulate and gaseous air pollution on cardiac autonomic control in subjects with coronary artery disease: The ULTRA study. J Expos Sci Environ Epidemiol; 16 332-41.

Tortora GJ, Anagnostakos NP. (1990) Principles of Anatomy and Physiology, 6th edition, New York: Harper-Collins. p.707

Tuomi T. (1985) Face seal leakage of half-masks and surgical masks. Am Ind Hyg Assoc J; 46 308-12.

UL. (2010) Underwriters Laboratories Inc., Firefighter Exposure to Smoke Particulates, http://www.ul.com/global/documents/offerings/industries/buildingmaterials/fireservice/WEBDOCUMENTS/EMW-2007-FP-02093.pdf (Accessed on Nov.15, 2012).

Wang A, Richardson AW, Hofacre KC. (2012) The Effect of Flow Pattern on Collection Efficiency of Respirator Filters. J Int Soc Resp Prot; 29 41.

FIGURES

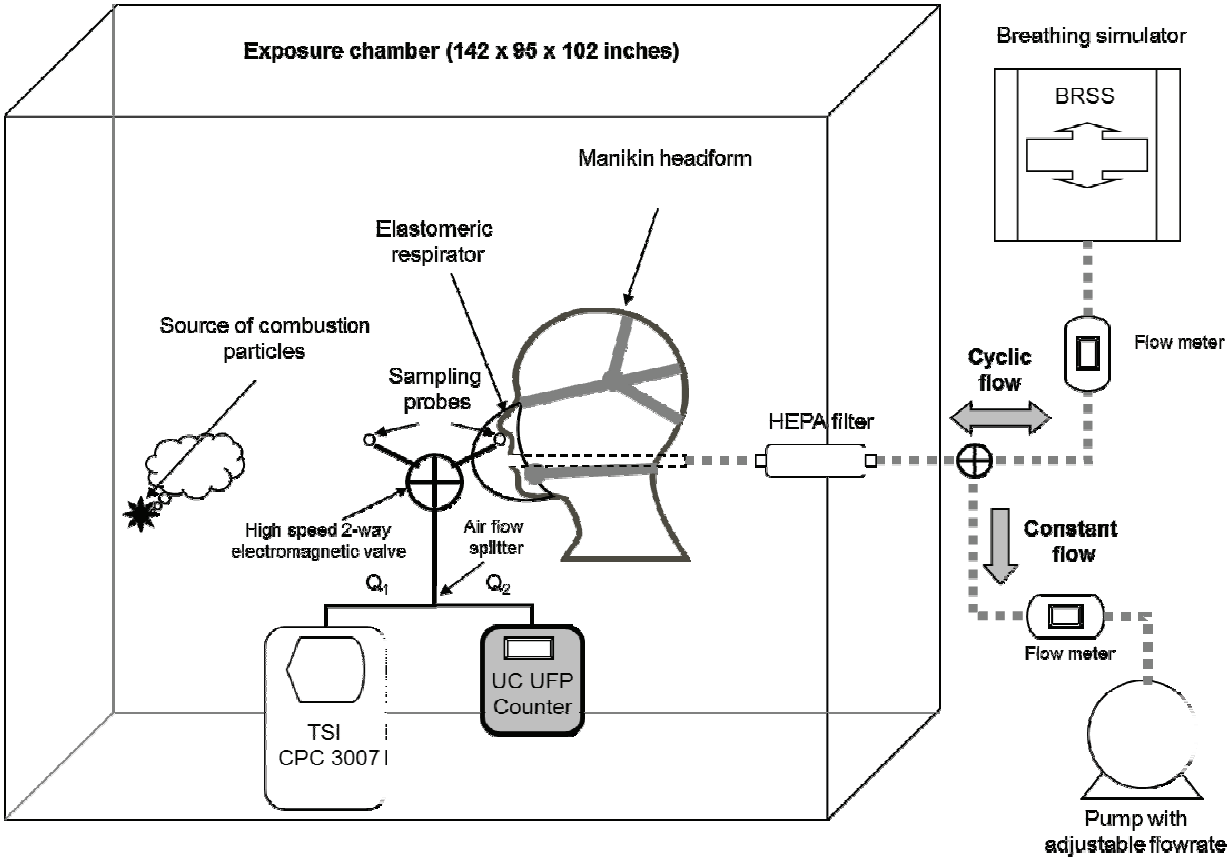

Figure 1-1. Experimental setup.

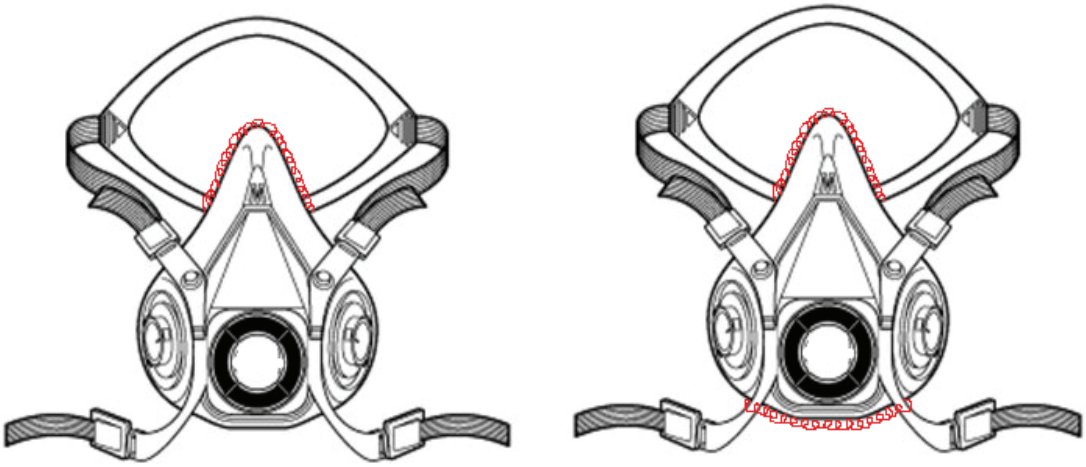

Figure 1-2. "Nose-only" and "nose & chin" sealed half-mask respirators. Respirator total length: 16 inches. Nose-only sealed length: 5 inches. Nose & chin sealed length: 4 inches.

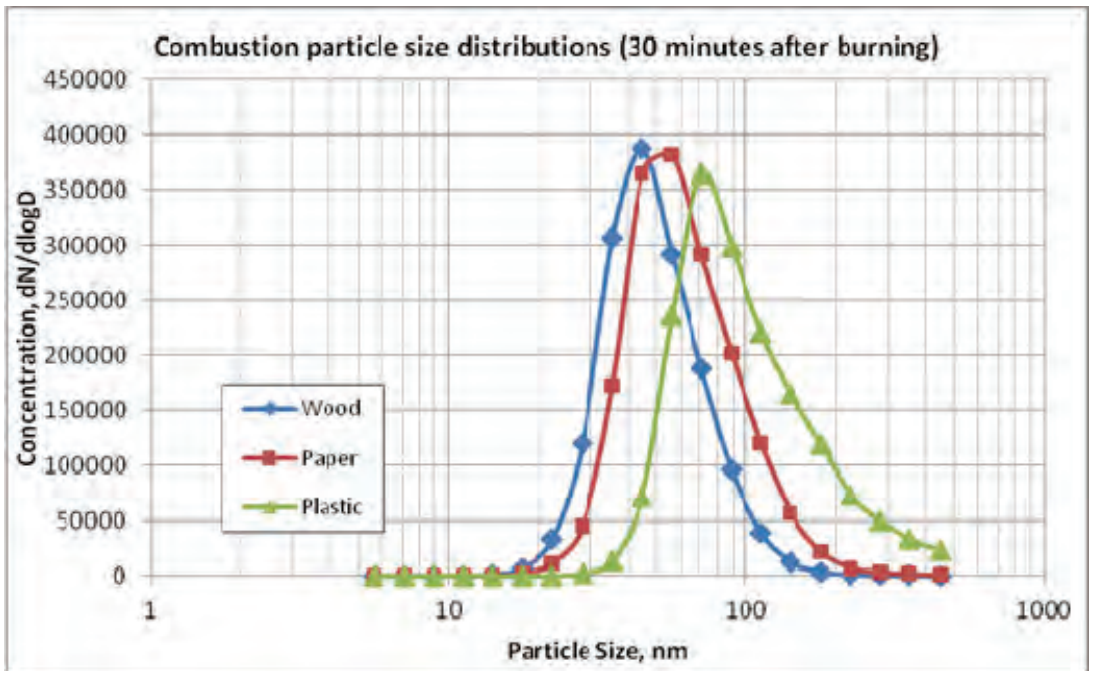

Figure 1-3. Size distributions of particles aerosolized from combustion of three tested materials: wood, paper and plastic. The measurement with a Nanoparticle Spectrometer was initiated 30 minutes after burning.

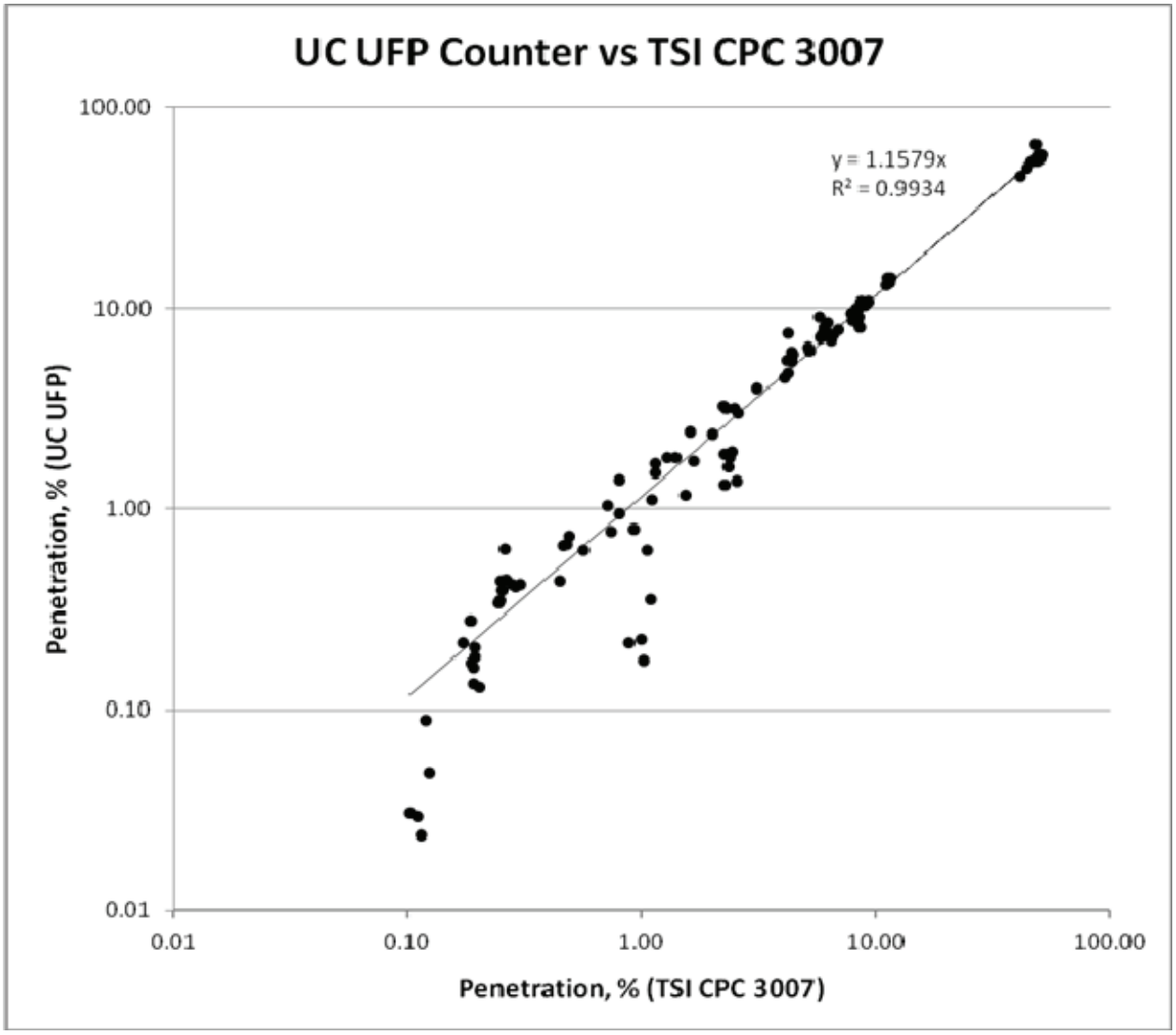

Figure 1-4. Comparison of particle penetration data obtained from the UC UFP counter and the TSI CPC 3007.

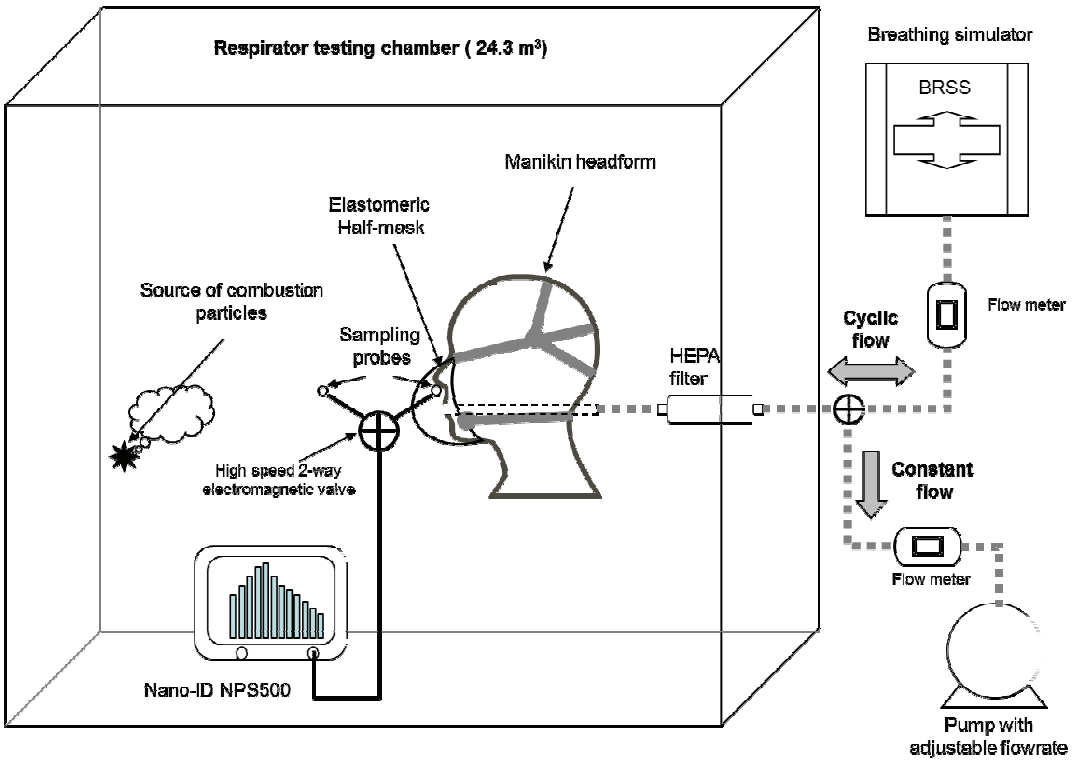

Figure 2-1. Schematic diagram of the experimental set-up (modified from He *et al.*, 2013).

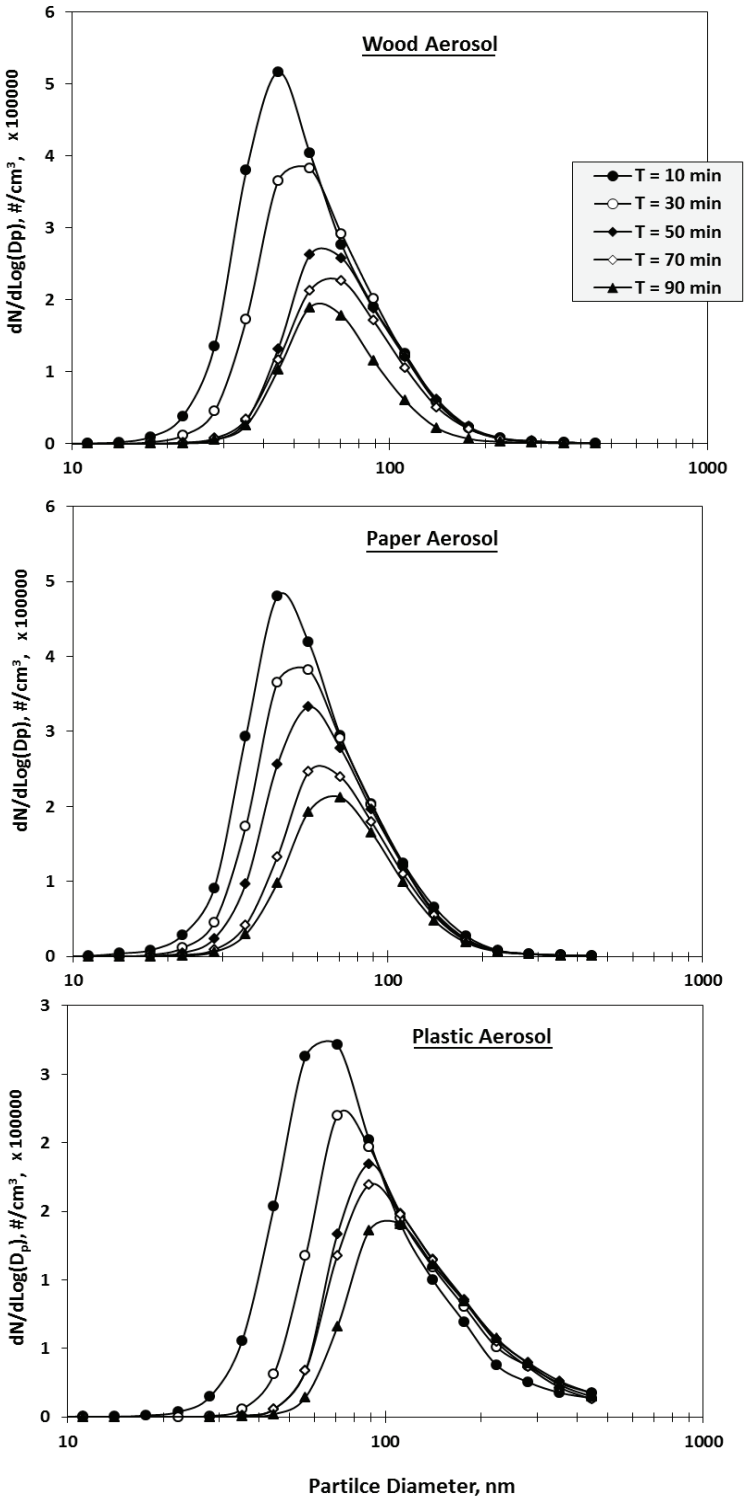

Figure 2-2. Particle size distributions of three combustion aerosols (wood, paper, and plastic) measured at 10, 30, 50, 70, and 90 minutes after the material burning stopped.

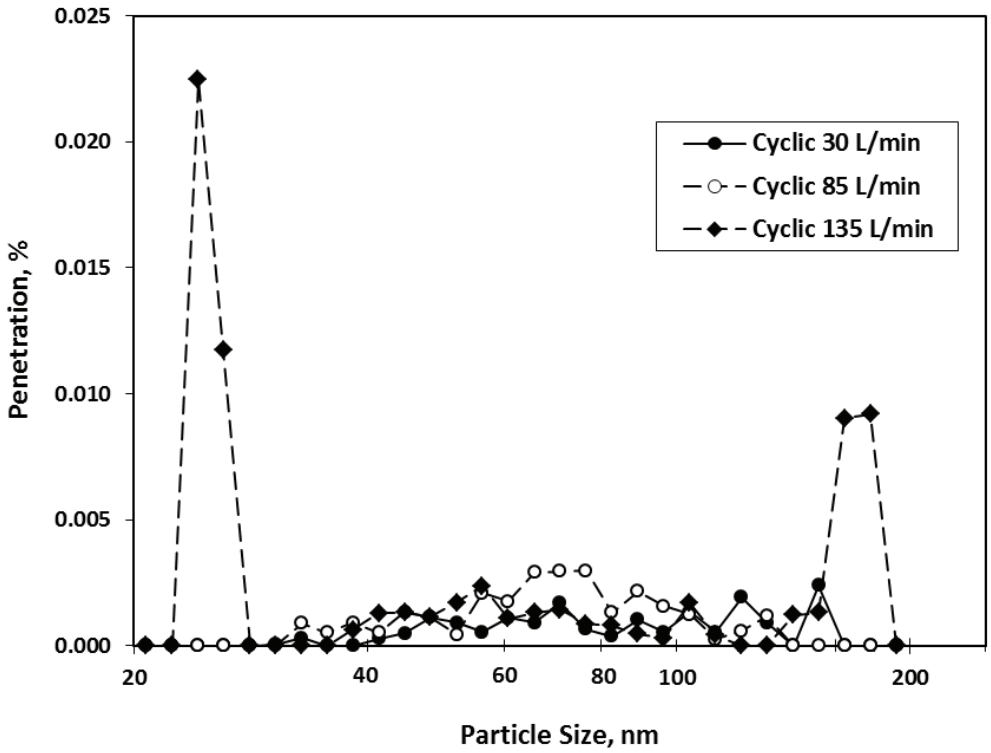

Figure 2-3. Penetration of wood combustion aerosol through a fully sealed half-mask equipped with two P-100 filters. Each data point represents the average of four replicates.

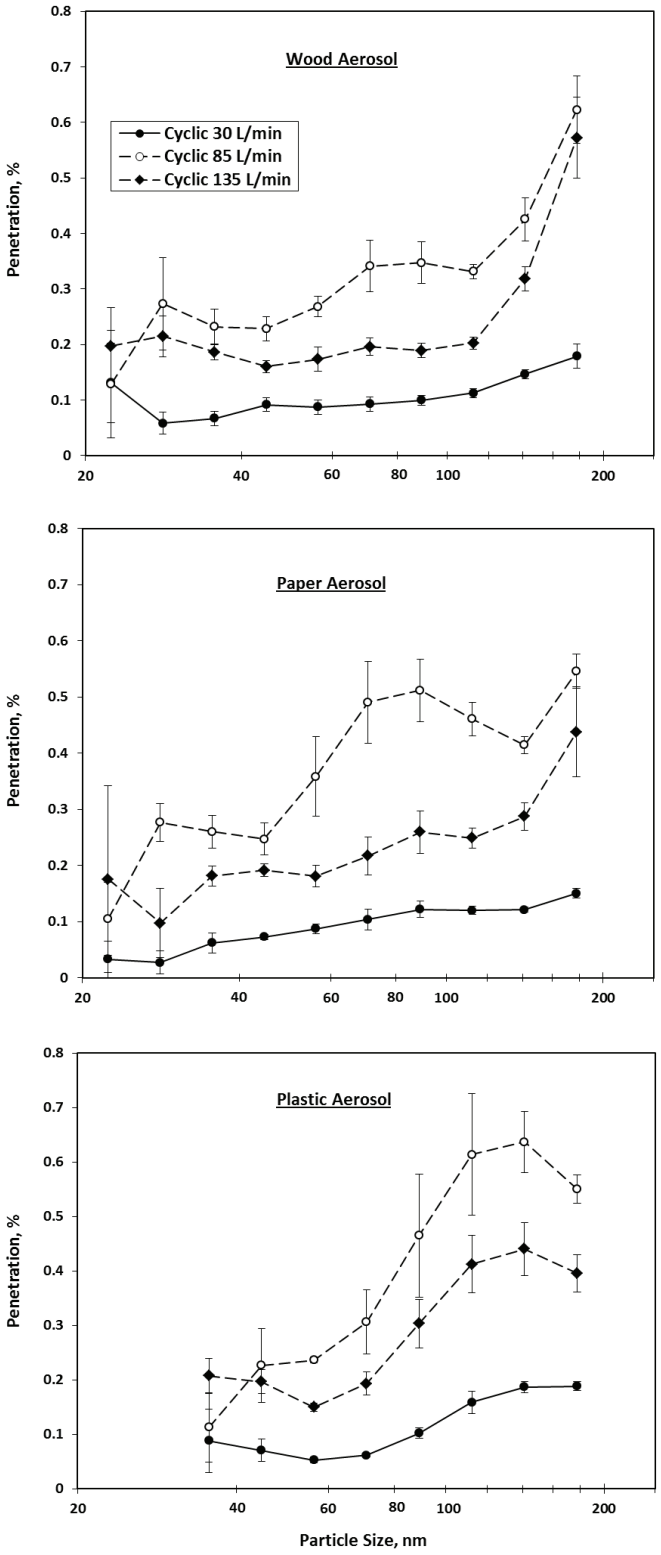

Figure 2-4. Penetration of wood, paper and plastic combustion aerosols through a partially sealed (nose area) half-mask equipped with two P-100 filters. Each point represents the average value of four replicates, and the error bar represents the standard error of the mean.

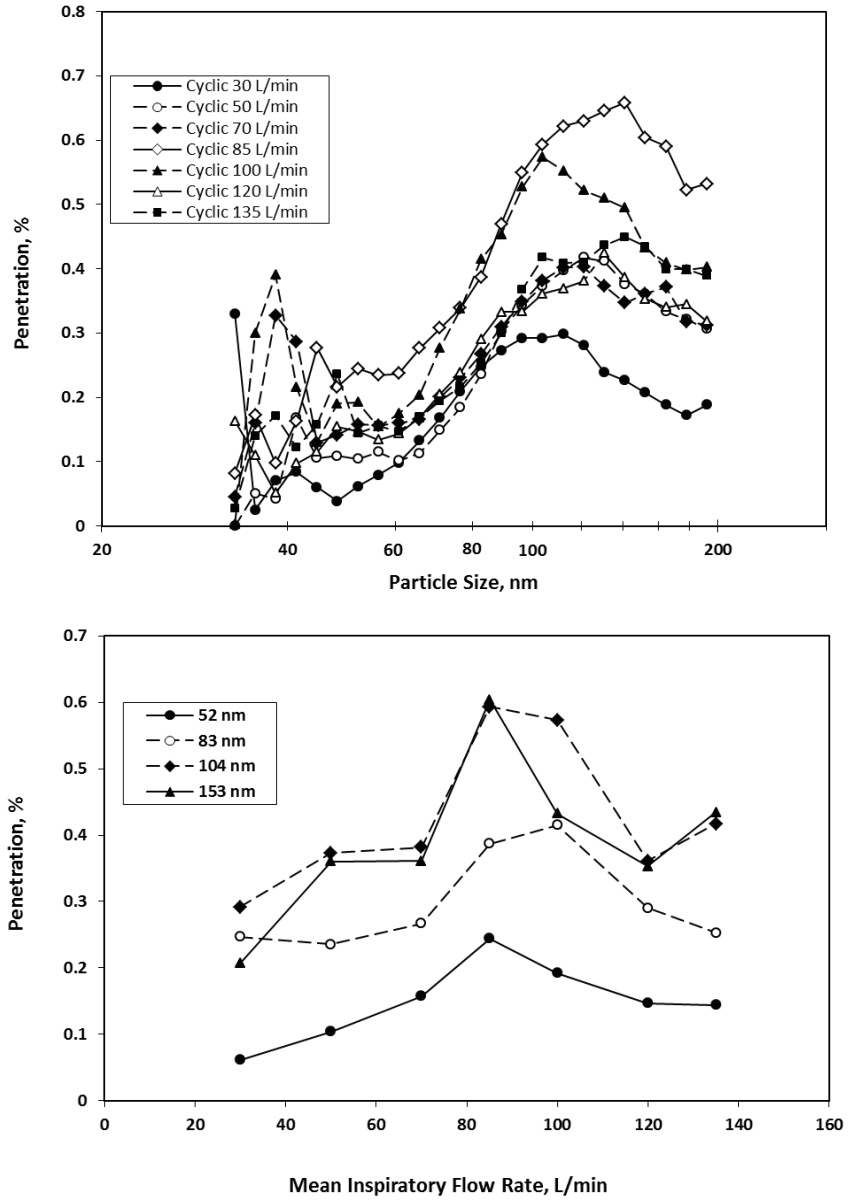

Figure 2-5. Penetration of plastic combustion particles through a partially sealed (nose area) half-mask equipped with two P-100 filters: dependence on particle size for fixed MIFs (upper figure), and dependence on the MIF for fixed particle sizes (lower figure). Each point represents the average value of four replicates.

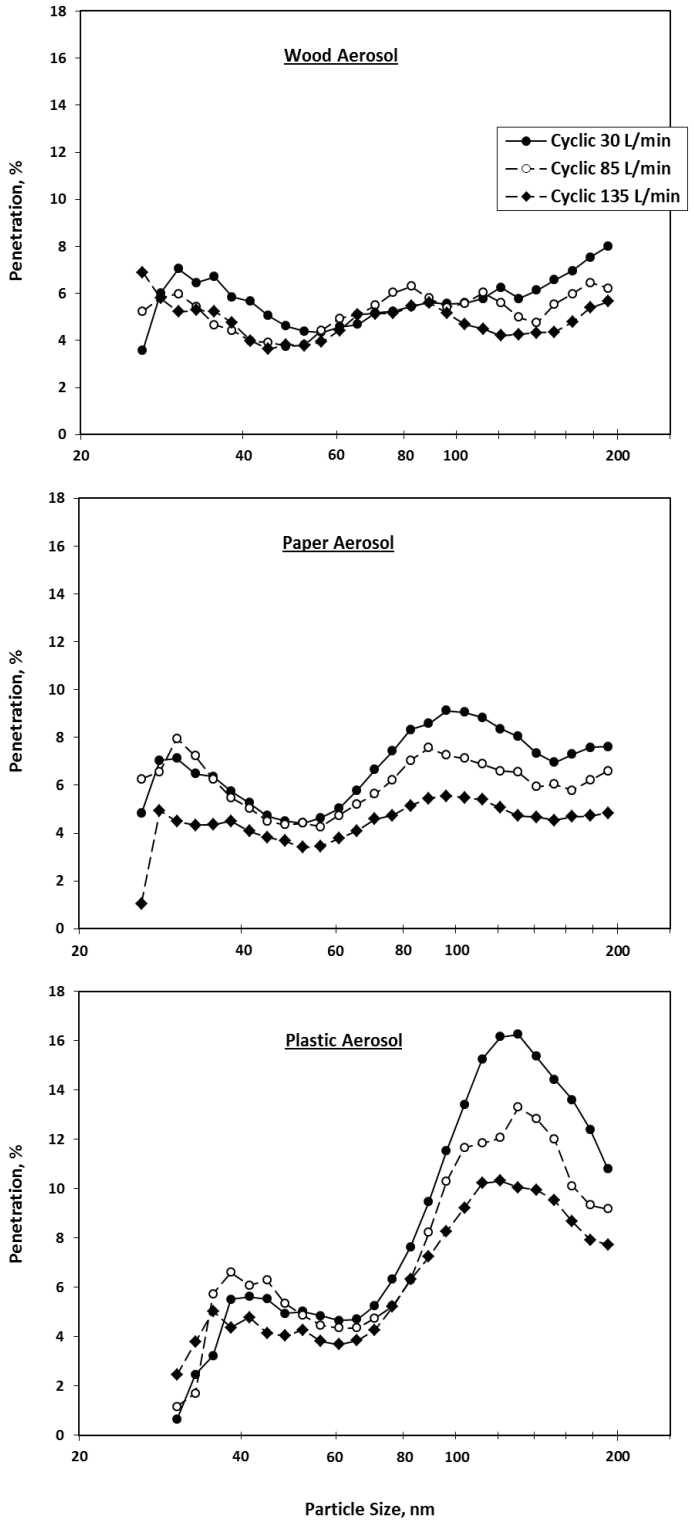

Figure 2-6. Penetration of wood, paper and plastic combustion aerosols through an unsealed half-mask equipped with two P-100 filters. Each point represents the average value of four replicates.

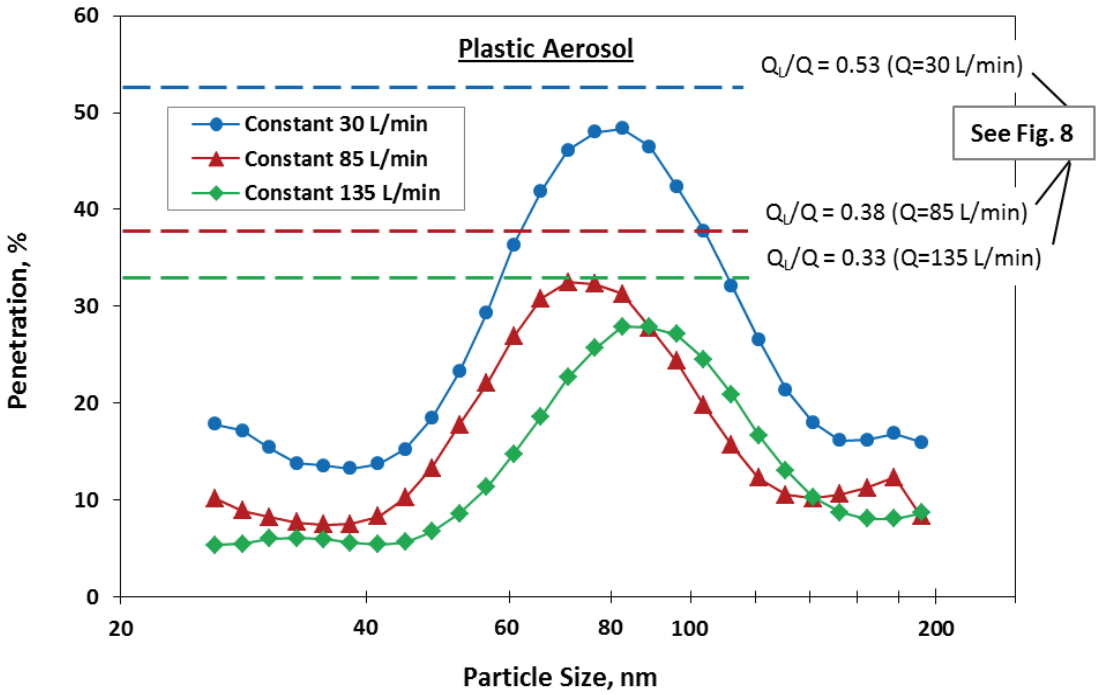

Figure 2-7. Penetration of the plastic combustion aerosol through an unsealed half-mask equipped with two P-100 filters under constant flow regime. Each point represents the average value of four replicates. Additionally, the graph shows three straight dotted lines representing Q_L/Q values at Q = 30, 85, and 135 L/min, which correspond to the maximum particle penetrations at these flow rates, as determined from Fig. 8.

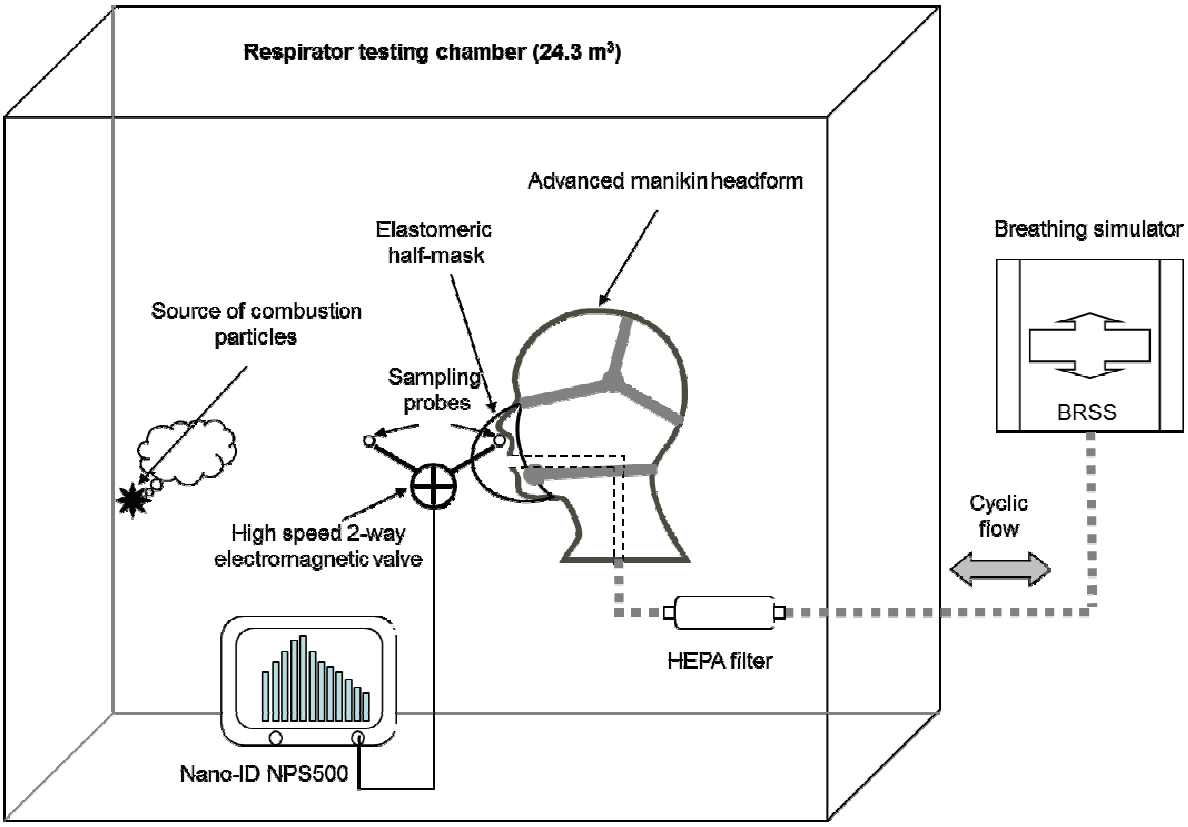

Figure 3-1. Schematic diagram of the experimental set-up (modified from He *et al.*, 2013a).

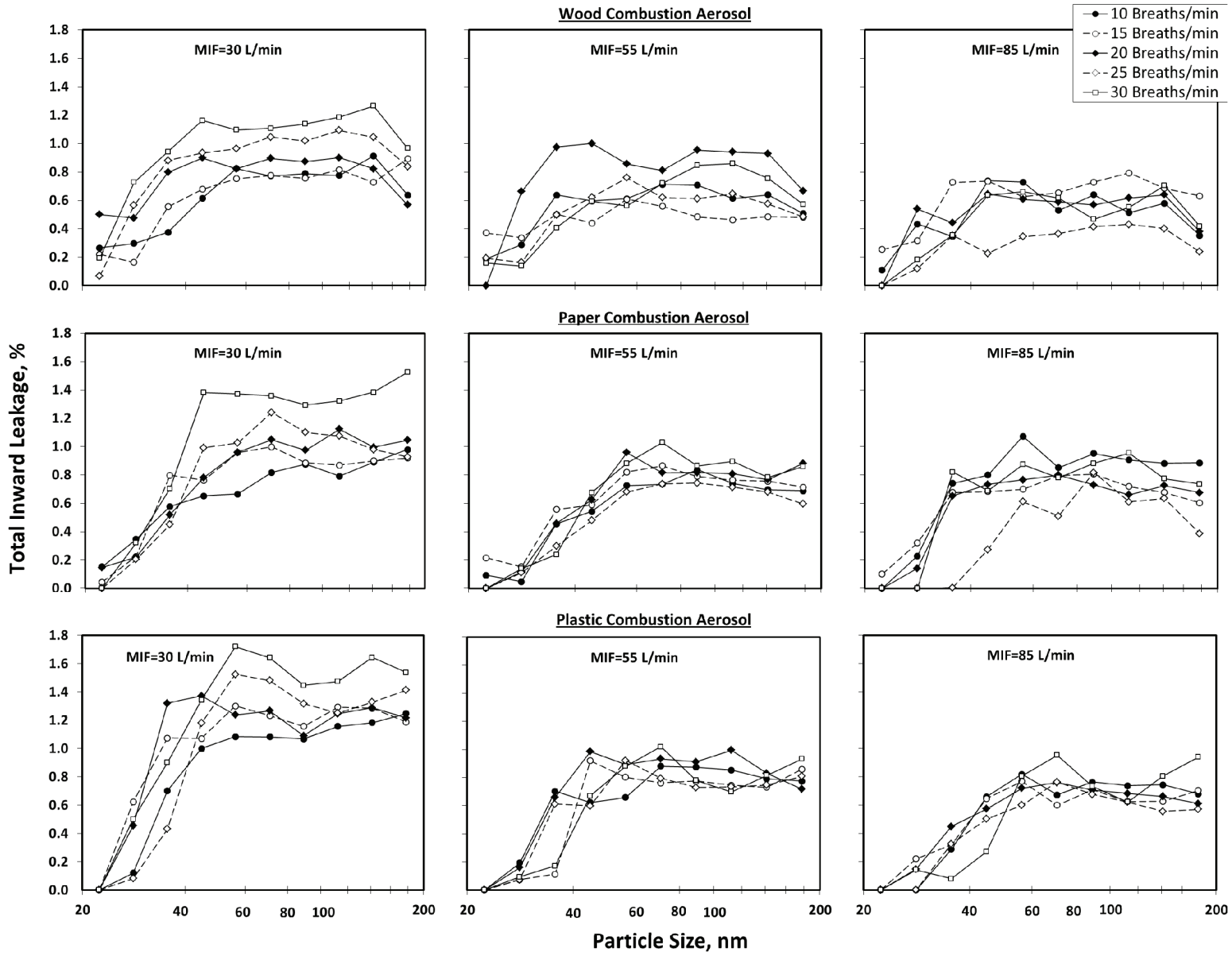

Figure 3-2. Size-selective total inward leakage values for an elastomeric half-mask respirator donned an advanced manikin headform while challenged with three combustion aerosols (wood, paper and plastic). Each point represents the average value of four replicates.

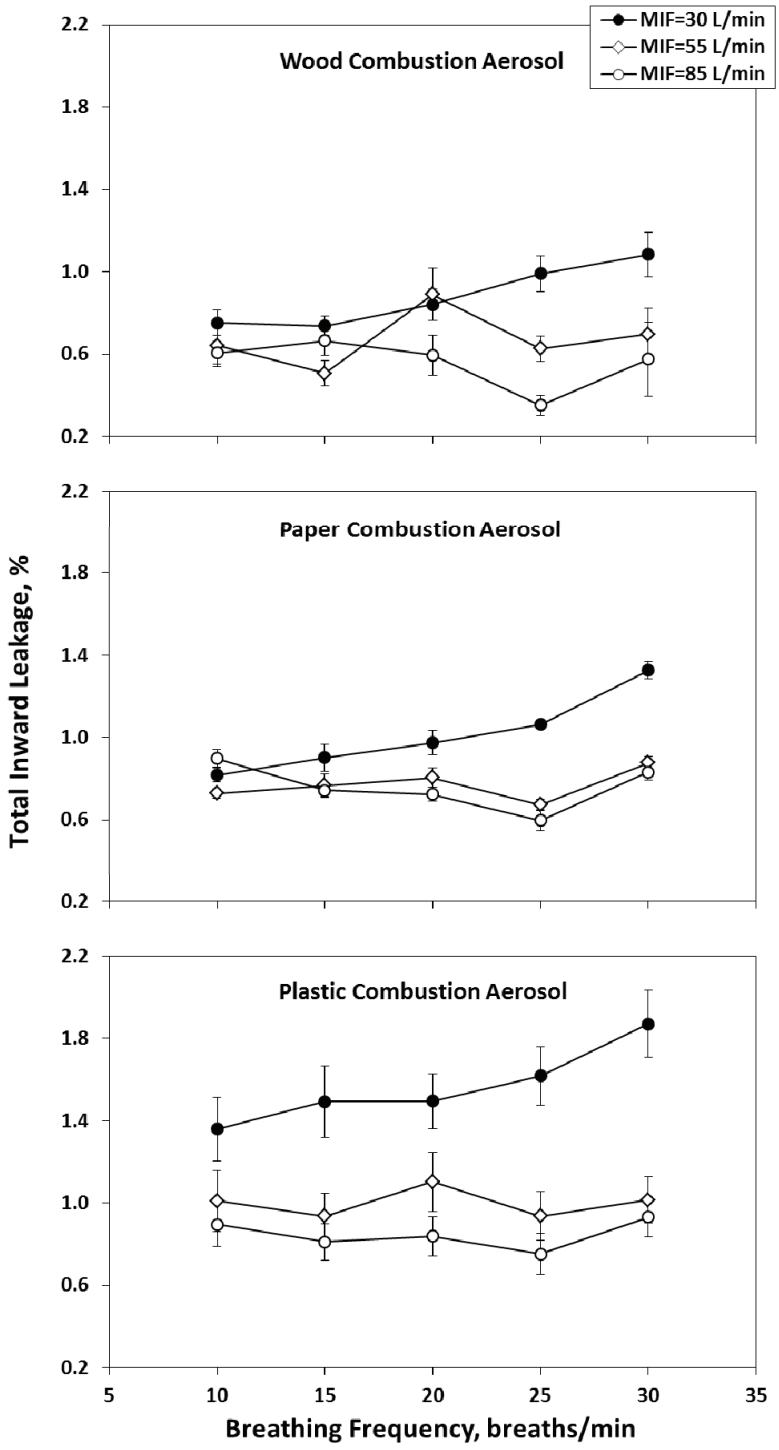

Figure 3-3. Size-independent (overall) total inward leakage values for an elastomeric half-mask respirator donned an advanced manikin headform while challenged with three combustion aerosols (wood, paper and plastic). Each point represents the average value of four replicates after combining all the channels between 20 to 200 nm, and the error bar represents the standard error of the mean.

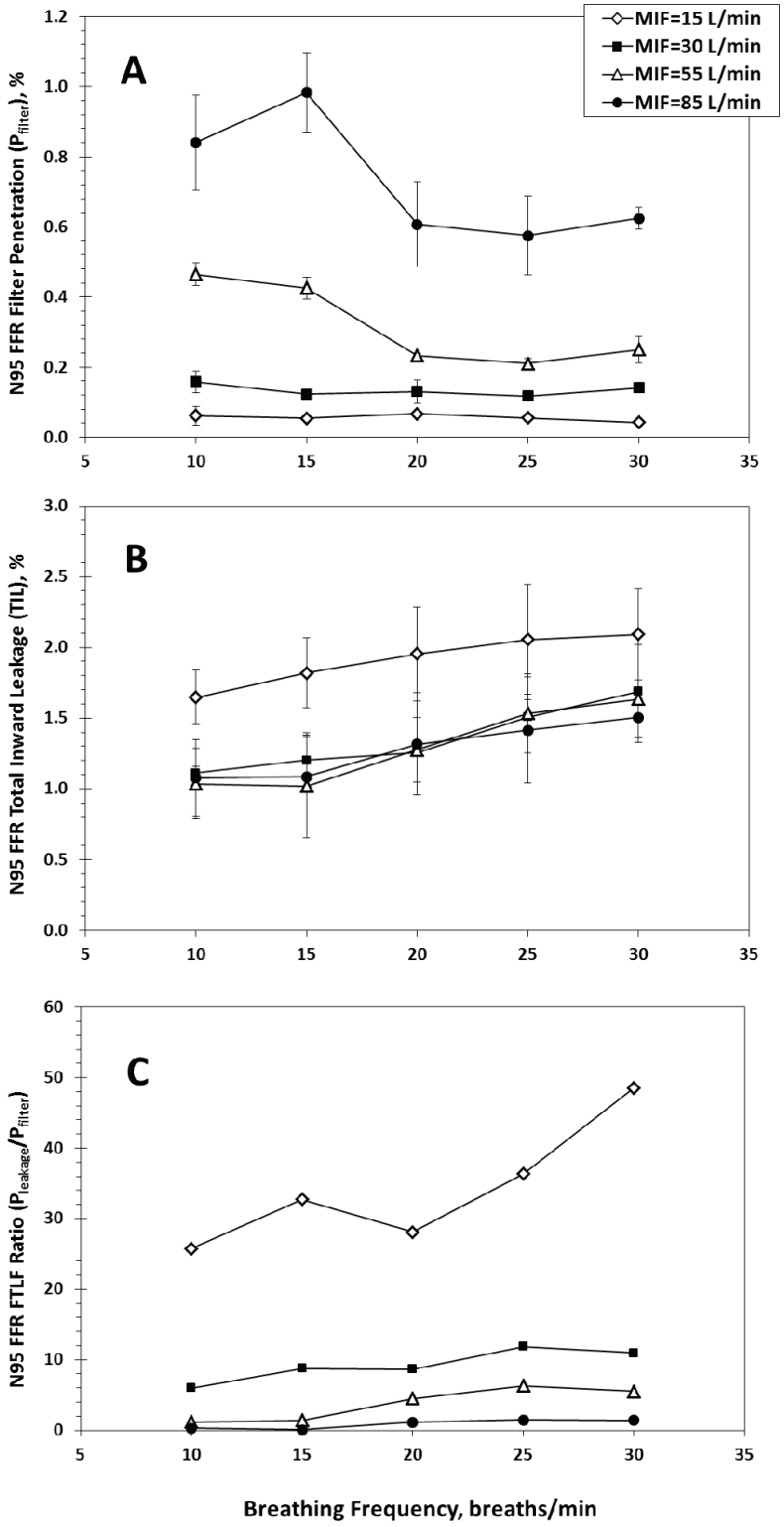

Figure 4-1. Filter penetration (A), Total Inward Leakage (TIL) (B), and faceseal leakage-to-filter (*FLTF*) ratio (C) for an N95 FFR sealed to a plastic manikin's face. No error bars for *FLTF* ratio as it was calculated from the mean $P_{leakage}$ (over 3 replicates) divided by the mean P_{filter} (over 3 replicates).

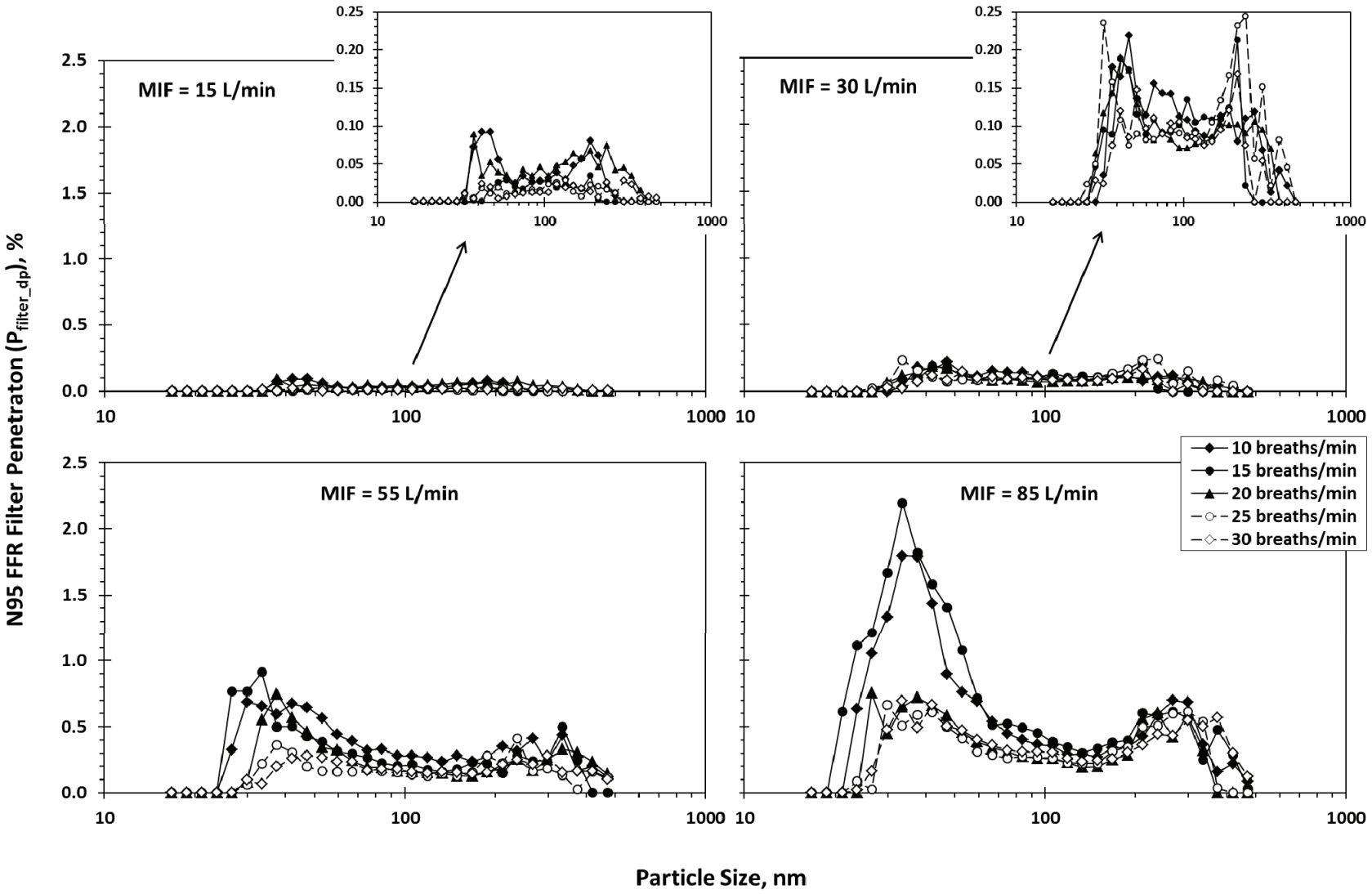

Figure 4-2. Size-specific filter penetration for an N95 FFR sealed to a plastic manikin's face while challenged with charge-equilibrated NaCl particles. Each point represents the mean value of three replicates.

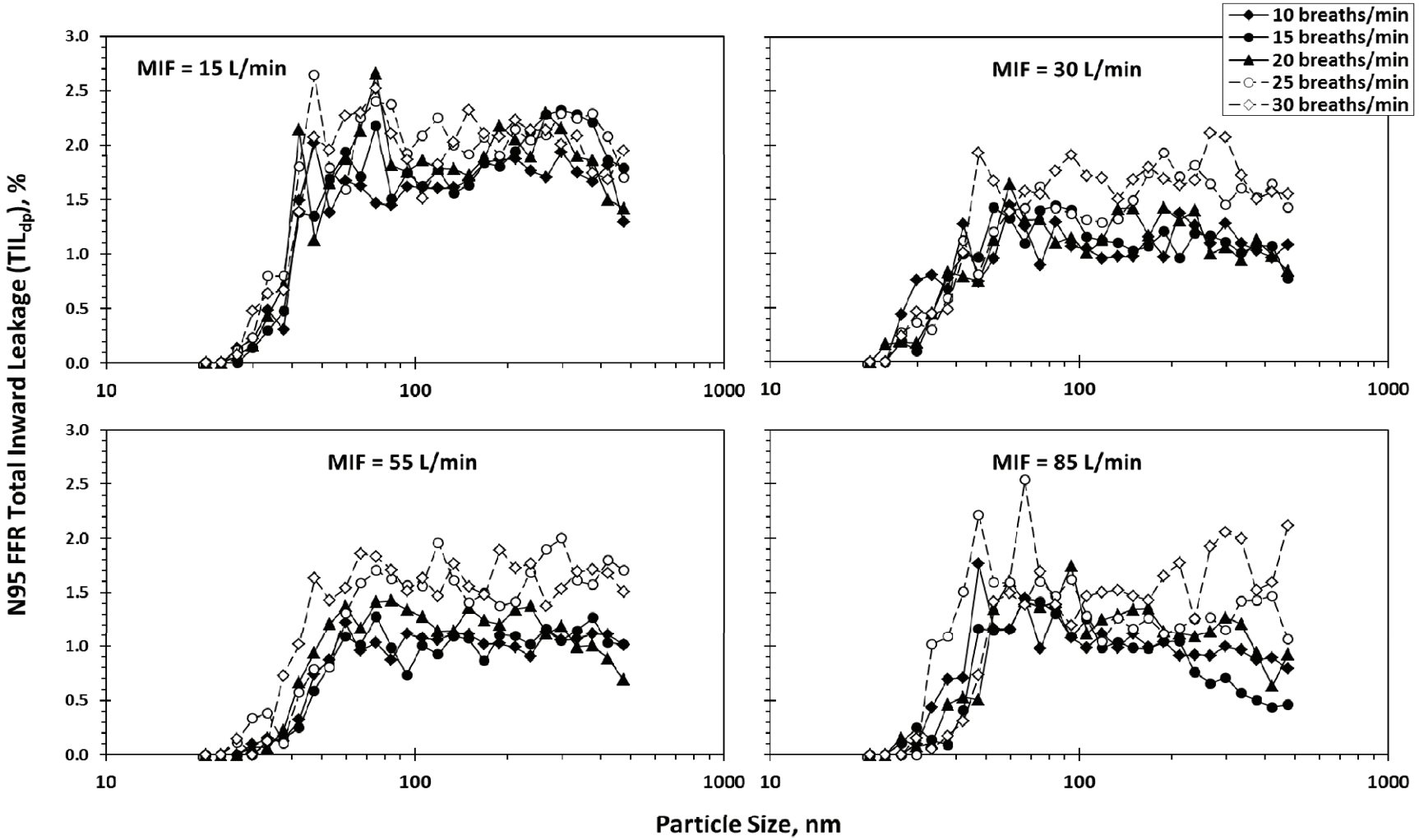

Figure 4-3. Size-specific total inward leakage for an N95 FFR donned on an advanced manikin headform while challenged with charge-equilibrated NaCl particles. Each point represents the mean value of three replicates.

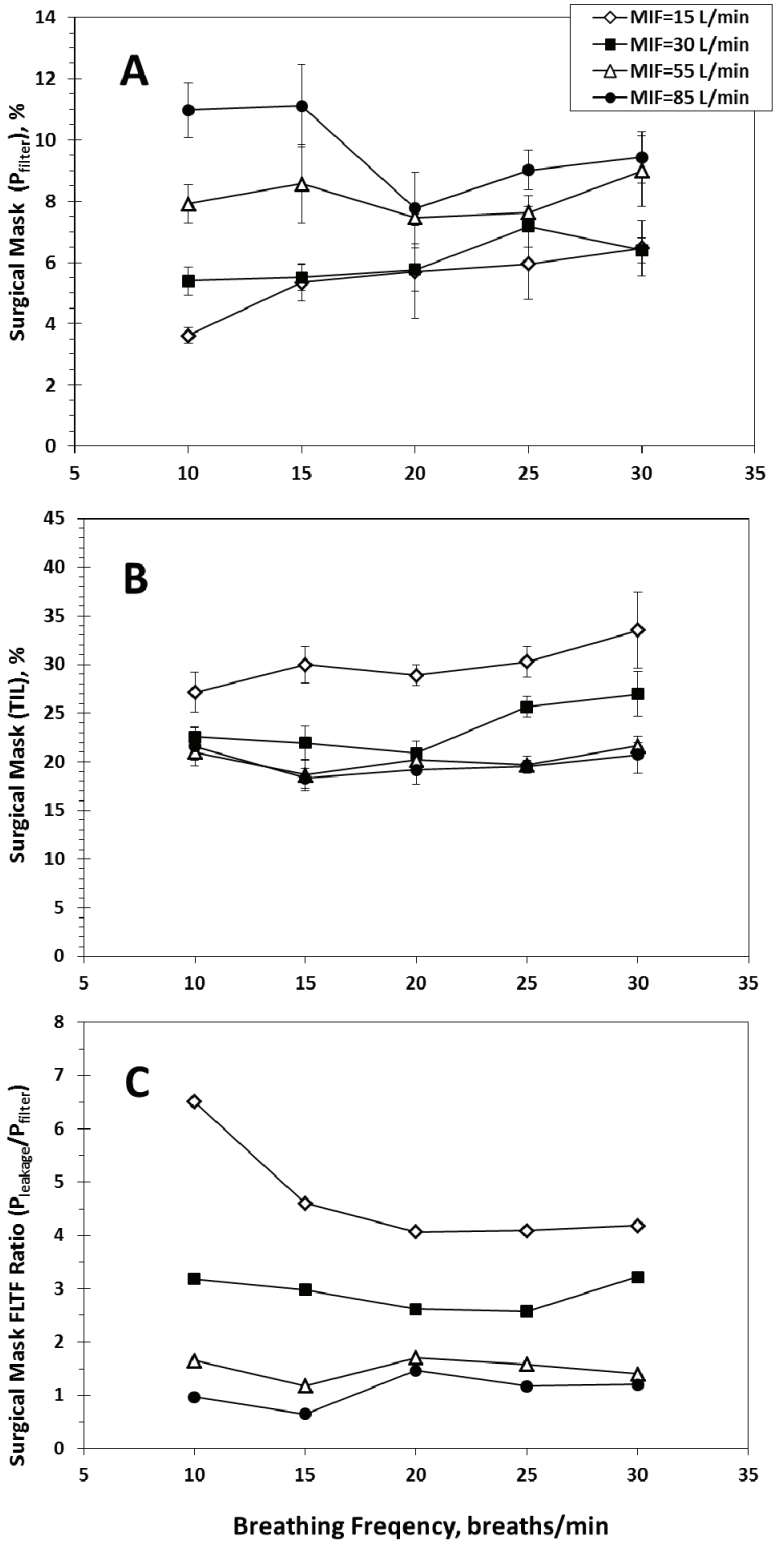

Figure 4-4. Filter penetration (A), Total Inward Leakage TIL (B), and faceseal leakage-to-filter (*FLTF*) ratio (C) for a surgical mask sealed to a plastic manikin's face. No error bars for *FLTF* ratio as it was calculated from the mean $P_{leakage}$ (over 3 replicates) divided by the mean P_{filter} (over 3 replicates).

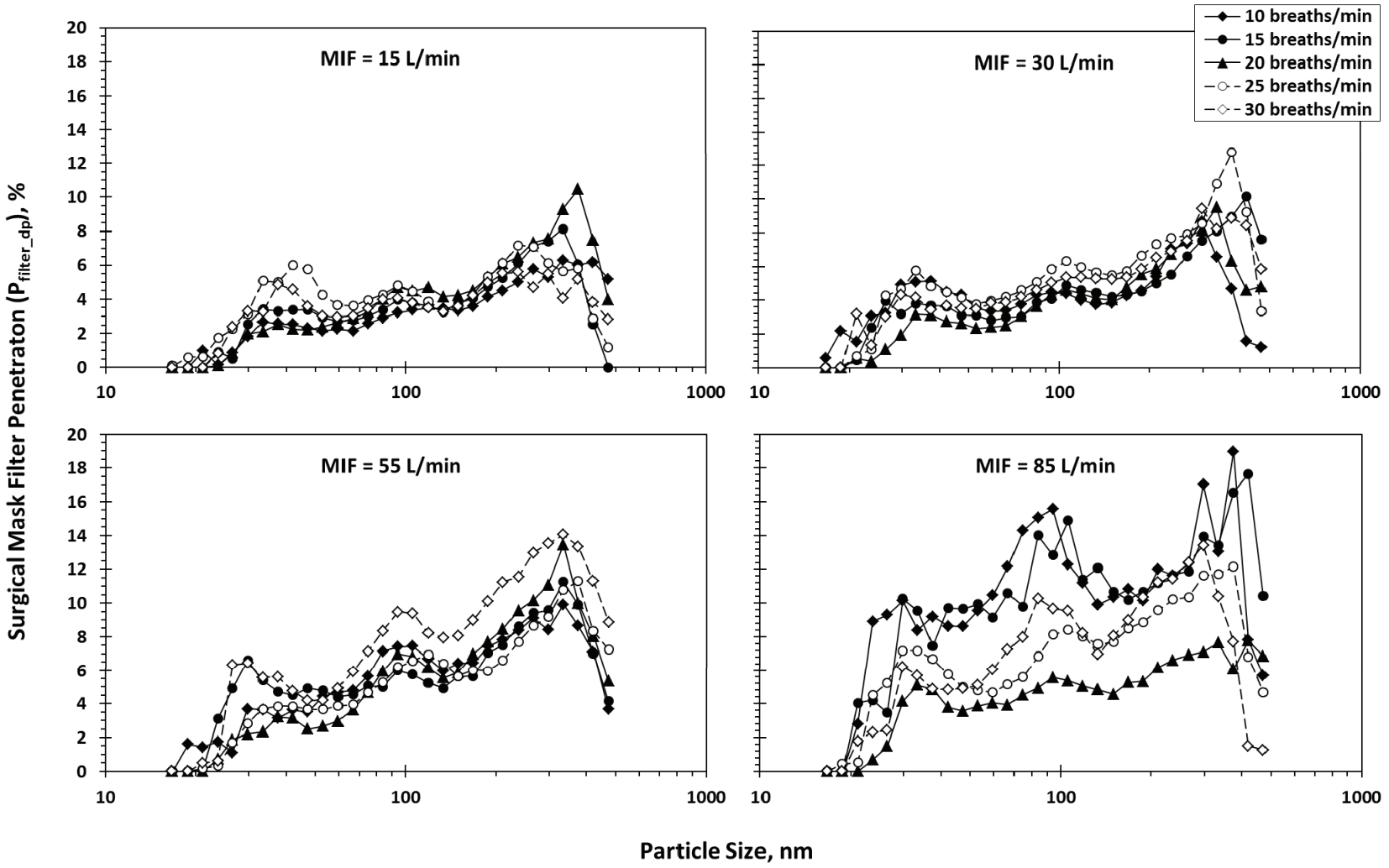

Figure 4-5. Size-specific filter penetration for a surgical mask sealed to a plastic manikin's face while challenged with charge-equilibrated NaCl particles. Each point represents the mean value of three replicates.

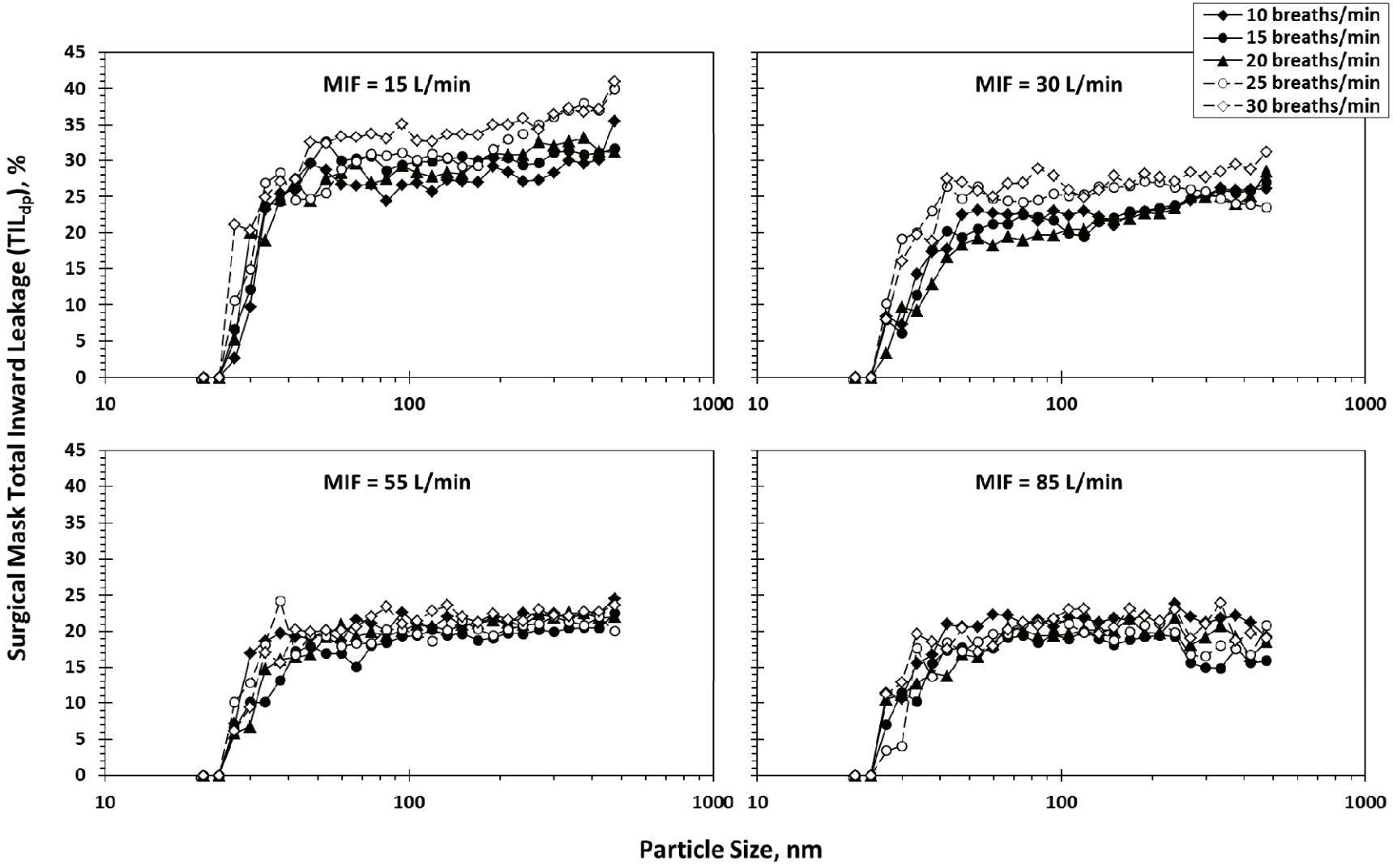

Figure 4-6. Size-specific total inward leakage for a surgical mask donned on an advanced manikin headform while challenged with charge-equilibrated NaCl particles. Each point represents the mean value of three replicates.

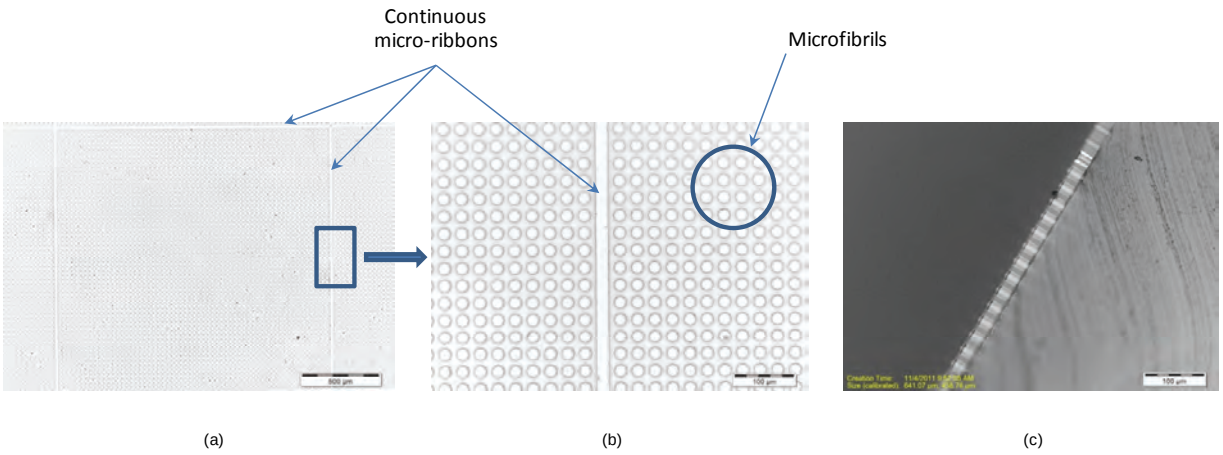

Figure 5-1. Optical microscope images of PU microfibrillar arrays incorporating micro-ribbons: (a) top view at a magnification of 40× – presents the structure inside the area bordered by the continuous micro-ribbons, (b) insert magnified at 400×; and (c) side view.

Figure 5- 2. A conventional elastomeric half-mask versus a modified elastomeric half-mask (same model).

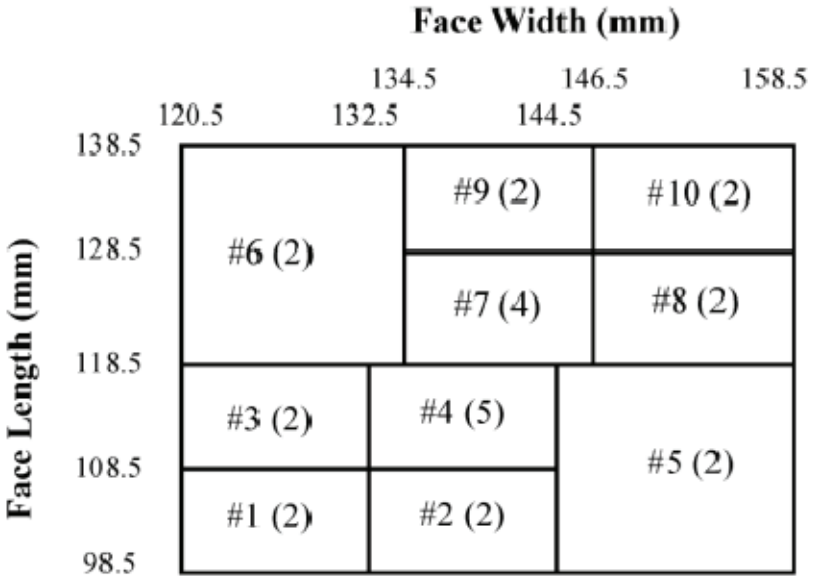

Figure 5-3. The NIOSH 25-subject bivariate panel. Number of subjects is given in parenthesis after the panel number.

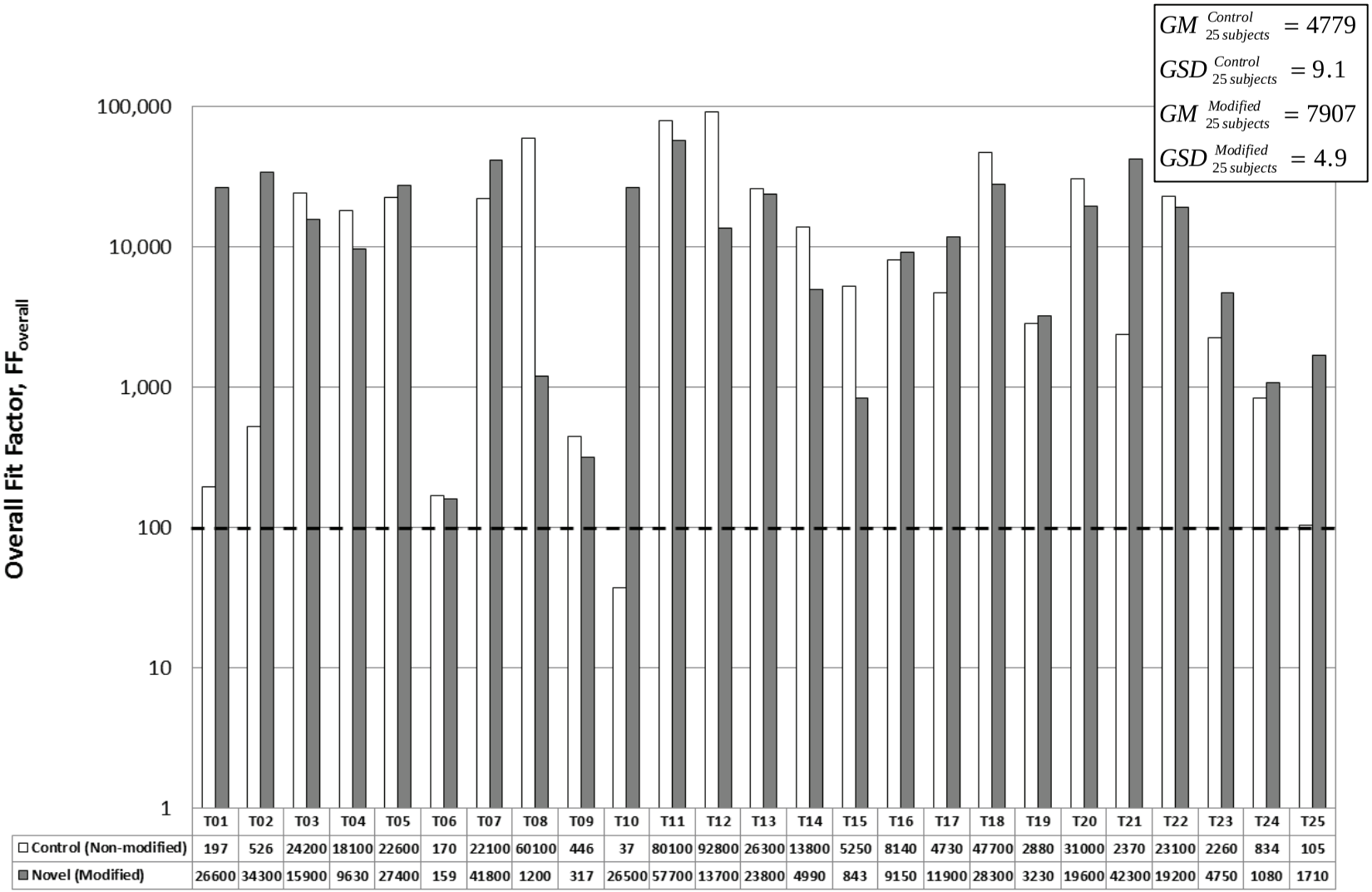

	T01	T02	T03	T04	T05	T06	T07	T08	T09	T10	T11	T12	T13	T14	T15	T16	T17	T18	T19	T20	T21	T22	T23	T24	T25
Control (Non-modified)	197	526	24200	18100	22600	170	22100	60100	446	37	80100	92800	26300	13800	5250	8140	4730	47700	2880	31000	2370	23100	2260	834	105
Novel (Modified)	26600	34300	15900	9630	27400	159	41800	1200	317	26500	57700	13700	23800	4990	843	9150	11900	28300	3230	19600	42300	19200	4750	1080	1710

Figure 5-4. Overall fit factors determined for 25 subjects with dry and well-shaved faces wearing a conventional (non-modified) and modified elastomeric half-mask respirators.

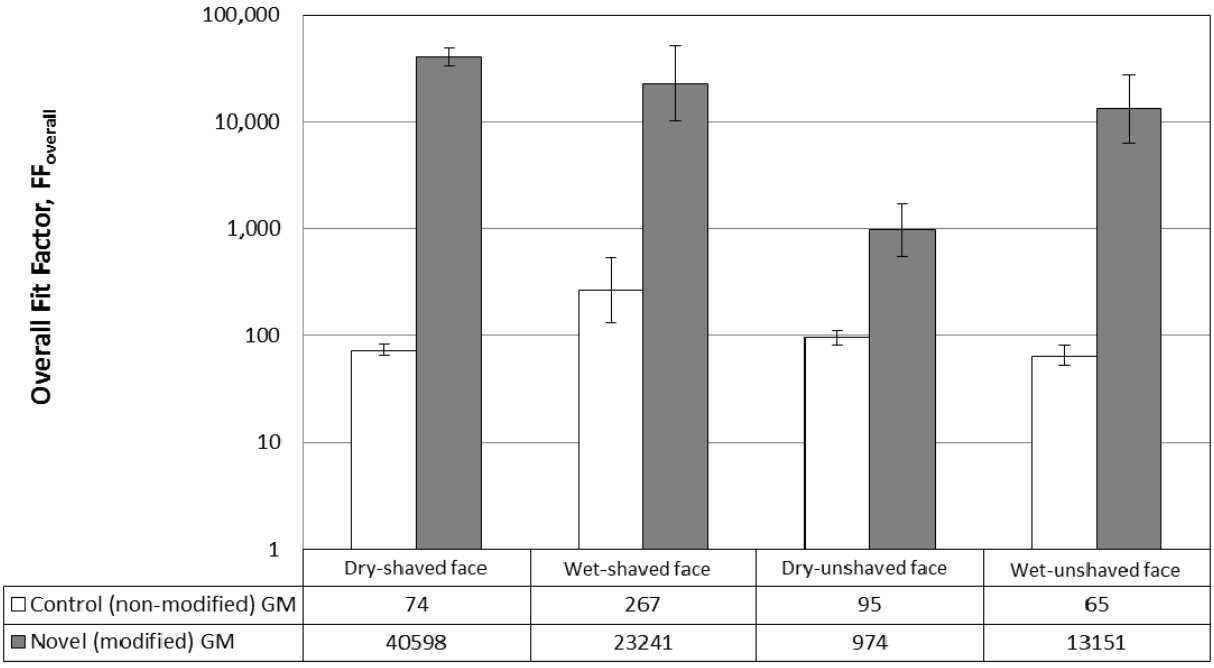

Figure 5-5. Overall fit factors determined for a subject with four facial conditions while wearing a conventional (non-modified) and novel (modified) elastomeric half-mask respirators. The bars represent geometric means; error bars represent the geometric standard deviations.

TABLES

Table 1-1. Summary of Experimental Conditions

Variable	Levels	
Respirator Type	Half-mask	Full mask
Sealing Condition	4 (unsealed, nose-only sealed, nose & chin sealed, fully sealed)	2 (unsealed, fully sealed)
Burning Material	3 (paper, wood, plastic)	3 (paper, wood, plastic)
Manikin Breathing Rate	1 constant (30 L/min) 3 cyclic (30, 85, 135 L/min)[a]	1 constant (30 L/min) 3 cyclic (30, 85, 135 L/min)[a]
Replicates	3	3
Total Runs:	3×4×4×3 = 144	3×4×2×3 = 72

a: The cyclic flows of MIF = 30, 85, and 135 L/min were applied at breathing rates of 15, 25, and 25 breaths/min, respectively.

Table 1-2. Penetration values for a half-mask elastomeric respirator

Material	Flow type[a], Flow rate (L/min)	Penetration, % (Mean ± SD)			
		Unsealed	Nose only Sealed	Nose & Chin Sealed	Fully Sealed
Wood	Constant, 30	43.97 ± 2.44	1.19 ± 0.08	0.33 ± 0.02	0.000 ± 0.000
	Cyclic, 30	8.27 ± 0.25	0.18 ± 0.01	0.23 ± 0.01	0.001 ± 0.000
	Cyclic, 85	6.63 ± 0.25	0.29 ± 0.01	0.34 ± 0.01	0.002 ± 0.000
	Cyclic, 135	5.37 ± 0.29	0.48 ± 0.01	0.29 ± 0.02	0.011 ± 0.003
Paper	Constant, 30	48.37 ± 0.15	0.66 ± 0.19	0.28 ± 0.11	0.000 ± 0.000
	Cyclic, 30	11.3 ± 0.26	0.11 ± 0.01	0.21 ± 0.02	0.001 ± 0.000
	Cyclic, 85	8.10 ± 0.44	0.19 ± 0.00	0.36 ± 0.01	0.002 ± 0.000
	Cyclic, 135	5.83 ± 0.06	0.25 ± 0.01	0.28 ± 0.01	0.011 ± 0.003
Plastic	Constant, 30	50.67 ± 0.61	0.69 ± 0.12	0.14 ± 0.04	0.000 ± 0.000
	Cyclic, 30	11.4 ± 0.10	0.12 ± 0.01	0.25 ± 0.00	0.000 ± 0.000
	Cyclic, 85	8.23 ± 0.25	0.20 ± 0.01	0.35 ± 0.02	0.002 ± 0.000
	Cyclic, 135	6.1 ± 0.10	0.25 ± 0.01	0.28 ± 0.01	0.011 ± 0.001

a: For cyclic flow regime, the number represents Mean Inspiratory Flow (MIF).

Table 1-3. ANOVA with Tukey's range test on the effects of the flow rate adjusted for material (half-mask)

Tukey Grouping[a]	Mean Penetration[b] (%)	Flow type Flow rate (L/min)
Unsealed		
A	47.7	Constant, 30
B	10.3	Cyclic, 30
C	7.7	Cyclic, 85
D	5.8	Cyclic, 135
Nose-only Sealed		
A	0.85	Constant, 30
B	0.33	Cyclic, 135
C	0.23	Cyclic, 85
C	0.14	Cyclic, 30
Nose & Chin Sealed		
A	0.35	Cyclic, 85
B	0.28	Cyclic, 135
B C	0.25	Constant, 30
C	0.23	Cyclic, 30
Full Sealed		
A	0.011	Cyclic, 135
B	0.002	Cyclic, 85
B	0.000	Cyclic, 30
B	0.000	Constant, 30

a: Means with the same letter are not significantly different (p-value > 0.05). The cyclic flows of MIF = 30, 85, and 135 L/min were applied at breathing rates of 15, 25, and 25 breaths/min, respectively.

b: Calculated over all combustion materials.

Table 1-4. ANOVA with Tukey's range test on the effects of the material adjusted for breathing flow (half-mask)

Tukey Grouping[a]	Mean Penetration[b] (%)	Material
Unsealed		
A	19.1	Plastic
A	18.4	Paper
B	16.1	Wood
Nose-only Sealed		
A	0.53	Wood
B	0.31	Plastic
B	0.30	Paper
Nose & Chin Sealed		
A	0.30	Wood
A B	0.28	Paper
B	0.26	Plastic
Full sealed		
A	0.003	Paper
A	0.003	Wood
A	0.003	Plastic

a: Means with the same letter are not significantly different (p-value > 0.05).
b: Calculated over all breathing flow type and flow rate.

Table 1-5. ANOVA with Tukey's range test on the effects of the sealing condition adjusted for material and breathing flow (half-mask)

Tukey Grouping[a]	Mean Penetration[b] (%)	Sealing Condition
A	17.9	Unsealed
B	0.38	Nose-only Sealed
B	0.28	Nose-chin Sealed
C	0.003	Fully Sealed

a: Means with the same letter are not significantly different (p-value > 0.05).
b: Calculated over all combustion material and breathing flow.

Table 1-6. Penetration values for the full facepiece elastomeric respirator

Material	Flow type Flow rate (L/min)	Penetration, % (Mean ± SD)	
		Unsealed	Fully Sealed
Wood	Constant, 30	0.017 ± 0.002	0.001 ± 0.000
	Cyclic, 30	0.003 ± 0.001	0.001 ± 0.000
	Cyclic, 85	0.010 ± 0.001	0.003 ± 0.000
	Cyclic, 135	0.019 ± 0.001	0.013 ± 0.002
Paper	Constant, 30	0.024 ± 0.000	0.000 ± 0.000
	Cyclic, 30	0.003 ± 0.001	0.000 ± 0.000
	Cyclic, 85	0.008 ± 0.000	0.002 ± 0.000
	Cyclic, 135	0.016 ± 0.001	0.010 ± 0.000
Plastic	Constant, 30	0.035 ± 0.001	0.001 ± 0.000
	Cyclic, 30	0.003 ± 0.001	0.001 ± 0.000
	Cyclic, 85	0.012 ± 0.001	0.002 ± 0.000
	Cyclic, 135	0.025 ± 0.002	0.011 ± 0.000

Table 3-1. Summary of the experimental conditions

Variable	Levels
Respirator Type	One elastomeric half-mask with P100 filters (Medium size, 3M 6000 series)
Challenge Aerosol	Paper, wood, and plastic combustion aerosols
Breathing Flow Rate	Cyclic 30, 55, and 85 L/min
Breathing Frequency	10, 15, 20, 25, and 30 breaths/min
Particle Size Range	20 – 200 nm (10 channels)
Replicates	4
Total Runs:	3×3×5×4 = 180

Table 3-2. Three-way ANOVA results for the size-independent (overall) TIL as a function of combustion aerosol, MIF and breathing frequency (B*f*)

Source	DF	ANOVA SS	Mean Square	F Value	*p*-value
Aerosol	2	5.81	2.90	28.40	<.0001
MIF	2	6.24	3.12	30.49	<.0001
Aerosol*MIF	4	1.43	0.35	3.49	0.0096
B*f*	4	0.86	0.21	2.10	0.0841
Aerosol*B*f*	8	0.09	0.01	0.12	0.9983
MIF*B*f*	8	1.38	0.17	1.68	0.1076
Aerosol*MIF*B*f*	16	0.23	0.01	0.14	1.0000

Note: B*f* stands for breathing frequency. Three-way ANOVA were performed on all levels of combustion aerosol, MIF and breathing frequency (pooled data). The asterisk (*) indicates an interaction between variables.

Table 3-3. Pairwise multiple comparisons: mean TIL values among three combustion aerosol groups (ANOVA with Tukey's range test)

Tukey Grouping[a]	Mean[b] TIL (%)	Aerosol
A	1.14	Plastic
B	0.85	Paper
C	0.70	Wood

a: Means with the same letter are not significantly different (p-value > 0.05).
b: Calculated using the size-independent (overall) TIL values.

Table 3-4. Pairwise multiple comparisons: mean TIL values among three MIF groups (ANOVA with Tukey's range test)

Tukey Grouping[a]	Mean[b] TIL (%)	MIF (L/min)
A	1.15	30
B	0.81	55
B	0.72	85

a: Means with the same letter are not significantly different (p-value > 0.05).
b: Calculated using the size-independent (overall) TIL values.

Table 3-5. Pairwise multiple comparisons: mean TIL values among five breathing frequency groups challenged with combustion aerosols (ANOVA with Tukey's range test)

Wood Combustion Aerosol				Paper Combustion Aerosol				Plastic Combustion Aerosol			
Tukey Grouping[a]	Mean[b] TIL (%)	Breathing Frequency (breaths/min)	*p*-value[c]	Tukey Grouping[a]	Mean[b] TIL (%)	Breathing Frequency (breaths/min)	*p*-value[c]	Tukey Grouping[a]	Mean[b] TIL (%)	Breathing Frequency (breaths/min)	*p*-value[c]
MIF = 30 L/min				MIF = 30 L/min				MIF = 30 L/min			
A	1.08	30	0.0265	A	1.33	30	< 0.0001	A	1.87	30	0.0476
A B	0.99	25		B	1.06	25		A B	1.62	25	
A B	0.84	20		B C	0.97	20		A B	1.50	20	
B	0.75	10		C D	0.90	15		A B	1.49	15	
B	0.74	15		D	0.82	10		B	1.36	10	
MIF = 55 L/min				MIF = 55 L/min				MIF = 55 L/min			
A	0.89	20	0.0373	A	0.88	30	0.0231	A	1.10	20	0.9890
A	0.70	30		A B	0.81	20		A	1.01	30	
A B	0.64	10		B C	0.77	15		A	1.01	10	
A B	0.63	25		B C	0.73	10		A	0.94	15	
B	0.51	15		C	0.67	25		A	0.94	25	
MIF = 85 L/min				MIF = 85 L/min				MIF = 85 L/min			
A	0.67	15	0.0391	A	0.90	10	0.0260	A	0.93	30	0.9689
A	0.61	10		A B	0.83	30		A	0.90	10	
A	0.60	20		A B	0.74	15		A	0.84	20	
A	0.58	30		B	0.73	20		A	0.81	15	
B	0.35	25		B	0.72	25		A	0.75	25	

a: Within each group of the combustion aerosol (wood, paper and plastic), means with the same letter are not significantly different (p-value > 0.05).
b: Calculated using the size-independent (overall) TIL values.
c: *P*-values were obtained from the one-way ANOVA performed to examine the effect of the breathing frequency on the size-independent TIL after stratifying the combustion aerosol and the MIF.

Table 4-1. Pairwise multiple comparisons for mean P_{filter} values among four MIFs and five breathing frequency groups (ANOVA with Tukey's range test) for an N95 FFR

Effect of MIF on P_{filter}				**Effect of Breathing Frequency on P_{filter}**			
MIF (L/min)	Tukey Grouping[a]	Mean[b] P_{filter} (%)	*p*-value[c]	Breathing Frequency (breaths/min)	Tukey Grouping[a]	Mean[b] P_{filter} (%)	*p*-value[d]
15	D	0.05	<0.0001	10	0.38	I	<0.0001
30	C	0.13		15	0.39	I	
55	B	0.31		20	0.25	II	
85	A	0.72		25	0.23	II	
				30	0.26	II	

a: Within each group of the MIF or the breathing frequency, means with the same letter are not significantly different (*p*-value > 0.05).
b: Calculated using the size-independent (overall) P_{filter} values.
c: *P*-values were obtained from the two-way ANOVA performed to examine the effect of the MIF on the filter penetration.
d: *P*-values were obtained from the two-way ANOVA performed to examine the effect of the breathing frequency on the filter penetration.

Table 4-2. Pairwise multiple comparisons for mean TIL values among four MIFs and five breathing frequency groups (ANOVA with Tukey's range test) for an N95 FFR

Effect of MIF on TIL				**Effect of Breathing Frequency TIL**			
MIF (L/min)	Tukey Grouping[a]	Mean[b] TIL (%)	*p*-value[c]	Breathing Frequency (breaths/min)	Tukey Grouping[a]	Mean[b] TIL (%)	*p*-value[d]
15	A	1.93		10	II	1.22	
30	B	1.37	0.0019	15	II	1.28	0.0025
55	B	1.31		20	I II	1.45	
85	B	1.29		25	I II	1.63	
				30	I	1.73	

a: Within each group of the MIF or the breathing frequency, means with the same letter are not significantly different (*p*-value > 0.05).
b: Calculated using the size-independent (overall) TIL values.
c: *P*-values were obtained from the two-way ANOVA performed to examine the effect of the MIF on the TIL.
d: *P*-values were obtained from the two-way ANOVA performed to examine the effect of the breathing frequency on the TIL.

Table 4-3. Pairwise multiple comparisons for mean P_{filter} values among four MIFs and five breathing frequency groups (ANOVA with Tukey's range test) for a surgical mask

Effect of MIF on P_{filter}				**Effect of Breathing Frequency on P_{filter}**			
MIF (L/min)	Tukey Grouping[a]	Mean[b] P_{filter} (%)	*p*-value[c]	Breathing Frequency (breaths/min)	Tukey Grouping[a]	Mean[b] P_{filter} (%)	*p*-value[d]
15	C	5.41	<0.0001	10	I II	6.97	<0.0143
30	C	6.04		15	I II	7.63	
55	B	8.11		20	II	6.67	
85	A	9.65		25	I II	7.43	
				30	I	7.81	

a: Within each group of the MIF or the breathing frequency, means with the same letter are not significantly different (*p*-value > 0.05).
b: Calculated using the size-independent (overall) P_{filter} values.
c: *P*-values were obtained from the two-way ANOVA performed to examine the effect of the MIF on the filter penetration.
d: *P*-values were obtained from the two-way ANOVA performed to examine the effect of the breathing frequency on the filter penetration.

Table 4-4. Pairwise multiple comparisons for mean TIL values among four MIFs and five breathing frequency groups (ANOVA with Tukey's range test) for a surgical mask

Effect of MIF on TIL				**Effect of Breathing Frequency TIL**			
MIF (L/min)	Tukey Grouping[a]	Mean[b] TIL (%)	*p*-value[c]	Breathing Frequency (breaths/min)	Tukey Grouping[a]	Mean[b] TIL (%)	*p*-value[d]
15	A	1.93		10	I II	23.1	
30	B	1.37	0.0019	15	II	22.2	0.0316
55	B	1.31		20	I II	22.3	
85	B	1.29		25	I II	23.8	
				30	I	25.7	

a: Within each group of the MIF or the breathing frequency, means with the same letter are not significantly different (*p*-value > 0.05).
b: Calculated using the size-independent (overall) TIL values.
c: *P*-values were obtained from the two-way ANOVA performed to examine the effect of the MIF on the TIL.
d: *P*-values were obtained from the two-way ANOVA performed to examine the effect of the breathing frequency on the TIL.

APPENDIX: Peer Reviewed Publications

Journal of Occupational and Environmental Hygiene, 10: 203–212
ISSN: 1545-9624 print / 1545-9632 online

DOI: 10.1080/15459624.2012.760063

Manikin-Based Performance Evaluation of Elastomeric Respirators Against Combustion Particles

Xinjian He,[1] Michael Yermakov,[1] Tiina Reponen,[1] Roy T. McKay,[1] Kelley James,[2] and Sergey A. Grinshpun[1]

[1]Center for Health-Related Aerosol Studies, Department of Environmental Health, University of Cincinnati, Cincinnati, Ohio
[2]Department of Mechanical Engineering, University of Cincinnati, Cincinnati, Ohio

This study investigated the effects of faceseal leakage, breathing flow, and combustion material on the overall (non-size-selective) penetration of combustion particles into P-100 half and full facepiece elastomeric respirators used by firefighters. Respirators were tested on a breathing manikin exposed to aerosols produced by combustion of three materials (wood, paper, and plastic) in a room-size exposure chamber. Testing was performed using a single constant flow (inspiratory flow rate = 30 L/min) and three cyclic flows (mean inspiratory flow rates = 30, 85, and 135 L/min). Four sealing conditions (unsealed, nose-only sealed, nose and chin sealed, and fully sealed) were examined to evaluate the respirator faceseal leakage. Total aerosol concentration was measured inside (C_{in}) and outside (C_{out}) the respirator using a condensation particle counter. The total penetration through the respirator was determined as a ratio of the two ($P = C_{in} / C_{out}$). Faceseal leakage, breathing flow type and rate, and combustion material were all significant factors affecting the performance of the half mask and full facepiece respirators. The efficiency of P-100 respirator filters met the NIOSH certification criteria (penetration ≤0.03%); it was not significantly influenced by the challenge aerosol and flow type, which supports the current NIOSH testing procedure using a single challenge aerosol and a constant airflow. However, contrary to the NIOSH total inward leakage (TIL) test protocol assuming that the result is independent on the type of the tested aerosol, this study revealed that the challenge aerosol significantly affects the particle penetration through unsealed and partially sealed half mask respirators. Increasing leak size increased total particle penetration. The findings point to some limitations of the existing TIL test in predicting protection levels offered by half mask elastomeric respirators.

Keywords combustion aerosol, elastomeric respirator, manikin, total penetration

Correspondence to: Sergey A. Grinshpun, University of Cincinnati, Department of Environmental Health, 3223 Eden Ave., P.O. Box 670056, Cincinnati, OH 45267; e-mail: sergey.grinshpun@uc.edu.

INTRODUCTION

While on duty, firefighters are exposed to a wide range of chemicals and particulate matter.[1] Smoke from a fire contains fine (≤1 μm) and ultrafine (≤0.1 μm) particle size fractions. In a large-scale fire test laboratory study, ultrafine particles accounted for more than 70% of the total number concentration of particles during fire knockdown and overhaul.[2] Fine particle exposures at various workplace environments have been associated with impairment of cardiovascular function and other adverse health outcomes.[3–5]

There are approximately 1.1 million firefighters in the United States (including 300,000 career firefighters). Their leading cause of death is heart disease.[6] Sudden cardiac death is responsible for 50% and 39% of the on-duty deaths for volunteer and professional firefighters, respectively.[7] Firefighters have greater mortality rates associated with cardiovascular disease and elevated cancer rates than the general population.[8,9]

Respirators used for structural fire fighting should meet the certification requirements of the National Institute for Occupational Safety and Health (NIOSH) and the National Fire Protection Association.[10,11] Ironically, there is limited information on the efficiency of the full facepiece used by firefighters during actual fire fighting. Furthermore, during fire overhaul (entering the structure after the fire has been extinguished) firefighters commonly use negative pressure elastomeric half mask or filtering facepiece respirators (FFR) or no respirators at all.[12,13] According to the Occupational Safety and Health Administration (OSHA), the assigned protection factors (APF) given for negative pressure air-purifying full and half mask respirators are 50 and 10,[14] which corresponds the equivalent penetration values of 2% and 10%, respectively, (P = 100/APF,%).

Respiratory protection offered by negative pressure respirators depends significantly (and often primarily) on the faceseal fit.[15,16] Little data is available on faceseal aerosol penetration under the cyclic flow regime, and even less is known about the filter vs. faceseal penetration under actual breathing conditions. The early investigation carried out by Hinds and Kraske[17] addressed the performance of half mask and single-use respirators by measuring particle penetration through the filter and the artificially induced cylindrical leaks; the tests were conducted under a constant flow regimen at rates between 2 to 150 L/min. Chen and Willeke,[18] who deployed a breathing manikin with artificially created slit-like or circular leaks to assess the faceseal vs. filter penetration for 0.5–5 μm particles, also tested under the constant flow regime. However, artificial fixed leaks and constant flows are not representative of real world conditions. Workplace protection factor (WPF) studies are representative of real world conditions with human subjects wearing respirators,[19–23] and thus, WPF results include both filter and faceseal penetration. However, the contribution of faceseal leakage to total penetration cannot be calculated from WPF.

The above limitations were overcome in recent studies[15,16,19,24,25] either by inclusion of human subjects without induced fixed leaks or through partial sealing of respirators on a manikin tested under cyclic flow. Grinshpun et al.[16] found that the primary particle penetration pathway was faceseal leakage for both an N95 FFR and a surgical mask. Cho et al.[15] reported that despite having a well-fitted N95 FFR, the majority of particles penetrated through the faceseal leaks, and penetration decreased with an increase in respiration flow and in particle size.

Finally, most of the published data on the performance of respirators was collected using an ambient aerosol or nebulizer-generated NaCl particles. Some investigators used polystyrene latex spheres as challenge aerosol in their tests.[26,27] Others used fungal spores, bacteria, or viruses.[20,27–29] Eninger et al.[29] compared the effects of NaCl and three virus aerosols (all having significant ultrafine components) on the performance of fully sealed N99 and N95 FFRs. The authors concluded that filter penetration of the tested biological aerosols did not exceed that of NaCl aerosol, which suggests that NaCl may generally be appropriate for modeling filter penetration of similarly sized virions. However, particles used in the above studies are not representative of the exposures experienced by firefighters. The differences are concerned with the particle shape, density, electric charge, and possibly other properties. To our knowledge, the effects of combustion material on respirator performance have not been previously studied.

The present investigation was designed to examine the effects of faceseal leakage, breathing flow type and rate, and combustion material on the overall (non-size selective) aerosol particle penetration through elastomeric half and full facepiece respirators equipped with P-100 filters.

MATERIALS AND METHODS

Experimental Design

Two elastomeric respirators (one half mask and the other a full facepiece) were tested on a breathing manikin exposed to aerosols produced by combustion of three different materials. Testing was performed using two different flow patterns (constant and cyclic breathing regimes). Cyclic flow testing was conducted at three flows selected to represent breathing at different work load levels. Four facepiece sealing conditions were established to evaluate faceseal leakage. Total aerosol concentration was measured inside (C_{in}) and outside (C_{out}) the respirator. Particle penetration (P) through the respirator was determined as C_{in} / C_{out}.

The experimental setup for investigating particle penetration through the respirator is schematically shown in Figure 1. Inside the exposure chamber ($142 \times 95 \times 102$ inches, L×W×H), the tested respirator was donned on a manikin headform made of hard plastic (Model: Full round molded male manikin display head; Allen Display, Midlothian, Va.). A copper pipe (1 inch diameter) was installed into the headform to simulate airflow through the upper respiratory tract. One end of the pipe was sealed between the upper and lower lips of the manikin. For cyclic flows, the other end was connected to an electromechanical Breathing Recording and Simulation System (BRSS; Koken Ltd., Tokyo, Japan) with a HEPA filter placed in between to keep particles from re-entering the respirator cavity with the exhalation airflow. The constant flow was created by a vacuum pump (Model G272X; Doerr Electric Corp., Cedarburg, Wis.). Aerosol concentrations inside and outside the respirator were measured with a condensation particle counter (CPC, Model 3007; TSI Inc., Shoreview, Minn.) that detects particles in a size range from 0.01 to >1.0 μm.

Respirators and Test Conditions

Two types of respirators were tested in this study: (1) half mask elastomeric respirator (size: medium) equipped with two P-100 filters, and (2) full facepiece elastomeric respirator (size: medium) equipped with the same type of P-100 filters.

Several studies have reported common facepiece leak locations as the nose, chin, and cheek.[30–32] In the present study, four sealing conditions ("unsealed," "nose-only sealed," "nose and chin sealed," and "fully sealed") were used when testing the half mask respirator. For the full facepiece respirator, only two sealing conditions (unsealed and fully sealed) were used because our pilot study revealed that these two conditions produced similar penetration levels, which made it unnecessary to evaluate partially sealed conditions. Silicone sealant was applied in between the manikin's face and the edge of the respirator to form seals. Sealing configurations for the half mask with nose-only and nose and chin sealing conditions are shown in Figure 2. Respirator straps were tightened and placed around the manikin's head and neck as conventionally used. For each sealing condition, once the respirator was

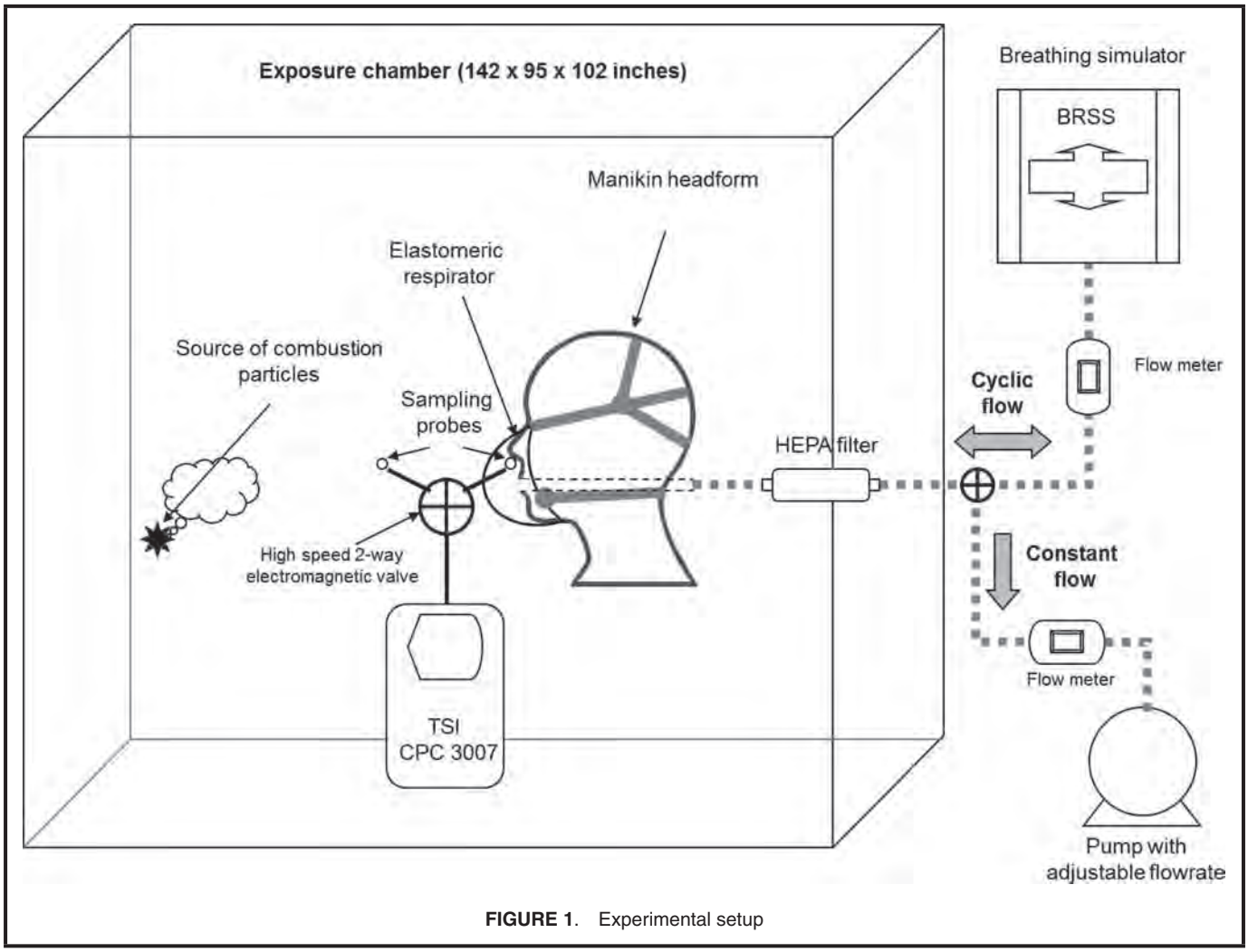

FIGURE 1. Experimental setup

positioned it was not removed until another sealing condition was evaluated.

Wood (BBQ long match, 0.23 ± 0.03 g), paper (Multifold brown paper towel, 0.25 ± 0.04 g), and plastic (Ziploc plastic bag, 0.24 ± 0.04 g) were selected for this study. Wood, paper, and plastic are the most common materials encountered by firefighters during fire activities. All three materials were ignited by a long-reach lighter and burned separately

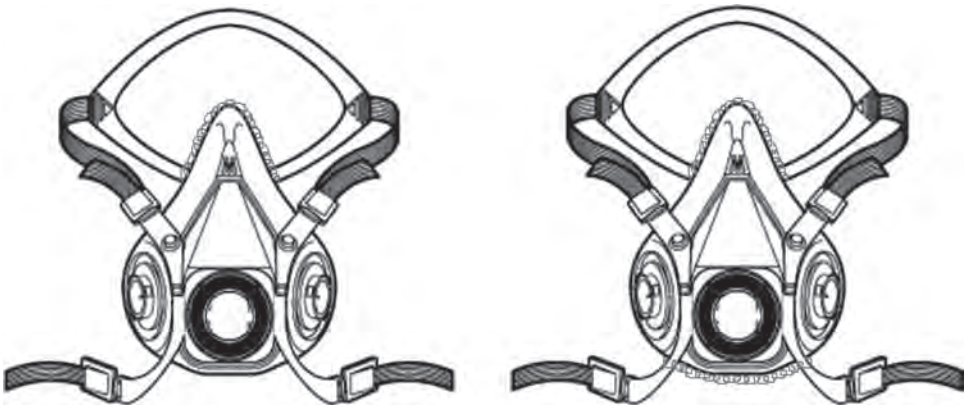

FIGURE 2. "Nose-only" and "nose and chin" sealed half mask respirators. Respirator total length: 16 inches. Nose-only sealed length: 5 inches. Nose and chin sealed length: 5 + 4 inches

TABLE I. Summary of Experimental Conditions

Variable	Levels	
Respirator type	Half mask	Full mask
Sealing condition	4 (unsealed, nose-only sealed, nose and chin sealed, fully sealed)	2 (unsealed, fully sealed)
Burning material	3 (paper, wood, plastic)	3 (paper, wood, plastic)
Manikin breathing rate	1 constant (30 L/min) 3 cyclic (30, 85, 135 L/min)[A]	1 constant (30 L/min) 3 cyclic (30, 85, 135 L/min)[A]
Replicates	3	3
Total runs	$3\times4\times4\times3 = 144$	$3\times4\times2\times3 = 72$

[A]The cyclic flows of MIF = 30, 85, and 135 L/min were applied at breathing rates of 15, 25, and 25 breaths/min, respectively.

inside the testing chamber. The aerosol measurements were initated15 min after burning to allow the combustion aerosol to reach a homogenous concentration. To assess the effect of breathing flow on the particle penetration through respirators, we selected three mean inspiratory flows (MIF) of 30, 85, and 135 L/min, with breathing rates of 15, 25, and 25 breaths/min (achieved by adjusting the tidal volume), respectively. These were established to simulate breathing at moderate, high, and strenuous workloads, respectively. The selection of the breathing rates was based on average respiratory rates reported in a healthy adult.[33,34] In addition, one constant flow (30 L/min) was selected to investigate the effects of the flow type (constant vs. cyclic).

Three replicates were conducted for each condition, resulting in 144 and 72 measurements for the half and full facepiece respirators, respectively. The manikin breathing flow with three replicates was completely randomized throughout the entire study. A summary of experimental conditions is listed in Table I.

Data Analysis

Collected data from the TSI CPC was entered into a spreadsheet, and descriptive and inferential statistical analyses were performed using SAS version 9.2 (SAS Institute Inc., Cary, N.C.). The total aerosol penetration was the sum of filter and faceseal penetration ($P = P_F + P_L$), where P_F is the penetration solely through the filter and P_L represents faceseal penetration. For each combination of experimental conditions, the average value of the overall penetration and the standard deviation were calculated from the three replicates. Analysis of variance (ANOVA) with Tukey's range test and paired *t*-test were performed to study effects of sealing condition, burning material, manikin breathing rate, and respirator type on aerosol penetration value. P-values of <0.05 were considered significant.

RESULTS AND DISCUSSION

Particle Size Distribution of Combustion Aerosols

Prior to the experiments involving respirators, challenge aerosols—produced by combustion of wood, paper, and plastic, respectively—were characterized with respect to their particle size distributions determined with a Nanoparticle Spectrometer (Nano-ID NPS500; Particle Measuring System, Inc., Boulder, Colo.). This instrument is capable of measuring particle diameter in a range of 5 to 500 nm. Particle size distribution curves obtained 30 min after burning are presented in Figure 3. The peak particle size for wood combustion aerosol was around 45 nm, and 95% of the particles fell within the size range of 20–200 nm. Peak sizes for paper and plastic combustion aerosols were 56 nm and 89 nm, respectively, with 95% of the particles falling in size ranges of 20–200 nm and 20–300 nm, respectively. In general, wood combustion produced smaller particles; all three peak concentrations were observed at particle sizes below 100 nm. More than 70% of particles generated by combustion of wood and paper, and slightly more than 50% of particles generated by plastic combustion, were ultrafine, which is consistent with the earlier findings.[2]

Half Mask Elastomeric Respirator with P-100 Filters

1. Respirator Donned on the Manikin (Unsealed)
   a. *Constant flow.* As shown in Table II, for the constant flow 30 L/min, the overall particle penetration was very high: average values were $43.97 \pm 2.44\%$ (wood aerosol), $48.37 \pm 0.15\%$ (paper aerosol), and $50.67 \pm 0.61\%$ (plastic aerosol). ANOVA revealed a statistically significant (p-value <0.05) effect of combustion material, but from the practical standpoint it does not play an important role since all measured penetration values fell between 40% and 52%. The important finding is that the obtained penetration level is over three orders of magnitude higher than the one expected, based solely on the filter efficiency. Indeed, the respirator was equipped with a P100 filter that has a collection efficiency 99.97% for the most penetrating particle size at a constant flow of 85 L/min, which corresponds to an overall penetration of $\leq 0.03\%$ at 85 L/min and even lower at 30 L/min (no data is available for 135 L/min). This means that most of the penetrated particles entered through the faceseal leakage; only one out of thousands of the penetrated particles entered through the filter media. When testing with

TABLE II. Penetration Values for a Half Mask Elastomeric Respirator

Material	Flow Type,[A] Flow Rate (L/min)	Penetration,% (Mean ± SD)			
		Unsealed	Nose-Only Sealed	Nose and Chin Sealed	Fully Sealed
Wood	Constant, 30	43.97 ± 2.44	1.19 ± 0.08	0.33 ± 0.02	0.000 ± 0.000
	Cyclic, 30	8.27 ± 0.25	0.18 ± 0.01	0.23 ± 0.01	0.001 ± 0.000
	Cyclic, 85	6.63 ± 0.25	0.29 ± 0.01	0.34 ± 0.01	0.002 ± 0.000
	Cyclic, 135	5.37 ± 0.29	0.48 ± 0.01	0.29 ± 0.02	0.011 ± 0.003
Paper	Constant, 30	48.37 ± 0.15	0.66 ± 0.19	0.28 ± 0.11	0.000 ± 0.000
	Cyclic, 30	11.3 ± 0.26	0.11 ± 0.01	0.21 ± 0.02	0.001 ± 0.000
	Cyclic, 85	8.10 ± 0.44	0.19 ± 0.00	0.36 ± 0.01	0.002 ± 0.000
	Cyclic, 135	5.83 ± 0.06	0.25 ± 0.01	0.28 ± 0.01	0.011 ± 0.003
Plastic	Constant, 30	50.67 ± 0.61	0.69 ± 0.12	0.14 ± 0.04	0.000 ± 0.000
	Cyclic, 30	11.4 ± 0.10	0.12 ± 0.01	0.25 ± 0.00	0.000 ± 0.000
	Cyclic, 85	8.23 ± 0.25	0.20 ± 0.01	0.35 ± 0.02	0.002 ± 0.000
	Cyclic, 135	6.1 ± 0.10	0.25 ± 0.01	0.28 ± 0.01	0.011 ± 0.001

[A]For cyclic flow regime, the number represents mean inspiratory flow.

an unsealed respirator, a sizeable gap (~1 mm) located around the nose of the manikin was observed, indicating a poor fit for the tested respirator donned on the manikin, which could result in unexpectedly high penetration values. This was likely because the manikin was made of hard plastic. Softer human skin would likely form a better seal, resulting in lower penetration values for the elastomeric half mask respirator.

The total particle penetration results from two components: the filter penetration (P_F) at the corresponding flow through the filter (Q_F), and the leakage penetration (P_L) at the corresponding air flow (Q_L). It can be expressed as:

$$P = \frac{C_{in}}{C_{out}} = \frac{N_{in}}{N_{out}} = \frac{N_F + N_L}{N_{out}} = \frac{N_F}{N_{out}} + \frac{N_L}{N_{out}} = \frac{P_F N_{out} \frac{Q_F}{Q}}{N_{out}} + \frac{P_L N_{out} \frac{Q_L}{Q}}{N_{out}} = P_F \frac{Q_F}{Q} + P_L \frac{Q_L}{Q} = P_F \frac{Q_F}{Q} + P_L \left(1 - \frac{Q_F}{Q}\right) \quad \textbf{(1)}$$

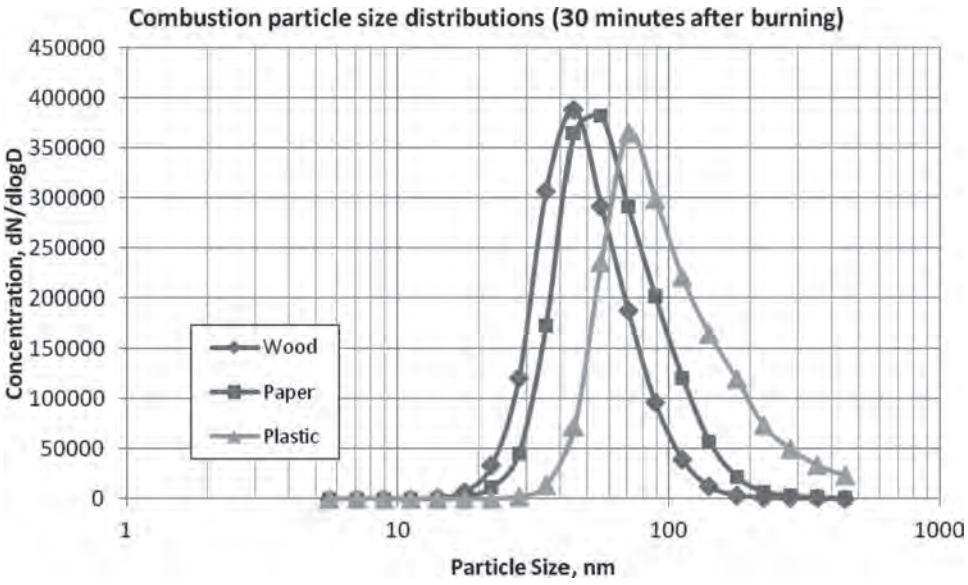

FIGURE 3. Size distributions of particles aerosolized from combustion of three tested materials: wood, paper, and plastic. Measurement with a nanoparticle spectrometer was initiated 30 min after burning.

where

N_{in} = Particle numbers inside the respirator
N_{out} = Particle number outside the respirator
N_F = Number of particle penetrating through the filters
N_L = Number of particles penetrating through the leakage
Q = Breathing flow = $Q_F + Q_L$.

We concluded from Eq. 1 that it is crucial to determine the relative contribution of the airflow through the filter to the total airflow. Therefore, a separate experiment was conducted to measure Q_F when the half mask was donned on the manikin. A flow meter (Model 4043; TSI) was placed between the filter and the respirator. Three breathing (constant) flows (30, 85, and 135 L/min) were selected. For each flow, the respirator was taken off the manikin and put back on. Then the filter flow was recorded after each redonning. Seven replicates were performed for each flow (a total run of 21). It was determined that the fraction of the breathing flow entering through the filter (Q_F/Q) was 56.0 ± 7.2% at 30 L/min, 61.7 ± 4.4% at 85 L/min, and 61.0 ± 4.0% at 135 L/min. Given that P_F of a P100 filter is negligibly low (<0.03%) compared to P_L, and Q_F and Q_L are comparable (according to the above experimental data), Eq. 1 can be simplified as:

$$P \approx P_L \left(1 - \frac{Q_F}{Q}\right) \quad \textbf{(2)}$$

Particle loss inside the gap (~1 mm) was negligibly low according to a classic particle diffusion theory.[35] For these conditions, P_L is close to 100%, which allows further simplifying the equation for the overall particle penetration:

$$P \approx 1 - \frac{Q_F}{Q} \quad \textbf{(3)}$$

According to this assessment, the overall penetration values are expected to be slightly below 50% at 30 L/min and about 40% at 85 and 135 L/min, which is in reasonable agreement with the penetration values experimentally obtained for an unsealed half mask tested against three combustion aerosols under constant flow of 30 L/min (listed in Table II). However, Eq. 3 is limited to constant flow only and cannot be applied to cyclic flow conditions representing a much more complex two-direction flow regime.

b. *Cyclic flow.* Data on the overall aerosol penetration through the *unsealed* half mask respirator obtained for different MIFs and different combustion materials is presented in Table II.

(i) *Cyclic vs. constant flow.* For wood combustion aerosol with a cyclic MIF of 30 L/min, the penetration was 8.27 ± 0.25%, which is approximately fivefold lower than the one obtained in the same experiment with constant flow (43.97 ± 2.44%). Similar results were observed for paper and plastic combustion aerosols. Overall, P_{cyclic} values were approximately 4–8 times lower than the corresponding $P_{constant}$ values. One reason for this difference is that with constant flow, aerosol particles continuously penetrate into the respirator (mostly through the leakage). However, under the cyclic flow regime, no particles enter during exhalation (half the period). The return flow is particle free since it is supplied back into the respirator through a HEPA filter installed between the manikin and the breathing simulator. This time factor causes a twofold decrease in aerosol concentration inside the respirator with cyclic breathing compared to constant flow, which explains a 50% drop in the measured penetration.

In addition, the returning clean airflow dilutes the particle-contaminated air inside the respirator by a volumetric factor of two, thus further decreasing the aerosol concentration C_{in}. Consequently, it should be anticipated that P_{cyclic} is at least four times below the corresponding $P_{constant}$. This explanation is valid when the majority of particles detected inside the respirator penetrate directly through facepiece leaks (not the filter). The situation is different when the aerosol enters solely through the filter (Table II, fully sealed respirator). In addition, with cyclic flow, the relative contribution of airflow through the faceseal leak and filter changes with time, which affects the difference between the penetration levels obtained in the two protocols (constant vs. cyclic flow). The large and consistent difference between $P_{constant}$ and P_{cyclic} found in this study points to a significant limitation of the existing respirator evaluation protocols that are based on the constant flow design.

(ii) *MIF effect on P_{cyclic}.* As MIF of the cyclic flow increased, the particle penetration decreased. This was observed for all three combustion materials and was statistically significant (Table III). One possible explanation is changing leak size with increasing cyclic flows. Higher flows can generate higher negative pressures inside the respirator during breathing, which improves the sealing performance of the respirator. It should be stressed that P_{cyclic} values that ranged from a low of 5.37 ± 0.29% (wood, 135 L/min) to a high of 11.4 ± 0.10% (plastic, 30 L/min) are still well above the expected penetration level of P100 filters (<0.03%). This suggests faceseal

TABLE III. ANOVA with Tukey's Range Test on the Effects of the Flow Rate Adjusted for Material (half mask)

Tukey Grouping[A]	Mean Penetration[B] (%)	Flow Type, Flow Rate (L/min)
Unsealed		
A	47.7	Constant, 30
B	10.3	Cyclic, 30
C	7.7	Cyclic, 85
D	5.8	Cyclic, 135
Nose-only sealed		
A	0.85	Constant, 30
B	0.33	Cyclic, 135
C	0.23	Cyclic, 85
C	0.14	Cyclic, 30
Nose and chin sealed		
A	0.35	Cyclic, 85
B	0.28	Cyclic, 135
B C	0.25	Constant, 30
C	0.23	Cyclic, 30
Fully sealed		
A	0.011	Cyclic, 135
B	0.002	Cyclic, 85
B	0.000	Cyclic, 30
B	0.000	Constant, 30

[A]Means with the same letter are not significantly different (p-value > 0.05). The cyclic flows of MIF = 30, 85, and 135 L/min were applied at breathing rates of 15, 25, and 25 breaths/min, respectively.
[B]Calculated over all combustion materials.

leakage was the primary penetration pathway for the unsealed half mask respirator.

(iii) Effect of combustion material on particle penetration. Data obtained with the three tested combustion materials revealed similar trends, with paper and plastic producing slightly higher penetrations than wood (Table IV). There was no statistically significant difference in penetration between paper and plastic combustion aerosols. As this study is the first one of its kind dealing with combustion aerosols, no direct comparisons can be made with previous studies.

2. Respirator Partially Sealed on the Manikin (Nose-Only Sealed and Nose and Chin Sealed)

a. *Effect of partial sealing on penetration.* As seen from Table II, penetration values obtained under these two conditions were significantly lower than those determined for the unsealed respirator (Table V). In most cases the decrease was almost two orders of magnitude. The data indicates that most of the leakage occurred around the manikin's nose.

TABLE IV. ANOVA with Tukey's Range Test on the Effects of the Material Adjusted for Breathing Flow (half mask)

Tukey Grouping[A]	Mean Penetration[B] (%)	Material
Unsealed		
A	19.1	Plastic
A	18.4	Paper
B	16.1	Wood
Nose-only sealed		
A	0.53	Wood
B	0.31	Plastic
B	0.30	Paper
Nose and chin sealed		
A	0.30	Wood
A B	0.28	Paper
B	0.26	Plastic
Fully sealed		
A	0.003	Paper
A	0.003	Wood
A	0.003	Plastic

[A]Means with the same letter are not significantly different (p-value >0.05).
[B]Calculated over all breathing flow type and flow rate.

b. *Difference between two types of partial sealing.* There were no significant differences in penetration between the two partial sealing conditions labeled as "nose-only" and "nose and chin" regardless of the combustion material and the breathing airflow (Table V). This further suggests that sealing the nose area (rather than the chin area) reduced penetration on average from approximately 5–11% (unsealed) to 0.11–0.48% (nose-only sealed) for the cyclic flow regime, and from approximately 44–51% (unsealed) to 0.66–1.19% (nose-only sealed) for the constant flow regime. This finding is consistent with other studies[30–32] that suggest the nose is frequently the primary leak location.

TABLE V. ANOVA with Tukey's Range Test on the Effects of the Sealing Condition Adjusted for Material and Breathing Flow (half mask)

Tukey Grouping[A]	Mean Penetration[B] (%)	Sealing Condition
A	17.9	Unsealed
B	0.38	Nose-only sealed
B	0.28	Nose and chin sealed
C	0.003	Fully sealed

[A]Means with the same letter are not significantly different (p-value > 0.05).
[B]Calculated over all combustion material and breathing flow.

c. *Penetration pathway.* Although partial sealing reduced the total particle penetration to the levels below 1%, these levels are still much higher than that for a P100 filter alone (<0.03% or <<0.3%). Thus, although offering much greater protection against combustion particles, partial sealing still left a considerable opportunity for penetration through faceseal leakages so that full advantage could not be taken of the efficient P100 filter deployed in a half mask elastomeric respirator.

d. *MIF effect on P_{cyclic}.* For nose-only sealed condition, we found that penetration remained at the same level at 30 and 85 L/min but was significantly higher at 135 L/min (Table III). For nose-chin sealed condition, there were significant differences between the outcome observed at three MIFs (30, 85, and 135 L/min). Compared to the unsealed condition, the P_{cyclic} values obtained for the two partial sealing conditions were 10 to 100 times lower as determined at the same MIF. The results also show that increasing the flow does not always reduce the faceseal penetration. In another study, Cho et al.[15] reported that faceseal penetration was reduced significantly (p-value <0.001) with increasing breathing flow. A different type of respirator (N95 FFR partially sealed on a manikin) tested in the quoted study may exhibit faceseal leaks of different sizes, which could cause the disagreement between the two studies.

e. *Effect of combustion material on penetration.* Penetration values were higher for wood combustion aerosol compared to paper and plastic combustion aerosols in both "nose-only" and "nose and chin" sealed conditions (Table IV). In contrast, for an unsealed respirator, plastic combustion aerosol exhibited the highest penetration. The finding suggests that a better sealing may produce different effect on the respiratory protection level for different aerosols, e.g., be more beneficial for protecting against plastic combustion particles than against other materials. This seems to have a significant practical relevance, especially given that burning plastic generates more toxic combustion particles, making their elimination by a respirator particularly important.

3. Respirator Fully Sealed on the Manikin

For a fully sealed half mask respirator, the total penetration should be equal to the filter penetration, which is supposed to be below 0.03% at 85 L/min for a NIOSH-certified P-100 filter. In our experiments, no particle penetration was detected at constant flow rate of 30 L/min. For low to moderate cyclic flows, filter penetration was 0.002% or below. At the highest flow (MIF = 135 L/min), the average penetration was around 0.011%.

The P-100 filter penetration values obtained in this study reflect the total particle count regardless of the particle size. The filter penetration generally depends on the particle size reaching the highest value for the most penetrating particle size (MPPS). One size-selective investigation revealed—for a specific P-100 FFR filter—that the penetration could be as high as 0.048% at the MMPS of 50–200 nm.[36]

TABLE VI. Penetration Values for a Full Facepiece Elastomeric Respirator

Material	Flow Type, Flow Rate (L/min)	Penetration, % (Mean ± SD)	
		Unsealed	Fully Sealed
Wood	Constant, 30	0.017 ± 0.002	0.001 ± 0.000
	Cyclic, 30	0.003 ± 0.001	0.001 ± 0.000
	Cyclic, 85	0.010 ± 0.001	0.003 ± 0.000
	Cyclic, 135	0.019 ± 0.001	0.013 ± 0.002
Paper	Constant, 30	0.024 ± 0.000	0.000 ± 0.000
	Cyclic, 30	0.003 ± 0.001	0.000 ± 0.000
	Cyclic, 85	0.008 ± 0.000	0.002 ± 0.000
	Cyclic, 135	0.016 ± 0.001	0.010 ± 0.000
Plastic	Constant, 30	0.035 ± 0.001	0.001 ± 0.000
	Cyclic, 30	0.003 ± 0.001	0.001 ± 0.000
	Cyclic, 85	0.012 ± 0.001	0.002 ± 0.000
	Cyclic, 135	0.025 ± 0.002	0.011 ± 0.000

Full Facepiece Elastomeric Respirator with P-100 Filters

1. *Respirator Donned on the Manikin (Unsealed)*

a. *Penetration values.* As seen from Table VI, penetration values for unsealed condition were extremely low for all flows and materials. At 30 L/min, $P_{constant}$ ranged from 0.017% (wood) to 0.035% (plastic). The values of P_{cyclic} were even lower: from 0.003% for MIF = 30 L/min (all three combustion materials) to 0.025% (135 L/min, plastic). These levels were approximately three orders of magnitude lower than the penetrations obtained for the half mask elastomeric respirator. This difference is likely associated with the leak size. The nose has been identified as the primary leak location for half mask respirators, whereas full facepiece does not have a nose leak (thus penetration dramatically reduced). The difference between the cyclic and constant flow regimens for the full facepiece was not as large as we observed with the half mask. Again, this also can be explained by the leak size. As the full facepiece does not have nose leak, it is more comparable to a partially sealed half mask than a fully sealed half mask.

b. *MIF effect on P_{cyclic}.* The lowest MIF (30 L/min) produced the lowest penetration; as the flow

increased, the penetration increased (p-value <0.05). Since the penetration values were so low and closer to those expected from the filter material, one would suggest that the role of faceseal leakage pathway is not as great for the full facepiece elastomeric respirator if compared to the half mask, and the particle deposition on the filter governs the process, at least to a significant extent. For ultrafine particles used in this study, the primary filtration mechanism is diffusion. As the flow increases, the residence time decreases, and the diffusion becomes less effective. This explains the observed effect of MIF on the particle penetration.

2. *Respirator Fully Sealed on the Manikin*
   Data obtained with the fully sealed full facepiece was similar to data obtained with the fully sealed half mask. This is understandable because testing of a fully sealed respirator (both half and full facepiece) is essentially equivalent to examining the performance of the respirator filter (with an exhalation valve attached). As the same type of filter was used for the half and full facepiece respirators, there was no significant difference in the filter efficiency. The results are consistent with the fact that the efficiency of a P100 filter is 0.03% or below at 85 L/min.

CONCLUSION

Two elastomeric respirators (half mask and full facepiece) were evaluated as to the overall particle penetration with respect to faceseal leakage, breathing flow type and rate, and combustion material. All these factors had significant impact on the performance of the respirators. The total penetration through the fully sealed half and full facepiece respirators did not exceed the NIOSH certification level established for P-100 respirator filters ($\leq$0.03%). Increasing leak size increased total penetration. Effects of combustion material and breathing flow were significant and heavily dependent on sealing condition. Results suggest that eliminating or minimizing faceseal leakage is the key aspect for improving the efficiency of elastomeric respirators used by firefighters against combustion particles regardless of particle composition and size distribution.

Significant difference in penetration was found between cyclic and constant flow; however, this difference was observed mainly for the unsealed half mask. For the half mask (fully sealed) and full facepiece (unsealed or fully sealed), the penetration remained the same when challenged with three different combustion aerosols (wood, paper, and plastic). While under sealing, conditions such as "nose-only," "nose and chin," and "unsealed," the combustion material did show a significant effect on the total penetration for the half mask. This effect was not consistent—plastic aerosol produced the highest penetration under the unsealed condition, whereas for the two partial sealing conditions, wood aerosol was associated with the highest penetrations.

This study provides meaningful information related to the NIOSH respirator testing program in accordance with Title 42 of the *Code of Federal Regulations*, Part 84.[37] Results indicate that the efficiency of a P-100 respirator filter is not significantly influenced by the challenge aerosol and the flow type (constant vs. cyclic). This supports the approach implemented in the current NIOSH respirator testing of P-100 filters that uses a non-combustion challenge aerosol and constant airflow. However, the NIOSH total inward leakage (TIL) test assumes that the result is independent on the type of the tested aerosol,[38] while this study revealed that the challenge aerosol significantly affects the particle penetration through unsealed and partially sealed half mask elastomeric respirators. The differences between the currently used challenge(s) and actual combustion aerosols are concerned with the particle shape, density, electric charge, and possibly other properties. The findings generated by the presently adopted TIL test protocol (using ambient or NaCl model aerosols) may have limitations in predicting protection levels offered by half mask elastomeric respirators.

One limitation of this study is that a stationary (non-moving) manikin headform was used. It is acknowledged that this type of headform is not capable of mimicking human speaking, head movements, or facial expressions, which could affect the leak size. We believe that the next step in testing the elastomeric half mask and full facepiece respirators could involve robotically articulating headforms.

ACKNOWLEDGMENTS

This study was supported by the NIOSH Targeted Research Training Program of the University of Cincinnati Education and Research Center grant (No. T42/OH008432-06) and the University of Cincinnati Graduate Assistantship and Scholarship.

REFERENCES

1. **National Institute for Occupational Safety and Health (NIOSH):** "Preventing Fire Fighter Fatalities Due to Heart Attacks and Other Sudden Cardiovascular Events 2007-133." 2007.
2. **Baxter, C.S., C.S. Ross, T. Fabian, et al.:** Ultrafine particle exposure during fire suppression—Is it an important contributory factor for coronary heart disease in firefighters? *J. Occup. Environ. Med. 52* (*8*): 791–796 (2010).
3. **Peters, A., H.E. Wichmann, T. Tuch, J. Heinrich, and J. Heyder:** Respiratory effects are associated with the number of ultrafine particles. *Am. J. Respir. Crit. Care Med. 155* (*4*): 1376–1383 (1997).
4. **Schwartz, J., D.W. Dockery, and L.M. Neas:** Is daily mortality associated specifically with fine particles? *J. Air Waste Manag. Assoc. 46* (*10*):927–939 (1996).
5. **Timonen, K.L., E. Vanninen, J. de Hartog, et al.:** Effects of ultrafine and fine particulate and gaseous air pollution on cardiac autonomic control in subjects with coronary artery disease: The ULTRA study. *J. Expos. Sci. Environ. Epidemiol. 16* (*4*):332–341 (2005).
6. **Fahy, R., P. LeBlanc, and J. Molis:** Firefighter fatalities in the United States—2008. *Quincy, Mass.: National Fire Protection Association*, 2009.

7. **Centers for Disease Control and Prevention (CDC):** Fatalities among volunteer and career firefighters—United States, 1994–2004. *MMWR 55*(*16*): 453–455 (2006).
8. **Yoo, H.L., and W.D. Franke:** Prevalence of cardiovascular disease risk factors in volunteer firefighters. *J. Occup. Environ. Med. 51* (*8*) :958–962 (2009).
9. **LeMasters, G.K., A.M. Genaidy, P. Succop, et al.:** Cancer risk among firefighters: A review and meta-analysis of 32 studies. *J. Occup. Environ. Med. 48* (*11*): 1189–1202 (2006).
10. **National Fire Protection Association (NFPA):** *Standard on Open-Circuit Self-Contained Breathing Apparatus (SCBA) for Emergency Services, 2007 Edition*. Quincy, Mass.: NFPA, 2007.
11. "Respiratory Protective Devices; Final Rules and Notices," *Federal Register 60*:*110* (8 June 1995). pp. 30335–30393.
12. **Bolstad-Johnson, D.M., J.L. Burgess, C.D. Crutchfield, S. Storment, R. Gerkin, and J.R. Wilson:** Characterization of firefighter exposures during fire overhaul. *Am. Ind. Hyg. Assoc. J. 61*: 636–641 (2000).
13. **Burgess, J.L., C.J. Nanson, D.M. Bolstad-Johnson, et al.:** Adverse respiratory effects following overhaul in firefighters. *J. Occup. Environ. Med. 43* (*5*):467–473 (2001).
14. "Respirator Protection," *Code of Federal Regulations Title* 29, Part 1910.134 (d)(3)(i)(A). 2006.
15. **Cho, K.J., T. Reponen, R. McKay, et al.:** Large particle penetration through N95 respirator filters and facepiece leaks with cyclic flow. *Ann. Occup. Hyg. 54* (*1*):68–77 (2010).
16. **Grinshpun, S.A., H. Haruta, R.M. Eninger, T. Reponen, R.T. McKay, and S.-A. Lee:** Performance of an N95 filtering facepiece particulate respirator and a surgical mask during human breathing: Two pathways for particle penetration. *J. Occup. Environ. Hyg. 6*:593–603 (2009).
17. **Hinds, W.C., and G. Kraske:** Performance of dust respirators with facial seal leaks: I. Experimental. *Am. Ind. Hyg. Assoc. J. 48*:836–841 (1987).
18. **Chen, C.C., and K. Willeke:** Characteristics of face seal leakage in filtering facepieces. *Am. Ind. Hyg. Assoc. J. 53*:533–539 (1992).
19. **Cho, K.J., S. Jones, G. Jones, et al.:** Effect of particle size on respiratory protection provided by two types of N95 respirators used in agricultural settings. *J. Occup. Environ. Hyg. 7*:622–627 (2010).
20. **Lee, S.-A., A. Adhikari, S.A. Grinshpun, et al.:** Respiratory protection provided by N95 filtering facepiece respirators against airborne dust and microorganisms in agricultural farms. *J. Occup. Environ. Hyg. 2*:577–585 (2005).
21. **Lee, S.-A., S.A. Grinshpun, A. Adhikari, et al.:** Laboratory and field evaluation of a new personal sampling system for assessing the protection provided by the N95 filtering facepiece respirators against particles. *Ann. Occup. Hyg. 49* (*3*):245–257 (2005).
22. **Myers, W.R., and Z. Zhuang:** Field performance measurements of half-facepiece respirators: Developing probability estimates to evaluate the adequacy of an APF of 10. *Am. Ind. Hyg. Assoc. J. 59*: 796–801 (1998).
23. **Myers, W.R., Z. Zhuang, and T. Nelson:** Field performance measurements of half-facepiece respirators—Foundry operations. *Am. Ind. Hyg. Assoc. J. 57*:166–174 (1996).
24. **Lee, S.-A., S.A. Grinshpun, and T. Reponen:** Respiratory performance offered by N95 respirators and surgical masks: Human subject evaluation with NaCl aerosol representing bacterial and viral particle size range. *Ann. Occup. Hyg. 52* (*3*):177–185 (2008).
25. **Reponen, T., S.-A. Lee, S.A. Grinshpun, E. Johnson, and R. McKay:** Effect of fit testing on the protection offered by N95 filtering facepiece respirators against fine particles in a laboratory setting. *Ann. Occup. Hyg. 55* (*3*):264–271 (2011).
26. **Myers, W.R., H. Kim, and N. Kadrichu:** Effect of particle size on assessment of faceseal leakage. *J. Int. Soc. Resp. Prot. 9* (*3*):6–21 (1991).
27. **Qian, Y., K. Willeke, S.A. Grinshpun, J. Donnelly, and C.C. Coffey:** Performance of N95 respirators: Filtration efficiency for airborne microbial and inert particles. *Am. Ind. Hyg. Assoc. J. 59* (*2*):128–132 (1998).
28. **Bałazy, A., M. Toivola, A. Adhikari, S.K. Sivasubramani, T. Reponen, and S.A. Grinshpun:** Do N95 respirators provide 95% protection level against airborne viruses, and how adequate are surgical masks? *Am. J. Infect. Control 34* (*2*):51–57 (2006).
29. **Eninger, R.M., T. Honda, A. Adhikari, H. Heinonen-Tanski, T. Reponen, and S.A. Grinshpun:** Filter performance of N99 and N95 facepiece respirators against viruses and ultrafine particles. *Ann. Occup. Hyg. 52* (*5*):385–396 (2008).
30. **Crutchfield, C.D., and D.L. Park:** Effect of leak location on measured respirator Fit. *Am. Ind. Hyg. Assoc. J. 58* (*6*):413–418 (1997).
31. **Oestenstad, R.K., and A.A. Bartolucci:** Factors affecting the location and shape of face seal leak sites on half-mask respirators. *J. Occup. Environ. Hyg. 7*:332–341 (2010).
32. **Oestenstad, R.K., and L.L. Perkins:** An assessment of critical anthropometric dimensions for predicting the fit of a half-mask respirator. *Am. Ind. Hyg. Assoc. J. 53*:639–644 (1992).
33. **Sherwood, L.:** *Fundamentals of Physiology: A Human Perspective, 3rd ed.* Belmont, Calif.: Brooks/Cole, Thomson Learning, 2006. p. 380.
34. **Tortora, G.J., and N.P. Anagnostakos:** *Principles of Anatomy and Physiology, 6th ed*. New York: Harper-Collins, 1990. p. 707.
35. **Kulkarni, P., P.A. Baron, and K. Willeke:** *Aerosol Measurement - Principles, Techniques, and Applications, 3rd ed.* Hoboken, N.J.: John Wiley & Sons, 2011.
36. **Eshbaugh, J.P., P.D. Gardner, A.W. Richardson, and K.C. Hofacre:** N95 and P100 respirator filter efficiency under high constant and cyclic flow. *J. Occup. Environ. Hyg. 6*:52–61 (2008).
37. "Respiratory Protection," *Code of Federal Regulations Title 42*, Part 84 1995. pp. 30382–30383.
38. **National Institute for Occupational Safety and Health (NIOSH):** "Total Inward Leakage for Half-mask Air-purifying Particulate Respirators." Available at http://www.cdc.gov/niosh/npptl/resources/certpgmspt/meetings/062607/pdfs/TILHandout_Procedure.pdf (accessed Oct. 20, 2012).

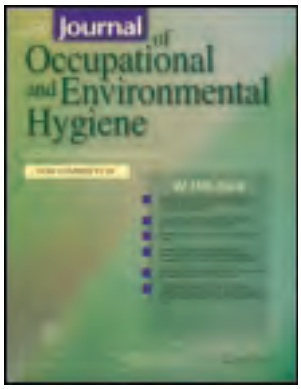

Journal of Occupational and Environmental Hygiene
Publication details, including instructions for authors and subscription information:
http://oeh.tandfonline.com/loi/uoeh20

Exploring a Novel Ultrafine Particle Counter for Utilization in Respiratory Protection Studies

Xinjian He [a] , Sang-Young Son [b] , Kelley James [b] , Michael Yermakov [a] , Tiina Reponen [a] , Roy T. McKay [a] & Sergey A. Grinshpun [a]

[a] Center for Health-Related Aerosol Studies, Department of Environmental Health, University of Cincinnati, Cincinnati, Ohio

[b] Department of Mechanical Engineering, University of Cincinnati, Cincinnati, Ohio

Accepted author version posted online: 22 Jan 2013.Version of record first published: 26 Feb 2013.

To cite this article: Xinjian He , Sang-Young Son , Kelley James , Michael Yermakov , Tiina Reponen , Roy T. McKay & Sergey A. Grinshpun (2013): Exploring a Novel Ultrafine Particle Counter for Utilization in Respiratory Protection Studies, Journal of Occupational and Environmental Hygiene, 10:4, D52-D54

To link to this article: http://dx.doi.org/10.1080/15459624.2013.766555

Journal of Occupational and Environmental Hygiene, 10: D52–D54
ISSN: 1545-9624 print / 1545-9632 online

DOI: 10.1080/15459624.2013.766555

Analytical Performance Issues
Exploring a Novel Ultrafine Particle Counter for Utilization in Respiratory Protection Studies

Exposure to ultrafine ($\leq$0.1 μm) particles is widespread at various workplaces. Several studies have revealed associations between ultrafine particle exposures and adverse health effects, including respiratory problems, impairment of cardiovascular function, and others.[1–3]

Condensation particle counters (CPCs) are conventionally deployed to measure the ultrafine particle concentrations in real time. For example, the P-Trak (Model 3007, TSI Inc., Shoreview, Minn.) is the most commonly used CPC in occupational environments. However, commercially available CPCs are typically too bulky to serve as workers' personal exposure monitors; furthermore, their performance is generally affected by their orientation. Several attempts have been made recently to design a better instrument for real-time personal exposure assessment, including a novel ultrafine particle counter (prototype) developed at the University of Cincinnati (UC UFP counter, Figure 1).[4,5] The operation principle of this device, like any CPC, involves condensation on nuclei; however, the novelty of this instrument is that the condensation takes place on nano-materials entering through the input channel. After passing a PM filter (cyclone), the particles enter a non-wetting, porous evaporation-condensation tube. Enlarged due to condensation growth, they are detected with an optical laser counter. Capillary force spontaneously generated on the surface of the non-wetting tube prevents flooding regardless of orientation and movement. This makes the instrument particularly advantageous for field applications. In addition, its time of response to a change in aerosol concentration is as low as approximately 0.3 sec. The detection particle size range is 4.5 nm to $>$1.0 μm that, in contrast to conventional CPCs, includes a low nano-scale. The present prototype of the UC UFP counter is portable; however, it is undergoing additional miniaturization to make the device wearable.

In this study, we examined the feasibility of using the UC UFP counter for measuring the aerosol particle penetration through an elastomeric half-mask respirator donned on a breathing manikin.[6,7] Elastomeric respirators are commonly used by firefighters and first responders. The UC UFP counter was tested against the TSI Model 3007 CPC operating side by side. Combustion particles (generated by burning wood, paper, or plastic) were used as challenge aerosols. Exposures to combustion aerosols at various workplace environments have been associated with adverse health outcomes.[2,3] More than 70% (by number) of particles in a fire-generated smoke are ultrafine.[8] The penetration values were obtained by measuring the aerosol concentrations inside and outside the respirator. The sampled airflow was split with 0.3 L/min directed to the UC UFP counter and 0.7 L/min to the TSI CPC. Measurements were conducted for four respirator sealing conditions (unsealed, sealed at the nose area, sealed at chin and nose, fully sealed) and for three cyclic breathing flow rates (mean inspiratory flow = 30, 85, and 135 L/min) and one constant flow rate (30 L/min).

Column Editor
Martin Harper

Reported by
Xinjian He[1]
Sang-Young Son[2]
Kelley James[2]
Michael Yermakov[1]
Tiina Reponen[1]
Roy T. McKay[1]
Sergey A. Grinshpun[1]

[1]Center for Health-Related Aerosol Studies, Department of Environmental Health, University of Cincinnati, Cincinnati, Ohio

[2]Department of Mechanical Engineering, University of Cincinnati, Cincinnati, Ohio

Correspondence to: Sergey Grinshpun, University of Cincinnati, Environmental Health, 3223 Eden Ave., P.O. 670056, Cincinnati, OH 45267; e-mail: sergey.grinshpun@uc.edu.

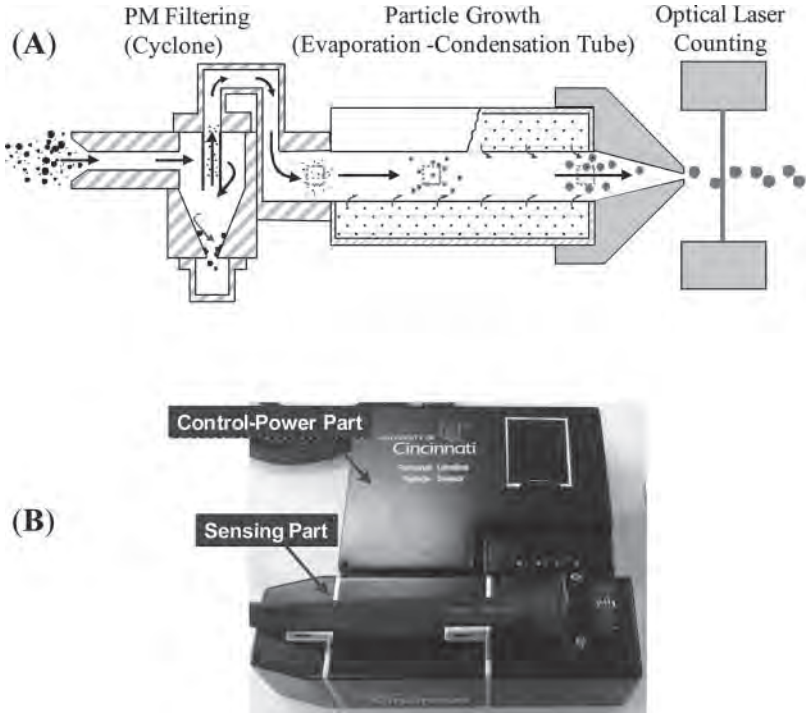

FIGURE 1. The UC UFP counter: schematics of operation (A) and picture (B).

The data are presented in Figure 2. The particle penetration falls into a wide range of values: from ~0.01% to ~60%, which reflects a variety of the sealing and breathing conditions. A favorable agreement between the two data sets was observed (slope $\approx$ 1.16, $R^2 \approx 0.99$; paired *t*-test: *p*-value = 0.91), suggesting that the new counter produced meaningful data comparable to a conventional TSI CPC instrument and was capable of measuring in the abovementioned wide range of parameters. We concluded that, once miniaturized to serve as a field compatible personal sampling device, the instrument can be successfully used for evaluating the performance of respirators directly at workplaces. Considering the data variability observed in this study (specifically two clusters at penetration levels around 0.1% and 1% as measured by the TSI CPC), a follow-up investigation is warranted to improve the sensitivity and stability of the UC UFP.

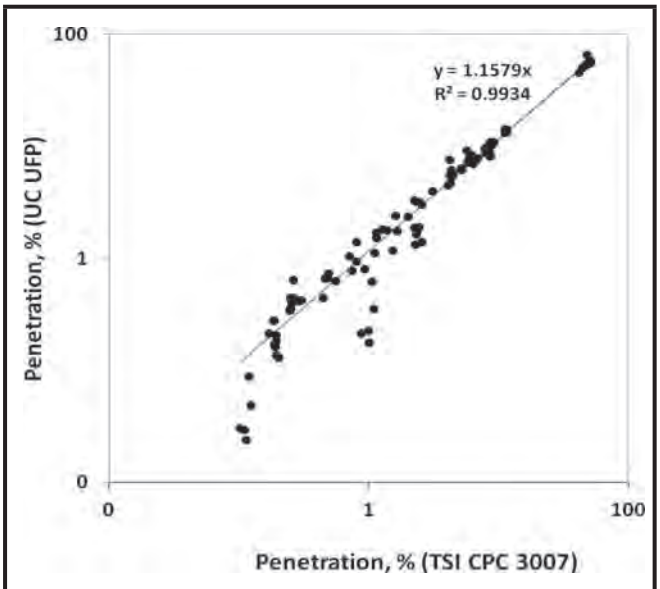

FIGURE 2. Particle penetration values measured with the novel UC UFP counter vs. the TSI CPC 3007.

ACKNOWLEDGMENTS

This study was supported by the NIOSH Targeted Research Training program of the University of Cincinnati Education and Research Center grant (No.T42/OH008432-06), NIH grant 5U01ES16123, and the University of Cincinnati Graduate Assistantship and Scholarship.

REFERENCES

1. **Peters, A., H.E. Wichmann, T. Tuch, J. Heinrich, and J. Heyder:** Respiratory effects are associated with the number of ultrafine particles. *Am. J. Respir. Crit. Care Med. 155*(*4*):1376–1383 (1997).
2. **Schwartz, J., D.W. Dockery, and L.M. Neas:** Is daily mortality associated specifically with fine particles? *J. Air Waste Manag. Assoc. 46*(*10*):927–939 (1996).
3. **Timonen, K.L., E. Vanninen, J. de Hartog, et al.:** Effects of ultrafine and fine particulate and gaseous air pollution on cardiac autonomic control in subjects with coronary artery disease: The ULTRA study. *J. Expos. Sci. Environ. Epidemiol. 16*(*4*):332–341 (2005).

4. **Son, S.Y., J.Y. Lee, H. Fu, S. Anand, F. Romay, and A. Collins:** Personal and wearable ultrafine particle counter. In *Proceedings of the AAAR 30th Annual Conference*, American Association for Aerosol Research, October 3–7, 2011, Orlando, Florida.
5. **Son, S.Y., J.Y. Lee, J. Lockey, and G. LeMasters:** 2010. Continuous droplet generator devices and methods. US Patent 20,100,180,765, filed Jan. 19, 2010.
6. **Grinshpun, S.A., H. Haruta, R.M. Eninger, T. Reponen, R.T. McKay, and S.-A. Lee:** Performance of an N95 filtering facepiece particulate respirator and a surgical mask during human breathing: Two pathways for particle penetration. *J. Occup. Environ. Hyg. 6*:593–603 (2009).
7. **He, X., M. Yermakov, T. Reponen, R. McKay, K. James, and S.A. Grinshpun:** Manikin-based performance evaluation of elastomeric respirators against combustion particles. *J. Occup. Environ. Hyg.* 10: 203–212.
8. **Baxter, C.S., C.S. Ross, T. Fabian, et al.:** Ultrafine particle exposure during fire suppression—Is it an important contributory factor for coronary heart disease in firefighters? *J. Occup. Environ. Med. 52*(*8*):791–796 (2010).

Ann. Occup. Hyg.

doi:10.1093/annhyg/met014

Laboratory Evaluation of the Particle Size Effect on the Performance of an Elastomeric Half-mask Respirator against Ultrafine Combustion Particles

XINJIAN HE[1], SERGEY A. GRINSHPUN[1]*, TIINA REPONEN[1], MICHAEL YERMAKOV[1], ROY MCKAY[1], HIROKI HARUTA[2] and KAZUSHI KIMURA[2]

[1]Center for Health-Related Aerosol Studies, Department of Environmental Health, University of Cincinnati, PO Box 670056, Cincinnati, OH 45267-0056, USA; [2]Koken Ltd, 7 Yonbancho, Chiyoda-ku, Tokyo 102–8459, Japan

Received 9 December 2012; in final form 1 February 2013

Objectives: This study quantified the particle size effect on the performance of elastomeric half-mask respirators, which are widely used by firefighters and first responders exposed to combustion aerosols.

Methods: One type of elastomeric half-mask respirator equipped with two P-100 filters was donned on a breathing manikin while challenged with three combustion aerosols (originated by burning wood, paper, and plastic). Testing was conducted with respirators that were fully sealed, partially sealed (nose area only), or unsealed to the face of a breathing manikin to simulate different faceseal leakages. Three cyclic flows with mean inspiratory flow (MIF) rates of 30, 85, and 135 L/min were tested for each combination of sealing condition and combustion material. Additional testing was performed with plastic combustion particles at other cyclic and constant flows. Particle penetration was determined by measuring particle number concentrations inside and outside the respirator with size ranges from 20 to 200 nm.

Results: Breathing flow rate, particle size, and combustion material all had significant effects on the performance of the respirator. For the partially sealed and unsealed respirators, the penetration through the faceseal leakage reached maximum at particle sizes >100 nm when challenged with plastic aerosol, whereas no clear peaks were observed for wood and paper aerosols. The particles aerosolized by burning plastic penetrated more readily into the unsealed half-mask than those aerosolized by the combustion of wood and paper. The difference may be attributed to the fact that plastic combustion particles differ from wood and paper particles by physical characteristics such as charge, shape, and density. For the partially sealed respirator, the highest penetration values were obtained at MIF = 85 L/min. The unsealed respirator had approximately 10-fold greater penetration than the one partially sealed around the bridge of the nose, which indicates that the nose area was the primary leak site.

Keywords: combustion aerosol; half-mask; manikin; particle size; penetration; respirator fit

INTRODUCTION

The US Bureau of Labor Statistics (BLS) has reported that firefighting ranks among the most dangerous occupations in the USA (BLS, 2003). Firefighters are known to have respiratory problems due to smoke inhalation resulting from combustion (Musk et al., 1982; Materna et al., 1992; CDC, 2006). First responders as well as other workers exposed to combustion aerosols are at a similar health risks as firefighters, although their associated health effects are not as well documented. Smoke generated from a fire consists

*Author to whom correspondence should be addressed: Tel: 1-513-558-0504; Fax: 1-513-558-2263; e-mail: sergey.grinshpun@uc.edu

primarily of fine (≤ 1 μm) and ultrafine (≤ 0.1 μm) particles. These smoke particles contain a variety of reactive free radicals and other chemical compounds, which pose a potential health risk (Leonard et al., 2007). Baxter et al. (2010) reported >70% (by number) of smoke particles present during fire knockdown and overhaul are ultrafine. With an increase in surface area, ultrafine particles can be toxicologically more reactive than those of larger sizes (Lam et al., 2004; Shvedova et al., 2005).

During fire overhaul (after the fire has been extinguished), firefighters enter the structure to examine areas for possible re-ignition. At that stage, it has been reported that firefighters may use elastomeric half-mask respirators equipped with a highly efficient P-100 filters (Bolstad-Johnson et al., 2000; Burgess et al., 2001). When subjected to the National Institute for Occupational Safety and Health (NIOSH) respirator certification test, a P-100 filter must provide at least a 99.97% efficiency when challenged to polydisperse dioctyl phthalate (DOP) particles having a count median diameter (CMD) of 185 ± 20 nm and a geometric standard deviation (GSD) of <1.60 (Shaffer and Rengasamy, 2009).

Numerous studies have been conducted to determine the filter efficiency of commercially available respirators (Martin and Moyer, 2000; Eninger et al., 2008; Eshbaugh et al., 2009; Rengasamy et al., 2008; Rengasamy et al., 2009). However, the respirator performance is affected not only by the filter efficiency but also by the faceseal leakage. Furthermore, several studies have shown that particle penetration through the faceseal leakage may be much higher than through the filter medium (Coffey et al., 1998; Zhuang et al., 1998; Grinshpun et al., 2009; Cho et al., 2010b). To account for these two penetration pathways, NIOSH has proposed the total inward leakage (TIL) method for testing respirators (NIOSH, 2009). However, the NIOSH TIL test does not consider particle size, as it is based on non–size selective measurement. TIL was investigated as a function of particle size (aerodynamic size: 0.04–1.3 μm) in our previous research performed with N95 respirators and surgical masks (Lee et al., 2008). The lowest protection factors (PFs) were observed in the size range of 0.04–0.2 μm (which includes the ultrafine fraction). Faceseal leaks on one brand of half-mask respirator (US Safety Series 200 Half-mask) worn by 73 subjects were studied by Oestenstad and Perkins (1992). They found respirator leakage was strongly affected by leaks at the nose and chin, and consideration should be given to including nasal dimensions when selecting a respirator for an individual wearer. Our recent study with a half-mask respirator tested on a breathing manikin revealed that the nose was the primary leak site (He et al., 2013).

There are no data available about the ultrafine particle penetration through faceseal leaks of elastomeric respirators even for a relatively simple case when the breathing flow rate is assumed to be constant. It is much more complex to quantify the particle penetration under actual breathing conditions (when the air flow through a respirator is not constant but has a cyclic nature). Early researchers addressed the effects of faceseal leakage on the particle penetration (Hinds and Kraske, 1987; Chen et al., 1990; Chen and Willeke, 1992). A recent study conducted by Rengasamy and Eimer (2011) investigated the TIL of nanoparticles through Filtering Facepiece Respirators (FFRs) and reported that penetration increased with increasing leak size. With smaller size leaks (< 1.65 mm), the penetration values measured for 50 nm size particles were ~2-fold higher than the values determined for 8 and 400 nm size particles. However, the quoted studies were conducted using either constant flow or artificially induced leaks. Cho et al. (2010b) investigated a more realistic faceseal leakage by partially sealing a N95 respirator on a manikin face with breathing patterns simulated (as a sinusoidal function) by a breathing simulator. That paper showed that most of particles penetrated into the respirator through the faceseal leakage, rather than through the filter. A similar conclusion was drawn by Grinshpun et al. (2009) for a N95 FFR and a surgical mask.

Different challenge aerosols (non-biological and biological) have been utilized for various respiratory protection research including NaCl, Ag, DOP, and viruses (enterobacteriophages MS2, T4, and Bacillus subtilis phage) (Balazy et al., 2006a; Huang et al., 2007; Eninger et al., 2008; Shaffer and Rengasamy, 2009; Cho et al., 2010a; Rengasamy and Eimer, 2011). In most of the previous respirator evaluation studies the challenge aerosol was charge neutralized/equilibrated. To our knowledge, besides our latest investigation (He et al., 2013), no peer-reviewed published study has yet reported respirator performance using combustion aerosols that likely have different charge, shape, and density.

The present investigation is a follow-up to the study of He et al. (2013) performed with challenge aerosols originating from the combustion of wood, paper, and plastic. Similar to our earlier

study, the present investigation aims at testing the performance of an elastomeric half-mask respirator; however, a distinct difference is that the current experimental design includes particle size as an independent variable. Accordingly, a particle size selective measurement technique was deployed in this effort to characterize the effect of particle size along with other factors such as inhalation flow, combustion material, and faceseal leakage on the efficiency of a half-mask respirator.

MATERIALS AND METHODS

Respirator and challenge aerosols

In this study an elastomeric half-mask respirator was tested, which is widely used by firefighters during fire overhaul. This type of respirator is also commonly used by first responders and other workers exposed to combustion aerosols. The model selection was also influenced by feedback from the Cincinnati Fire Department, which indicated that their firefighters frequently wear elastomeric 3M 6000 series half-mask respirators with P-100 filters for medical responses and fire overhaul. Based on this rationale, a medium size 3M 6000 series half-mask respirator equipped with two 3M 2091 P-100 filters was chosen for this study. This same make and model was tested in our latest study on the overall (non-particle-size-selective) particle penetration (He et al., 2013).

Three combustion aerosols were generated by burning the following materials inside a test chamber: wood (24 cm BBQ long matches, 1.9 ± 0.5 g), paper (23 cm × 24 cm brown multifold paper towel, 2.1 ± 0.2 g), and plastic (23 cm × 20 cm Ziploc™ sandwich bags, single layer, 1.7 ± 0.3 g). Wood, paper, and plastic were selected to represent common sources of combustion particles in the environments encountered by firefighters and first responders. It is noted that aerosol particles originated by combustion are usually highly charged; unlike many earlier investigations, no charge neutralization or equilibration was conducted in this study in order to preserve the original properties of combustion particles.

Study design and experimental set-up

The experiments were carried out in the University of Cincinnati indoor testing chamber (volume = 24.3 m^3). The experimental set-up is presented in Fig. 1.

In each experiment, the elastomeric half-mask respirator was donned on a breathing manikin and challenged with one of the three test combustion aerosols. Tests were conducted at three cyclic flows, with mean inspiratory flows (MIFs) of 30, 85, and 135 L/min. These flows represent breathing at medium, high, and strenuous workloads (Lafortuna et al., 1984; Anderson et al., 2006). The cyclic breathing was simulated by a Breathing Recording and Simulation System (BRSS, Koken Ltd., Tokyo, Japan). The BRSS consists of an electromechanical drive-cylinder and two air cylinders connected to each other. A sinusoidal air flow is generated as the electromechanical cylinder moves back (inspiratory duration, half a period) and forth (expiratory duration, half a period) (Haruta et al., 2008). The cylinder moving distance simulates the human tidal volume. By adjusting the speed and distance of the cylinder, the breathing frequency was set at 25 breaths/min for all three cyclic flows. Choosing the same breathing frequency for all cyclic flows eliminated frequency as an additional variable from the study design.

To examine the effect of the faceseal leakage on the performance of the respirator, three sealing conditions, namely 'fully sealed', 'partially (nose area) sealed', and 'unsealed', were established. A silicone sealant was applied to the respirator when it was necessary to seal the facepiece to the manikin. The fully sealed condition essentially targeted the efficiency of the P-100 filters installed on the half-mask respirator, assuming no penetration through the exhalation valve. The unsealed and partially sealed conditions permitted evaluation for both penetration pathways: filter penetration and faceseal leakage. Several studies have reported that faceseal leakage occurs mostly in the nose and chin area (Holton et al., 1987; Crutchfield and Park, 1997; Oestenstad et al., 2007; Oestenstad and Bartolucci, 2010). Our previous study (He et al., 2013) showed that there was no significant difference between two conditions 'nose-only sealed' and 'nose & chin sealed' in terms of the penetration level for the same half-mask respirator. Based on this rationale, only one partially sealed condition—a nose area seal—was chosen for this study (the length of the seal was 12.7 cm, which is ~30% of the 40.6 cm total respirator sealing length).

For each combination of the test conditions, the experiment was repeated four times. The particle concentrations outside and inside of the respirator were measured size-selectively using a recently developed Nanoparticle Spectrometer (Model: Nano-ID NPS500, Naneum Ltd., Kent, UK). To sample from inside the respirator, the half-mask was probed between the nose and upper lip of the

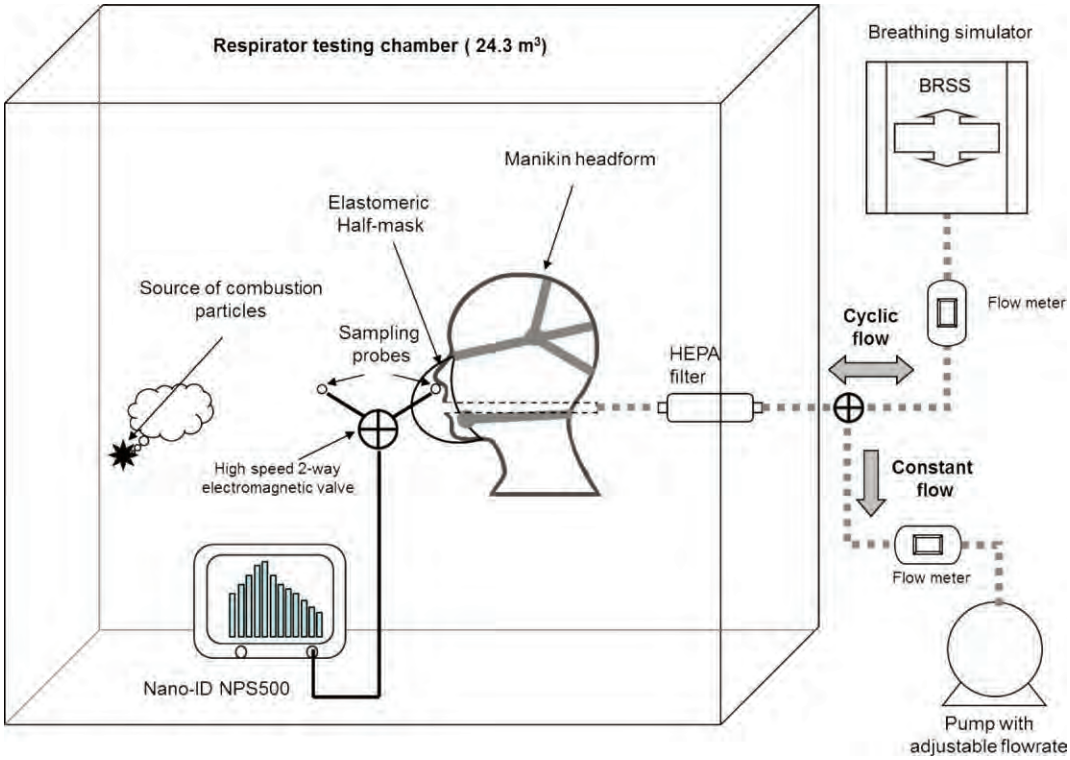

Fig. 1. Schematic diagram of the experimental set-up (modified from He et al., 2013).

manikin using the TSI Model 8025-N95 Fit Test Probe Kit. The Nano-ID is capable of measuring an aerosol particle size distribution over a range of mobility diameters (an equivalent diameter of a spherical particle of the same mobility, Kulkarni et al., 2011) from 5 to 500 nm (referred to as a scan range). The particle counts are recorded in up to 128 user-selectable channels at a sampling flow rate 0.2 L/min, which is sufficiently low (compared with the breathing flow 30–135 L/min) and, therefore, is unlikely to cause significant influence in the measured particle concentration inside the respirator. Myers et al. (1988) stated that biased sampling often occurs because aerosol does not mix well within the respirator cavity during the inhalation phase of the respiratory cycle. To minimize the effect of non-homogeneity of the concentration inside the respirator, resulting from poor mixing, a 3-min scan time was chosen for each measurement; this time allows integrating many cycles in one measurement, e.g. as many as 75 cycles in 3 min at 25 breaths/min.

The particle penetration (through both pathways) was determined for each particle size (d_p) as the ratio of inside and outside concentrations:

$$P(d_p) = \frac{C_{in}}{C_{out}} \times 100\% \quad (1)$$

Data analysis

For each combination of experimental conditions, the mean value of the total penetration and the standard deviation were calculated from the four replicates. One-way analyses of Variance (ANOVA) was performed to quantify the effect of sealing condition on the particle penetration, and three-way ANOVA was used to study the significance of combustion material, breathing flow, and particle size using SAS version 9.2 (SAS Institute Inc., Cary, NC). *P*-values of <0.05 were considered to represent significant differences in the outcomes.

RESULTS AND DISCUSSION

Particle size distribution of challenge combustion aerosols

Fig. 2 shows the particle size distributions of the three combustion aerosols measured at 10, 30, 50, 70, and 90 min after the burning was stopped.

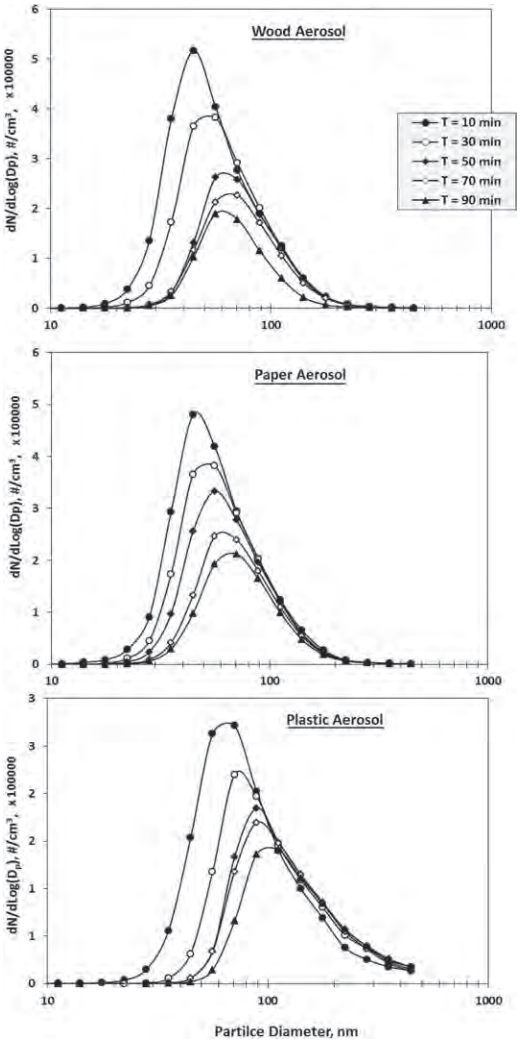

Fig. 2. Particle size distributions of three combustion aerosols (wood, paper, and plastic) measured at 10, 30, 50, 70, and 90 min after the material burning stopped.

Each aerosol produced a single-mode distribution. The peak concentrations occurred in the mobility diameter range of 40–80 nm for wood and paper combustion aerosols, whereas the peaks shifted slightly toward a larger size range (50–100 nm) for plastic combustion aerosols.

The majority of particles detected by the Nanoparticle Spectrometer fell between 20 and 200 nm. This is in a good agreement with the above quoted findings of Baxter et al. (2010), who suggested that the scan range could be narrowed down. In addition to a better representation of the challenge aerosol, a narrower scan range improves the instrument performance in a specific time interval (by providing a more accurate particle count per channel). Accordingly, the size range of 20–200 nm discriminated through 30 scan channels (representing 30 particle size fractions) was selected. The above choice was consistent with an important aim of the particle size selective sampling—to identify the most penetrating particle size (MPPS).

The natural decay of airborne particle concentration was found to be dependent on particle size. It is seen in Fig. 2 that the natural decay was very slow for wood and paper combustion particles >80 nm and plastic combustion particles >100 nm. The slower decay for larger particles can be explained by weakening diffusion as well as continuous coagulation (Kulkarni et al., 2011). The curves demonstrate a pronounced concentration decrease during approximately the first 50 min, which slowed down afterwards. On average, ~40% of particles remained airborne after 90 min. This assured a sufficient number of particles available for counting in each Nano-ID channel.

Fully sealed half-mask respirator with P-100 filters

The fully sealed respirator prevented particles from penetrating through the faceseal leakage. Therefore, total particle penetration equals filter penetration ($P = P_{filter}$), assuming no penetration through the exhalation valve. A separate experiment was conducted to test the assumption that exhalation valve operated properly, thus introducing no additional pathway for particles to penetrate inside the respirator. In this experiment, the same respirator with a functional exhalation valve was compared with a sealed valve. The penetration was determined at a constant flow of 135 L/min as well as at a cyclic flow of MIF=135 L/min. For either flow conditions, no significant difference in the penetration values was found. The results confirmed that the exhalation valve had no influence on particle penetration, which supports the fundamental postulate of our study design of only two particle penetration pathways (filter and faceseal).

Fig. 3 presents the particle penetration values for the fully sealed half-mask respirator equipped with two P-100 filters challenged with particles aerosolized by wood combustion. Our previous study (He et al., 2013) conducted with an identical fully sealed half-mask indicated that the effect of combustion material on the particle penetration was not significant (*P*-value >0.05); therefore, only one combustion material (wood) was tested here. Except

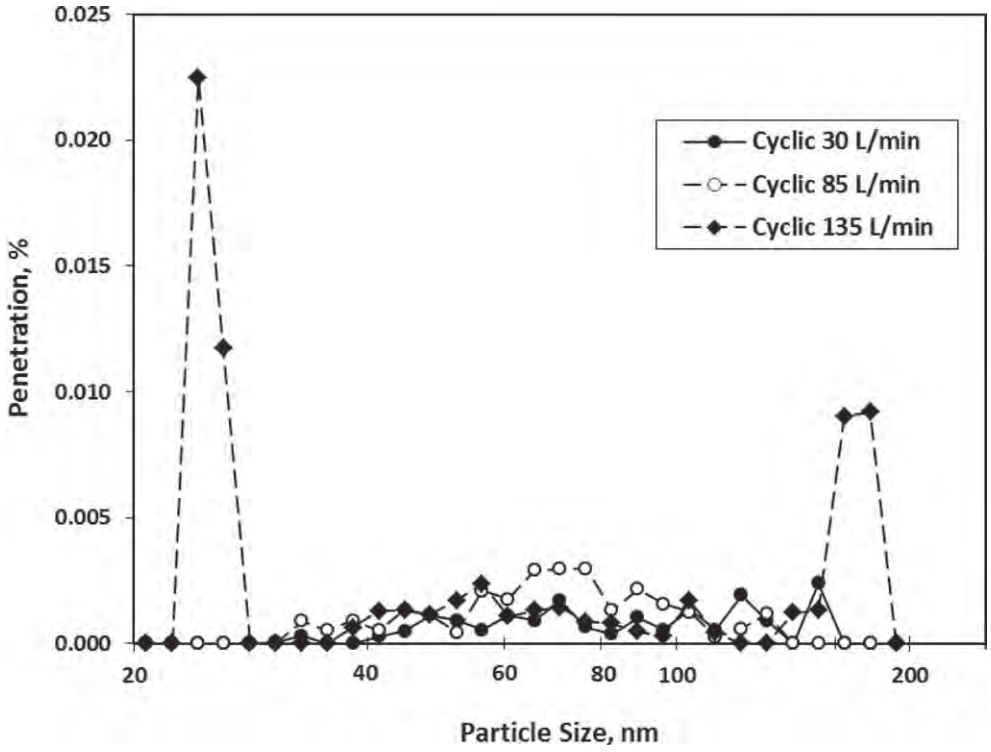

Fig. 3. Penetration of 'wood' combustion aerosol through a fully sealed half-mask equipped with two P-100 filters. Each data point represents the average of four replicates.

for a few points obtained at 135 L/min, all the other values were <0.005% regardless of the particle size and flow rate. The two peak points that occurred at the lower (~30 nm) and higher (~180 nm) sizes could be outliers as there were not sufficient number of particles (C_{out} <10 000 particles/channel, C_{in} <1 particle/channel) generated at those two sizes especially after 90-min measurement (see Fig. 2, Wood Aerosol). However, even if these two peaks were considered as valid data points, the maximum filter penetration would still fall <0.025% (Fig. 3). Overall, the results demonstrate that the tested P-100 filters exhibited the efficiency levels exceeding the NIOSH certification requirement (P ≤0.03%). This finding is in agreement with our earlier results obtained using a non-particle-size-selective aerosol measurement technique (He et al., 2013). Several other studies also reported similarly low particle penetration for P-100 filters (Eshbaugh et al., 2009; Rengasamy and Eimer, 2011).

Partially (nose area) sealed half-mask respirator with P-100 filters

Fig. 4 presents the particle penetration data for partially sealed half-mask with two P-100 filters, which was tested at three MIFs (30, 85, and 135 L/min) while exposed to three combustion aerosols (wood, paper, and plastic). Data analysis revealed that combustion material and particle size had a significant effect on penetration values (*P*-value < 0.001). For all three materials, the highest particle penetration values occurred at 85 L/min throughout the entire tested particle size range (20–200 nm) except for the first channel; the 135 L/min flow generated the second highest penetration levels followed by 30 L/min. All penetration values obtained with the three combustion aerosols were approximately between 0.05 and 0.7% except a few points obtained for smaller particles at 30 L/min. Insufficient number of particles detected by the Nanoparticle Spectrometer (C_{out} <1000 particles/channel, C_{in} <1 particle/channel) prevented us from reporting penetration values for plastic particles between 20 and ~30 nm (see Fig. 2, Plastic Aerosol).

Compared with the fully sealed test condition, even the lowest penetration values obtained for the partially sealed half-mask at 30 L/min were at least 10-fold greater, regardless of flow rates (30, 85, and 135 L/min). This shows that any additional

faceseal leakage can substantially compromise the protection offered by a half-mask respirator.

The penetration curves obtained for wood and paper combustion aerosols were of similar shapes. While not perfectly monotonic, the curves showed an overall increase of penetration with increasing particle size. For plastic combustion particles, the curves are slightly different from those found for wood and paper aerosols with the penetration reaching the maximum approximately at 120–160 nm at 85 and 135 L/min. One possible reason is that wood and paper combustion aerosol particles are expected to have similar physical and chemical properties while the particles originated by burning plastic, a synthetic material, may differ in composition and physical characteristics such as a charge, shape, and density. It is worth of mentioning that, although effects associated with electrical charges on particles as well as on respirator and manikin surfaces fell outside of the scope of this study, electric forces may have a major contribution to the differences associated with combustion material. It is also to be noted that the measurement of particles in this study was based on their electrical mobility (not an aerodynamic diameters), and there are no data, to our knowledge, that would allow establishing a relationship between the two, at least, for the challenge aerosol. All these factors may explain the material-associated differences and similarities observed in our experiments.

The order of curves in Fig. 4 was somewhat unexpected: at the same particle size the penetration increased as the MIF increased from 30 to 85 L/min but then decreased as the flow continued rising from 85 to 135 L/min at MIF. In order to identify the flow rate(s) associated with the maximum particle penetration, four more cyclic flows (50, 70, 100, and 120 L/min) were added to the testing program for the partially sealed half-mask. This additional experiment was conducted using plastic combustion aerosol only. It is believed that the finding would have higher practical significance because plastic aerosol is comparatively more toxic and more health relevant than the ones produced by burning wood or paper (Underwriters Laboratories Inc, 2010). Thus, seven flows (30, 50, 70, 85, 100, 120, and 135 L/min) were tested at the same manikin breathing frequency (25 breaths/min) with four replicates for each flow. The experimental results are presented in Fig. 5. The penetration values are shown for particle sizes of and above of 30 nm (as mentioned earlier, the count of plastic combustion particles <30 nm was insufficient).

Firstly, the curves (upper section of Fig. 5) corresponding to seven different MIFs are similarly non-monotonic. Although the trend is not completely clear for particle diameters up to 40–50 nm, all the curves indicated that penetration increased with increasing particle size up to

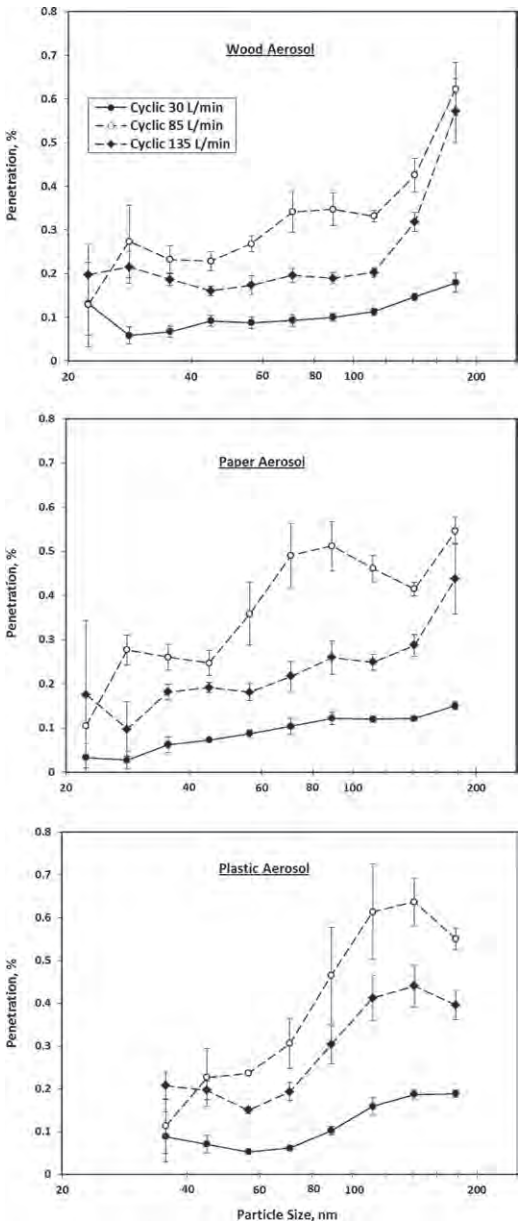

Fig. 4. Penetration of wood, paper, and plastic combustion aerosols through a partially sealed (nose area) half-mask equipped with two P-100 filters. Each point represents the average value of four replicates, and the error bar represents the standard error of the mean.

~100–140 nm (depending on the flow rate) and then decreased for larger particles. The flow rate of 85 L/min indeed appeared to be the one producing the highest penetration values when particle size was >40 nm. The flow rate of 100 L/min produced the second highest penetration (the values are approximately the same compared with 85 L/min in the particle size range of 80 to 100 nm). Further increase in flow rate resulted in decrease in penetration. Results also showed the lowest penetration values at the lowest tested MIF (30 L/min). The following explanations are offered to address the flow effect: as the breathing flow increased from 30 to 85 L/min, more combustion particles were brought into the respirator cavity (greater penetration) while the outside concentration remained unchanged. However, it is anticipated that at higher flows (>85 L/min) the negative pressure inside the respirator during inhalation became sufficiently high to suck the respirator toward the face of the manikin and consequently reduce faceseal leak size. In turn, a smaller leak could correspond to a lower relative contribution of the total air flow entering the facepiece, resulting in penetration of fewer particles. During exhalation, exhaled air is released primarily through the exhalation valve (rather than the faceseal leakage or filters) of the half-mask respirator so that a higher flow should not substantially increase the leak size during exhalation.

Secondly, the lower section of Fig. 5 shows the particle penetration as a function of MIF at four particle sizes (52, 83, 104 and 153 nm) that were selected to fairly represent the entire scan range. This figure conveys that the particle penetration was largely dependent on the cyclic breathing flow, with the highest penetration values occurred at the MIF = 85 L/min. As particle size increased from 52 nm to 104 nm, the penetration values showed a clear increasing trend regardless of the flow rate. However, penetration values obtained at the larger particle size (153 nm) were close to or higher than those acquired at 104 nm (depending on the flow rate). This indicates that the MPPS for this partially sealed half-mask (nose area only) was within a size range of ~100 to 160 nm when challenged to plastic combustion aerosols.

Unsealed half-mask respirator with P-100 filters

The findings for the unsealed half-mask are presented in Fig. 6. The ANOVA results showed that both particle size and material type had strong significant effects (P-value < 0.001) on the particle penetration. The penetration values ranged from 4 to 8% for wood aerosol, from 3 to 10% for paper aerosol, and from 3 to 16% for plastic aerosol. Plastic aerosol produced higher penetration values for particles between 100 and 200 nm compared with wood and paper combustion aerosols. This finding is important in light of previously published evidence that combustion of plastic generates toxic particles that may be associated with human health effects (Linak et al., 1989; Wong et al., 2007).

The average penetration of the unsealed half-mask respirator exceeded that of fully sealed respirator by a factor of >100, given that most of penetration values obtained for the fully sealed half-mask were <0.05% (see Fig. 3). Therefore, more than 99% of particles entering the unsealed half-mask respirator cavity penetrated through faceseal leakage (not through the P-100 filter medium). This finding is consistent with the conclusions presented in He et al. (2013) for the same type of respirator based on total particle concentration measurement (non-size selective).

For plastic aerosol, the size of particles most readily penetrating through faceseal leakage fell in a range of 120–140 nm for all three MIFs, whereas it is difficult to determine the MPPS for wood and paper aerosols as the penetration curves do not show clear peaks in the particle size range of 20–200 nm. Many previous studies on respirator filter efficiency have reported the MPPS for tested filters (Brown, 1993; Martin and Moyer, 2000; Grafe et al., 2001; Bałazy et al., 2006a, 2006b; Eninger et al., 2008). However, there are very limited data available on the MPPS for respirator faceseal leakage. Rengasamy and Eimer (2011) reported that the MPPS for a cylindered leak (<1.65 mm diameter) was ~50 nm. It is commonly assumed that size and location of faceseal leakage are constantly changing during breathing, talking, and head/body movement (Myers et al., 1996), which contributes to additional variability when trying to determine the MPPS. Additional challenge is that the MPPS can be affected by aerosol type as shown in this study.

Unlike the fully sealed condition, an unsealed respirator involves two primary particle penetration pathways (filter medium and faceseal leakage). While numerous studies have addressed the effect of breathing flow on the filter efficiency (e.g. increasing flow rate was shown to promote higher penetration of ultrafine particles due to diffusion) (Bałazy et al., 2006a, 2006b; Eninger et al., 2008; Rengasamy and Eimer, 2011), it is less certain how the breathing flow affects

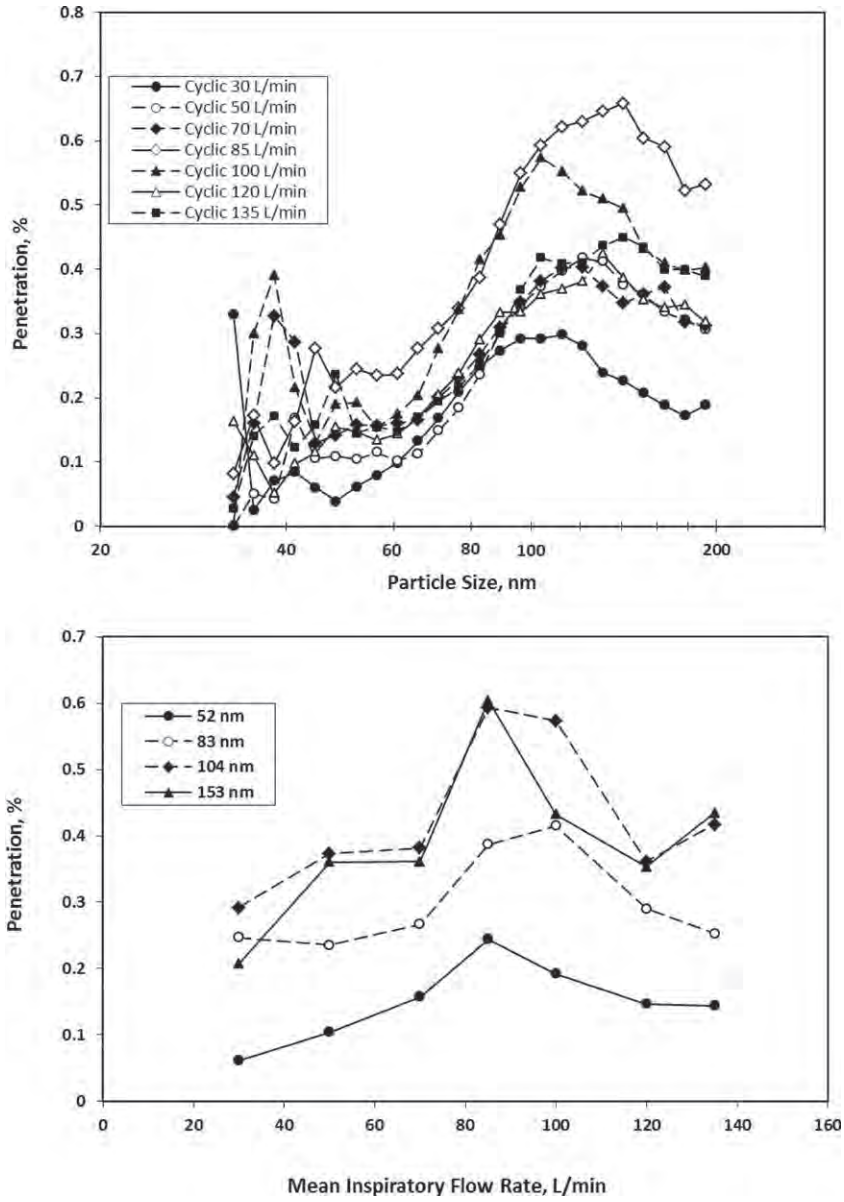

Fig. 5. Penetration of 'plastic' combustion particles through a partially sealed (nose area) half-mask equipped with two P-100 filters: dependence on particle size for fixed MIFs (upper figure) and dependence on the MIF for fixed particle sizes (lower figure). Each point represents the average value of four replicates.

the faceseal penetration. Interestingly, several published FFR studies have documented that faceseal penetration decreased with increase in breathing flow when challenged with particles >500 nm (Chen et al., 1990; Huang et al., 2007; Cho et al., 2010b). On the other hand, another FFR evaluation effort failed to observe significant increase or decrease in faceseal penetration when increasing the breathing flow (Rengasamy and Eimer, 2011) for particles ranging from 8 to 400 nm. In our study, increasing flow seemed to decrease particle penetration through the faceseal leakage, and such effect was most dominant for plastic aerosol and particle size of >100 nm (see Fig. 6). It is acknowledged that our study tested a different respirator (elastomeric half-mask) with different challenge aerosols compared with the three studies referenced above.

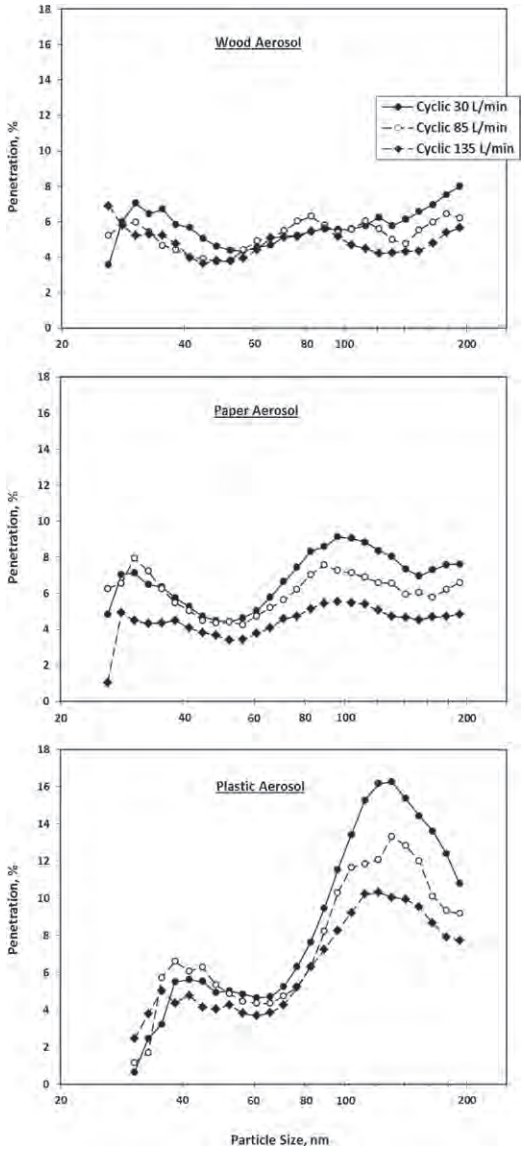

Fig. 6. Penetration of wood, paper, and plastic combustion aerosols through an unsealed half-mask equipped with two P-100 filters. Each point represents the average value of four replicates.

To interpret the above finding (faceseal penetration decreases with increasing flow rate), an experiment with breathing flow held constant was conducted. The same unsealed half-mask was tested using three constant flow rates (30, 85, and 135 L/min) while challenged with plastic aerosol. The results are shown in Fig. 7. First, constant inhalation flow produced much higher penetration values than cyclic flow. Peak penetration was close to 50% for a constant flow rate of 30 L/min (Fig. 7) compared with 16% for cyclic flow of the same MIF (Fig. 6); similar trends were observed for 85 and 135 L/min. These differences were explained in our previous study (He et al., 2013). The important finding is that increasing constant flow was generally associated with a decrease in particle penetration (with the exception of data obtained at 85 versus 135 L/min for larger particles). Due to the high efficiency of the P-100 filter, the total particle penetration through the half-mask elastomeric respirator is almost fully determined by the number of particles penetrating through faceseal leakage. Most of tested particles are small enough to have their motion governed primarily by diffusion and electrostatics. Assuming that (a) the exhalation valve provides a perfect seal, (b) the particle loss inside the faceseal leakage is negligibly small, and (c) the capture efficiency of the P-100 filter is close to 100%; the total particle penetration (P_{Total}) into a respirator is determined by the relative contributions of the air flows through the filter and the leakage (He et al., 2013):

$$P_{Total} \approx 1 - \frac{Q_F}{Q} = \frac{Q_L}{Q} \times 100\% \qquad (2)$$

Where Q_F is the constant air flow through filter media, Q_L is the constant air flow through faceseal leakage, and $Q = Q_F + Q_L$ is the constant total flow. If the respirator is equipped with an absolute filter, the penetration value calculated by equation (2) can be considered as maximum possible particle penetration.

Depending on the position of the respirator and the tightness of the straps, the gap between the respirator and the face of the manikin is likely variable. In our experiment, the most sizeable leakage (~1 mm) was observed around the nose area. However, in areas around the chin and cheeks the faceseal leakage could be 0.1 mm or lower. According to the classic particle diffusion theory (Kulkarni et al., 2011), the particle losses inside a 1-mm gap are estimated to be negligibly low (with the Brownian displacement of ~0.01 mm). At the same time, the diffusional deposition inside a 0.1 mm gap is not negligible, especially for particles below ~50 nm. Larger particles (well above 50 nm) are not subjected to appreciable diffusional deposition, but some of them may carry substantial electrical charges, which could cause losses inside the faceseal leakage and consequently decrease the particle penetration. This

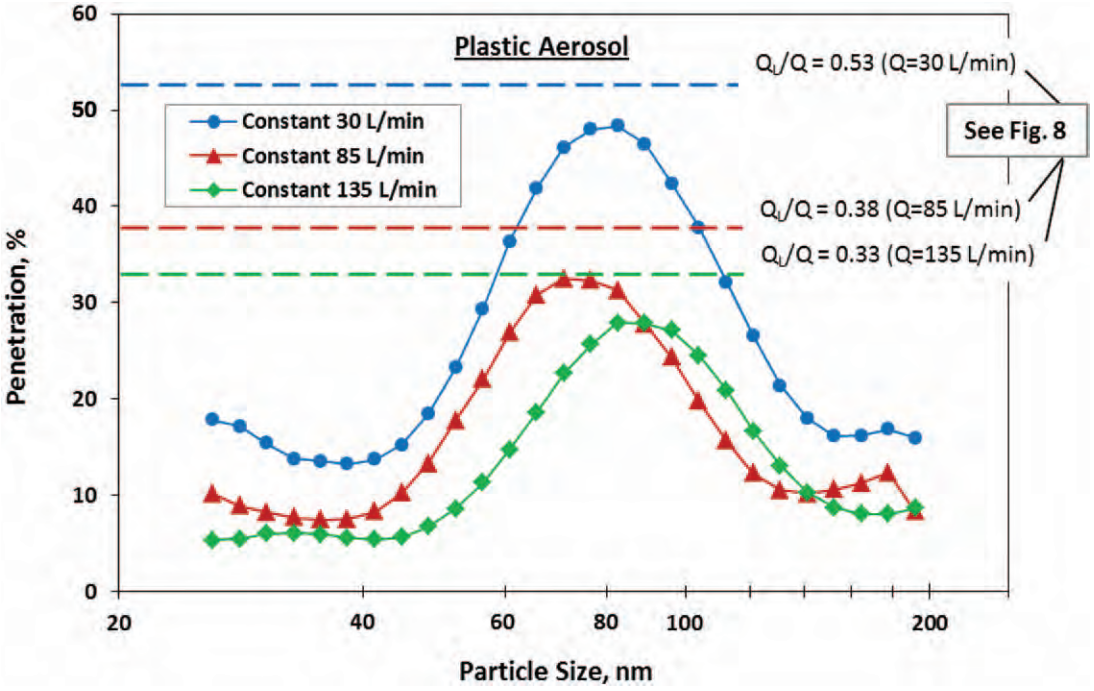

Fig. 7. Penetration of the plastic combustion aerosol through an unsealed half-mask equipped with two P-100 filters under constant flow regime. Each point represents the average value of four replicates. Additionally, the graph shows three straight dotted lines representing Q_L/Q values at Q = 30, 85, and 135 L/min, which correspond to the maximum particle penetrations at these flow rates, as determined from Fig. 8.

effect is expected to be more pronounced as the particle size increases (further increase of the particle size adds interception and impaction losses). The above explains the non-monotonic curves shown in Fig. 7. The MPPSs ranging ~70–90 nm (depending on the flow rate) represent the condition when the particles are too large for substantial diffusional losses inside the leakage but at the same time too small to expect notable deposition due to electrostatic mechanism, interception, and impaction. In these cases, the penetration is close to the theoretically maximum level, Q_L/Q [Eq. (2)]. These thresholds are shown in Fig. 7 for each of the three flow rates as straight lines.

The proportion of total flow through the faceseal leakage was experimentally determined for an unsealed half-mask donned on the manikin under the constant flow condition. This was done as follows. First, the respirator was fully sealed on the manikin, and the air flow was established (entirely through the filter in absence of the faceseal leakage). By adjusting the speed of a vacuum pump, seven constant flow rates (Q_F) ranging from 10 to 100 L/min were achieved and the seven corresponding static pressures (pressure drop) were recorded. Second, an unsealed respirator was donned on the manikin with both P-100 filters removed and all inhalation openings fully covered to allow the air pass solely through the leakage. Using the same pre-recorded static pressures, seven flow rates (Q_L) were established by adjusting the vacuum pump. Subsequently, the seven total flow rates were calculated ($Q = Q_F + Q_L$, see Fig. 8 for the seven tested Q-values marked as black dots).

The relationship between Q_L/Q and total flow Q is plotted in Fig. 8. The graph reveals that Q_L/Q values decreased along with increasing total flow rate. As indicated above, this likely occurred due to high negative pressure inside of the respirator that sucks it towards the manikin surface, thus reducing the faceseal leakage and producing higher flow resistance, which, in turn, reduced the proportion of total flow (Q_L/Q) passing through the leakage. Increase in total flow decreased the slope of the curve shown in Fig. 8. At a total flow of 30 L/min, the ratio of Q_L/Q was as high as 53%, which, based on our theoretical considerations presented above, was

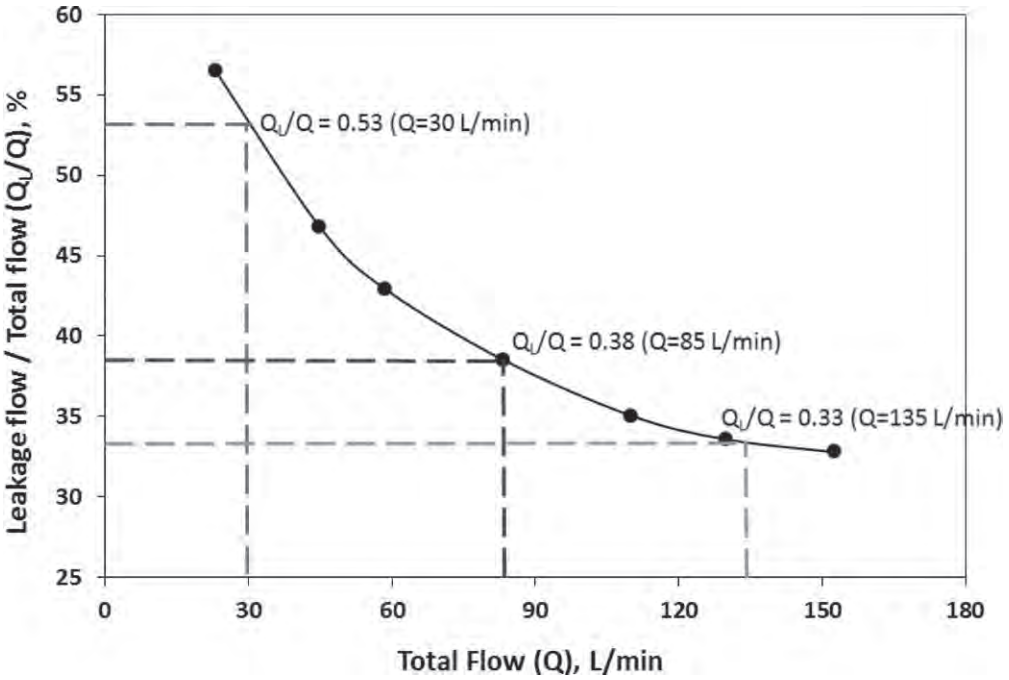

Fig. 8. The relationship between the leakage-portion of total flow (Q_L/Q) and the total flow (Q) under constant flow regime. Each black dot represents the flow measurement for a certain static pressure. The dotted lines represent Q_L/Q values at Q = 30, 85, and 135 L/min.

supposed to produce $P_{Total} \approx Q_L/Q = 53\%$ (see Fig. 7, the 53% straight line). Similarly, when the total flow was 85 and 135 L/min, the Q_L/Q was 38 and 33%, respectively.

The above explanations can be applied to a more complex case of the cyclic flow regime, which—in contrast to the constant flow—exhibits both inhalation and exhalation. During exhalation, particle concentration inside the respirator is diluted by the purified exhalation air (in our experimental set-up, a HEPA filter installed between the manikin and the breathing simulator). At the same time, the particles cannot be entirely removed from the respirator cavity as there are always particles trapped inside the respirator after exhalation. Thus, the particle penetration obtained under the cyclic flow regime is expected to be lower than those obtained under the constant flow regime (see a more detailed explanation in He et al., 2013). However, the effects of the flow rate on the faceseal penetration remained the same for both constant flow and cyclic flow regimes—higher flow associated with lower penetration, which was proven by the theoretical calculation [equation (2)] combined with the flow measurements (Fig. 8). No previously published studies were found to address the flow type (cyclic versus constant) effect on the total inward leakage for the elastomeric half-masks.

CONCLUSIONS

Performance of the elastomeric half-mask respirator was significantly affected by the particle size (*P*-value < 0.001). When testing the partially sealed half-mask, the highest penetration was detected at 180 nm for wood and paper combustion aerosols and at ~120–160 nm for plastic aerosol. Under the unsealed conditions, the peak penetration occurred at 120 nm for plastic combustion aerosol, while no clear peaks were identified for wood and paper. Results suggest that the MPPS for the faceseal leakage was >100 nm for the partially sealed and unsealed conditions when challenged with plastic aerosol. The partially sealed (nose area only) half-mask respirator resulted in 10-fold lower penetration levels when compared with the unsealed condition. This suggests that the nose area was a primary leak site.

Material type was another significant factor (*P*-value < 0.001). For the unsealed half-mask challenged with plastic combustion aerosol, higher penetration values were observed compared with wood and paper aerosols for particles >100 nm.

The effect of cyclic flow rate was found to be significant as well (P-value < 0.001). For the partially sealed respirator, increasing flow rate was associated with an increase in penetration up to MIF = 85 L/min. For higher flow rates, the trend changed to a decrease in penetration as the flow increased. For unsealed conditions, increasing flow rate resulted in consistent decrease of penetration and this trend was most apparent for the plastic aerosol with size >100 nm.

One major limitation of this study is that a hard plastic manikin headform was used, which was not capable of mimicking the texture and softness of human skin. This may potentially create larger leaks for equivalent strap tension. An advanced headform covered with soft skin-like material may be considered as an appropriate alternative in future studies. Only one model of the elastomeric half-mask was tested, which also represents a study limitation. Additionally, it is acknowledged that all the cyclic flows tested in this study used the same breathing frequency (25 breaths/min), which may not fully represent the real-world situation. Future studies are needed to investigate the effects of the breathing frequency on the performance of respiratory protection devices.

FUNDING

NIOSH Targeted Research Training program of the University of Cincinnati Education and Research Center grant (No.T42/OH008432-06) and the University of Cincinnati Graduate Assistantship and Scholarship.

REFERENCES

Anderson NJ, Cassidy PE, Janssen LL, Dengel DR. (2006) Peak Inspiratory Flows of Adults Exercising at Light, Moderate and Heavy Work Loads. J. Int. Soc. Res. Prot; 23: 53–63.

Balazy A, Toivola M, Adhikari A *et al.* (2006a) Do N95 respirators provide 95% protection level against airborne viruses, and how adequate are surgical masks? Am J Infect Control; 34: 51–7.

Balazy A, Toivola M, Reponen T *et al.* (2006b) Manikin-based performance evaluation of N95 filtering-facepiece respirators challenged with nanoparticles. Ann Occup Hyg; 50: 259–69.

Baxter CS, Ross CS, Fabian T *et al.* (2010) Ultrafine particle exposure during fire suppression–is it an important contributory factor for coronary heart disease in firefighters? J Occup Environ Med; 52: 791–6.

BLS. (2003) Occupational Injuries and Illnesses in the US by Industry International Association of Firefighters. Washington, DC: US Bureau of Labor Statistics. 1995–1996.

Bolstad-Johnson DM, Burgess JL, Crutchfield CD *et al.* (2000) Characterization of firefighter exposures during fire overhaul. AIHAJ; 61: 636–41.

Brown RC. (1993) Air filtration: An integrated approach to the theory and applications of fibrous filters. Oxford: Pergamon Press. p.109. ISBN: 0080412742.

Burgess JL, Nanson CJ, Bolstad-Johnson DM *et al.* (2001) Adverse respiratory effects following overhaul in firefighters. J Occup Environ Med; 43: 467–73.

CDC. (2006) Fatalities among volunteer and career firefighters—United States, 1994–2004. The Journal of the American Medical Association; 295: 2594–96.

Chen CC, Ruuskanen J, Pilacinski W *et al.* (1990) Filter and leak penetration characteristics of a dust and mist filtering facepiece. Am Ind Hyg Assoc J; 51: 632–9.

Chen CC, Willeke K. (1992) Characteristics of face seal leakage in filtering facepieces. Am Ind Hyg Assoc J; 53: 533–9.

Cho KJ, Jones S, Jones G *et al.* (2010a) Effect of particle size on respiratory protection provided by two types of N95 respirators used in agricultural settings. J Occup Environ Hyg; 7: 622–7.

Cho KJ, Reponen T, McKay R *et al.* (2010b) Large particle penetration through N95 respirator filters and facepiece leaks with cyclic flow. Ann Occup Hyg; 54: 68–77.

Coffey CC, Zhuang Z, Campbell, D.L. Myers, W.R. (1998) Quantitative fit testing of N95 respirators: part II - results, effect of filter penetration, fit test, and pass/fail criteria. J Int Soc Res Prot; 16(1–4): 25–36.

Crutchfield CD, Park DL. (1997) Effect of leak location on measured respirator fit. Am Ind Hyg Assoc J; 58: 413–7.

Eninger RM, Honda T, Adhikari A *et al.* (2008) Filter performance of n99 and n95 facepiece respirators against viruses and ultrafine particles. Ann Occup Hyg; 52: 385–96.

Eshbaugh JP, Gardner PD, Richardson AW *et al.* (2009) N95 and p100 respirator filter efficiency under high constant and cyclic flow. J Occup Environ Hyg; 6: 52–61.

Grafe T, Gogins M, Barris M, Schaefer J, Canepa R. (2001) "Nanofibers in Filtration Applications in Transportation". Filtration 2001 Conference Proceedings. Chicago, IL, pp 1–15.

Grinshpun SA, Haruta H, Eninger RM *et al.* (2009) Performance of an N95 filtering facepiece particulate respirator and a surgical mask during human breathing: two pathways for particle penetration. J Occup Environ Hyg; 6: 593–603.

Haruta H, Honda T, Eninger RM, Reponen T, McKay R, Grinshpun SA. (2008) Experimental and theoretical investigation of the performance of N95 respirator filters against ultrafine aerosol particles tested at constant and cyclic flows. J Int Soc Res Prot; 25: 75–88.

He X, Yermakov M, Reponen T, McKay R, James K, Grinshpun SA. (2013) Manikin-based performance evaluation of elastomeric respirators against combustion particles. J Environ Occup Hyg; 10: 203–12.

Hinds WC, Kraske G. (1987) Performance of dust respirators with facial seal leaks: I. Experimental. Am Ind Hyg Assoc J; 48: 836–41.

Holton PM, Tackett DL, Willeke K. (1987) Particle size-dependent leakage and losses of aerosols in respirators. Am Ind Hyg Assoc J; 48: 848–54.

Huang S-H, Chen C-W, Chang C-P, Lai C-Y, Chen C-C. (2007) Penetration of 4.5 nm to aerosol particles through fibrous filters. J Aerosol Sci; 38: 719–27.

Kulkarni P, Baron PA, Willeke K. (2011) Aerosol Measurement - Principles, Techniques, and Applications. 3rd edn. New Jersey: John Wiley & Sons.

Lafortuna CL, Minetti AE, Mognoni P. (1984) Inspiratory flow pattern in humans. J Appl Physiol; 57: 1111–9.

Lam CW, James JT, McCluskey R *et al.* (2004) Pulmonary toxicity of single-wall carbon nanotubes in mice 7 and 90 days after intratracheal instillation. Toxicol Sci; 77: 126–34.

Lee SA, Grinshpun SA, Reponen T. (2008) Respiratory performance offered by N95 respirators and surgical masks: human subject evaluation with NaCl aerosol representing bacterial and viral particle size range. Ann Occup Hyg; 52: 177–85.

Leonard SS, Castranova V, Chen BT *et al.* (2007) Particle size-dependent radical generation from wildland fire smoke. Toxicology; 236: 103–13.

Linak WP, Ryan JV, Perry E *et al.* (1989) Chemical and biological characterization of products of incomplete combustion from the simulated field burning of agricultural plastic. JAPCA; 39: 836–46.

Martin SB Jr, Moyer ES. (2000) Electrostatic respirator filter media: filter efficiency and most penetrating particle size effects. Appl Occup Environ Hyg; 15: 609–17.

Materna BL, Jones JR, Sutton PM *et al.* (1992) Occupational exposures in California wildland fire fighting. Am Ind Hyg Assoc J; 53: 69–76.

Musk AW, Peters JM, Bernstein L *et al.* (1982) Pulmonary function in firefighters: a six-year follow-up in the Boston Fire Department. Am J Ind Med; 3: 3–9.

Myers WR, Allender JR, Iskander W *et al.* (1988) Causes of in-facepiece sampling bias–I. Half-facepiece respirators. Ann Occup Hyg; 32: 345–59.

Myers WR, Zhuang Z, Nelson T. (1996) Field performance measurements of half-facepiece respirators–foundry operations. Am Ind Hyg Assoc J; 57: 166–74.

NIOSH. (2009) "Total Inward Leakage for Half-mask Air-purifying Respirators" http://www.cdc.gov/niosh/docket/archive/docket137.html. Accessed 17 November 2012.

Oestenstad RK, Bartolucci AA. (2010) Factors affecting the location and shape of face seal leak sites on half-mask respirators. J Occup Environ Hyg; 7: 332–41.

Oestenstad RK, Elliott LJ, Beasley TM. (2007) The effect of gender and respirator brand on the association of respirator fit with facial dimensions. J Occup Environ Hyg; 4: 923–30.

Oestenstad RK, Perkins LL. (1992) An assessment of critical anthropometric dimensions for predicting the fit of a half-mask respirator. Am Ind Hyg Assoc J; 53: 639–44.

Rengasamy S, Eimer BC. (2011) Total inward leakage of nanoparticles through filtering facepiece respirators. Ann Occup Hyg; 55: 253–63.

Rengasamy S, Eimer BC, Shaffer RE. (2009) Comparison of nanoparticle filtration performance of NIOSH-approved and CE-marked particulate filtering facepiece respirators. Ann Occup Hyg; 53: 117–28.

Rengasamy S, King WP, Eimer BC *et al.* (2008) Filtration performance of NIOSH-approved N95 and P100 filtering facepiece respirators against 4 to 30 nanometer-size nanoparticles. J Occup Environ Hyg; 5: 556–64.

Shaffer R, Rengasamy S. (2009) Respiratory protection against airborne nanoparticles: a review. J Nanoparticle Res; 11: 1661–72.

Shvedova AA, Kisin ER, Mercer R *et al.* (2005) Unusual inflammatory and fibrogenic pulmonary responses to single-walled carbon nanotubes in mice. Am J Physiol Lung Cell Mol Physiol; 289: L698–708.

Underwriters Laboratories Inc. (2010) Firefighter Exposure to Smoke Particulates. Available at http://www.ul.com/global/documents/offerings/industries/buildingmaterials/fireservice/WEBDOCUMENTS/EMW-2007-FP-02093.pdf. Accessed 15 November 2012).

Wong MH, Wu SC, Deng WJ *et al.* (2007) Export of toxic chemicals - a review of the case of uncontrolled electronic-waste recycling. Environ Pollut; 149: 131–40.

Zhuang Z, Coffey CC, Myers WR, Yang J, Campbell DL. (1998) Quantitative Fit-Testing of N95 Respirators: Part I-Method Development. J Int Soc Res Prot; 16: 11–24.

Effect of Breathing Frequency on the Total Inward Leakage of an Elastomeric Half-Mask Donned on an Advanced Manikin Headform

Journal:	*Annals of Occupational Hygiene*
Manuscript ID:	Draft
Manuscript Type:	Original Articles
Date Submitted by the Author:	n/a
Complete List of Authors:	Grinshpun, Sergey; University of Cincinnati, Department of Environmental Health He, Xinjian; University of Cincinnati, Environ Health Reponen, Tiina; University of Cincinnati, Environ Health McKay, Roy; University of Cincinnati, Environmental Health Bergman, Michael; NIOSH/NPPTL, Zhuang, Z; NIOSH/NPPTL,
Keywords:	breathing frequency, half-mask, total inward leakage, combustion aerosol, manikin

Effect of Breathing Frequency on the Total Inward Leakage of an Elastomeric Half-Mask Donned on an Advanced Manikin Headform

Xinjian He[1], Sergey A. Grinshpun[1]*, Tiina Reponen[1], Roy McKay[1], Michael S. Bergman[2], and Ziqing Zhuang[2]

[1]Center for Health-Related Aerosol Studies, Department of Environmental Health, University of Cincinnati, Cincinnati, OH, USA;

[2]Technology Research Branch, National Personal Protective Technology Laboratory, National Institute for Occupational Safety and Health, Pittsburgh, PA, USA

To be submitted to

The Annals of Occupational Hygiene

March 6, 2013

Corresponding author: Sergey A. Grinshpun: sergey.grinshpun@uc.edu

ABSTRACT

Objective: To investigate the effect of breathing frequency on the total inward leakage (TIL) of an elastomeric half-mask donned on an advanced manikin headform and challenged with combustion aerosols.

Methods: An elastomeric half-mask respirator equipped with P100 filters was donned on an advanced manikin headform covered with life-like soft skin and challenged with aerosols originated by burning three materials: wood, paper and plastic (polyethylene). TIL was determined as the ratio of aerosol concentrations inside (C_{in}) and outside (C_{out}) of the respirator (C_{in}/C_{out}) measured with a nanoparticle spectrometer operating in the particle size range of 20 to 200 nm. The testing was performed under three cyclic breathing flows (mean inspiratory flow, MIF, of 30, 55, and 85 L/min) and five breathing frequencies (10, 15, 20, 25, and 30 breaths/min). A completely randomized factorial study design was chosen with four replicates for each combination of breathing flow rate and frequency.

Results: Particle size, MIF and combustion material had significant ($p < 0.001$) effects on TIL regardless of breathing frequency. Increasing breathing flow decreased TIL. Testing with plastic aerosol produced higher mean TIL values than wood and paper aerosols. The effect of the breathing frequency was complex. When analyzed using all combustion aerosols and MIFs (pooled data), breathing frequency did not significantly ($p = 0.08$) affect TIL. However, once the data were stratified according to combustion aerosol and MIF, the effect of breathing frequency became significant ($p < 0.05$) for all MIFs challenged with wood and paper combustion aerosols, and for MIF = 30 L/min only when challenged with plastic combustion aerosol.

Conclusions: The effect of breathing frequency on TIL is less significant than the effects of combustion aerosol and breathing flow rate for the tested elastomeric half-mask respirator. The greatest penetration occurred when challenged with plastic aerosol at 30 L/min and at a breathing frequency of 30 breaths/min.

Keywords: breathing frequency, half-mask, total inward leakage, combustion aerosol, manikin

INTRODUCTION

The U.S. Occupational Safety and Health Administration (OSHA) requires respirators be provided to employees whenever engineering and work practice control measures are not adequate to reduce the employees' exposure to acceptable levels (OSHA, 2006). Among the non-powered air purifying respirators, filtering facepiece respirators (FFRs) are the most commonly used respiratory protection devices (share = 49%) followed by elastomeric half-masks (34%), according to the survey conducted in private industry by the U.S. Bureau of Labor Statistics (BLS) and the National Institute for Occupational Safety and Health (NIOSH) (BLS/NIOSH, 2003).

Smoke from a fire contains primarily ultrafine particles (< 0.1 μm). The latter were found to account for more than 70% of airborne particles (by number) measured in a large-scale fire test laboratory study (Baxter *et al.*, 2010). Exposure to ultrafine particles has been associated with impairment of cardiovascular function and other adverse health outcomes (Schwartz *et al.*, 1996; Peters *et al.*, 1997; Timonen *et al.*, 2005; Schulte *et al.*, 2008).

Many studies have evaluated the most penetrating particle size (MPPS) (Martin and Moyer, 2000; Grafe *et al.*, 2001; Bałazy *et al.*, 2006a; 2006b; Eninger *et al.*, 2008; Rengasamy *et al.*, 2008; Cho *et al.*, 2010a) of NIOSH-certified N95 FFRs. These studies consistently report a MPPS in a range of 30 to 100 nm. Elastomeric half-masks, which offer the benefits of reusability, improved face seal, and enhanced user seal check capability – and can be decontaminated multiple times – (Roberge *et al.*, 2010), have not been studied as extensively as N95 FFRs. One study involving three half-masks and 10 FFRs tested on a panel of 10 human subjects concluded that the fit factors of elastomeric half-masks were higher than those of FFRs (Han and Lee,

2005). Another study (Lawrence *et al.*, 2006) involving a panel of 25 subjects with varying face sizes reported superior performance of elastomeric N95 half-masks (15 models tested) over N95 FFRs (15 models tested) and surgical masks (6 models tested). However, these investigations used non-size-selective aerosol measurement devices that did not allow exploring potential differences in penetration by different particle sizes, and none of these studies studied the effect of breathing frequency.

Respirator filter efficiency is significantly affected by breathing flow rate. This has been demonstrated for mechanical and "electret" filters tested under constant and cyclic flow conditions (Brosseau *et al*., 1990; Chen *et al.*, 1990; Brown, 1993; Qian *et al.*, 1998; Martin and Moyer, 2000; Bałazy *et al.*, 2006b; Huang *et al.*, 2007; Eninger *et al.*, 2008; Rengasamy *et al.*, 2008; Rengasamy *et al.*, 2009; Cho *et al.*, 2010b). A constant inhalation flow rate of 85 L/min is currently used in the NIOSH respirator certification program (NIOSH, 1995); however, constant flow does not accurately represent human breathing patterns. Stafford *et al* (1973) reported that human breathing is more reasonably approximated by a sinusoidal waveform, which can be better approximated with different flow rates and breathing frequencies (breaths/min) (Haruta *et al.*, 2008). Breathing frequency differs between population groups (e.g., healthy vs. sick, young vs. old) and is significantly affected by the level of physical activity (e.g., rest vs. active) (Tortora and Anagnostakos, 1990; Sherwood, 2006). Several studies using cyclic flow, have reported an effect of flow rate on filter efficiency and faceseal leakage (Myers *et al.*, 1991; Eshbaugh *et al.*, 2008; Haruta *et al.*, 2008; Cho *et al.*, 2010b). However, with exception to Wang et al. (2012) no published study has yet fully addressed the effect of the breathing frequency. Wang *et al.* (2012) did investigate two breathing frequencies (32 and 50 breaths/min) with a single MIF (100 L/min), but the data generated in their study were too limited to draw

conclusions about breathing frequency. Furthermore, they selected a breathing frequency (50 breaths/min) that is excessive for most workplace populations.

Respiratory protection offered by negative pressure respirators is dependent not only on the filter efficiency but also on faceseal leakage (Zhuang *et al.*, 1998; Grinshpun *et al.*, 2009; Cho *et al.*, 2010b). To account for these two penetration pathways, NIOSH has proposed the total inward leakage (TIL) method for testing respirators (NIOSH/CDC, 2009). Several studies addressed this issue by creating artificial slit-like or circular leaks to assess the faceseal leakage (Hinds and Bellin, 1987; Myers *et al.*, 1991; Chen and Willeke, 1992; Rengasamy and Eimer, 2011). However, artificial fixed leaks are not representative of actual conditions when a respirator is worn by humans. It is commonly assumed that size and location of faceseal leaks are constantly changing during breathing, talking, and head/body movement (Myers *et al.*, 1996). Some studies tested respirators worn by human subjects (Zhuang *et al.*, 1998; Grinshpun *et al.*, 2009) but these were, obviously, limited to a non-toxic challenge aerosol (NaCl). Comprehensive testing of respirator performance in a toxic aerosol environment and at higher challenge concentrations requires use of a manikin headform. Conventional static manikin headforms (either made of a rigid material or coated with a thin layer of rubber, plastic, or other compressible materials) have been shown in the literature to have high TIL levels for half-mask elastomeric respirators and filtering facepiece respirators (Cooper *et al.*, 1983; Tuomi, 1985; Golshahi *et al.*, 2012). These older type headforms do not simulate the properties of human facial tissue (e.g., skin softness and local depth) which deforms under stress in ways that solid elastomers cannot simulate (Hanson and Priya, 2007). To address this gap, an advanced manikin headform was developed that is capable of mimicking the softness and thicknesses of the human skin (Hanson *et al.*, 2006; Bergman *et al.*, 2013).

This study is a follow-up to recent studies (He *et al.*, 2013a; 2013b) conducted in the same laboratory on the performance of elastomeric respirators challenged with combustion aerosols. The present study specifically addresses the effect of breathing frequency on TIL of an elastomeric half-mask respirator on an advanced, soft-skinned manikin headform.

MATERIALS AND METHODS

Respirator

An elastomeric 3M 6000 series half-mask respirator equipped with two 3M 2091 P100 filters (3M Corp., St. Paul, MN, USA) was chosen for the testing to assure the continuity of our previous research (He *et al.*, 2013a; 2013b). The rationale for selecting the above respirator was described in detail in He *et al.* (2013a).

Challenge Aerosols

The challenge aerosols were separately generated by burning the following three materials inside a test chamber: wood (24 cm long pellets, 1.9 ± 0.5 g), paper (23 cm × 24 cm brown multifold paper towel, 2.1 ± 0.2 g), and polyethylene (23 cm × 20 cm, 1.7 ± 0.3 g – further referred to as plastic) (He *et al.*, 2013a). Each material held by a caliper was ignited by a long reach lighter and completely burnt inside the chamber. All burnt materials were captured in a water-filled basin placed on the floor. The measurements were initiated 15 minutes after burning to allow the combustion aerosol to reach a special uniformity. As our previous measurements revealed that 90% of particles so generated were within the range 20 to 200 nm (He *et al.*, 2013a), we focused on this size range.

Advanced Manikin Headform

The specifications of the advanced manikin headform chosen for this study were reported in detail by Bergman *et al.* (2013). Briefly, the headform is of the medium size defined by the NIOSH Principal Component Analysis panel created using data from a large-scale anthropometric survey of U.S. workers conducted in 2003 (Zhuang *et al.*, 2007). A human-like skin with locally correct thicknesses was mounted on the headform skull. The material used to generate the skin is called Frubber™ (Hanson and White, 2004), a fluid-filled cellular matrix composed of an elastomer that compresses, elongates and otherwise deforms in ways that simulates human skin (Hanson and White, 2004).

Experimental Design and Test Conditions

The experimental set-up is shown in Figure 1. The respirator was donned on the advanced manikin headform, which was then challenged with one of three combustion aerosols (wood, paper and plastic). The donning was performed according to the manufacturer's user instructions. After donning, the respirator was not re-donned or repositioned until the completion of the study, which allowed maintaining the size and shape of the faceseal leaks. Obviously, the static headform design did not allow fit testing of the respirator prior to the study. The P100 filters were changed after every 15 runs to minimize the effect of loading of combustion products on the filter medium. The filters were changed in a careful way to minimize the effect of this procedure on the respirator faceseal leakage. After each filter change, the particle penetration was measured to assure that the size of the leak was consistent with the one existing before the change under the same experimental conditions. Temperature and relative humidity were kept at 17-22 ℃ and 30-50 %.

The headform was connected to a Breathing Recording and Simulation System (BRSS, Koken Ltd., Tokyo, Japan) with a HEPA filter placed in between to keep particles from re-entering the respirator cavity in exhaled air. The BRSS consists of an electro-mechanical drive-cylinder coupled with two air cylinders. As the electromechanical cylinder stroke moves back (inspiratory duration, half a period) and forth (expiratory duration, half a period), a sinusoidal air flow is generated (Haruta *et al.*, 2008). The stroke moving distance and frequency can be adjusted with a resolution of 0.1 mm and 0.01 Hz, respectively, thus allowing for precise changes to breathing flow rate and frequency when human breathing is simulated (Haruta *et al.*, 2008).

The test were conducted under three cyclic breathing flows (mean inspiratory flow – time weighted average flow rate over the width of an inspiration, MIF = 30, 55 and 85 L/min) and five breathing frequencies (10, 15, 20, 25 and 30 breaths/min). A completely randomized factorial study design was chosen with four replicates for each combination of the tested breathing flow rate and frequency. A summary of the experimental conditions is presented in Table 1. Aerosol concentrations inside (C_{in}) and outside (C_{out}) the respirator were measured using a nanoparticle spectrometer (Nano-ID NPS500, Naneum Ltd., Kent, UK) size-selectively in 10 channels between 20 and 200 nm. Each concentration measurement took 3 minutes. The corresponding mean sizes for the 10 chosen channels were 22.4, 28.2, 35.5, 44.7, 56.2, 70.8, 89.1, 112.2, 141.3 and 177.8 nm. TIL was determined for each particle size (d_p) as the ratio of inside to outside concentration:

$$\mathrm{TIL}_{d_p} = \frac{C_{\mathrm{in},d_p}}{C_{\mathrm{out},d_p}} \times 100\% \quad \textbf{(1)}$$

In addition, by combining the 10 channels, size-independent (overall) TIL was calculated for all combustion particles ranging from 20 to 200:

$$\mathrm{TIL} = \frac{\sum_{i=1}^{10} N_{\mathrm{in},i}}{\sum_{i=1}^{10} N_{\mathrm{out},i}} \times 100\% \quad \textbf{(2)}$$

where N_{in} is the number of particles measured in a specific channel inside the respirator, N_{out} is the number of particles measured in a specific channel outside the respirator, and i is the i^{th} particle size channel.

Data analysis

Data analysis was performed using SAS version 9.3 (SAS Institute Inc., Cary, NC, USA). For the size-selective TIL, the effect of particle size was analyzed using the one-way analysis of variance (ANOVA) on the pooled data. Three-way ANOVA was used to study the significance of combustion material, breathing flow and breathing frequency for the size-independent TIL. One-way ANOVA was performed to quantify the effect of breathing frequency on the size-independent TIL after stratifying the data by the combustion material and breathing flow. All pairwise comparisons were performed using Tukey's range test. P-values < 0.05 were considered significant.

RESULTS AND DISCUSSION

Size-selective Total Inward Leakage (TIL_{d_p})

The size-selective TIL values determined within the chosen ten-channel size range are shown in Figure 2. The graphs represent three MIFs, five breathing frequencies, and three combustion aerosols (error bars are not shown as they make it difficult to see the data lines for each breathing frequency).

First, the graphs in figure 2 demonstrate particle size affected TIL_{d_p} ($p < 0.0001$). For all three aerosols, the TIL_{d_p} values obtained at the lowest tested sizes, 20–40 nm, fell below those obtained at > 40 nm regardless of the breathing flow and frequency. This can be explained by the diffusional deposition which is more pronounced for smaller particles (consequently, a smaller fraction could penetrate inside the respirator more readily). For particles 40~50 nm and larger, the TIL_{d_p} curves showed no consistent increasing or decreasing trend. Furthermore, ANOVA results showed no significant differences in TIL_{d_p} ($p = 0.36$) among the six channels between 45 to 200 nm. The relatively flat curves obtained for the half-mask indicate a wide range for the MPPS. No TIL MPPS data were available in the literature for elastomeric respirators until our recent study (He *et al.*, 2013a), which measured an MPPS of 120–140 nm for the same half-mask donned on a plastic manikin headform and challenged with plastic combustion aerosol. The cited study failed to detect an MPPS for wood and paper aerosols due to multiple peaks in the TIL_{d_p} curves. Previous TIL studies have focused on N95 FFRs or surgical masks, for which the particle size effect was found significant and the TIL values were close to the penetration levels observed for the filters only (Myers *et al.*, 1991; Cho *et al.*, 2010a; Rengasamy and Eimer, 2011). At the same time, little information has been generated with respect to the MPPS for faceseal leakage. When testing N95 FFRs with artificially created cylindered leaks, Rengasamy and Eimer (2011) found that for leak diameters ≤ 1.65 mm the MPPS was ~50 nm; we believe that

this value likely represents the N95 filter penetration, whereas the TIL of the respirator used in this study (equipped with P100 filters) is primarily governed by the faceseal leakage penetration. This likely explains the suppressed peaks or the plateaus seen in the curves presented in Figure 2.

The effect of breathing frequency on TIL_{d_p} was complex. When challenged with wood combustion aerosol, frequencies of 30, 20 and 15 breaths/min produced the highest TIL_{d_p} values at MIF = 30, 55 and 85 L/min, for most size channels between 20 to 200 nm. MIF = 30 L/min produced the most notable effect of the breathing frequency on the TIL_{d_p}. The TIL_{d_p} curves obtained from testing with paper combustion aerosol showed some peaks at 30 and 10 breaths/min at MIF = 30 and 85 L/min, but no clear peak was identified for MIF = 55 L/min. The graphs representing TILs for plastic aerosol revealed separations between the TIL_{d_p} curves at MIF = 30 L/min, which essentially diminished at higher flow rates.

Increasing the MIF resulted in a decrease in the average TIL values for all challenge aerosols (wood, paper and plastic). For example, for the wood combustion aerosol, the average TIL values were 0.6~1.0 % at MIF = 30 L/min, 0.5~0.8 % at 55 L/min, and 0.3~0.6 % at 85 L/min. Several published FFR studies also reported that faceseal penetration decreased with increase in breathing flow when challenged with particles larger than 500 nm (Chen *et al.*, 1990; Huang *et al.*, 2007; Cho *et al.*, 2010b). On the other hand, another FFR study observed no significant increase or decrease in faceseal penetration by 8–400 nm particles associated with increasing breathing flow (Rengasamy and Eimer, 2011).

We have previously tested the filter penetration of wood, paper and plastic combustion aerosol through a fully sealed half-mask equipped with two P100 filters (and found that all penetration values were below 0.03% (He *et al.*, 2013a). An additional experiment was

conducted and confirmed that the evaluate exhalation valve did not leak. Based on the comparison of the TIL and filter penetration data, we concluded that the primary particle penetration pathway for the tested elastomeric half-mask was faceseal leakage.

The average size-selective TIL values obtained from this study were comparable to those reported in our previous study with a partially sealed (nose or nose-chin area) half-mask donned on a hard plastic manikin headform (He *et al.*, 2013a, 2013b), and 5~10-fold lower than those obtained with the unsealed half-mask donned on the plastic headform. This improvement can be attributed to the softness of the manikin skin, which deforms under stress, thus increasing the contact surface area and consequently forming a better seal.

Size-independent (overall) Total Inward Leakage (TIL)

The size-independent (overall) TIL values for the half-mask respirator challenged with the three tested combustion aerosols are presented in Figure 3. The highest TIL values were determined at MIF = 30 L/min and 30 breaths/min for all three challenge aerosols (peak TIL = 1.08%, 1.33% and 1.87% for wood, paper and plastic, respectively). The lowest TIL values (0.35%, 0.60% and 0.75% for wood, paper and plastic, respectively) were obtained at MIF = 85 L/min combined with 25 breaths/min. ANOVA with Tukey's range test was performed to study the effects of combustion material, breathing flow and breathing frequency on the TIL, and the data analysis results are presented in Tables 2 through 5.

Effect of the combustion aerosol. A three-way ANOVA (see Table 2) shows that the non-size selective combustion aerosol significantly affected TIL ($p < 0.0001$). Pair wise multiple comparison analysis revealed the mean overall TIL values for wood, paper and plastic combustion aerosol were significantly ($p < 0.05$) different from each other (see Table 3). The

plastic aerosol produced the highest mean TIL (1.14%) followed by wood (0.85%) and paper (0.70%). This finding is in agreement with our recent study (He et al., 2010b) conducted with the same type of half-mask donned on a hard plastic manikin headform. The difference in TIL can be attributed to differences in particle shape, density, electric charge, and possibly other properties. Plastic (polyethylene) is pure hydrocarbon, paper is cellulose (plus various additives and coatings), and wood is half cellulose and half lignin, which includes aromatics and relatively little hydrogen.

Effect of the breathing flow (MIF). Breathing flow had a significant effect on TIL (p <0.0001) as shown in Table 2. The interaction between the challenge aerosol and breathing flow (Aerosol*MIF) was significant (p = 0.0096). The pairwise comparison results for three MIF groups (30, 55 and 85 L/min) are presented in Table 4. The mean TIL obtained at MIF = 30 L/min was significantly ($p < 0.05$) higher than those determined for MIF = 55 and 85 L/min. The differences between the data series obtained at 55 and 85 L/min were not significant ($p > 0.05$). One possible explanation is that a higher breathing flow can create a higher negative pressure inside the half-mask respirator, which sucks the respirator toward the manikin's face, thus helping make a tighter contact with the manikin headform. The consequent reduction in faceseal leakage with an increase from 30 to 55 L/min affects the TIL; however, this effect becomes less pronounced at higher flow rates.

Effect of the breathing frequency. Breathing frequency did not show a significant effect on the TIL($p > 0.05$, see Table 2) regardless of combustion aerosol, MIF and breathing frequency (pooled data). When the data was stratified by combustion aerosol and MIF (see Table 5), the effect of the breathing frequency became significant ($p < 0.05$) for all conditions challenged with wood and paper combustion aerosols, and for MIF = 30 L/min only if challenged with plastic

aerosol. However, no significant breathing frequency effect was found at MIF = 55 L/min (p = 0.99) and MIF = 85 L/min (p = 0.97) for plastic aerosol. The pairwise multiple comparisons confirmed that the frequency of 30 breath/min produced the highest mean TIL value when MIF = 30 L/min, which was true for all three combustion aerosols (see Table 5). The findings were consistent with the results of size-selective TIL measurements (see Figure 2). At MIF = 55 L/min, the highest mean TIL values were recorded at 20 breaths/min for wood combustion aerosol (TIL = 0.89%) and at 30 breaths/min for paper aerosol (TIL = 0.88%); no peak TIL value was observed for plastic aerosol. For the MIF = 85 L/min, the highest mean TIL values were recorded at 15 breaths/min for wood combustion aerosol (TIL = 0.67%), at 10 breaths/min for paper aerosol (TIL = 0.90%); again, no peak TIL value was found for plastic aerosol.

In summary, the data suggest that the breathing frequency effect is rather complex and dependent on the combustion aerosol and MIF. It is concluded that the breathing frequency affects the TIL less than factors such as combustion aerosol and breathing flow rate. This finding points to the importance of a proper selection of challenge aerosol and MIF when testing the performance of the elastomeric half-mask respirators. Nevertheless, for a certain chosen aerosol and MIF, different breathing frequencies can produce significant differences among the TIL values. For example, for wood aerosol and MIF = 30 L/min, the highest TIL (1.08%) obtained at 30 breaths/min was almost 1.5-fold higher than the one (0.74%) obtained at 15 breaths/min. At MIF = 85 L/min, the highest TIL found for the wood aerosol (0.67% at 15 breaths/min) was almost twice greater than the lowest TIL (0.35% at 25 breaths/min). In addition to characterizing the role of breathing frequency in the performance evaluation of an elastomeric respirator, the findings of this study support testing with cyclic flow (the present NIOSH certification protocol utilizes the constant flow condition). A similar conclusion was

made for other types of respirators (Eshbaugh *et al.*, 2008; Haruta *et al.*, 2008; Grinshpun *et al.*, 2009).

A limitation of the study is that only one model of elastomeric half-mask respirators was tested. Generally, the results may differ from one model to another. In addition, only a single donning was conducted so that a contaminated respirator would not be subjected to a replicate testing. It remains unknown how the results would differ given that the respirator model characteristics and between-donning variability may cause leaks of different sizes and shapes. While we believe that the major trends would remain the same, it seems meaningful to expand the present study in the future involving alternative experimental designs and other half-mask models as well as, possibly, other classes of respirators (i.e., full facepiece and filtering facepiece respirators).

CONCLUSIONS

Particle size, combustion material and breathing flow had significant ($p < 0.001$) effects on the TIL regardless of the level of the breathing frequency. The relatively flat curves generated in the size-selective experiments between approximately 40 to 200 nm serve as an evidence of a wide size range of particles, which most readily penetrate through faceseal leaks of half-mask respirators.

The effect of the breathing frequency was complex and differed for different combinations of the combustion aerosol and the MIF. For pooled data, the breathing frequency had no significant ($p = 0.08$) effect on the non-size selective TIL. However, after stratifying the data according to combustion aerosol and MIF, the breathing frequency effect became significant ($p < 0.05$) for all MIFs when challenged with wood and paper combustion aerosols, and

specifically for MIF = 30 L/min when challenged with plastic aerosol. More studies are needed to fully understand the effect of breathing frequency.

Plastic aerosols produced higher overall mean TIL values ($p < 0.05$) as compared to wood and paper aerosols, suggesting potentially higher exposure to a wearer. The highest penetration occurred when challenged plastic aerosol, at 30 L/min, and at a breathing frequency of 30 breaths/min. The results also showed that an increase in the MIF leads to a decrease in TIL — a trend which lost its significant difference as the flow rate exceeded 55 L/min.

ACKNOWLEDGEMENT

This study was supported by the NIOSH Targeted Research Training Program and Pilot Research Project Training Program (University of Cincinnati, Education and Research Center, Grant T42/OH008432-07). The BRSS was made available thanks to courtesy of Koken Ltd. (Tokyo, Japan). The authors are grateful to Dr. Joseph Wander who provided numerous valuable comments to the draft of this manuscript.

REFERENCES

Bałazy A, Toivola M, Adhikari A, Sivasubramani SK, Reponen T, Grinshpun SA. (2006a) Do N95 respirators provide 95% protection level against airborne viruses, and how adequate are surgical masks? Am. J. Infect. Control; 34 51-57.

Bałazy A, Toivola M, Reponen T, Podgorski A, Zimmer A, Grinshpun SA. (2006b) Manikin-Based Performance Evaluation of N95 Filtering-Facepiece Respirators Challenged with Nanoparticles. Ann. Occup. Hyg.; 50 259-69.

Baxter CS, Ross CS, Fabian T, Borgerson JL, Shawon J, Gandhi PD, Dalton JM, Lockey JE. (2010) Ultrafine Particle Exposure During Fire Suppression-Is It an Important Contributory Factor for Coronary Heart Disease in Firefighters? J. Occup. Environ. Med.; 52 791-96.

Bergman MS, Zhuang Z, Wander J, Hanson D, Heimbuch BK, McDonald M, Palmiero A, Shaffer RE, Husband M. (2013) Development of an Advanced Respirator Fit Test Headform. (To be submitted).

BLS/NIOSH. (2003) "Respirator Usage in Private Sector Firms, 2001"U.S. Department of Labor, Bureau of Labor Statistics/U.S. Department of Health and Human Services, Public Health Service, Centers for Disease Control and Prevention, National Institute for Occupational Safety and Health

Brown RC. (1993) Air filtration: An integrated approach to the theory and applications of fibrous filters. Oxford: Pergamon Press; p.109, Book (ISBN 0080412742).

Brosseau LM, Ellenbecker MJ, Evans JS. (1990) Collection of Silica and Asbestos Aerosols by Respirators at Steady and Cyclic Flow. Am. Ind. Hyg. Assoc. J.; 51 420-26.

Chen CC, Ruuskanen J, Pilacinski W, Willeke K. (1990) Filter and leak penetration characteristics of a dust and mist filtering facepiece. Am. Ind. Hyg. Assoc. J.; 51 632-39.

Chen CC, Willeke K. (1992) Characteristics of face seal leakage in filtering facepieces. Am. Ind. Hyg. Assoc. J.; 53 533-39.

Cho KJ, Jones S, Jones G, McKay R, Grinshpun SA, Dwivedi A, Shukla R, Singh U, Reponen T. (2010a) Effect of Particle Size on Respiratory Protection Provided by Two Types of N95 Respirators Used in Agricultural Settings. J. Occup. Environ. Hyg.; 7 622-27.

Cho KJ, Reponen T, McKay R, Shukla R, Haruta H, Sekar P, Grinshpun SA. (2010b) Large Particle Penetration through N95 Respirator Filters and Facepiece Leaks with Cyclic Flow. Ann. Occup. Hyg.; 54 68-77.

Cooper DW, Hinds WC, Price JM, Weker R, Yee HS. (1983) Common materials for emergency respiratory protection: leakage tests with a manikin. Am. Ind. Hyg. Assoc. J.; 44 720-26.

Eninger RM, Honda T, Adhikari A, Heinonen-Tanski H, Reponen T, Grinshpun SA. (2008) Filter Performance of N99 and N95 Facepiece Respirators Against Viruses and Ultrafine Particles. Ann. Occup. Hyg.; 52 385-96.

Eshbaugh JP, Gardner PD, Richardson AW, Hofacre KC. (2008) N95 and P100 Respirator Filter Efficiency Under High Constant and Cyclic Flow. J. Occup. Environ. Hyg.; 6 52-61.

Golshahi L, Telidetzki K, King B, Shaw D, Finlay WH. (2012) A pilot study on the use of geometrically accurate face models to replicate ex vivo N95 mask fit. Am. J. Infect. Control.

Grafe T, Gogins M, Barris M, Schaefer J, Canepa R. (2001) "Nanofibers in Filtration Applications in Transportation". Filtration 2001 Conference Proceedings, Chicago, IL; 1-15.

Grinshpun SA, Haruta H, Eninger RM, Reponen T, McKay RT, Lee S-A. (2009) Performance of an N95 Filtering Facepiece Particulate Respirator and a Surgical Mask During Human Breathing: Two Pathways for Particle Penetration. J. Occup. Environ. Hyg.; 6 593-603.

Han D-H, Lee J. (2005) Evaluation of Particulate Filtering Respirators Using Inward Leakage (IL) or Total Inward Leakage (TIL) Testing—Korean Experience. Ann. Occup. Hyg.; 49 569-74.

Hanson D, Bergs R, Tadesse Y, White V, Priya S. (2006) Enhancement of EAP Actuated Facial Expressions by Designed Chamber Geometry in Elastomers. Proc. SPIE's Electroactive Polymer Actuators and Devices Conf., 10th Smart Structures and Materials Symposium, San Diego.

Hanson D, Priya S. (2007) An Actuated Skin for Robotic Facial Expressions, NSF Phase 1 Final Report. National Science Foundation STTR award, NSF 05-557.

Hanson D, White V. (2004) Converging the Capabilities of ElectroActive Polymer Artificial Muscles and the Requirements of Bio-inspired Robotics. Proc. SPIE's Electroactive Polymer Actuators and Devices Conf., 10th Smart Structures and Materials Symposium, San Diego.

Haruta H, Honda T, Eninger RM, Reponen T, McKay R, Grinshpun SA. (2008) Experimental and theoretical investigation of the performance of N95 respirator filters against ultrafine aerosol particles tested at constant and cyclic flows. J. Int. Soc. Res. Prot.; 25 75-88.

He X, Grinshpun SA, Reponen T, Yermakov M, McKay R, Haruta H, Kimura K. (2013a) Laboratory Evaluation of the Particle Size Effect on the Performance of an Elastomeric Half-mask Respirator against Ultrafine Combustion Particles. (Submitted). Ann. Occup. Hyg.

He X, Yermakov M, Reponen T, McKay R, James K, Grinshpun SA. (2013b) Manikin-based performance evaluation of elastomeric respirators against combustion particles. (Accepted) J. Environ. Occup. Hyg.

Hinds WC, Bellin P. (1987) Performance of Dust Respirators with Facial Seal Leaks: II. Predictive Model. Am. Ind. Hyg. Assoc. J.; 48 842-47.

Huang S-H, Chen C-W, Chang C-P, Lai C-Y, Chen C-C. (2007) Penetration of 4.5 nm to aerosol particles through fibrous filters. Journal of aerosol science; 38 719-27.

Lawrence RB, Duling MG, Calvert CA, Coffey CC. (2006) Comparison of Performance of Three Different Types of Respiratory Protection Devices. Journal of Occupational and Environmental Hygiene; 3 465-74.

Martin SB, Moyer ES. (2000) Electrostatic Respirator Filter Media: Filter Efficiency and Most Penetrating Particle Size Effects. Applied Occupational and Environmental Hygiene; 15 609-17.

Myers WR, Kim H, Kadrichu N. (1991) Effect of particle size on assessment of faceseal leakage. J. Int. Soc. Res. Prot.; 6-21.

Myers WR, Zhuang Z, Nelson T. (1996) Field Performance Measurements of Half-Facepiece Respirators - Foundry Operations. Am. Ind. Hyg. Assoc. J.; 57 166-74.

NIOSH. (1995) National Institute for Occupational Safety and Health. US DHHS, Public Health Service. "Respiratory Protective Devices; Final Rules and Notices" Federal Register 60:110, pp. 30335-30393.

NIOSH/CDC. (2009) National Institute for Occupational Safety and Health. US DHHS, Public Health Service. "Total Inward Leakage for Half-mask Air-purifying Respirators".

OSHA. (2006) "Respirator Protection", 29 CFR 1910.134.

Peters A, Wichmann HE, Tuch T, Heinrich J, Heyder J. (1997) Respiratory effects are associated with the number of ultrafine particles. Am. J. Respir. Crit. Care Med.; 155 1376-83.

Qian Y, Willeke K, Grinshpun SA, Donnelly J, Coffey CC. (1998) Performance of N95 Respirators: Filtration Efficiency for Airborne Microbial and Inert Particles. Am. Ind. Hyg. Assoc. J.; 59 128-32.

Rengasamy S, Eimer BC. (2011) Total Inward Leakage of Nanoparticles Through Filtering Facepiece Respirators. Ann. Occup. Hyg.; 55 253-63.

Rengasamy S, Eimer BC, Shaffer RE. (2009) Comparison of Nanoparticle Filtration Performance of NIOSH-approved and CE-Marked Particulate Filtering Facepiece Respirators. Ann. Occup. Hyg.; 53 117-28.

Rengasamy S, King WP, Eimer BC, Shaffer RE. (2008) Filtration Performance of NIOSH-Approved N95 and P100 Filtering Facepiece Respirators Against 4 to 30 Nanometer-Size Nanoparticles. J. Occup. Environ. Hyg.; 5 556-64.

Roberge RJ, Coca A, Williams WJ, Powell JB, Palmiero AJ. (2010) Reusable elastomeric air-purifying respirators: Physiologic impact on health care workers. Am. J. Infect. Control; 38 381-86.

Schulte P, Geraci C, Zumwalde R, Hoover M, Kuempel E. (2008) Occupational Risk Management of Engineered Nanoparticles. J. Occup. Environ. Hyg.; 5 239-49.

Schwartz J, Dockery DW, Neas LM. (1996) Is Daily Mortality Associated Specifically with Fine Particles? J. Air Waste Manag. Assoc.; 46 927-39.

Sherwood L. (2006) Fundamentals of Physiology: A Human Perspective. Thomson Brooks/Cole, p.380.

Stafford RG, Ettinger HJ, Rowland TJ. (1973) Respirator Cartridge Filter Efficiency under Cyclic- and Steady-Flow Conditions. Am. Ind. Hyg. Assoc. J.; 34 182-92.

Timonen KL, Vanninen E, de Hartog J, Ibald-Mulli A, Brunekreef B, Gold DR, Heinrich J, Hoek G, Lanki T, Peters A, *et al.* (2005) Effects of ultrafine and fine particulate and gaseous air pollution on cardiac autonomic control in subjects with coronary artery disease: The ULTRA study. J Expos Sci Environ Epidemiol; 16 332-41.

Tortora GJ, Anagnostakos NP. (1990) Principles of Anatomy and Physiology, 6th edition, New York: Harper-Collins. p.707

Tuomi T. (1985) Face seal leakage of half-masks and surgical masks. Am. Ind. Hyg. Assoc. J.; 46 308-12.

UL. (2010) Underwriters Laboratories Inc., Firefighter Exposure to Smoke Particulates, http://www.ul.com/global/documents/offerings/industries/buildingmaterials/fireservice/WEBDOCUMENTS/EMW-2007-FP-02093.pdf (Accessed on Nov.15, 2012).

Wang A, Richardson AW, Hofacre KC. (2012) The Effect of Flow Pattern on Collection Efficiency of Respirator Filters. J. Int. Soc. Res. Prot.; 29 41.

Zhuang Z, Coffey CC, Myers WR, Yang J, Campbell DL. (1998) Quantitative Fit-Testing of N95 Respirators: Part I-Method Development. International Society for Respiratory Protection; 16 11-24.

Zhuang ZQ, Bradtmiller B, Shaffer RE. (2007) New respirator fit test panels representing the current US civilian work force. J. Occup. Environ. Hyg.; 4 647-59.

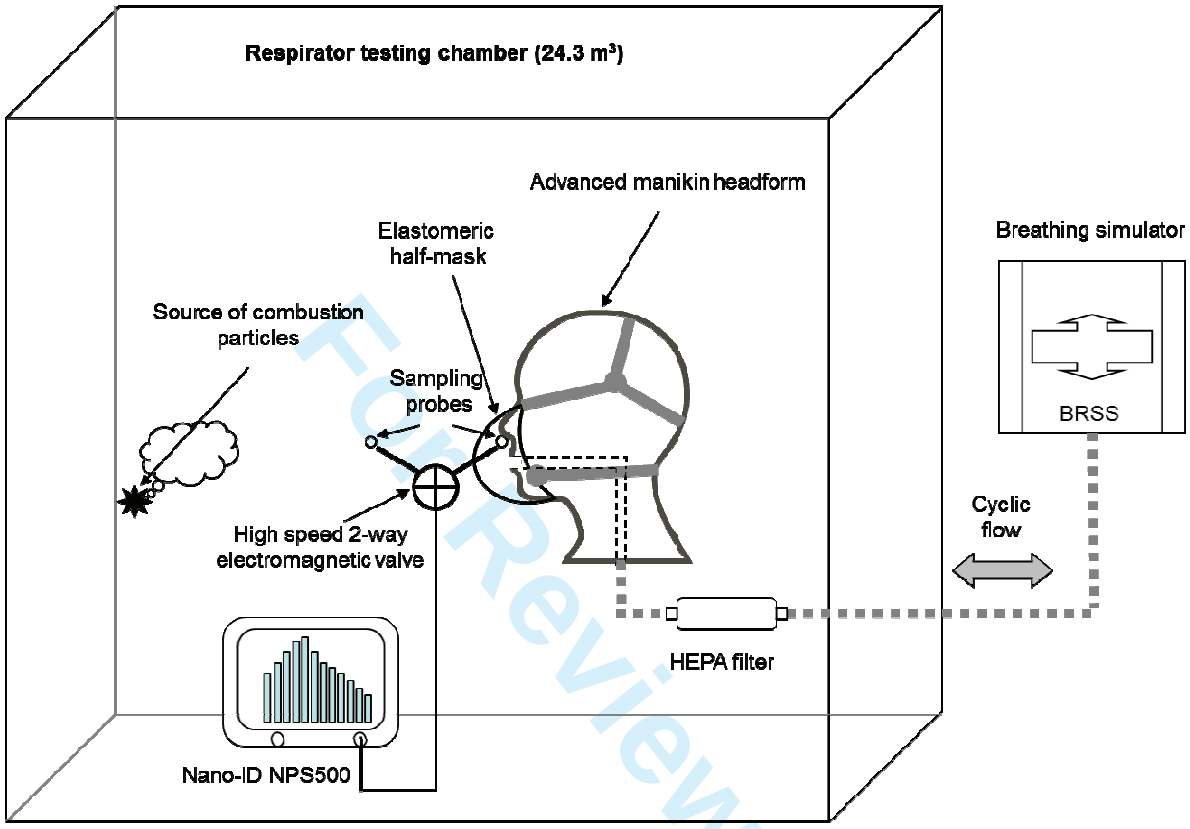

Fig. 1. Schematic diagram of the experimental set-up (modified from He *et al.*, 2013a).

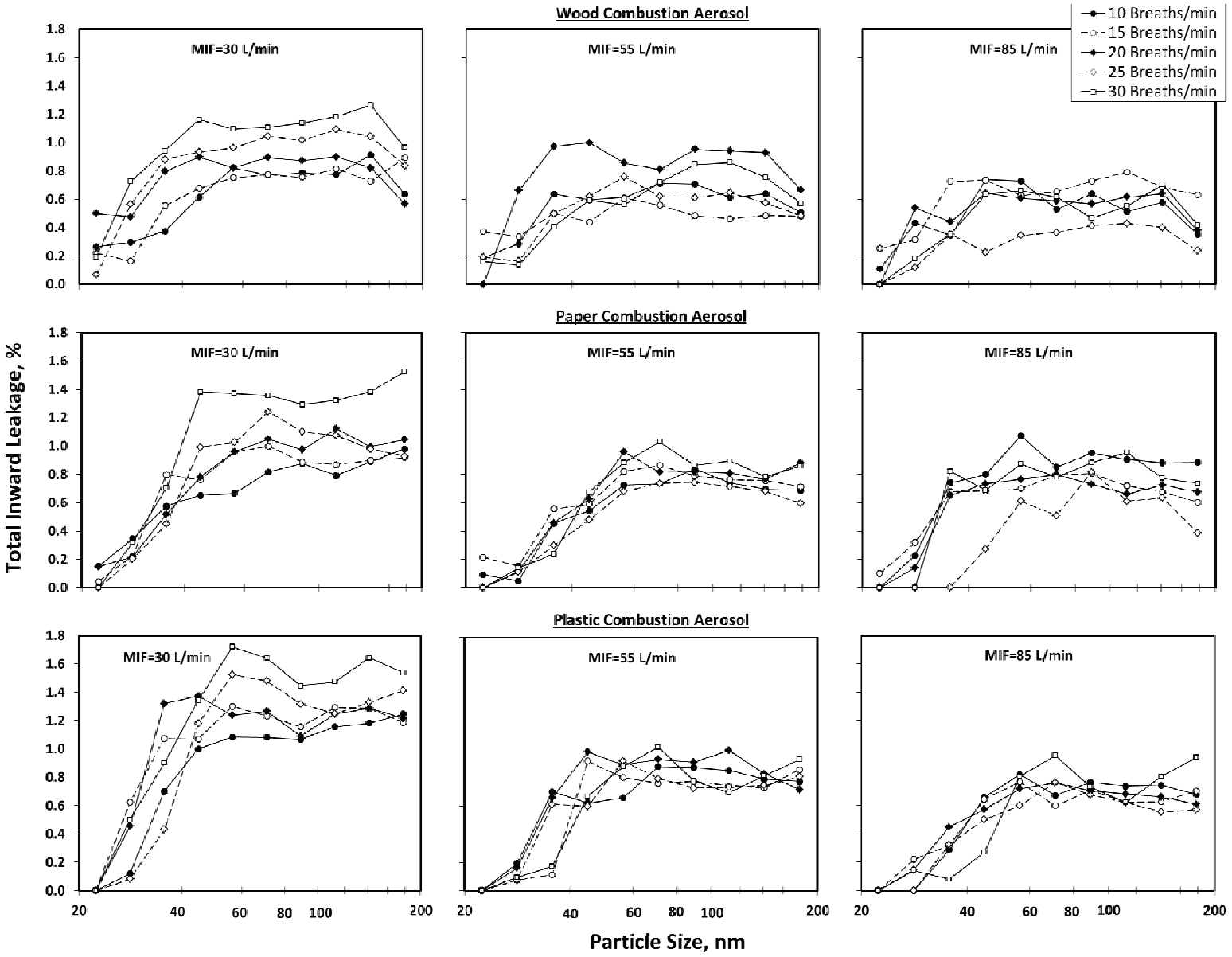

Fig. 2. Size-selective total inward leakage values for an elastomeric half-mask respirator donned an advanced manikin headform while challenged with three combustion aerosols (wood, paper and plastic). Each point represents the average value of four replicates.

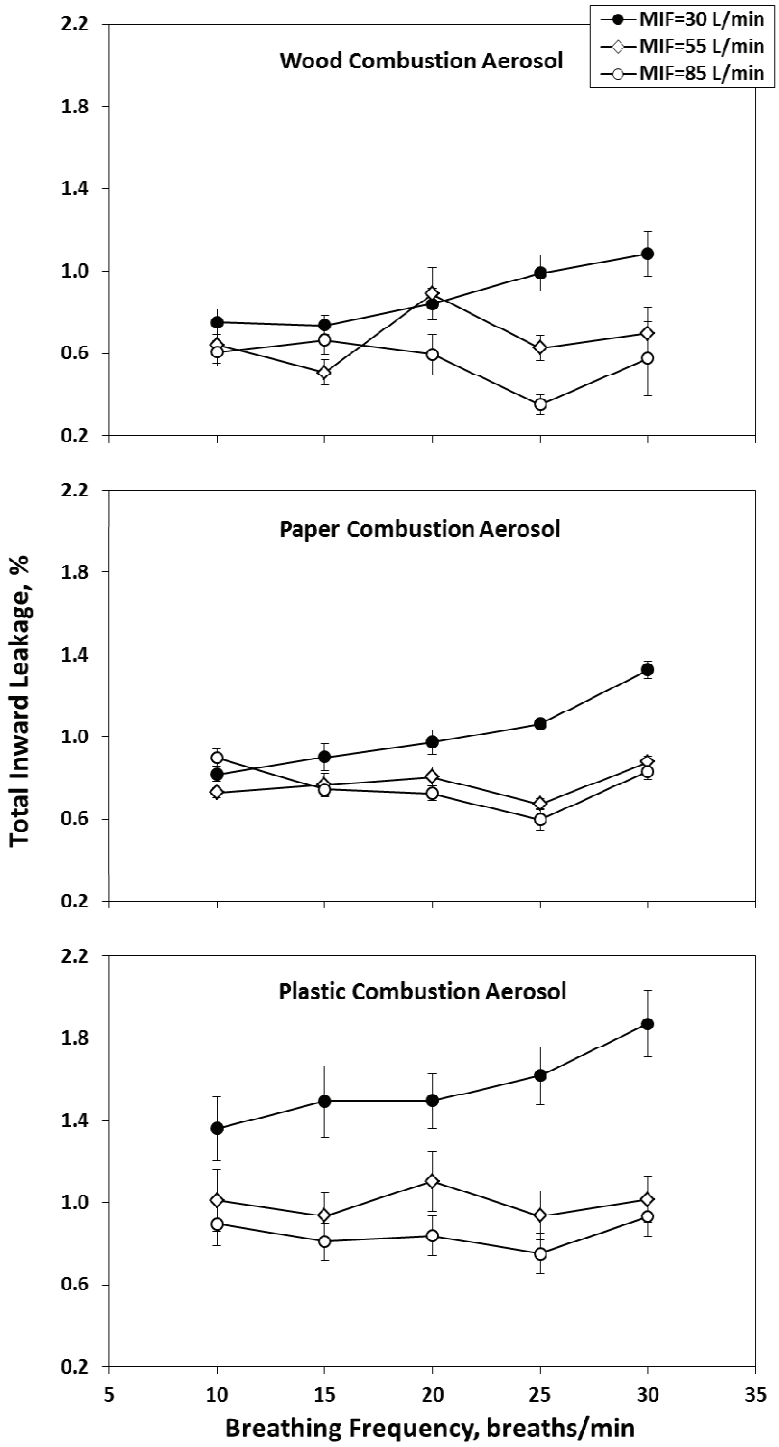

Fig. 3. Size-independent (overall) total inward leakage values for an elastomeric half-mask respirator donned an advanced manikin headform while challenged with three combustion aerosols (wood, paper and plastic). Each point represents the average value of four replicates after combining all the channels between 20 to 200 nm, and the error bar represents the standard error of the mean.

Table 1. Summary of the experimental conditions

Variable	Levels
Respirator Type	One elastomeric half-mask with P100 filters (Medium size, 3M 6000 series)
Challenge Aerosol	Paper, wood, and plastic combustion aerosols
Breathing Flow Rate	Cyclic 30, 55, and 85 L/min
Breathing Frequency	10, 15, 20, 25, and 30 breaths/min
Particle Size Range	20 – 200 nm (10 channels)
Replicates	4
Total Runs:	3×3×5×4 = 180

Table 2. Three-way ANOVA results for the size-independent (overall) TIL as a function of combustion aerosol, MIF and breathing frequency (B*f*).

Source	DF	ANOVA SS	Mean Square	F Value	*p*-value
Aerosol	2	5.81	2.90	28.40	<.0001
MIF	2	6.24	3.12	30.49	<.0001
Aerosol*MIF	4	1.43	0.35	3.49	0.0096
B*f*	4	0.86	0.21	2.10	0.0841
Aerosol*B*f*	8	0.09	0.01	0.12	0.9983
MIF*B*f*	8	1.38	0.17	1.68	0.1076
Aerosol*MIF*B*f*	16	0.23	0.01	0.14	1.0000

Note: B*f* stands for breathing frequency. Three-way ANOVA were performed on all levels of combustion aerosol, MIF and breathing frequency (pooled data). The asterisk (*) indicates an interaction between variables.

Table 3. Pairwise multiple comparisons: mean TIL values among three combustion aerosol groups (ANOVA with Tukey's range test)

Tukey Grouping[a]	Mean[b] TIL (%)	Aerosol
A	1.14	Plastic
B	0.85	Paper
C	0.70	Wood

a: Means with the same letter are not significantly different (p-value > 0.05).
b: Calculated using the size-independent (overall) TIL values.

Table 4. Pairwise multiple comparisons: mean TIL values among three MIF groups (ANOVA with Tukey's range test)

Tukey Grouping[a]	Mean[b] TIL (%)	MIF (L/min)
A	1.15	30
B	0.81	55
B	0.72	85

a: Means with the same letter are not significantly different (p-value > 0.05).
b: Calculated using the size-independent (overall) TIL values.

Table 5. Pairwise multiple comparisons: mean TIL values among five breathing frequency groups challenged with combustion aerosols (ANOVA with Tukey's range test)

Wood Combustion Aerosol				Paper Combustion Aerosol				Plastic Combustion Aerosol			
Tukey Grouping[a]	Mean[b] TIL (%)	Breathing Frequency (breaths/min)	*p*-value[c]	Tukey Grouping[a]	Mean[b] TIL (%)	Breathing Frequency (breaths/min)	*p*-value[c]	Tukey Grouping[a]	Mean[b] TIL (%)	Breathing Frequency (breaths/min)	*p*-value[c]
MIF = 30 L/min				MIF = 30 L/min				MIF = 30 L/min			
A	1.08	30		A	1.33	30		A	1.87	30	
A B	0.99	25	0.0265	B	1.06	25	< 0.0001	A B	1.62	25	0.0476
A B	0.84	20		B C	0.97	20		A B	1.50	20	
B	0.75	10		C D	0.90	15		A B	1.49	15	
B	0.74	15		D	0.82	10		B	1.36	10	
MIF = 55 L/min				MIF = 55 L/min				MIF = 55 L/min			
A	0.89	20		A	0.88	30		A	1.10	20	
A	0.70	30	0.0373	A B	0.81	20	0.0231	A	1.01	30	0.9890
A B	0.64	10		B C	0.77	15		A	1.01	10	
A B	0.63	25		B C	0.73	10		A	0.94	15	
B	0.51	15		C	0.67	25		A	0.94	25	
MIF = 85 L/min				MIF = 85 L/min				MIF = 85 L/min			
A	0.67	15		A	0.90	10		A	0.93	30	
A	0.61	10	0.0391	A B	0.83	30	0.0260	A	0.90	10	0.9689
A	0.60	20		A B	0.74	15		A	0.84	20	
A	0.58	30		B	0.73	20		A	0.81	15	
B	0.35	25		B	0.72	25		A	0.75	25	

a: Within each group of the combustion aerosol (wood, paper and plastic), means with the same letter are not significantly different (p-value > 0.05).

b: Calculated using the size-independent (overall) TIL values.

c: *P*-values were obtained from the one-way ANOVA performed to examine the effect of the breathing frequency on the size-independent TIL after stratifying the combustion aerosol and the MIF.

Journal of Occupational and Environmental Hygiene

How does breathing frequency affect the performance of an N95 filtering facepiece respirator and a surgical mask against surrogates of viral particles?

Journal:	*Journal of Occupational & Environmental Hygiene*
Manuscript ID:	JOEH-13-0112
Manuscript Type:	Technical Manuscript
Date Submitted by the Author:	10-May-2013
Complete List of Authors:	Grinshpun, Sergey A.; University of Cincinnati, Environ Health He, Xinjian; University of Cincinnati, Environmental Health Reponen, Tiina; University of Cincinnati, Environmental Health McKay, Roy; University of Cincinnati, Environmental Health
Keyword:	breathing frequency, N95, respirator, surgical mask, manikin

How does breathing frequency affect the performance of an N95 filtering facepiece respirator and a surgical mask against surrogates of viral particles?

Xinjian He, Tiina Reponen, Roy McKay, and Sergey A. Grinshpun*

Center for Health-Related Aerosol Studies, Department of Environmental Health, University of Cincinnati, Cincinnati, OH

Word count of the exposition only: 3008

Keywords: breathing frequency; N95; respirator; surgical mask; manikin

To be submitted to the

Journal of Occupational and Environmental Hygiene

May 10, 2013

Corresponding author: Sergey A. Grinshpun: sergey.grinshpun@uc.edu

ABSTRACT

Background: Breathing frequency (breaths/min) differs between individuals and levels of physical activity. Particles enter respirators through two principle penetration pathways: faceseal leakage and filter penetration. However, it is unknown how breathing frequency affects the overall performance of N95 filtering facepiece respirators (FFRs) and surgical masks (SMs) against viral particles, as well as other health-relevant submicrometer particles.

Methods: A breathing manikin was tested at four mean inspiratory flows (MIFs) (15, 30, 55 and 85 L/min) and five breathing frequencies (10, 15, 20, 25 and 30 breaths/min). Filter penetration (P_{filter}) and total inward leakage (TIL) were determined for the tested respiratory protection devices against sodium chloride (NaCl) aerosol particles in the size range of 20 to 500 nm. "Faceseal leakage-to-filter" (*FLTF*) penetration ratios were calculated.

Results: Both MIF and breathing frequency showed significant effects ($p<0.05$) on P_{filter} and TIL. Increasing breathing frequency increased TIL for the N95 FFR whereas no clear trends were observed for the SM. Increasing MIF increased P_{filter} and decreased TIL resulting in decreasing *FLTF* ratio. Most of *FLTF* ratios were >1, suggesting that the faceseal leakage was the primary particle penetration pathway at various breathing frequencies.

Conclusions: Breathing frequency is another factor (besides MIF) that can significantly affect the performance of N95 FFRs, with higher breathing frequencies increasing TIL.

INTRODUCTION

The National Institute for Occupational Safety and Health (NIOSH) certified N95 filtering facepiece respirators (FFRs) are widely used in various occupational environments to reduce the workers' exposure to hazardous aerosols. In healthcare environments, N95 FFRs and surgical masks (SMs) are the most commonly used devices to prevent transmission of infectious diseases.[1] N95 FFRs are certified by NIOSH in accordance with Title 42 of the Code of Federal Regulations.[2] The letter 'N' stands for non-oil-resistance, and the number '95' denotes the filter efficiency of at least 95% when the filter is challenged with NaCl aerosols having a mass median aerodynamic particle diameter of 300 nm (the most penetrating particle size, MPPS, for mechanical filters) at a constant flow of 85 L/min.[3] Presently, the vast majority of FFRs are manufactured utilizing electrostatic fibers, which feature much smaller MPPS: 30 to 100 nm.[4-11] The latter range includes many viral species. SMs are not subject to NIOSH filter certification approval; instead they are regulated by the US Food and Drug Administration (FDA). Previous studies have shown that the filter efficiency for SMs is much lower than that for N95 FFRs.[4, 12-14]

Besides filter penetration, faceseal leakage can have a significant impact on the performance of N95 FFRs and SMs. One study showed that the efficiency of N95 FFRs was high when sealed to a manikin headform but decreased significantly due to faceseal leakage when the same respirators were tested on human subjects.[15] NIOSH has proposed total inward leakage (TIL) testing to assess respirator performance since it takes into account both penetration pathways.[16] Grinshpun and colleagues quantified the relative contributions of the two pathways for an N95 FFR and a SM by determining the filter penetration (P_{filter}) and faceseal leakage penetration ($P_{leakage}$) using manikin-based and human subject-based experimental protocols.[12]

The "faceseal leakage-to-filter" ratio ($FLTF = P_{leakage}/P_{filter}$) was > 1, indicating a greater number of particles penetrated through faceseal leaks than the filter media.[12] While the quoted study addressed a wide range of particle sizes (30 – 1000 nm), it did not examine breathing frequency.

Viral airborne particles (known as virions) are generally much smaller than airborne bacteria. Most viruses referenced in the literature are between 20 and 300 nm in diameter.[17] For instance, coronavirus, the causative agent of severe acute respiratory syndrome (SARS), has a primary physical size ranging from 80 to 140 nm; the avian influenza virus (H5N1 and H1N1) is between 80 to 120 nm.[18, 19] Exposure to viral particles is best characterized by the number of inhaled particles rather than mass concentration.[20]

The Institute of Medicine estimates that during an influenza pandemic, more than 13 million health care workers, patients, family members and friends may need respiratory protection devices to protect them from receiving or spreading infectious illness.[21] Between population groups (e.g., young vs. old, small vs. large, healthy vs. sick), breathing frequency (breaths/min) differs and will differ significantly with level of physical activity (e.g., at rest vs. active).[22, 23] In addition, one study, which examined the physiologic impact of respirators on healthcare workers, reported that wearing a respirator significantly decreased the breathing frequency at both low and high work rates compared to controls not wearing a respirator.[24] Various studies have addressed the effect of flow rate on filter efficiency and faceseal leakage.[25-28] However, with exception to our recent study in which an elastomeric half-mask respirator was tested,[29] no published study has evaluated the effect of breathing frequency on the performance of N95 FFRs and SMs when both filter and faceseal leakage penetration pathways are present.

Although the nature of an inert aerosol (e.g., NaCl) differs from that of bioaerosols, several studies have confirmed that filter performance against biological particles is consistent with that determined using non-biological particles of the same size.[4, 6, 15] This suggests that inert aerosol surrogates such as NaCl particles may generally be appropriate for predicting penetration of similarly sized virions. The present manikin-based study addresses the effects of breathing frequency and flow rate on the filter efficiency and faceseal leakage of an N95 FFR and a SM challenged with NaCl particles representative of viral size ranges, as well as other health-relavent particles (e.g., combustion generated or engineered nanoparticles). The tested N95 FFR/SM was sealed to plastic manikin headform to investigate filter performance. It was also donned without sealing to a different advanced manikin headform to quantify TIL. The advanced manikin utilized in this study was recently developed to mimic the properties of the human face.[30, 31] Faceseal leakage represents the difference between TIL and filter penetration.

MATERIALS AND METHODS

Tested N95 FFR and Surgical Mask

One N95 FFR and one SM were chosen for the study. Both models are commercially available and widely used in health-care environments. The model of the N95 FFR was identical to the one tested in our previous studies.[4, 5] It has three principle layers with the middle layer composed of electrically charged polypropylene fibers to enhance filter capture efficiency.[4] The selected SM, according to the manufacturer, is fluid resistant and capable of providing at least 95% filter efficiency for 100 nm particles.

For filter efficiency testing, the FFR/SM was sealed to the face of a hard plastic manikin headform. For the TIL tests, it was donned on an advanced manikin headform according to the

FFR/SM manufacturer's user instruction. After 20 tests, the tested FFR/SM was removed from the manikin and replaced with a new one to minimize the effect of NaCl loading on the filter media.

Challenge Aerosol

To produce the challenge agent (NaCl), a liquid salt solution was aerosolized using a particle generator (Model: 8026, TSI Inc., Shoreview, MN) and charge-equilibrated by passing through a ^{85}Kr electrical charge equilibrator (Model: 3054, TSI Inc., Shoreview, MN) prior to being released inside the test chamber. Before each experiment, the particle generator operated for at least one hour to achieve a uniform NaCl concentration in the chamber; it continued operating during the testing to maintain a stable particle concentration level. The challenge aerosol was log normally distributed with a size range of 20 – 500 nm, a count geometric mean of 125.4 nm, and a geometric standard deviation of 1.68 as measured with a Nanoparticle Spectrometer (Nano-ID NPS500, Naneum Ltd., Kent, UK). This size range covers the size of individual and aggregate virus particles.

Experimental Design and Test Conditions

Experiments were carried out in a room-size (24.3 m^3) test chamber described in recent studies.[29, 32] Temperature and relative humidity inside the chamber were kept at 17–22 ℃ and 30–60 %, respectively. The headform was connected to a Breathing Recording and Simulation System (BRSS, Koken Ltd., Tokyo, Japan) with a HEPA filter placed in-between to keep particles from re-entering the respirator cavity during exhalation cycles. Details regarding the BRSS are described in our previous studies.[27, 29, 32, 33]

The experiments were conducted at four cyclic breathing flows (mean inspiratory flow, MIF =15, 30, 55 and 85 L/min) and five breathing frequencies (10, 15, 20, 25 and 30 breaths/min). Completely randomized factorial design was implemented for the breathing frequency and flow rate with three replicates. Particle size-independent (overall) concentrations inside and outside the FFR/SM were obtained using a condensation particle counter (Model: 3007, TSI Inc., Shoreview, MN) having a total sampling time of 3 min with a time resolution of 1 sec.

Filter Penetration (P_{filter}) Test

The filter penetration (P_{filter}) was determined as the ratio of concentrations inside [$C_{in\_(Sealed)}$] and outside [$C_{out\_(Sealed)}$] of the FFR/SM sealed to the plastic headform:

$$P_{filter} = \frac{C_{in\_(Sealed)}}{C_{out\_(Sealed)}} \times 100\% \quad \textbf{(1)}$$

Total Inward Leakage (TIL) Test

For TIL, the same experimental protocol and test conditions were used except the FFR/SM was not sealed onto the advanced manikin headform. TIL values were determined as the ratio of concentrations inside [$C_{in\_(Donned)}$] and outside [$C_{out\_(Donned)}$] of the FFR/SM:

$$TIL = \frac{C_{in\_(Donned)}}{C_{out\_(Donned)}} \times 100\% \quad \textbf{(2)}$$

Faceseal Leakage to Filter (FLTF) Ratio

The TIL test measures total penetration through the filter and faceseal leakage (TIL = $P_{filter} + P_{leakage}$). The *FLTF* ratio represents the relative contribution for each and was calculated as:

$$FLTF = \frac{P_{leakage}}{P_{filter}} = \frac{TIL - P_{filter}}{P_{filter}} \quad \textbf{(5)}$$

In this study, the *FLTF* ratio was calculated using the average TIL and P_{filter} values over three replicates in order to identify the primary penetration pathway (leakage or filter penetration) for the entire particle size range of interest.

Data analysis

SAS version 9.3 (SAS Institute Inc., Cary, NC, USA) was used for data analysis. Two-way Analysis of Variance (ANOVA) was performed to analyze the effect of breathing frequency and flow rate on the filter penetration and TIL. All pairwise comparisons were conducted using Tukey's range test. *P*-values < 0.05 were considered significant.

RESULTS AND DISCUSSION

1. N95 Filtering Facepiece Respirator

N95 Filter Penetration (P_{filter})

Filter penetration results for the N95 FFR are presented in Figure 1A. Filter penetration (P_{filter}) consistently increased with increasing MIF. This result can be explained by the differences in linear air velocities. Penetration of very small particles, which deposit on filter fibers primarily due to diffusion, increases with a decreasing residence time (also known as

removal time). Thus, small particles are more likely to penetrate the filter at higher breathing flows. At the higher flows (MIF = 55 and 85 L/min), the P_{filter} curves are not flat, in contrast to those at the 15 and 30 L/min, suggesting that the effect of lower breathing frequencies are more pronounced at higher MIFs.

Two-way ANOVA performed on the P_{filter} data revealed that both the MIF and breathing frequency had a significant effect on filter penetration (p <0.0001, see Table I). Pairwise multiple comparison results (see Table I) show that the four MIFs produced four different P_{filter} groups with the highest mean P_{filter} (0.72%, Tukey grouping "A") occurring at the highest MIF of 85 L/min, and the lowest mean P_{filter} (0.05%, Tukey grouping "D") occurring at the lowest MIF of 15 L/min. The breathing frequency comparisons show that 10 and 15 breaths/min produced higher values of P_{filter} (0.39% and 0.38%, Tukey grouping "I") than those observed at 20, 25 and 30 breaths/min (0.25%, 0.23% and 0.26%, respectively, Tukey grouping "II").

N95 Total Inward Leakage (TIL)

Figure 1B presents the results obtained from the TIL measurements for the tested N95 FFR. It is seen that the MIF of 15 L/min produced the highest TILs. Interestingly, the TIL increased with increasing the breathing frequency, especially at MIF = 15 L/min. The exhaled particle-free air dilutes the aerosol in the respirator cavity. At a higher breathing frequency, the dilution air volume per breathing cycle is lower, which results in a less efficient dilution and consequently increases the aerosol concentration inside the respirator. This explains why a higher breathing frequency produced a higher TIL. This finding suggests that fast-breathing people (e.g., children and adults with various health impairments) may benefit less from wearing N95 FFRs. It is acknowledged though that the latter statement is acceptable only as the first

approximation. The aerosol particle transport into a FFR/SM worn by a human is more complex than the one when it is donned on a manikin (e.g., the exhalation air generally carries particles to the cavity).

Statistical analysis revealed significant effects of MIF (p =0.0019) and breathing frequency (p =0.0025) on TIL (see Table II). The pairwise multiple comparison results presented in Table II show that the lowest MIF (15 L/min) was associated with the highest mean TIL (1.93%, Tukey grouping "A"). The mean TIL values among the three higher MIFs (30, 55 and 85 L/min) were not significantly different from each other (1.37%, 1.31% and 1.29%, Tukey grouping "B"). The highest breathing frequency (30 breaths/min) produced the highest mean TIL (1.73%, Tukey grouping "I") compared to the lowest mean TIL (1.22%, Tukey grouping "II") with the lowest breathing frequency (10 breaths/min). The highest and lowest breathing frequencies were significantly different (Tukey groups I & II). As was pointed out in our previous study on elastomeric respirators, [29] higher MIF may create a higher sucking force that made a tighter contact between the respirator and the soft skin of the headform, possibly reducing the leak size. We anticipate that the quoted effect showed up when MIF increased to 30 L/min. The finding is consistent with previous FFR performance studies conducted using hard manikins and challenge aerosol particles above 500 nm.[25, 34, 35]

N95 Faceseal Leakage-to-Filter (FLTF) Ratio

The size-independent (overall) *FLTF* ratios calculated by Eq. (3) are presented in Figure 1C as a function of the breathing frequency and MIF. Except for MIF = 85 L/min, all the *FLTF* ratios were > 1, which suggests that overall particle penetration through faceseal leaks exceeded N95 filter penetration at lower breathing rates. Remarkably, at the lowest MIF (15 L/min) the

FLTF ratios ranged from 25 to 47, suggesting that the absolute majority of the measured virus-size aerosol particles penetrated through faceseal leaks. At MIF = 15 L/min, increase in breathing frequency was generally associated with increase in *FLTF* ratio. However, the breathing frequency effect was not clearly seen for the three higher MIFs (30, 55 and 85 L/min).

It is seen that increasing MIF resulted in decreasing *FLTF* ratio. This finding agrees with two other N95 FFR studies.[12, 36] Grinshpun *et al* tested an N95 FFR using 25 human subjects, and reported that "deep breathing" produced higher *FLTF* ratios compared to "normal breathing".[12] Rengasamy and Eimer also reported higher *FLTF* ratios occurred at higher flow rates when testing the N95 FFRs with artificially created leaks.[36] In both quoted studies, all the *FLTF* ratios exceeded the unity, indicating that the faceseal leakage was the primary penetration pathway for N95 FFRs.

2. Surgical Mask

SM Filter Penetration (P_{filter})

The data on filter penetrations (P_{filter}) for the tested SM are shown in Figure 2A. Compared to the N95 FFR, the SM had a much higher filter penetration. This is not surprising given the less stringent filter penetration test requirements for SMs. In fact, previous studies have reported SMs providing much lower levels of respiratory protection than N95 FFRs when challenged with biological or non-biological particles.[4, 12-14] Increasing MIF frequently resulted in an increase in filter penetration, especially at the lowest breathing frequency. Statistical analysis suggests that the effects of MIF and breathing frequency on the P_{filter} were both significant (p <0.05; see Table III). The pairwise multiple comparisons (see Table III) show the highest MIF (85 L/min) produced the highest mean P_{filter} (9.65%, Tukey grouping "A"), whereas

the lowest P_{filter} (5.41%, Tukey grouping "C") occurred at the lowest MIF (15 L/min). Table III also shows that the mean P_{filter} = 7.81% (Tukey grouping "I") obtained at 30 breaths/min was significantly higher (p <0.05) than P_{filter} = 6.67% (Tukey grouping "II") obtained at 20 breaths/min. However, no consistent trend was identified throughout the frequency scale.

SM Total Inward Leakage (TIL)

TIL results for the SM are presented in Figure 2B. The average TIL values ranged from 17% to 35% compared to filter penetrations of 3 – 12%, suggesting that faceseal leakage had a greater effect on the mask performance. Increasing MIF caused the mean TIL to decrease FFR (see Table IV), which is in agreement with the finding reported for the N95.

While ANOVA revealed that both MIF and breathing frequency had a significant effect on the TIL (p <0.05; see Table IV), no consistent trend of increase or decrease of TIL with breathing frequency was observed. For instance, increasing the breathing frequency from 10 to 15 breaths/min was associated with a decrease in TIL, whereas changing the frequency from 10 to 30 breaths/min at MIF = 55 or 85 L/min resulted in essentially no change in TIL. When comparing the mean TIL values among the five breathing frequencies, the highest mean TIL (25.7%, Tukey grouping "I") occurred at 30 breaths/min, and the lowest mean TIL (22.2%, Tukey grouping "II") at 15 breaths/min.

At the same time, the data produced by a pairwise comparison presented in Table IV demonstrate that increasing MIF indeed decreased the TIL with MIF = 15 L/min generating the highest mean TIL (30%, Tukey grouping "A") and 85 L/min producing the lowest mean TIL (19.9%, Tukey grouping "C").

SM Faceseal Leakage-To-Filter (FLTF) Ratio

The *FLTF* ratios calculated from the overall P_{filter} and the TIL data are presented in Figure 2C. It is seen that increasing MIF from 15 to 55 L/min resulted in a decrease in *FLTF*, with most of the *FLTF* ratios were > 1 (which means $P_{leakage} > P_{filter}$). Increasing MIF from 55 to 85 L/min had less effect, with FLTF ratios < 2 and even < 1 at the highest MIF (85 L/min) for the two lowest frequencies of 10 and 15 breaths/min. The results had a similar pattern to those presented for the N95 FFR. However, the *FLTF* ratios for the SM were lower. For example, at MIF = 15 L/min, the *FLTF* ratios for the SM were between 4 and 7 while those found for the N95 FFR ranged from 24 to 50. This difference is attributed to much higher filter penetration of the SM as compared to the N95 FFR.[12]

No clear trend was identified between the breathing frequency and the *FLTF* ratio for the three highest flows (MIF = 30, 55 and 85 L/min), where the curves are relatively flat (Figure 2C). For the lowest flow rate (15 L/min), increasing breathing frequency initially decreased *FLTF*, but this too leveled off.

CONCLUSIONS

Breathing frequency was found to be another factor (in addition to MIF) that can significantly affect the performance of N95 FFRs and SMs. For the tested N95 FFR, the increase of breathing frequency caused an increase in TIL, thus allowing more particles to penetrate inside the respirator. No consistent trend of increase or decrease of TIL with either MIF or breathing frequency was observed for the tested SM.

The *FLTF* ratios obtained for the N95 FFR were generally higher than those for the SM for all tested breathing frequencies and MIFs. It is primarily because of the higher efficiency of

the N95 filter. Increasing MIF was also generally associated with decreasing *FLTF* ratio for the tested FFR/SM. Except for MIF = 85 L/min, all the calculated *FLTF* ratios were > 1, suggesting that the faceseal leakage was the primary particle penetration pathway for the tested FFR/SM at various breathing frequencies.

ACKNOWLEDGEMENT

This research was supported by the NIOSH Targeted Research Training Program and Pilot Research Project Training Program (University of Cincinnati, Education and Research Center, Grant T42/OH008432-07). The BRSS was made available thanks to courtesy of Koken Ltd. (Tokyo, Japan); the advanced manikin headform was provided by Mr. Michael S. Bergman, and Dr. Ziqing Zhuang of NIOSH.

REFERENCES

1 **OSHA:** Occupational Safety & Health Administration. Pandemic influenza preparedness and response guidance for healthcare workers and healthcare employers. (2007).

2 **CFR:** Code of Federal Regulations Title 42, Part 84. "Respirator Protection"(1995. pp.30382-30383).

3 **NIOSH:** National Institute for Occupational Safety and Health. US DHHS, Public Health Service. "Respiratory Protective Devices; Final Rules and Notices" *Federal Register 60:110, pp. 30335-30393.* (1995).

4 **Bałazy, A., M. Toivola, A. Adhikari, S.K. Sivasubramani, T. Reponen, and S.A. Grinshpun:** Do N95 respirators provide 95% protection level against airborne viruses, and how adequate are surgical masks? *Am. J. Infect. Control* 34(2): 51-57 (2006).

5 **Bałazy, A., M. Toivola, T. Reponen, A. Podgorski, A. Zimmer, and S.A. Grinshpun:** Manikin-Based Performance Evaluation of N95 Filtering-Facepiece Respirators Challenged with Nanoparticles. *Ann. Occup. Hyg.* 50(3): 259-269 (2006).

6 **Eninger, R.M., T. Honda, A. Adhikari, H. Heinonen-Tanski, T. Reponen, and S.A. Grinshpun:** Filter Performance of N99 and N95 Facepiece Respirators Against Viruses and Ultrafine Particles. *Ann. Occup. Hyg.* 52(5): 385-396 (2008).

7 **Grafe, T., M. Gogins, M. Barris, J. Schaefer, and R. Canepa:** "Nanofibers in Filtration Applications in Transportation". *Filtration 2001 Conference Proceedings, Chicago, IL; 1-15* (2001).

8 **Martin, S.B., and E.S. Moyer:** Electrostatic Respirator Filter Media: Filter Efficiency and Most Penetrating Particle Size Effects. *Appl. Occup. Environ. Hyg.* 15(8): 609-617 (2000).

9 **Rengasamy, S., W.P. King, B.C. Eimer, and R.E. Shaffer:** Filtration Performance of NIOSH-Approved N95 and P100 Filtering Facepiece Respirators Against 4 to 30 Nanometer-Size Nanoparticles. *J. Occup. Environ. Hyg.* 5(9): 556-564 (2008).

10 **Cho, K.J., S. Jones, G. Jones, R. McKay, S.A. Grinshpun, A. Dwivedi et al.:** Effect of Particle Size on Respiratory Protection Provided by Two Types of N95 Respirators Used in Agricultural Settings. *J. Occup. Environ. Hyg.* 7(11): 622-627 (2010a).

11 **Zuo, Z., T.H. Kuehn, and D.Y.H. Pui:** Performance evaluation of filtering facepiece respirators using virus aerosols. *Am. J. Infect. Control* 41(1): 80-82 (2013).

12 **Grinshpun, S.A., H. Haruta, R.M. Eninger, T. Reponen, R.T. McKay, and S.A. Lee:** Performance of an N95 filtering facepiece particulate respirator and a surgical mask during human breathing: two pathways for particle penetration. *J. Occup. Environ. Hyg.* 6(10): 593-603 (2009).

13 **Lee, S.A., S.A. Grinshpun, and T. Reponen:** Respiratory performance offered by N95 respirators and surgical masks: human subject evaluation with NaCl aerosol representing bacterial and viral particle size range. *Ann Occup Hyg* 52(3): 177-185 (2008b).

14 **Willeke, K., Y. Qian, J. Donnelly, S. Grinshpun, and V. Ulevicius:** Penetration of Airborne Microorganisms Through a Surgical Mask and a Dust/Mist Respirator. *Am. Ind. Hyg. Assoc. J.* 57(4): 348-355 (1996).

15 **Qian, Y., K. Willeke, S.A. Grinshpun, J. Donnelly, and C.C. Coffey:** Performance of N95 Respirators: Filtration Efficiency for Airborne Microbial and Inert Particles. *Am. Ind. Hyg. Assoc. J.* 59(2): 128-132 (1998).

16 **NIOSH/CDC:** National Institute for Occupational Safety and Health. US DHHS, Public Health Service. "Total Inward Leakage for Half-mask Air-purifying Respirators"(2009).

17 **Collier, L., A. Balows, and M. Sussman:** *Topley and Wilson's Microbiology and Microbial Infections, Volume 1, Virology*: Hodder Arnold Publishers, 1998.

18 **Ksiazek, T.G., D. Erdman, C.S. Goldsmith, S.R. Zaki, T. Peret, S. Emery et al.:** A Novel Coronavirus Associated with Severe Acute Respiratory Syndrome. *N. Engl. J. Med.* 348(20): 1953-1966 (2003).

19 **Mandell, G.L., J.E. Bennett, and R.D. Dolin:** *Principles and practice of infectious diseases*. New York: Churchill Livingstone, 1995.

20 **Kulkarni, P., P.A. Baron, and K. Willeke:** Aerosol Measurement - Principles, Techniques, and Applications, 3rd Edition. *John Wiley & Sons, New Jersey*. (2011).

21 **IOM:** Institute of Medicine. Preparing for an Influenza Pandemic: Personal Protective Equipment for Healthcare Workers(2008).

22 **Sherwood, L.:** Fundamentals of Physiology: A Human Perspective. *Thomson Brooks/Cole, p.380* (2006).

23 **Tortora, G.J., and N.P. Anagnostakos:** Principles of Anatomy and Physiology, 6th edition, New York: Harper-Collins. p.707 (1990).

24 **Roberge, R.J., A. Coca, W.J. Williams, J.B. Powell, and A.J. Palmiero:** Reusable elastomeric air-purifying respirators: Physiologic impact on health care workers. *Am. J. Infect. Control* 38(5): 381-386 (2010).

25 **Cho, K.J., T. Reponen, R. McKay, R. Shukla, H. Haruta, P. Sekar et al.:** Large Particle Penetration through N95 Respirator Filters and Facepiece Leaks with Cyclic Flow. *Ann. Occup. Hyg.* 54(1): 68-77 (2010b).

26 **Eshbaugh, J.P., P.D. Gardner, A.W. Richardson, and K.C. Hofacre:** N95 and P100 Respirator Filter Efficiency Under High Constant and Cyclic Flow. *J. Occup. Environ. Hyg.* 6(1): 52-61 (2008).

27 **Haruta, H., T. Honda, R.M. Eninger, T. Reponen, R. McKay, and S.A. Grinshpun:** Experimental and theoretical investigation of the performance of N95 respirator filters against ultrafine aerosol particles tested at constant and cyclic flows. *J. Int. Soc. Resp. Prot.* 25: 75-88 (2008).

28 **Myers, W.R., H. Kim, and N. Kadrichu:** Effect of particle size on assessment of faceseal leakage. *J. Int. Soc. Resp. Prot.* (9): 6-21 (1991).

29 **He, X., S.A. Grinshpun, T. Reponen, R. McKay, S.M. Bergman, and Z. Zhuang:** Effect of Breathing Frequency on the Total Inward Leakage of an Elastomeric Half-Mask Donned on an Advanced Manikin Headform. *Submitted to the Annals of Occupational Hygiene* (2013c).

30 **Bergman, M.S., Z. Zhuang, J. Wander, D. Hanson, B.K. Heimbuch, M. McDonald et al.:** Development of an Advanced Respirator Fit Test Headform. *(To be submitted)* (2013).

31 **Hanson, D., R. Bergs, Y. Tadesse, V. White, and S. Priya:** Enhancement of EAP Actuated Facial Expressions by Designed Chamber Geometry in Elastomers. Proc. SPIE's Electroactive Polymer Actuators and Devices Conf., 10th Smart Structures and Materials Symposium, San Diego(2006).

32 **He, X., S.A. Grinshpun, T. Reponen, M. Yermakov, R. McKay, H. Haruta et al.:** Laboratory Evaluation of the Particle Size Effect on the Performance of an Elastomeric Half-mask Respirator against Ultrafine Combustion Particles. (Accepted). *Ann. Occup. Hyg.* (2013a).

33 **He, X., M. Yermakov, T. Reponen, R. McKay, K. James, and S.A. Grinshpun:** Manikin-based performance evaluation of elastomeric respirators against combustion particles. *J. Environ. Occup. Hyg.* 10: 203-212 (2013b).

34 **Chen, C.C., J. Ruuskanen, W. Pilacinski, and K. Willeke:** Filter and leak penetration characteristics of a dust and mist filtering facepiece. *Am. Ind. Hyg. Assoc. J.* 51(12): 632-639 (1990).

35 **Huang, S.-H., C.-W. Chen, C.-P. Chang, C.-Y. Lai, and C.-C. Chen:** Penetration of 4.5 nm to aerosol particles through fibrous filters. *J. Aerosol. Sci.* 38(7): 719-727 (2007).

36 **Rengasamy, S., and B.C. Eimer:** Total Inward Leakage of Nanoparticles Through Filtering Facepiece Respirators. *Ann. Occup. Hyg.* 55(3): 253-263 (2011).

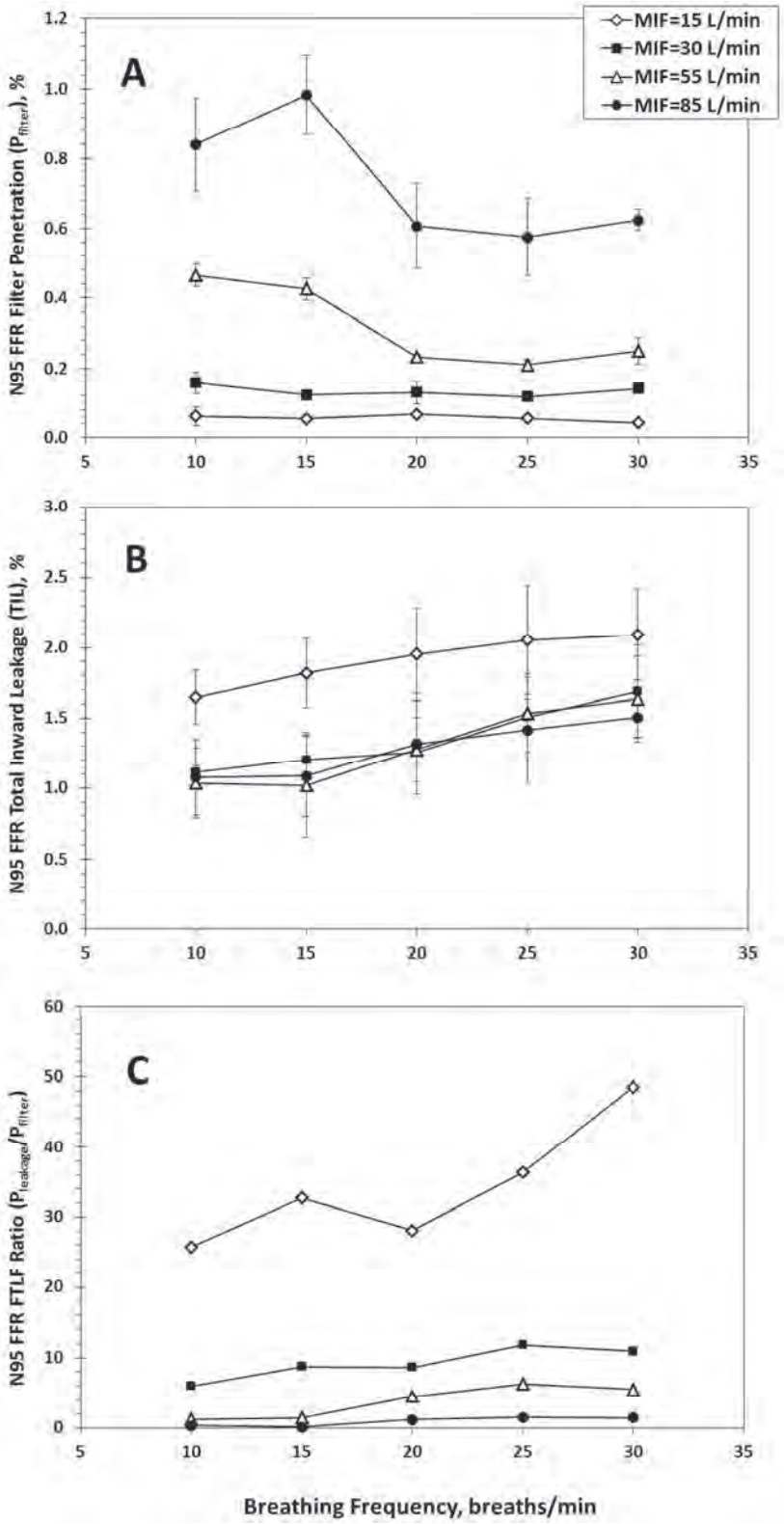

Fig 1. Filter penetration (A), Total Inward Leakage (TIL) (B), and faceseal leakage-to-filter (*FLTF*) ratio (C) for an N95 FFR sealed to a plastic manikin's face. No error bars for *FLTF* ratio as it was calculated from the mean $P_{leakage}$ (over 3 replicates) divided by the mean P_{filter} (over 3 replicates).

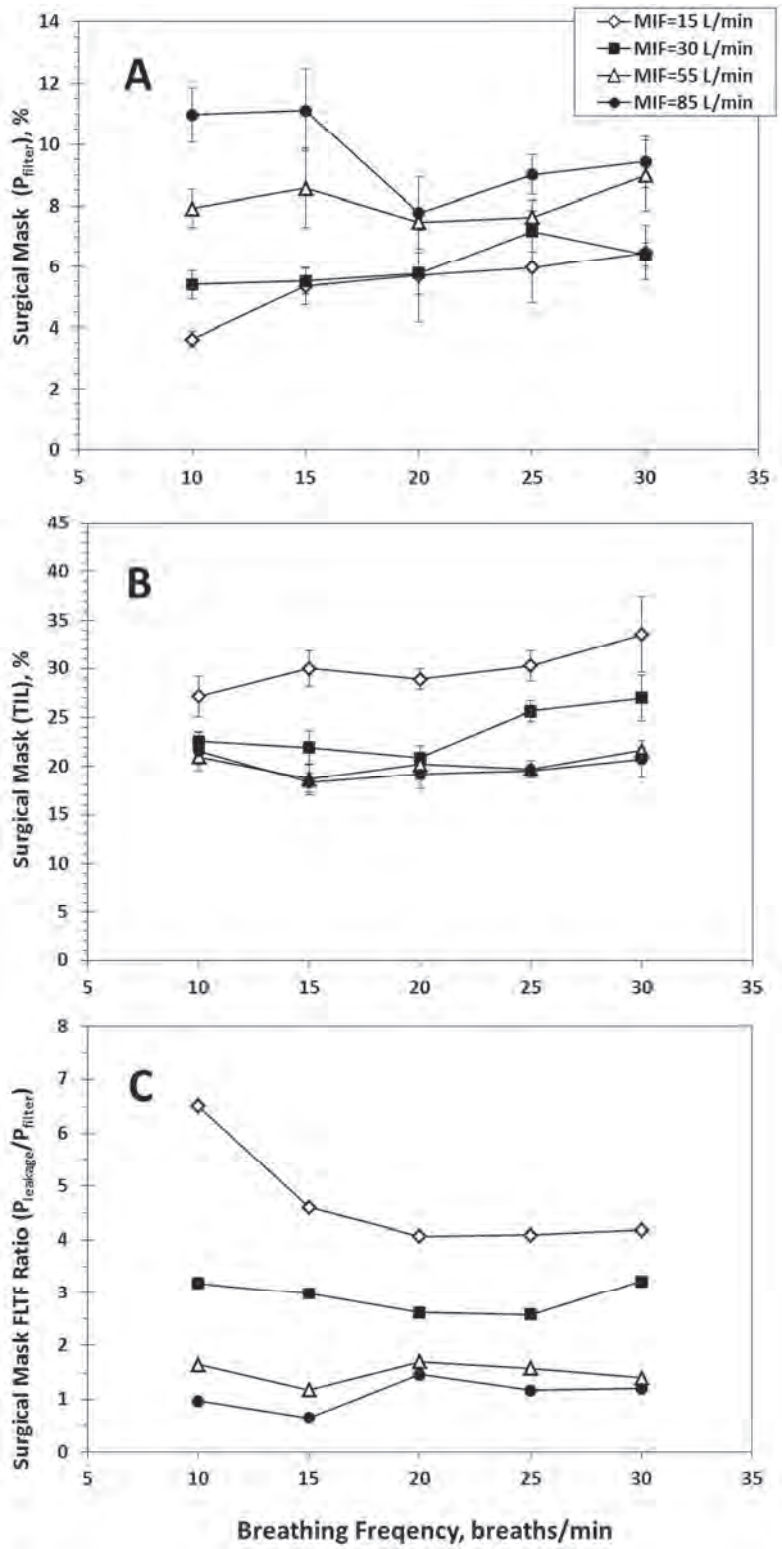

Fig 2. Filter penetration (A), Total Inward Leakage TIL (B), and faceseal leakage-to-filter (*FLTF*) ratio (C) for a surgical mask sealed to a plastic manikin's face. No error bars for *FLTF* ratio as it was calculated from the mean $P_{leakage}$ (over 3 replicates) divided by the mean P_{filter} (over 3 replicates).

TABLE I. Pairwise multiple comparisons for mean P_{filter} values among four MIFs and five breathing frequency groups (ANOVA with Tukey's range test) for an N95 FFR

Effect of MIF on P_{filter}				Effect of Breathing Frequency on P_{filter}			
MIF (L/min)	Tukey Grouping[a]	Mean[b] P_{filter} (%)	*p*-value[c]	Breathing Frequency (breaths/min)	Tukey Grouping[a]	Mean[b] P_{filter} (%)	*p*-value[d]
15	D	0.05	<0.0001	10	0.38	I	<0.0001
30	C	0.13		15	0.39	I	
55	B	0.31		20	0.25	II	
85	A	0.72		25	0.23	II	
				30	0.26	II	

a: Within each group of the MIF or the breathing frequency, means with the same letter are not significantly different (*p*-value > 0.05).
b: Calculated using the size-independent (overall) P_{filter} values.
c: *P*-values were obtained from the two-way ANOVA performed to examine the effect of the MIF on the filter penetration.
d: *P*-values were obtained from the two-way ANOVA performed to examine the effect of the breathing frequency on the filter penetration.

TABLE II. Pairwise multiple comparisons for mean TIL values among four MIFs and five breathing frequency groups (ANOVA with Tukey's range test) for an N95 FFR

Effect of MIF on TIL				Effect of Breathing Frequency TIL			
MIF (L/min)	Tukey Grouping[a]	Mean[b] TIL (%)	*p*-value[c]	Breathing Frequency (breaths/min)	Tukey Grouping[a]	Mean[b] TIL (%)	*p*-value[d]
15	A	1.93	0.0019	10	II	1.22	0.0025
30	B	1.37		15	II	1.28	
55	B	1.31		20	I II	1.45	
85	B	1.29		25	I II	1.63	
				30	I	1.73	

a: Within each group of the MIF or the breathing frequency, means with the same letter are not significantly different (p-value > 0.05).
b: Calculated using the size-independent (overall) TIL values.
c: *P*-values were obtained from the two-way ANOVA performed to examine the effect of the MIF on the TIL.
d: *P*-values were obtained from the two-way ANOVA performed to examine the effect of the breathing frequency on the TIL.

TABLE III. Pairwise multiple comparisons for mean P_{filter} values among four MIFs and five breathing frequency groups (ANOVA with Tukey's range test) for a surgical mask

Effect of MIF on P_{filter}				Effect of Breathing Frequency on P_{filter}			
MIF (L/min)	Tukey Grouping[a]	Mean[b] P_{filter} (%)	*p*-value[c]	Breathing Frequency (breaths/min)	Tukey Grouping[a]	Mean[b] P_{filter} (%)	*p*-value[d]
15	C	5.41	<0.0001	10	I II	6.97	<0.0143
30	C	6.04		15	I II	7.63	
55	B	8.11		20	II	6.67	
85	A	9.65		25	I II	7.43	
				30	I	7.81	

a: Within each group of the MIF or the breathing frequency, means with the same letter are not significantly different (*p*-value > 0.05).
b: Calculated using the size-independent (overall) P_{filter} values.
c: *P*-values were obtained from the two-way ANOVA performed to examine the effect of the MIF on the filter penetration.
d: *P*-values were obtained from the two-way ANOVA performed to examine the effect of the breathing frequency on the filter penetration.

TABLE IV. Pairwise multiple comparisons for mean TIL values among four MIFs and five breathing frequency groups (ANOVA with Tukey's range test) for a surgical mask

Effect of MIF on TIL				Effect of Breathing Frequency TIL			
MIF (L/min)	Tukey Grouping[a]	Mean[b] TIL (%)	*p*-value[c]	Breathing Frequency (breaths/min)	Tukey Grouping[a]	Mean[b] TIL (%)	*p*-value[d]
15	A	1.93	0.0019	10	I II	23.1	0.0316
30	B	1.37		15	II	22.2	
55	B	1.31		20	I II	22.3	
85	B	1.29		25	I II	23.8	
				30	I	25.7	

a: Within each group of the MIF or the breathing frequency, means with the same letter are not significantly different (*p*-value > 0.05).
b: Calculated using the size-independent (overall) TIL values.
c: *P*-values were obtained from the two-way ANOVA performed to examine the effect of the MIF on the TIL.
d: *P*-values were obtained from the two-way ANOVA performed to examine the effect of the breathing frequency on the TIL.

Effect of Particle Size on the Performance of an N95 Filtering Facepiece Respirator and a Surgical Mask at Various Breathing Conditions

Journal:	*Aerosol Science & Technology*
Manuscript ID:	AST-MS-2013-110
Manuscript Type:	Original Manuscript
Date Submitted by the Author:	26-May-2013
Complete List of Authors:	Grinshpun, Sergey; University of Cincinnati, Dept of Environmental Health; He, Xinjian; University of Cincinnati, Dept of Environmental Health Reponen, Tiina; University of Cincinnati, Dept of Environmental Health McKay, Roy; University of Cincinnati, Dept of Environmental Health
Keywords:	respirator, filter, total inward leakage, breathing frequency, particle size

Effect of Particle Size on the Performance of an N95 Filtering Facepiece Respirator and a Surgical Mask at Various Breathing Conditions

Xinjian He, Tiina Reponen, Roy T. McKay, and Sergey A. Grinshpun*

Center for Health-Related Aerosol Studies, Department of Environmental Health, University of Cincinnati, Cincinnati, OH

Keywords: respirator, filter, total inward leakage, breathing frequency, particle size

To be submitted to the

Aerosol Science and Technology

May 26, 2013

Corresponding author: Sergey A. Grinshpun: sergey.grinshpun@uc.edu

ABSTRACT

The effect of aerosol particle size on the performance of an N95 filtering facepiece respirator (FFR) and a surgical mask (SM) was evaluated under different breathing conditions, including breathing frequency and mean inspiratory flow (MIF) rate. The FFR and SM were sealed on a manikin headform and challenged to charge-equilibrated NaCl aerosol. Filter penetration (P_{filter}) was determined as the ratio of aerosol concentrations inside and outside the FFR/SM size-selectively (28 channels) within a range of 20 to 500 nm. In addition, the same models of the FFR and SM were donned, but not sealed, on an advanced manikin headform covered with skin-like material. Total inward leakage (TIL), which represents the total particle penetration, was measured under conditions identical to the filter penetration experiment. Testing was conducted at four mean MIFs (15, 30, 55 and 85 L/min) combined with five breathing frequencies (10, 15, 20, 25 and 30 breaths/min). P_{filter} was significantly affected by particle size and breathing flow rate (p <0.05) for the tested FFR and SM. Surprisingly, for both respiratory protection devices, P_{filter} as a function of the particle size exhibited more than one peak under all tested breathing conditions. The effect of breathing frequency on P_{filter} was generally less pronounced, especially for lower MIFs. For the FFR and SM, TIL increased with increasing particle size up to about 50 nm; for particles above 50 nm, the total penetration was not significantly affected by particle size and breathing frequency; however, the effect of MIF remained significant.

INTRODUCTION

N95 filtering facepiece respirators (FFRs) are commonly used to prevent occupational aerosol exposures. When certified by the National Institute for Occupational Safety and Health (NIOSH), N95 filters have a collection efficiency of at least 95% when tested against non-oil particles (e.g., NaCl) having a count median diameter (CMD) of 75±20 nm with a geometric standard deviation (GSD) of <1.86 and a mass median aerodynamic diameter of ~300 nm (NIOSH 1995). Presently, the vast majority of FFRs are manufactured utilizing electrostatic fibers to enhance filter efficiency and, at the same time, reduce breathing resistance. Studies have reported that the most penetrating particle size (MPPS) for N95 FFRs ranges from 30 to 100 nm (Bałazy et al. 2006a; 2006b; Cho et al. 2010a; Eninger et al. 2008; Grafe et al. 2001; Martin et al. 2000; Rengasamy et al. 2008: Shaffer and Rengasamy 2009). Surgical masks (SMs) have a different intended purpose, and were originally designed to reduce bioaerosol dissemination from the wearer rather than to control wearer's exposure to ambient aerosols. Previous research have demonstrated that the filter efficiency for SMs is much lower than that for N95 FFRs (Bałazy et al. 2006a; Grinshpun et al. 2009; Lee et al. 2008b; Willeke et al. 1996).

The protection offered by an undamaged negative pressure air purifying device (including N95 FFR and SM) depends on two principle factors: filter penetration (P_{filter}) and faceseal leakage ($P_{leakage}$) (Cho et al. 2010b; Grinshpun et al. 2009; Zhuang et al. 1998). The efficiency of respirator filter media has been assessed in several previous studies by measuring the aerosol concentration inside and outside of the FFR/SM while it was sealed to a manikin headform using constant or cyclic breathing flow (Bałazy et al. 2006b; Cho et al. 2010b; He et al. 2013d; Rengasamy et al. 2011; Richardson et al. 2007). To simulate faceseal leakage, artificially

created slit-like or circular leaks have been commonly used in manikin-based respiratory protection research (Chen et al. 1992; Hinds et al. 1987; Myers et al. 1991; Rengasamy et al. 2011). The limitation of most of the previous manikin-based faceseal leakage studies was that the headforms had rigid surfaces, which were unable to simulate the characteristics of the human skin. Ideally, it would be preferred to measure faceseal leakage while the respiratory protection device is donned on a human subject, not a manikin. However, respirator testing using humans has its own limitations, most importantly, the subjects cannot be exposed to hazardous aerosol challenges and it is impossible to maintain a constant leak size, shape, mean inspiratory flow (MIF), and breathing frequency (Wander et al. 2012). To partially address this limitation, an advanced manikin headform was recently developed with capabilities of mimicking the softness and thicknesses of the human skin (Bergman et al. 2013; Hanson et al. 2006).

Manikin-based respirator testing protocols using cyclic flow (as opposite to constant flow) produce data that more closely represents actual respirator use conditions. While evaluating respirators with cyclic flow, breathing frequency (breaths/min) and flow rate (L/min) should be tested as these two factors vary between populations (e.g., body size, age, health, etc.). Numerous studies have been conducted to evaluate effects of breathing flow rate and particle size on the performance of respiratory protection devices (Bałazy et al. 2006a; Bałazy et al. 2006b; Chen et al. 1990; Cho et al. 2010a; Eninger et al. 2008; He et al. 2013d; Lee et al. 2008b; Martin et al. 2000; Myers et al. 1991; Rengasamy et al. 2008). In contrast, the breathing frequency has been addressed only in a few investigations. One study (Wang et al. 2012) presented data only for two values, 32 and 50 breaths/min (which likely exceeds the breathing frequency for most worker populations that wear N95 FFRs and SMs) and a single MIF rate of 100 L/min (which is also higher than observed at nearly all workplace use conditions). Another

investigation by our team evaluated the performance of an elastomeric half-mask respirator at different breathing frequencies, but not N95 FFRs and SMs (He et al. 2013a).

The present study is a follow-up to our recent effort in which the effect of breathing frequency on the performance of an N95 FFR and SM was examined particle-size-independently (He et al. 2013c). The experimental design used in the present study includes particle size as the main independent variable when testing the FFR/SM under various breathing conditions.

MATERIALS AND METHODS

Tested N95 FFR and Surgical Mask

A widely used, commercially available N95 FFR having three layers with the middle being electrically charged to enhance the filter capture efficiency was chosen for this study. A conventional fluid resistant SM capable of providing at least 95% filter efficiency for 100 nm particles (according to the manufacturer) was also tested. To allow comparison with previous studies by our team, the selected FFR and SM was the same make and model as used previously (He et al. 2013c). To evaluate filter efficiency, the FFR/SM was fully sealed on a hard plastic manikin headform. The outcome of this experiment is not dependent on the properties of the manikin surface as long as a perfect sealing is achieved, which was confirmed using an air bubble detector. Additionally, the tested FFR/SM was donned on an advanced manikin headform without seal for the purpose of the Total Inward Leakage (TIL = $P_{filter} + P_{leakage}$) testing. As the TIL depends on the headform surface properties (i.e., faceseal leakage), the advanced manikin with skin-like surface properties was utilized. After 20 consecutive tests, the FFR/SM was replaced with a brand new one to minimize the effect of the challenge aerosol loading on the filter media. Following each replacement, the particle concentrations inside and outside the

FFR/SM were assessed to assure that the size of the leak was consistent with the one that existed before the change under the same experimental conditions. In addition, paired t-tests were performed to study the donning effect between the first 20 tests (before changing the FFR/SM) and the next 20 tests (after changing the FFR/SM), and the results showed that this effect was not significant (p >0.05).

Experimental Design and Test Conditions

The experiments were carried out in a room-size (24.3 m^3) respirator test chamber. The experimental set-up was described in detail elsewhere (He et al. 2013c). In brief, NaCl particles (CMD = 125 nm, GSD = 1.68) generated with a particle generator (Model: 8026, TSI Inc., Shoreview, MN, USA) were first charge-equilibrated by passing through a ^{85}Kr electrical charge equilibrator (Model: 3054, TSI Inc., Shoreview, MN, USA) and then released into the test chamber. The headform with FFR/SM (either sealed in a filter penetration test, or donned in a total penetration test), was connected to a Breathing Recording and Simulation System (BRSS, Koken Ltd., Tokyo, Japan). To keep particles from re-entering into the respirator cavity during exhalation cycles, a HEPA filter was placed between the headform and the BRSS. Prior to each experiment, the particle generator operated for at least one hour to allow a uniform NaCl concentration inside the chamber, and continued operating during the testing to maintain a stable concentration level. Temperature and relative humidity inside the chamber were kept at 17–22 ℃ and 30–60 %, respectively.

Cyclic breathing flows with MIF rates of 15, 30, 55 and 85 L/min and breathing frequencies of 10, 15, 20, 25 and 30 breaths/min were examined (total of 20 combinations). Each combination was tested in three replicates. Particle size-specific concentrations inside ($C_{\mathrm{in}\_d_\mathrm{p}}$)

and outside ($C_{\text{out}\_d_p}$) of the FFR/SM were measured using a nanoparticle spectrometer (Nano-ID NPS500, Naneum Ltd., Kent, UK) operating in 28 channels within a range of d_p = 20 – 500 nm at a sampling flow rate of 0.2 L/min. Each particle size-specific concentration ($C_{\text{in}\_d_p}$ or $C_{\text{out}\_d_p}$) was determined based on a 6-min sampling.

For each particle size, the filter penetration ($P_{\text{filter}\_d_p}$) was determined as the ratio of the corresponding size-specific concentrations inside ($C_{in\_d_p(Sealed)}$) and outside ($C_{out\_d_p(Sealed)}$) of the FFR/SM sealed to the plastic headform:

$$P_{filter\_d_p} = \frac{C_{in\_d_p(Sealed)}}{C_{out\_d_p(Sealed)}} \times 100\% \quad \textbf{(1)}$$

The same experimental protocol and test conditions were used with FFR/SM donned (not sealed) on the advanced manikin headform for TIL measurements. Accordingly, the size-specific TIL values were determined as follows:

$$TIL_{d_p} = \frac{C_{in\_d_p(Donned)}}{C_{out\_d_p(Donned)}} \times 100\% \quad \textbf{(2)}$$

Data analysis

Statistical data analysis was conducted using SAS version 9.3 (SAS Institute Inc., Cary, NC). Three-way Analysis of Variance (ANOVA) was performed to study the effects of particle size, breathing frequency, and flow rate on the P_{filter} and TIL separately. A t-test was used to examine the differences in P_{filter} and TIL between the N95 FFR and the SM. For all data analyses, $p < 0.05$ represented significance.

RESULTS AND DISCUSSION

1. N95 Filtering Facepiece Respirator

N95 FFR Filter Penetration ($P_{filter\_d_p}$)

Figure 1 presents the size-specific $P_{filter\_d_p}$ values for the tested N95 FFR. It is seen that filter penetration increased with increasing MIF (p <0.05), which is consistent with the results of many previous N95 FFR studies (Bałazy et al. 2006b; Cho et al. 2010a; Eninger et al. 2008; He et al. 2013a; Rengasamy et al. 2008).

Particle size had a significant effect on the $P_{filter\_d_p}$ (p <0.05). Interestingly, all the filter penetration curves show two peaks for all MIFs and breathing frequencies, indicating two possible MPPS for the tested N95 FFR. The first MPPS occurred at 30–40 nm, which was expected for N95 FFRs composed of electrically charged fibers. Several studies have reported that the MPPS for a N95 FFR "electret" filter is < 100 nm while a "mechanical" filter has a MPPS of approximately 300 nm (Bałazy et al. 2006a; Bałazy et al. 2006b; Eninger et al. 2008; Huang et al. 2007; Martin et al. 2000; Rengasamy et al. 2009). The second MPPS identified at ~300 nm (Figure 1) was not reported in any of the above quoted studies. One reason is that the quoted investigations utilized a constant flow design, whereas the present effort represents a cyclic flow condition. It is possible that under the cyclic flow some particles are trapped inside the respirator cavity. This phenomenon "artificially" increases the particle count inside the FFR, thus affecting the filter penetration calculated by Eq. (1). The effect is expected to be particularly pronounced at low $C_{out\_d_p}$. The tested aerosol is characterized by a rapidly decreasing concentration in the particle size range of 200 to 400 nm – the area where the second

peak was identified (Figure 1). The other possible reason of the observed departure of $P_{filter} = f(d_p)$ from the conventional single-mode function could be associated with a three-layer filter structure of the tested N95 FFR of which only the middle layer was electrostatically charged. The combination of electrostatic (the middle layer) and mechanical (the two outer layers) characteristics may produce a compound penetration function involving particle diffusion, polarization force, interception and impaction, which is capable of generating two peaks.

The effect of breathing frequency on filter penetration was complex and heavily dependent on the particle size and the MIF. This effect was most clearly seen for particles around the MPPS (Figure 1). For example, at the first MPPS (30 – 40 nm) the lower breathing frequencies (10, 15 and 20 breaths/min) produced higher penetration values for MIF = 15, 55 and 85, but not for 30 L/min. It is hard to differentiate the breathing frequency effect on the penetration at the second MPPS at 200 – 300 nm for all four MIFs. Such complexity of breathing frequency effect was also reported in our recent investigation that utilized an elastomeric half-mask respirator equipped with P100 filters (He et al. 2013a). As expected, the N95 FFR had P_{filter} below 5% for any particle size, breathing frequency, and MIF tested in the present study.

N95 FFR Total Inward Leakage (TIL_{d_p})

The size-specific TIL results for the tested N95 FFR donned on an advanced manikin headform are presented in Figure 2. The TIL_{d_p} increased as the particle size increased from 20 to ~50 nm regardless of the MIF and the breathing frequency, which is consistent with the fact that the diffusional deposition effect is stronger for smaller particles. However, at the particle size of ~50 nm, the TIL_{d_p} curves reached a plateau. The effect of particle size on the TIL_{d_p} was not significant (p >0.05) for particles larger than 50 nm for any MIF and breathing frequency used in

this study. One possible reason is that the penetration through the faceseal leakage (unlike the filter media) is not very sensitive to the particle size. Once the particles are large enough (for a typical leakage dimension, the estimated size must be above 40 – 70 nm) to have a low diffusional deposition efficiency (Kulkarni et al. 2011), their penetration through the faceseal leak is essentially particle size independent in a wide size range. This differs from P_{filter}, which is influenced by other particle deposition mechanisms. As seen from the data presented in Figures 1 and 2, TIL values are at least 10- fold greater than P_{filter} results. This suggests that the leakage represents the major penetration pathway and thus has the major effect on the TIL, which explains the lack of its particle size dependence at > 50 nm. This finding is consistent with the conclusion of our recent study in which the performance of an elastomeric respirator was examined while it was donned on the same advanced manikin headform (He et al. 2013a). Little information is available about the MPPS for faceseal leakage of N95 FFRs. One investigation that determined the MPPS for N95 FFRs with artificially created leaks, reported MPPS ~50 nm for leak diameters as small as < 1.65 mm (Rengasamy et al. 2011). Experimental protocols with artificial faceseal leaks have a number of limitations because (i) the outcome may be dependent not only on the leak size but factors such as the leak shape, location and others unaccounted for and (ii) in reality, the leak is continuously changing as a wearer is breathing, talking and moving.

Statistical analysis showed that increasing MIF was associated with a decrease in TIL_{d_p} (p <0.05). Other FFR performance studies have reported decreased inward leakage with increasing the breathing flow (Cho et al. 2010b; He et al. 2013c; Rengasamy et al. 2011). As communicated earlier, a possible explanation is that higher MIF creates a greater negative pressure during the inspiratory cycle that pulls the facepiece towards the manikin surface with a

reduction in leak size (Richardson et al. 2007). This may be particularly evident when testing with the advanced manikin headform with simulated soft skin.

Surgical Mask

SM Filter Penetration ($P_{filter\_d_p}$)

The filter penetration ($P_{filter\_d_p}$) results for the tested SM are presented in Figure 3. Compared to the N95 FFR, the SM had a much higher filter penetration (p <0.05), which is expected given its primary function to protect others from the aerosol exhaled by the wearer. Previous studies have reported that a typical SM provided much lower protection than a N95 FFR when challenged with biological or non-biological particles (Bałazy et al. 2006a; Chen et al. 1990; Grinshpun et al. 2009; He et al. 2013c; Lee et al. 2008b; Willeke et al. 1996). It is also evident from Figure 3 that the filter penetration curves deviate from a single-peak function expected from a conventional mechanical filter. Similar to the interpretation offered above for the N95 FFR, we attribute this difference to cyclic flow tested in this study compared to constant flow utilized by other researchers. No previous study has reported a multiple P_{filter} peaks for SMs. In the current investigation, three peaks were observed for P_{filter}: at ~30, ~100 and ~300 nm. The most prominent MPPS was ~300 nm for all MIFs and breathing frequencies. This is much higher than the most prominent MPPS obtained for the N95 FFR (30 – 40 nm). The latter is consistent with the fact that the tested SM had a mechanical filter with no electrically charged fibers (or the charges were negligible). These filters are known for their relatively low-efficiency and MPPS of ~300 nm.

As evident from Figure 3, the curves corresponding to different breathing frequencies were not distinct for MIF = 15 and 30 L/min and largely also for 55 L/min; the curve separation

suggests that a more prominent effect of breathing frequency was observed at 85 L/min with the 10 and 15 breaths/min producing higher $P_{filter\_d_p}$ values and 20 breaths/min generating the lowest $P_{filter\_d_p}$ curve. This suggests that the MPPS was not directly affected by the MIF and the breathing frequency.

Although the SM model chosen for this study is expected to provide at least 95% filter efficiency for particles of 100 nm (according to its manufacturer, no flow rate is specified), Figure 3 shows that the filter penetration of 100 nm particles was > 5% at various breathing frequencies, especially when MIFs ≥ 55 L/min. This finding suggests that the tested SM may not provide the expected filter efficiency at higher breathing flows. Particles of 100-400 nm penetrated through the SM filter more readily. From this perspective, the 100 nm size used by the manufacturer as a reference point does not seem appropriate unless the SM is deployed specifically against ≤ 100 nm particles.

SM Total Inward Leakage (TIL_{d_p})

Figure 4 presents the total particle penetration data for the SM. Similar to N95 FFR, the TIL_{d_p} of the SM increased rapidly with the particle diameter increasing up to 30 – 50 nm, but then its dependence on d_p became less pronounced (p >0.05). TIL_{d_p} was not significantly affected by breathing frequency (p >0.05) but had slightly different patterns at different MIFs. For particles >30 nm, a slow increase was observed at the lowest MIF (15 L/min), but this gradually leveled off as MIF increased to 85 L/min. This suggests a wide range of sizes producing essentially the same TIL (approximately 20% at MIF=85 L/min). It is also noticed that the variability in the total penetration obtained for the SM was lower than that for the N95 FFR. The total particle penetration into the SM was about 10-fold greater than the penetration into the FFR,

which means that the particle count inside the N95 FFR was an order of magnitude lower than that inside the SM (given that C_{out} is the same). Lower count is usually associated with higher variability, which explains our finding. To our knowledge, no published study has reported the TIL's MPPS for surgical masks. Even though SMs are not rated high as personal respiratory protective devices, there are many circumstances where SMs are used to reduce human exposure to hazardous aerosols. In fact, the use of SMs as personal protective devices world-wide likely exceeds the use of N95 FFRs. Given that the size of most infectious airborne virions (Collier et al. 1998), diesel particles (Castranova et al. 2001), combustion particles generated from fire smoke (He et al. 2013b), and other hazardous aerosols falls into the above-indicated range (20 – 500 nm), the data suggest that the tested SM may not be able to provide substantial protection against these particles at any relevant combination of the breathing frequency and flow rate.

CONCLUSIONS

For the tested N95 FFR and SM, the filter penetration was significantly affected by the particle size and breathing flow rate, whereas the breathing frequency effect on P_{filter} was generally less pronounced and less important from the practical viewpoint, especially for lower MIFs. Surprisingly, the P_{filter} curves had two peaks for the tested N95 FFR and three peaks for the SM, which has not been reported in previous respirator filter studies (it is noted that these studies implemented a constant flow test protocol). Consequently, using data from a single MPPS may not always be representative of the filter performance, especially if the tested respirator is intended to be deployed against particles of a wide size range.

For the FFR and SM, the total penetration increased with increasing particle size up to ~50 nm; when challenged with particles greater than 50 nm, only the breathing flow rate

remained a significant factor affecting the TIL, whereas the influence of particle size and breathing frequency was not significant. Increasing the MIF increased the filter penetration, but decreased the total penetration for both the FFR and SM. The SM produced much higher P_{filter} and TIL values than the N95 FFR, and the predominant MPPS was also higher for the SM (~300 nm) than for the N95 FFR (30 – 40 nm). The results suggest that the tested SM may not be able to provide substantial protection against aerosol particles at least up to ~500 nm at any relevant combination of the breathing frequency and flow rate.

ACKNOWLEDGEMENT

This research was supported by the NIOSH Targeted Research Training Program and Pilot Research Project Training Program (University of Cincinnati, Education and Research Center, Grant T42/OH008432). The advanced manikin headform was provided by Mr. Michael S. Bergman, and Dr. Ziqing Zhuang of NIOSH (Pittsburgh, PA, USA). The Breathing Recording and Simulation System was made available courtesy of Koken Ltd. (Tokyo, Japan)

REFERENCES

Bałazy, A., Toivola, M., Adhikari, A., Sivasubramani, S. K., Reponen, T. and Grinshpun, S. A. (2006a). Do N95 respirators provide 95% protection level against airborne viruses, and how adequate are surgical masks? *Am. J. Infect. Control* 34:51-57.

Bałazy, A., Toivola, M., Reponen, T., Podgorski, A., Zimmer, A. and Grinshpun, S. A. (2006b). Manikin-based performance evaluation of N95 filtering-facepiece respirators challenged with nanoparticles. *Ann. Occup. Hyg.* 50:259-269.

Bergman, M. S., Zhuang, Z., Wander, J., Hanson, D., Heimbuch, B. K., McDonald, M., Palmiero, A., Shaffer, R. E. and Husband, M. (2013). Development of an advanced respirator fit test headform. *(Submitted)*.

Castranova, V., Ma, J., Yang, H.-M., Antonini, J. M., Butterworth, L., Barger, M. W., Roberts, J. and Ma, J. (2001). Effect of exposure to diesel exhaust particles on the susceptibility of the lung to infection. *Environ. Health Perspect.* 109:609.

Chen, C. C., Ruuskanen, J., Pilacinski, W. and Willeke, K. (1990). Filter and leak penetration characteristics of a dust and mist filtering facepiece. *Am. Ind. Hyg. Assoc. J.* 51:632-639.

Chen, C. C. and Willeke, K. (1992). Characteristics of face seal leakage in filtering facepieces. *Am. Ind. Hyg. Assoc. J.* 53:533-539.

Cho, K. J., Jones, S., Jones, G., McKay, R., Grinshpun, S. A., Dwivedi, A., Shukla, R., Singh, U. and Reponen, T. (2010a). Effect of particle size on respiratory protection provided by two types of N95 respirators used in agricultural settings. *J. Occup. Environ. Hyg.* 7:622-627.

Cho, K. J., Reponen, T., McKay, R., Shukla, R., Haruta, H., Sekar, P. and Grinshpun, S. A. (2010b). Large particle penetration through N95 respirator filters and facepiece leaks with cyclic flow. *Ann. Occup. Hyg.* 54:68-77.

Collier, L., Balows, A. and Sussman, M. (1998). *Topley and Wilson's Microbiology and Microbial Infections, Volume 1, Virology*. Hodder Arnold Publishers.

Eninger, R. M., Honda, T., Adhikari, A., Heinonen-Tanski, H., Reponen, T. and Grinshpun, S. A. (2008). Filter performance of N99 and N95 facepiece respirators against viruses and ultrafine particles. *Ann. Occup. Hyg.* 52:385-396.

Grafe, T., Gogins, M., Barris, M., Schaefer, J. and Canepa, R. (2001). "Nanofibers in Filtration Applications in Transportation". *Filtration 2001 Conference Proceedings, Chicago, IL; 1-15*.

Grinshpun, S. A., Haruta, H., Eninger, R. M., Reponen, T., McKay, R. T. and Lee, S.-A. (2009). Performance of an N95 filtering facepiece particulate respirator and a surgical mask during human breathing: two pathways for particle penetration. *J. Occup. Environ. Hyg.* 6:593-603.

Hanson, D., Bergs, R., Tadesse, Y., White, V. and Priya, S. (2006). Enhancement of EAP Actuated Facial Expressions by Designed Chamber Geometry in Elastomers. Proc. SPIE's Electroactive Polymer Actuators and Devices Conf., 10th Smart Structures and Materials Symposium, San Diego.

He, X., Grinshpun, S. A., Reponen, T., McKay, R., Bergman, S. M. and Zhuang, Z. (2013a). Effect of breathing frequency on the total inward leakage of an elastomeric half-mask donned on an advanced manikin headform. *Submitted to the Annals of Occupational Hygiene*.

He, X., Grinshpun, S. A., Reponen, T., Yermakov, M., McKay, R., Haruta, H. and Kimura, K. (2013b). Laboratory evaluation of the particle size effect on the performance of an elastomeric half-mask respirator against ultrafine combustion particles. (Accepted). *Ann. Occup. Hyg.*

He, X., Reponen, T., McKay, R. and Grinshpun, S. A. (2013c). How does breathing frequency affect the performance of an N95 filtering facepiece respirator and a surgical mask against surrogates of viral particles? (Submitted) *J. Occup. Environ. Hyg.*

He, X., Yermakov, M., Reponen, T., McKay, R., James, K. and Grinshpun, S. A. (2013d). Manikin-based performance evaluation of elastomeric respirators against combustion particles. *J. Environ. Occup. Hyg.* 10:203-212.

Hinds, W. C. and Bellin, P. (1987). Performance of dust respirators with facial seal leaks: II. Predictive model. *Am. Ind. Hyg. Assoc. J.* 48:842-847.

Huang, S.-H., Chen, C.-W., Chang, C.-P., Lai, C.-Y. and Chen, C.-C. (2007). Penetration of 4.5 nm to aerosol particles through fibrous filters. *J. Aerosol. Sci.* 38:719-727.

Kulkarni, P., Baron, P. A. and Willeke, K. (2011). Aerosol Measurement - Principles, Techniques, and Applications, 3rd Edition. *John Wiley & Sons, New Jersey.*

Lee, S. A., Grinshpun, S. A. and Reponen, T. (2008b). Respiratory performance offered by N95 respirators and surgical masks: human subject evaluation with NaCl aerosol representing bacterial and viral particle size range. *Ann Occup Hyg* 52:177-185.

Martin, S. B. and Moyer, E. S. (2000). Electrostatic respirator filter media: filter efficiency and most penetrating particle size effects. *Appl. Occup. Environ. Hyg.* 15:609-617.

Myers, W. R., Kim, H. and Kadrichu, N. (1991). Effect of particle size on assessment of faceseal leakage. *J. Int. Soc. Resp. Prot.*:6-21.

NIOSH (1995). National Institute for Occupational Safety and Health. US DHHS, Public Health Service. "Respiratory Protective Devices; Final Rules and Notices" *Federal Register 60:110, pp. 30335-30393.*

Rengasamy, S. and Eimer, B. C. (2011). Total inward leakage of nanoparticles through filtering facepiece respirators. *Ann. Occup. Hyg.* 55:253-263.

Rengasamy, S., Eimer, B. C. and Shaffer, R. E. (2009). Comparison of nanoparticle filtration performance of NIOSH-approved and CE-marked particulate filtering facepiece respirators. *Ann. Occup. Hyg.* 53:117-128.

Rengasamy, S., King, W. P., Eimer, B. C. and Shaffer, R. E. (2008). Filtration performance of niosh-approved N95 and P100 filtering facepiece respirators against 4 to 30 nanometer-size nanoparticles. *J. Occup. Environ. Hyg.* 5:556-564.

Richardson, A., Wang, A. and Hofacre, K. (2007). Development of Skin-Like Material to Accommodate Respirator Sealing with Manikin Head Forms, in *Report to U.S. Army Edgewood Chemical Biological Center*.

Shaffer, R. E., & Rengasamy, S. (2009). Respiratory protection against airborne nanoparticles: a review. Journal of Nanoparticle Research, 11(7): 1661-1672.

Wander, J., HANSON, D. and Margolin, R. (2012). Humanlike Articulate Robotic Headform to Replace Human Volunteers in Respirator Fit Testing, Air Force Research Laboratory Materials and Manufacturing Directorate.

Wang, A., Richardson, A. W. and Hofacre, K. C. (2012). The effect of flow pattern on collection efficiency of respirator filters. *J. Int. Soc. Resp. Prot.* 29:41.

Willeke, K., Qian, Y., Donnelly, J., Grinshpun, S. and Ulevicius, V. (1996). Penetration of airborne microorganisms through a surgical mask and a dust/mist respirator. *Am. Ind. Hyg. Assoc. J.* 57:348-355.

Zhuang, Z., Coffey, C. C., Myers, W. R., Yang, J. and Campbell, D. L. (1998). Quantitative fit-testing of n95 respirators: part I-method development. *International Society for Respiratory Protection* 16:11-24.

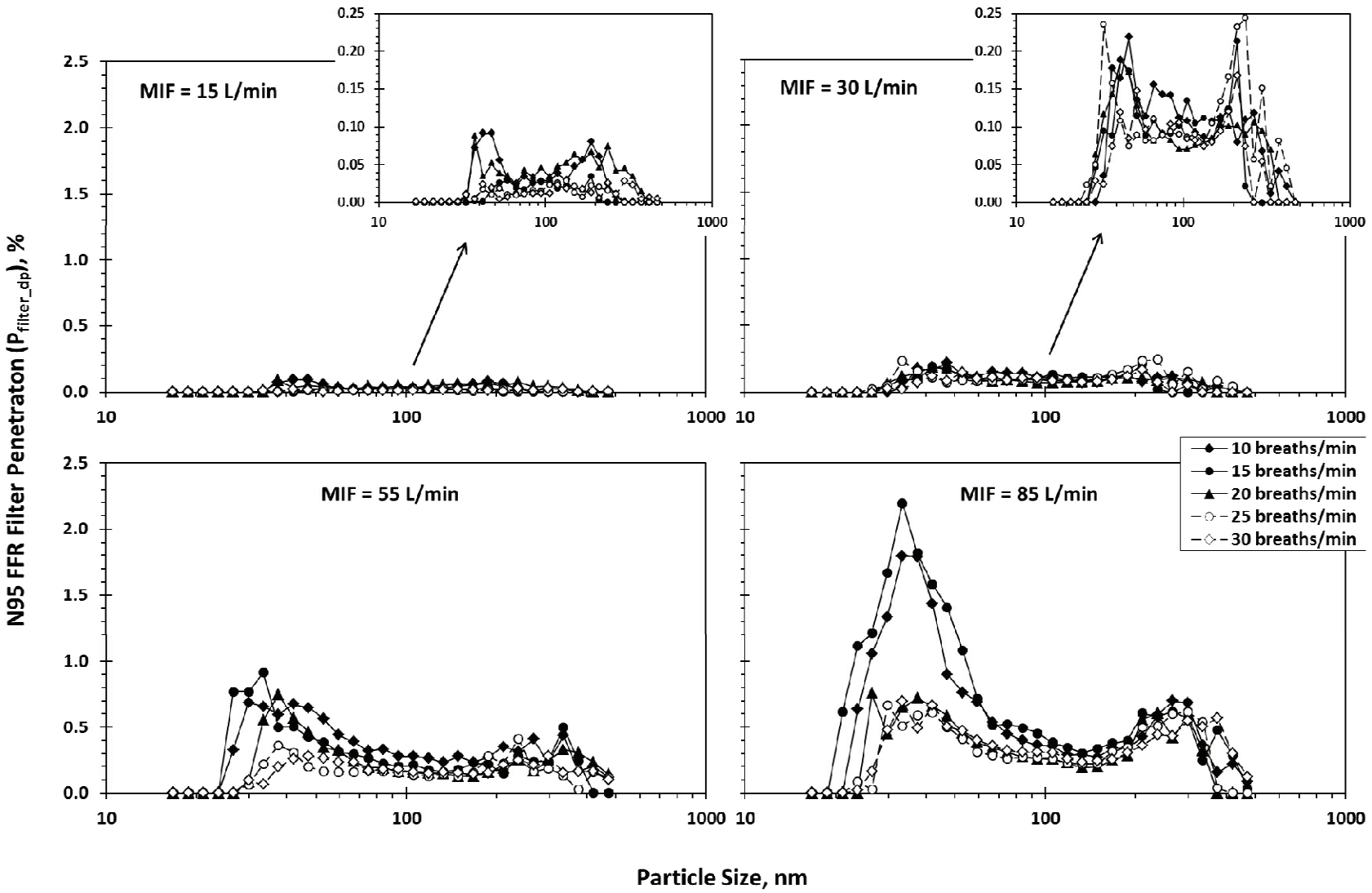

Fig 1. Size-specific filter penetration for an N95 FFR sealed to a plastic manikin's face while challenged with charge-equilibrated NaCl particles. Each point represents the mean value of three replicates. Calculated coefficient of variation (CV) has a mean of 0.42 and a standard deviation of 0.31.

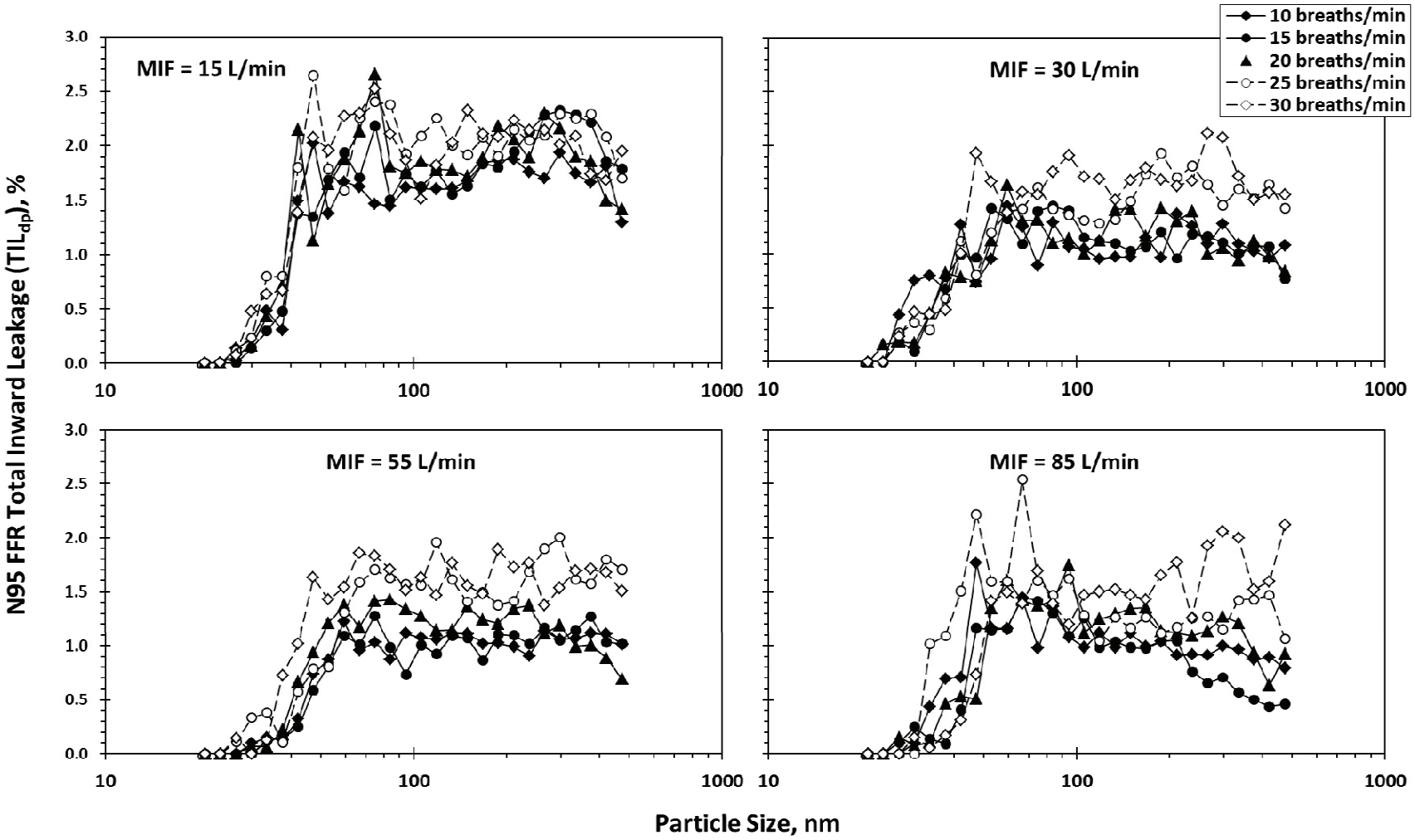

Fig 2. Size-specific total inward leakage for an N95 FFR donned on an advanced manikin headform while challenged with charge-equilibrated NaCl particles. Each point represents the mean value of three replicates. Calculated coefficient of variation (CV) has a mean of 0.40 and a standard deviation of 0.32.

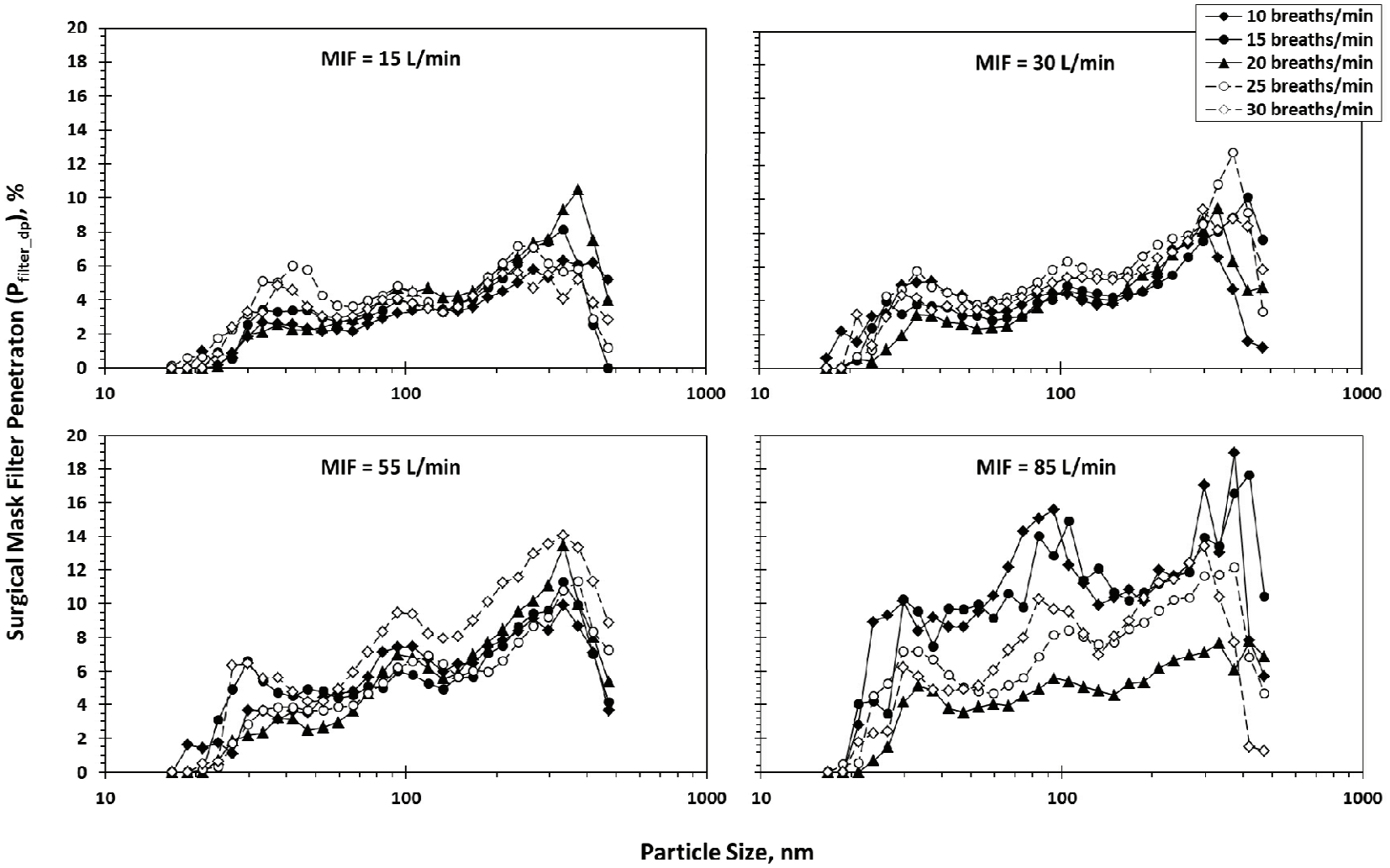

Fig 3. Size-specific filter penetration for a surgical mask sealed to a plastic manikin's face while challenged with charge-equilibrated NaCl particles. Each point represents the mean value of three replicates. Calculated coefficient of variation (CV) has a mean of 0.45 and a standard deviation of 0.29.

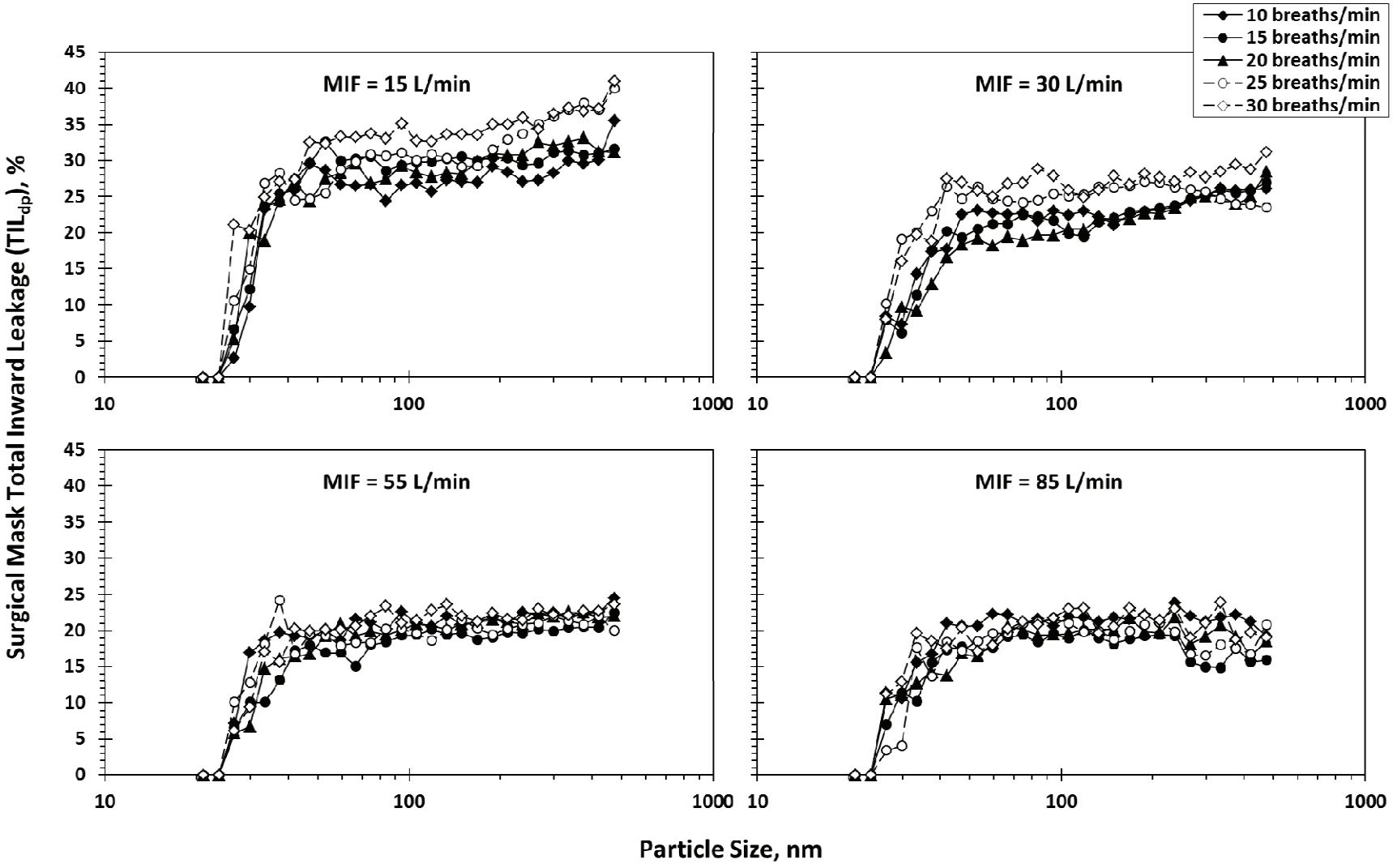

Fig 4. Size-specific total inward leakage for a surgical mask donned on an advanced manikin headform while challenged with charge-equilibrated NaCl particles. Each point represents the mean value of three replicates. Calculated coefficient of variation (CV) has a mean of 0.18 and a standard deviation of 0.17.

Performance Characteristics of an Elastomeric Half-mask Respirator Modified with a Polymer Micro-Patterned Adhesive

Xinjian He[1], Sergey A. Grinshpun*[1], Roy T. McKay[1], Mikhail Yermakov, Tiina Reponen[1], Jue Lu[2], and Parviz Soroushian[2]

[1]*Center for Health-Related Aerosol Studies, Department of Environmental Health, University of Cincinnati, Cincinnati, 3223 Eden Ave., OH, USA;*

[2]*Technova Corporation, 1926 Turner Street, Lansing, MI 48906, USA.*

Submitted to

Journal of the International Society for Respiratory Protection

July 9, 2013

Corresponding author: Sergey A. Grinshpun: sergey.grinshpun@uc.edu

ABSTRACT

Objective: To evaluate the fitting characteristics of an elastomeric half-mask respirator modified with a polymer micro-patterned adhesive applied to the sealing surface; to compare the performance of the modified respirator to that of a conventional (non-modified) one.

Methods: Twenty-five adult subjects representing a NIOSH bivariate panel were tested with a modified and non-modified elastomeric half-mask respirators while participating in a standard OSHA fit testing protocol. NaCl particles were generated as the challenge aerosol and the concentrations inside and outside of the respirator were measured to determine the fit factor for each subject. Additional tests were performed with one subject under challenge facial conditions, including wet and/or unshaved face.

Results: The modified respirator produced a geometric mean (GM) fit factor of 7,907 with a geometric standard deviation (GSD) of 4.9 compared to GM=4,779 and GSD = 9.1 for the non-modified respirator (p =0.07, paired t-test). For all challenge facial conditions, the modified half-mask prototype was consistently achieving significantly (p <0.05) higher fit factors than the conventional half-mask.

Conclusion: Applying a polymer micro-patterned adhesive to the sealing surface of an elastomeric half-mask respirator was found to improve respirator fit and showed promise towards improving performance with various facial conditions.

Keywords: elastomeric half-mask, polymer micro-patterned adhesive, fit testing

INTRODUCTION

Elastomeric respirators are commonly used to protect workers from various hazardous airborne particulates, e.g., firefighters are reported to use elastomeric half-masks equipped with highly efficient P100 filters during fire overhaul (after the fire has been extinguished) (Bolstad-Johnson *et al.*, 2000; Burgess *et al.*, 2001). Unlike filtering facepiece respirators (FFRs), elastomeric half-masks offer the benefits of reusability, enhanced user seal check capability, improved face seal, and can be decontaminated multiple times (Roberge *et al.*, 2010).

According to the U.S. Occupational Safety and Health Administration (OSHA), every worker required to wear a tight fitting respirator such as the elastomeric half-mask shall be fit tested prior to initial use of the respirator (OSHA, 2006). There are two categories of fit testing: 1) qualitative fit test (QLFT), which relies on the wearer's ability to sense a test agent by taste, smell, or irritation, and 2) quantitative fit test (QNFT), which assesses the adequacy of respirator fit by numerically measuring the amount of leakage into the respirator, such as measuring the concentration of a test agent outside (C_{out}) and inside (C_{in}) the respirator. The ratio of the two (C_{out}/C_{in}) is called the fit factor (FF) (OSHA, 2006). A fit factor of 100 is the OSHA pass criterion for negative pressure elastomeric half-mask respirators.

One study involving three half-masks and ten FFRs tested on a panel of ten human subjects concluded that the FFs of elastomeric half-masks are higher than those of FFRs (Han *et al.*, 2005). Considering that elastomeric respirators are equipped with P-100 filters that offer a collection efficiency at least as high as 99.97%, the overall performance of these respirators is largely dependent on their fit (Eshbaugh *et al.*, 2008; Rengasamy *et al.*, 2008; He *et al.*, 2013a). Thus, efforts should be directed towards improving the fit of elastomeric respirators by reducing

faceseal leakage. Many factors can interfere with a good face-to-respirator seal, e.g., positioning, strap adjustment, facial hair, facial scars, high cheekbones, excessive makeup, etc. Prior to the fit testing, a subject shall be free of stubble beard growth, beard, mustache or sideburns which cross the respirator sealing surface; no wetness on the subject's face is allowed. Accordingly, respirator fit-testing studies have usually been conducted under normal skin conditions (dry and clean-shaved). Thus, there are less data on respirator performance using other challenge conditions such as wet and/or unshaved skin.

Conventional elastomeric respirators have a flexible smooth sealing surface extending around the periphery and exhibit a uniform seal surface contour, which aims at creating a good faceseal (Beard, 1994; Starr *et al.*, 1996; Barnett *et al.*, 1999; Belfer *et al.*, 1999). One component of obtaining an effective seal is to be clean shaven prior to respirator donning. However, this requirement, cannot be met consistently in certain situations, e.g., in the battlefield or when respirators are needed during unforeseen emergency situations. The presence of sweat, facial hair, oil, dirt, or acne on facial skin could compromise the effectiveness of peripheral seals and thus negatively affect the performance of a conventional elastomeric respirator. To address the faceseal leakage issues, a conventional elastomeric half-mask was modified to reduce the faceseal leakage. A polymer micro-patterned adhesive (PMA) inspired by gecko-foot was applied to the peripheral area of the half-mask to improve its fit performance. The micro-and nano-fibrillar structure and unique capabilities of gecko-foot have intrigued biologists and engineers for many years. Development of PMA has been actively pursued in recent years (Del Campo and Arzt, 2007; Del Campo, Greiner*, et al.*, 2007; Greiner *et al.*, 2007; Murphy *et al.*, 2009); PMAs based on arrays of relatively soft elastomeric fibrils such as polydimethylsiloxane (PDMS) and polyurethane (PU) have been fabricated to mimic gecko's adhesion mechanism

(Kim *et al.*, 2006; Del Campo and Arzt, 2007). The adhesion capacity of these synthetic adhesives can reach or even surpass that of gecko-foot (Qu *et al.*, 2008). However, PMAs are not inherently leak-resistant; permeation can occur through the gaps between the micro-fibrils, compromising their sealing qualities (Lu *et al.*, 2012).

For this study, the sealing qualities of PMA was enhanced through patterning of polymer microfibrillar structure by incorporating continuous micro-ribbons around fibrillar regions (Lu *et al.*, 2012); and a conventional elastomeric respirator was modified with the PMA applied to the sealing surface. The modified respirator was then fit tested on a NIOSH bivariate (face length and width) 25-subject panel using the standard OSHA fit testing protocol (OSHA, 2006; Zhuang *et al.*, 2007). One of these 25 subjects then participated in a pilot study designed to investigate the fitting characteristics of the modified respirator with less than ideal facial conditions.

MATERIALS AND METHODS

Fabrication of Polymer Micro-patterned Adhesive (PMA)

PMA was produced by soft-molding of elastomeric precursors on a photolithographically formed master template. The template was fabricated following a procedure described elsewhere (Del Campo, Greiner*, et al.*, 2007). Fibrillar arrays were made with PU (ST-3040, Tustin, Inc., Tustin, CA, USA). The templates were silanized with heptadecafluoro-1,1,2,2-tetrahydrooctyltrichlorosilane (hepta-fluorosilane). Gas-phase silanization was performed in an evacuated desiccator for one hour, followed by baking at 95°C for one hour. The PU ST-3040 A and B (20:17 by weight) mixture was degassed and poured on the silanized template. After curing at room temperature in light vacuum over 24 hours, the PU was demolded to avoid rupture of the polymer micro-fibrillar array. The micro-patterned structure had micro-fibrils 20

μm in diameter and 20 μm long with a center-to-center distance of 30 μm. In addition, every 60 rows of micro-fibrils were incorporated with one continuous micro-ribbon 20 μm wide, as shown in Figure 1. The total thickness of the elastomer sheet (with fibrillar surface) was approximately 1 mm.

Respirators

This study was performed using a conventional elastomeric half-mask respirator equipped with two P100 pancake-shaped filters (Model: 2091, 3M, Minneapolis, MN, USA). The chosen respirator model (Model: 6000 series, 3M) is widely used in a variety of occupational environments; it was examined in our recent studies (He *et al.*, 2013a; 2013b) and available in three sizes (small, medium and large). The respirator was modified by manually attaching PMA strips with 2 cm width onto the presumed sealing surface of the half-mask respirator. A non-modified version of the same respirator model and size was used for comparison. The two half-masks (conventional and modified) are shown in Figure 2. An 11 mm long flush probe with a 14 mm diameter flange and a 4 mm diameter inlet was mounted on the surface of the respirator centerline approximately 25 mm from the manikin's nose/mouth. The end of the probe (14 mm flange) was flush with the interior surface of the half-mask.

The modified and non-modified respirators were tested on a given subject in random order. After each fit test the straps and yoke were removed from the respirator body and attached to the alternative respirator; this was accomplished without any adjustment to the straps themselves. We expected that the above procedure would eliminate and/or reduce variability due to strap adjustment.

Human Subjects and Test Conditions

Initially, 120 subjects were identified as available for screening. Twenty-five of these adult subjects were selected for fit testing. The selected subjects included all ten cells of the NIOSH bivariate 25-subject panel (see Figure 3). Of the selected subjects, six had relatively small faces (cells # 1, 2, and 3), six had large faces (cells # 8, 9, and 10), and thirteen had medium faces (cells # 4, 5, 6, and 7). The tested cohort included 17 male and 8 female subjects; among them 13 were Caucasians, 8 Asians, and 4 African Americans/African origins. All subjects were medically cleared by completing an OSHA respirator medical clearance questionnaire. The study received an approval from the University of Cincinnati Institutional Review Board.

The subjects were asked not to eat or drink for at least one hour prior to the fit test. The main phase of this study was performed according to the standard OSHA fit testing protocol; accordingly, the 25 subjects involved in this phase were clean-shaved with dry faces and were fit-tested once with each respirator. For the pilot study, one male subject was fit tested with both respirators under the following facial conditions: dry-shaved (non-challenge condition), wet-shaved, dry-unshaved, and wet-unshaved. The "unshaved" facial condition was created after not shaving for ~40 hours. This condition is believed to reflect many real-life respirator usage situations in the military, the general population, and during certain unforeseen emergency situations. The "wet" face condition was created by applying a handful of water to the face using two hands, patting lightly with a napkin to remove large water droplets, and then waited for 30 seconds before donning the respirator. This condition was intended to simulate a wet sealing when a respirator is worn for some time. In this phase of the study, three replicates were conducted for each of the four above-listed combinations.

Measurements

The study was conducted in a room-size respirator test chamber (24.3 m^3). The challenge aerosol, NaCl, was generated using a particle generator (Model: 8026, TSI Inc., St. Paul, MN, USA). The concentration inside the chamber was maintained at 30,000 to 60,000 particles/cm^3 (such high ambient concentrations were chosen to assure that enough particles would be detected inside a well-fit respirator). For each subject, two fit tests were performed: one with the non-modified half-mask respirator and the other modified with the PMA. A PortaCount Plus (Model: 8020, TSI Inc.) was used to measure the aerosol concentrations outside and inside the respirator.

Prior to fit testing, all respirators were visually examined to eliminate any obvious defects or damages. Each tested subject was asked to select the respirator size (small, medium, or large) that provided the most comfortable fit. Prior to donning each subject was shown how to don the respirator and how to adjust strap tension. After the respirator was donned and straps were properly adjusted, a positive pressure user seal check was performed. Subsequently, the subject was fit-tested while performing the standard set of OSHA respiratory fit testing exercises: 1) normal breathing, 2) deep breathing, 3) turning head side to side, 4) moving head up and down, 5) talking, 6) grimace, 7) bending over and 8) returning to normal breathing. The individual and overall FFs were recorded for each subject. Based on the PortaCount-measured concentrations, each exercise-specific FF value was calculated as below:

$$FF_i = \frac{(C_{out})_i}{(C_{in})_i} \quad \textbf{(1)}$$

where FF_i is the fit factor for the i^{th} exercise, $(C_{out})_i$ and $(C_{in})_i$ are the aerosol concentrations measured outside and inside the respirator, respectively, for each exercise. The overall fit factor

(FF) was determined according to the OSHA fit testing protocol with exclusion of the fit factor for the grimace exercise (OSHA, 2006).

Data Analysis

Data analysis was performed using SAS version 9.3 (SAS Institute Inc., Cary, NC, USA). The FF data were log-transformed. For comparison of respirator type (non-modified versus modified), paired *t*-test was performed using all 25 subjects' FF data. One-way analysis of variance (ANOVA) was performed to study the differences among exercise-specific FFs. For FF results obtained under various facial challenge conditions, paired *t*-test was performed to compare the difference in FF between the non-modified and the modified respirator.

RESULTS AND DISCUSSION

Tests under Normal Facial Condition (Dry and Shaved Face, 25 Subjects)

The overall fit factor data for the non-modified and modified half-masks are presented in Figure 4. FF values for the modified half-mask ranged from 159 (subject #T06) to 57,700 (subject #T11); geometric mean (GM) = 7,907 and geometric standard deviation (GSD) = 4.9. Since each respirator was equipped with P100 filters that are known to be at least 99.97% efficient when used against NaCl particles (results presented in He *et al*., 2013a). Therefore, a FF < 3,333 indicates face seal leakage, and 28% of subjects wearing the modified half-mask had FF < 3,333. Consequently, 72% of the tested modified respirators exhibited the particle penetration solely within the filter efficiency limit (allowing no measurable penetration through the face seal leakage. Furthermore, the majority of fit tests on the modified respirators had FF

greater than 10,000. Only two subjects (#T06 and #T09) had overall FF's between 100 and 1,000.

The non-modified respirator had overall FF's ranging from 37 (subject #T10) to 92,800 (subject #12), with a GM = 4,779 and GSD = 9.1. The range and variability of the non-modified respirator were considerably greater than those for the modified one. Ten subjects (40%) had FF < 3,333 suggesting faceseal leakage was present in the non-modified respirator compared to 28% tested with the modified respirator.

Based on the comparison of the data presented in Figure 4, the performance of the modified half-mask appeared to be better than that of the non-modified. When tested with the modified respirators, FF values exceeded 100 (the OSHA fit test passing criterion) for all 25 subjects, whereas 24 of 25 subjects wearing the non-modified respirators had FF > 100. However, paired *t*-test showed that this difference was not significant ($p = 0.07$, considered to be a boarder-line significance). Very high fit factors and between-subject variability were identified in this study, especially for the non-modified respirator, which presents a challenge in identifying statistical significance.

Comparison of Four Facial Conditions (Dry/Wet, Shaved/Unshaved, One Subject)

Four facial conditions were compared: dry-shaved face, wet-shaved face, dry-unshaved face, and wet-unshaved face. One subject (#T01) participated in this evaluation with the non-modified and modified respirators with three repeats for each condition. The results of this pilot evaluation are presented in Figure 5. The PMA modified respirator produced higher mean FFs under all tested conditions compared to the non-modified respirator. For example, for the wet-shaved facial condition, the modified half-mask achieved a mean FF of 23,241 compared with

267 for the non-modified half-mask. Even the least remarkable difference identified for the dry-unshaved face was an order of magnitude higher for the modified respirator (mean FF = 974 vs. 95). Paired *t*-test results showed that the modified respirator had significantly (p <0.05) higher mean FFs for all facial conditions (dry-shaved, wet-shaved, dry-unshaved, and wet-unshaved). These test results indicate that the surface of the PMA material improved contact against a facial skin under various challenge conditions (shaved, unshaved, dry, and wet).

When the non-modified respirator was tested with the dry skin condition, the fit was higher for the unshaved face than for the shaved face condition (mean FF = 95 vs.74). This observation was made from a single subject and contradicts the conventional wisdom and our own experience that an unshaved facial condition will compromise respirator fit. However, the difference was not statistically significant ($p > 0.05$). In the clean-shaved condition, the non-modified respirator fit this subject poorly with a mean FF below 100. The effect of facial hair may be less significant when respirators fit poorly. When the same subject participated in the 25-subject panel with a clean shaven face, his fit factor was higher (FF = 197 from Figure 4). This demonstrates the potentially high variability between donnings and the limitation of single-subject generated data. With respect to facial hair, it was an important observation that the PMA modified respirator initially fit very well, but FF dropped significantly ($p < 0.05$) after 40 hours of stubble. Although this finding is once again from a single subject, it demonstrates the potentially adverse effect of facial hair when respirators initially fit well in a clean shaven condition.

LIMITATIONS

The non-modified respirator selected for this study had very good fitting characteristics prior to adding the adhesive surface. It is challenging to demonstrate statistically significant

improvement in fit when the "referenced" respirator already fitted well in most of the tests. Additionally, improvement in fit created a situation whereby the number of in-facepiece particles detected by the instrument was very small, which increased the margin of error and decreased the confidence in the measured FFs. However, this concern should have affected both the modified and non-modified respirators similarly since the donning order was randomized. Another limitation was the lack of a "control" respirator consisting of a material with similar thickness and width applied to the sealing surfaces but without the surface characteristics of the PMA. Lastly, conclusions regarding improved performance of the modified respirator using different facial (un-shave and/or wet) are preliminary as they derived from only a single subject with three replicate measurements. A follow-up study seems to be warranted to address the above limitations.

CONCLUSIONS

An elastomeric half-mask respirator was modified by applying a polymer micro-patterned adhesive (PMA) material to the sealing surface. Twenty-five subjects with dry and clean-shaven faces and facial dimensions representing the NIOHS bivariate panel were fit tested using the modified respirator and its non-modified version. The modified respirator produced a geometric mean fit factor of 7,907 with a GSD of 4.9 compared to 4,779 (GSD = 9.1) for the non-modified respirator (p =0.07, paired t-test). In addition, pilot data were generated by testing a single subject under various facial conditions (shaved, unshaved, dry, and wet). The modified half-mask prototype was consistently achieving significantly (p <0.05) higher fit factors than the conventional half-mask. Future studies are needed to include more subjects with various face dimensions along with different shaving and wetting/sweating conditions.

Overall, the addition of a polymer micro-patterned adhesive to the sealing surface of an elastomeric half-mask respirator showed potential for improving the fitting characteristics and possibly respirator performance with less than ideal facial conditions.

ACKNOWLEDGEMENT

This study was supported in parts by the Chemical and Biological Defense (CBD) SBIR program (Contract No. W911NF-10-C-0060) as well as by the NIOSH Pilot Research Project Training Program and Targeted Research Training Program (University of Cincinnati, Education and Research Center, Grant T42/OH008432-07).

REFERENCES

Barnett SS, M. HP, Sabo KK, Scarberry EN. (1999) Respiratory Mask Facial Seal. Respironics, Inc.

Beard M. (1994) Seal for Respiratory Mask. European Patent Office.

Belfer WA, Petillo P. (1999) Strapless Respiratory Facial Mask for Customerizing to the Wearer's Face. US 6,196,223 B1.

Bolstad-Johnson DM, Burgess JL, Crutchfield CD, Storment S, Gerkin R, Wilson JR. (2000) Characterization of Firefighter Exposures During Fire Overhaul. *Am. Ind. Hyg. Assoc. J.* 61:636-41.

Burgess JL, Nanson CJ, Bolstad-Johnson DM, Gerkin R, Hysong TA, Lantz RC, Sherrill DL, Crutchfield CD, Quan SF, Bernard AM*, et al.* (2001) Adverse Respiratory Effects Following Overhaul in Firefighters. *J. Occup. Environ. Hyg.* 43:467-73.

Del Campo A, Arzt E. (2007) Design Parameters and Current Fabrication Approaches for Developing Bioinspired Dry Adhesives. *Macromol. Biosci.* 7:118-27.

Del Campo A, Greiner C, Arzt E. (2007) Contact Shape Controls Adhesion of Bioinspired Fibrillar Surfaces. Langmuir 23:10235-43.

Eshbaugh JP, Gardner PD, Richardson AW, Hofacre KC. (2008) N95 and P100 Respirator Filter Efficiency under High Constant and Cyclic Flow. *J. Occup. Environ. Hyg.* 6:52-61.

Greiner C, Del Campo A, Eduard A. (2007) Adhesion of Bioinspired Micropatterned Surfaces: Effects of Pillar Radius, Aspect Ratio, and Preload. Langmuir 23:3495-502.

Han D-H, Lee J. (2005) Evaluation of Particulate Filtering Respirators Using Inward Leakage (IL) or Total Inward Leakage (TIL) Testing—Korean Experience. *Ann. Occup. Hyg.* 49:569-74.

He X, Grinshpun SA, Reponen T, Yermakov M, McKay R, Haruta H, Kimura K. (2013a) Laboratory Evaluation of the Particle Size Effect on the Performance of an Elastomeric Half-Mask Respirator against Ultrafine Combustion Particles. (in Press). *Ann. Occup. Hyg.*

He X, Yermakov M, Reponen T, McKay RT, James K, Grinshpun SA. (2013b) Manikin-Based Performance Evaluation of Elastomeric Respirators against Combustion Particles. *J. Occup. Environ. Hyg.* 10:203-12.

Kim S, Sitti M. (2006) Biologically Inspired Polymer Microfibers with Spatulate Tips as Repeatable Fibrillar Adhesives. *Appl. Phys. Lett.* 89.

Lu J, Soroushian P. (2012) Micropatterned Structures for Forming a Seal with the Face Skin and Other Surfaces and Method of Make. US Patent Application.

Murphy MP, Aksak B, Sitti M. (2009) Gecko-Inspired Directional and Controllable Adhesion. *Small.* 5:170-75.

OSHA. (2006) Occupational Safety & Health Administration. "Respirator Protection", 29 Cfr 1910.134.

Qu LT, Dai LM, Stone M, Xia ZH, Wang ZL. (2008) Carbon Nanotube Arrays with Strong Shear Binding-on and Easy Normal Lifting-Off. *Science.* 322:238-42.

Rengasamy S, King WP, Eimer BC, Shaffer RE. (2008) Filtration Performance of Niosh-Approved N95 and P100 Filtering Facepiece Respirators against 4 to 30 Nanometer-Size Nanoparticles. *J. Occup. Environ. Hyg.* 5:556-64.

Roberge RJ, Coca A, Williams WJ, Powell JB, Palmiero AJ. (2010) Reusable Elastomeric Air-Purifying Respirators: Physiologic Impact on Health Care Workers. *Am. J. Infect. Control* 38:381-86.

Starr EW, Starr JR, Walthour MT. (1996) Respiratory Mask Facial Seal. Respironics Inc. US 5,540,223.

Zhuang Z, Bradtmiller B, Shaffer RE. (2007) New Respirator Fit Test Panels Representing the Current Us Civilian Work Force. *J. Occup. Environ. Hyg.* 4:647-59.

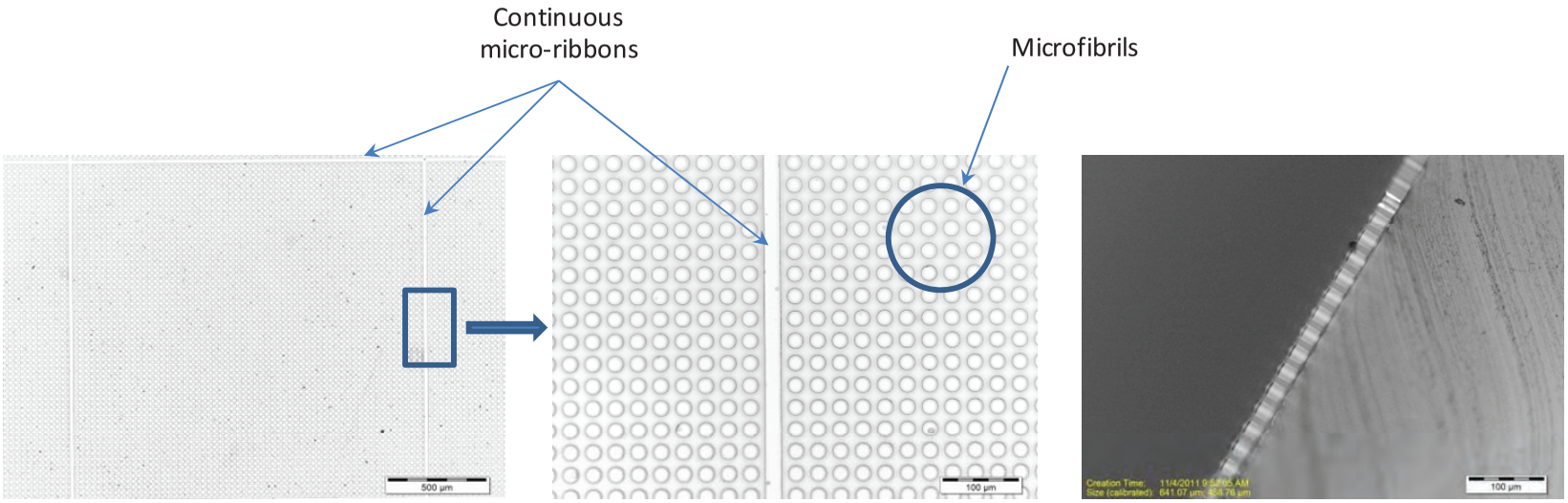

Figure 1. Optical microscope images of PU microfibrillar arrays incorporating micro-ribbons: (a) top view at a magnification of 40× – presents the structure inside the area bordered by the continuous micro-ribbons, (b) insert magnified at 400×; and (c) side view.

Figure 2. A conventional and modified elastomeric half-mask respirators (same model).

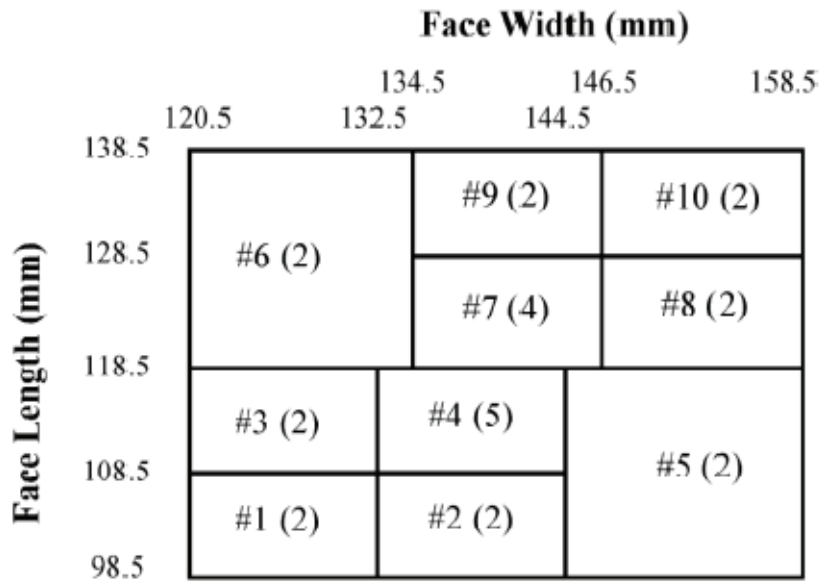

Figure 3. The NIOSH 25-subject bivariate panel. Number of subjects is given in parenthesis after the panel number.

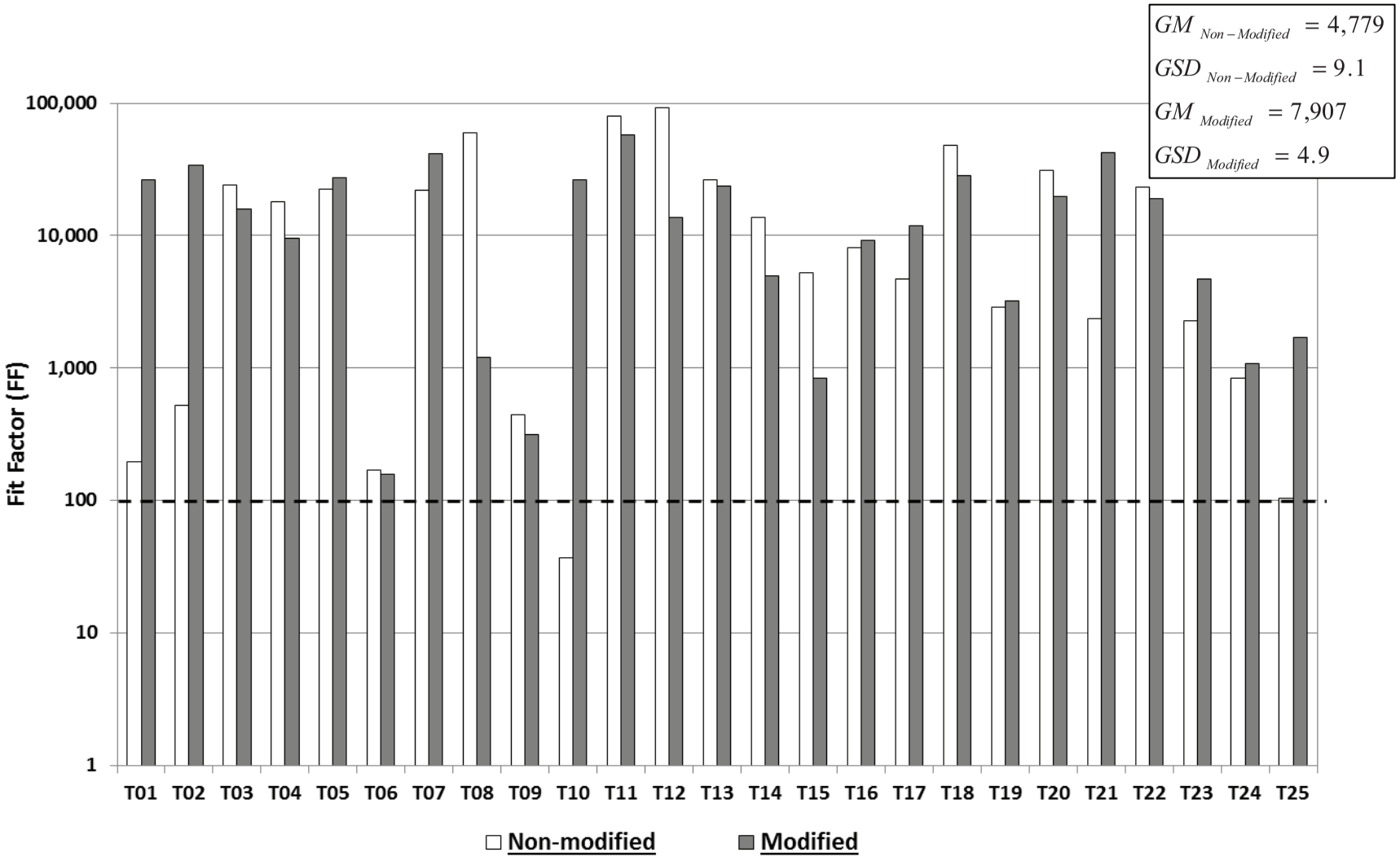

Figure 4. Fit factors (FFs) determined for 25 subjects with dry and clean-shaved faces wearing a conventional (non-modified) and modified elastomeric half-mask respirators.

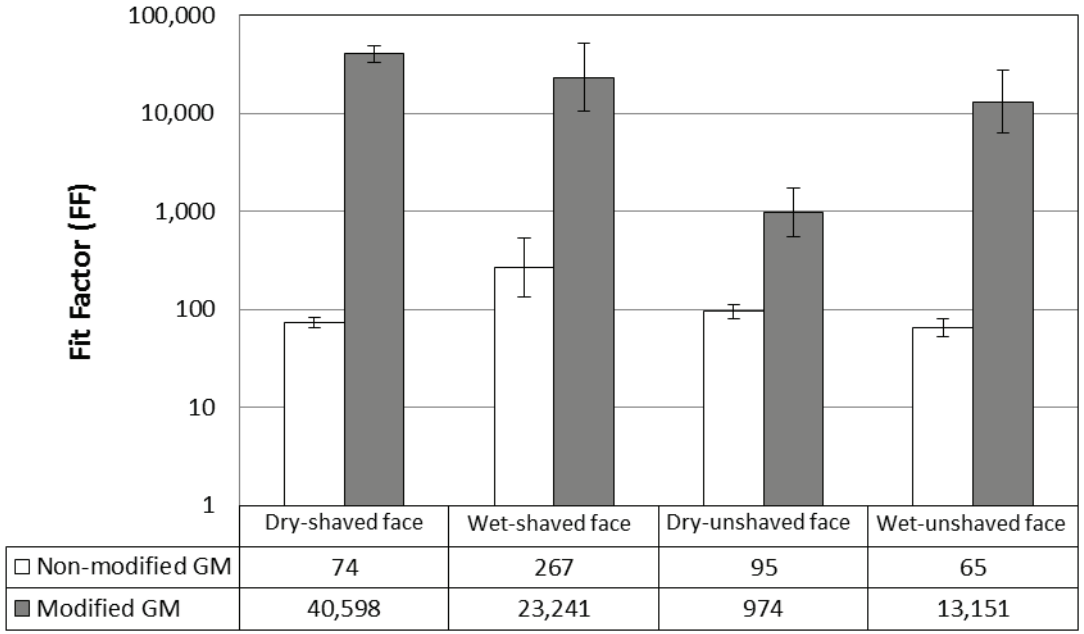

Figure 5. Fit factors (FFs) determined for a subject with four facial conditions while wearing a conventional (non-modified) and modified elastomeric half-mask respirators. The bars represent geometric means; error bars represent the geometric standard deviations of three replicates. (GM: geometric mean).